1994

The Molecular Genetics Of Mouse Catalase

Dorothy L. Reimer

ACKNOWLEDGEMENTS

I would like to thank the members of my advisory committee, Drs. Gerry Kidder, Burr Atkinson and Chris Naus for their guidance and assis_ance throughout my research project.

I would also like to thank my colleagues who gave me support when I needed it and for sharing their laughter and friendship. The numerous lunch hour "conversations" were worth it and I could not have succeeded without them.

Special thanks to Louise Milligan for helping me to keep my sanity when I thought I was about to lose it. Thanks also to Martina Celerin for her words of abuse and encouragement in addition to "running stories" which were instrumental to my success. I wish to express by gratitude to Ian MacPhee for keeping Martina and I both laughing and for graciously letting me win all our squash matches. Further thanks to Daniel and Chantelle MacPhee for keeping the lanster under control. I also thank the MacPhees for providing Tracer when I needed companionship. Thanks to Rebecca Ott for helping make this thesis error free, and to Mary Martin for going above the call of duty and providing me with more than deemed necessary.

I am indebted to my family for providing love, support and understanding during the years of :ny continued pursuit for a career. Sometimes the road gets bumpy, and without them to cushion the ride, the path would have been much rougher.

Most of all I would like to thank my supervisor, Shiva Singh for providing me with the opportunity to pursue my goals. I greatly appreciated all the guidance, support and criticisms that I endured along the way. Shiva. You will never be forgotten.

ISBN 0-315-93188-4

Canada

LIST OF FIGURES

FIGURE Page

To my Mother, Dorothy M. Reimer

to whom I dedicate

this thesis.

ACKNOWLEDGEMENTS

I would like to thank the members of my advisory committee, Drs. Gerry Kidder, Burr Atkinson and Chris Naus for their guidance and assistance throughout my research project.

I would also like to thank my colleagues who gave me support when I needed it and for sharing their laughter and friendship. The numerous lunch hour "conversations" were worth it and I could not have succeeded without them.

Special thanks to Louise Milligan for helping me to keep my sanity when I thought I was about to lose it. Thanks also to Martina Celerin for her words of abuse and encouragement in addition to "running stories" which were instrumental to my success. I wish to express by gratitude to Ian MacPhee for keeping Martina and I both laughing and for graciously letting me win all our squash matches. Further thanks to Daniel and Chantelle MacPhee for keeping the lanster under control. I also thank the MacPhees for providing Tracer when I needed companionship. Thanks to Rebecca Ott for helping make this thesis error free, and to Mary Martin for going above the call of duty and providing me with more than deemed necessary.

I am indebted to my family for providing love, support and understanding during the years of my continued pursuit for a career. Sometimes the road gets bumpy, and without them to cushion the ride, the path would have been much rougher.

Most of all I would like to thank my supervisor, Shiva Singh for providing me with the opportunity to pursue my goals. I greatly appreciated all the guidance, support and criticisms that I endured along the way. Shiva. You will never be forgotten.

TABLE OF CONTENTS

LIST OF TABLES

TABLE Page

LIST OF FIGURES

FIGURE Page

GLOSSARY

A	adenine
aa	amino acid
bp	base pair
C	cytosine
BCIP	5-bromo-4-chloro-3-indolyl phosphate
Cas-1	gene coding for catalase in mice
CAT	gene coding for catalase in humans
cDNA	complementary DNA
cM	centimorgans
cRNA	complementary RNA
DEPC	diethyl pyrocarbonate
DNA	deoxyribonucleic acid
G	guanine
GSH-Px	glutathione peroxidase
H_2O_2	hydrogen peroxide
kb	kilobase
kDa	kilodaltons
LB	Luria Bertani medium
M	molar
mA	milliamperes
mRNA	messenger ribonucleic acid
m7G	7 methyl guanine
NBT	nitroblue tetrazolium
nm	nanometer
nt	nucleotide
pB 4.6	genomic DNA clone with 5' region of *Cas-1*
PBS	phosphate buffered saline
PCR	polymerase chain reaction
pMCT-1	cDNA clone of *Cas-1*
pmol	picomole
R.I.	recombinant inbred mouse line
RNA	ribonucleic acid
RNAsin	RNase inhibitor
rRNA	ribosomal RNA
SDS	sodium dodecyl sulfate
SDS-PAGE	SDS polyacrylamide gel electrophoresis
SEM	standard error of the mean
SSC	standard saline citrate
SSCP	single strand conformation polymorphism
SOD	superoxide dismutase
T	thymine
tRNA	transfer RNA
UTR	untranslated region
UV	ultraviolet light - 254 nm
V	volts

CHAPTER 1

INTRODUCTION

1.1. Oxygen Free Radicals:

Oxygen free radicals (e.g. superoxide radical, hydrogen peroxide and the hydroxyl radical) are oxidants which are generated by all aerobic cells during normal oxygen metabolism, enzymatic reactions and electron flow in the respiratory chain (Sies and Cadenas, 1983, Halliwell and Gutteridge, 1990). They are also generated as a consequence of cellular exposure to radiation and toxic chemicals (Fridovich, 1977; Cerutti, 1985). Although oxygen free radicals are short lived at extremely low cellular concentrations, they are unstable and highly reactive because they bear one or more unpaired electrons in their outer shell. As a result they can damage macromolecules, including DNA, lipids and proteins. Oxidants have been implicated in a number of human diseases including pulmonary dysfunction (Southorn and Powis, 1988), aging (Harman, 1982; Saul *et al.*, 1987) cerebrovascular damage (Kontos, 1985), atherosclerosis (Hessler *et al.*, 1983), cataractogenesis (Varma *et al.*, 1984) and cancer (Ames, 1983; Kensler and Trush, 1984; Cerutti, 1985; Stadtman and Oliver, 1991).

Oxygen free radicals are normally metabolized by antioxidant enzymatic mechanisms that offer a defense against these noxious moieties and maintain cellular integrity. They include scavenging enzymes such as superoxide dismutase (SOD; EC 1.15.1.1), glutathione peroxidase (GSH-Px; EC 1.11.1.9) and catalase (H_2O_2: H_2O_2 oxidoreductase; EC 1.11.1.6). It is the concerted action of these antioxidant enzymes which enables the cell to function in an otherwise pernicious environment. The cooperative roles of these antioxidant enzymes in eliminating oxygen radicals is shown in Figure 1. During normal cellular metabolism, an electron reduction of O_2 produces the superoxide radical, O_2^-, which subsequently undergoes dismutation ($2O_2^- + 2H^+ \rightarrow H_2O_2 + O_2$) by the scavenger enzyme SOD (Fridovich, 1986) to produce H_2O_2. Cellular H_2O_2 can also be produced via flavin enzymes such as acyl-CoA oxidase, monoamine oxidase, uricase, and glutathione oxidase, as well as autooxidation of compounds like those that contain thiols, ascorbate and hydrazine (Percy,

Figure 1. Sources of intracellular hydrogen peroxide (H_2O_2) and its antioxidant enzyme mediated destruction. (A) Superoxide dismutase (SOD). (B) Flavin enzymes (e.g., uricase, monoamine oxidase, acyl-CoA oxidase and glutathione oxidase). (C) Autooxidation reactions (e.g., of thiol compounds, ascorbate and hydrazine). R represents a hydrogen donor and GSH-Px represents glutathione peroxidase.

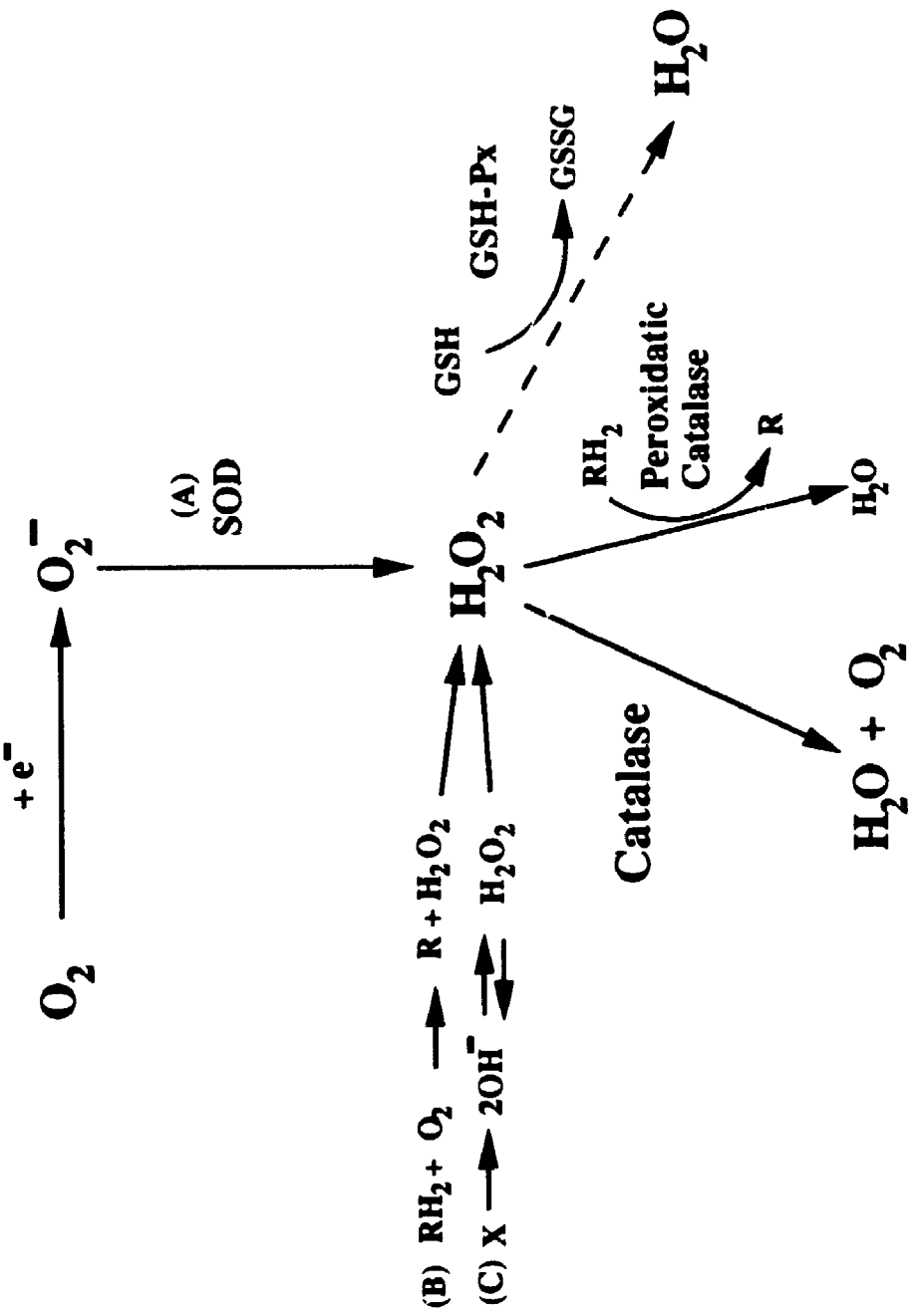
O_2
$+e^-$
O_2^-
(A)
SOD
H_2O_2
(B) $RH_2 + O_2 \rightarrow R + H_2O_2$
(C) $X \rightarrow 2OH^- \rightleftharpoons H_2O_2$
GSH
GSH-Px
GSSG
H_2O
RH_2
Peroxidatic
Catalase
R
H_2O
Catalase
$H_2O + O_2$

1984). The buildup of H_2O_2 is prevented by two classes of related enzymes, the catalases and the peroxidases. GSH-Px is a minor pathway for the breakdown of H_2O_2 and is effective in scavenging H_2O_2 at low concentrations ($<10^{-6}$ M). Furthermore, it acts upon a wide range of hydroperoxides in addition to H_2O_2 and therefore eliminates the toxicity of lipid peroxides (Fridovich, 1977). Catalase is well suited to the scavenging of H_2O_2 over a wide range of concentrations. It therefore provides the major and most fundamental mechanism toward the detoxification of H_2O_2.

Catalase functions in one of two ways depending on the concentration of H_2O_2. If the steady state concentration of H_2O_2 is high, catalase acts mainly as a decomposing catalyst where H_2O_2 acts as both substrate and hydrogen donor in the reaction $H_2O_2 + H_2O_2 \rightarrow O_2 + 2H_2O$ (Aebi and Suter, 1971; Aebi, 1984). At low H_2O_2 concentrations however ($<10^{-6}$ M) and in the presence of a suitable hydrogen donor such as methanol, ethanol or formate, catalase functions mainly as a peroxidase in the reaction $H_2R + H_2O_2 \rightarrow R + 2H_2O$ where R is the hydrogen donor (Smith and Taylor, 1982). Although the protective role of this enzyme is well documented, the specific role and significance of this housekeeping enzyme in this pathway remains poorly understood.

Catalase is ubiquitously expressed in most aerobic organisms including prokaryotes and eukaryotes and is thought to have evolved about two billion years ago when the earth developed an oxygenated atmosphere and organisms developed mechanisms for eradicating toxic effects of cellular metabolites (von Ossowski *et al.*, 1993). Catalases represent a well conserved group of proteins. Amino acid sequence alignments from 20 different organisms including prokaryotes and eukaryotes suggest that there are two major classes of catalases with distinct ancestry. Although the bacterial catalases fail to form a monophyletic group, animal and fungal catalases appear to be derived from a single prokaryotic ancestor. In comparison, plant catalases which form the second major class of catalases may have arisen from a different prokaryotic ancestor (von Ossowski *et al.*, 1993). The fact that the four prokaryotic catalases do not cluster may result from the small number of species available for analysis. Catalase sequences from additional prokaryotes, in particular the cyanobacteria and green algae, may more accurately establish the evolution of catalases in general and mammalian catalases in particular.

1.2. Mammalian Catalase:

In most mammalian cells, catalase, a ubiquitous metalloenzyme, is located primarily within peroxisomes (de Duve and Baudin, 1966; Chance *et al.*, 1979) and in the cytosol (Aviram and Shaklai, 1981; Masters *et al.*, 1986). Mammalian catalase is encoded by a single structural gene and four monomeric subunits are arranged in a tetrahedrally symmetric ellipsoid (Vainshtein, 1974). Each subunit has a molecular weight of approximately 60 kDa and contains a single hematin (Fe-(III)-protoporphyrin IX) group. The total molecular weight of this housekeeping enzyme is ~240 kDa (Schonbaum and Chance, 1976).

The structure of beef liver catalase was among the first to be elucidated (Fita and Rossmann, 1985). The structure of each subunit from beef liver catalase has been extensively studied and consists of four structural domains (Figure 2). The first domain includes an amino terminal region of about 70 residues, which forms an arm extending from each subunit. This arm contains two α-helices and is involved in intersubunit interaction. The second domain is the largest domain (244 amino acids) and forms a large eight-stranded antiparallel β-barrel which interacts with the heme molecule. The β-barrel consists of two topologically similar four stranded antiparallel sheets connected by three α-helices. The third domain (115 amino acids) is referred to as the "wrapping domain" and forms the outer layer of each subunit. The fourth domain which includes the carboxy terminus (69 amino acids) is folded into a four-helical domain and contributes to the formation of the hydrophobic channel leading to the heme. Although the biochemistry of mammalian catalase is now well established, the molecular mechanisms involved in regulating the expression of the catalase gene are still unknown.

Despite the central role of catalase as an antioxidant, a wide range of variation in the level of erythrocyte catalase has been shown in a number of vertebrates (Feinstein, 1970; Holmes and Masters, 1972). For example, ducks and beagle dogs have relatively low concentrations of blood catalase activity (1-23 perborate units/ml blood) while rabbits and humans have comparably higher levels (325-455 perborate units/ml blood). A significant reduction in catalase activity is observed in rare cases of human acatalasemia in Japanese and Swiss populations (Crawford *et al.*, 1988; Wen *et al.*, 1990; Ogata, 1991). This genetically heterogeneous disorder is inherited as an autosomal recessive trait.

Figure 2. Diagrammatic representation of the secondary structure of one subunit of liver catalase. The α and β pleats are marked and the heme molecule is highlighted. (adapted from Fita and Rossmann, 1985)

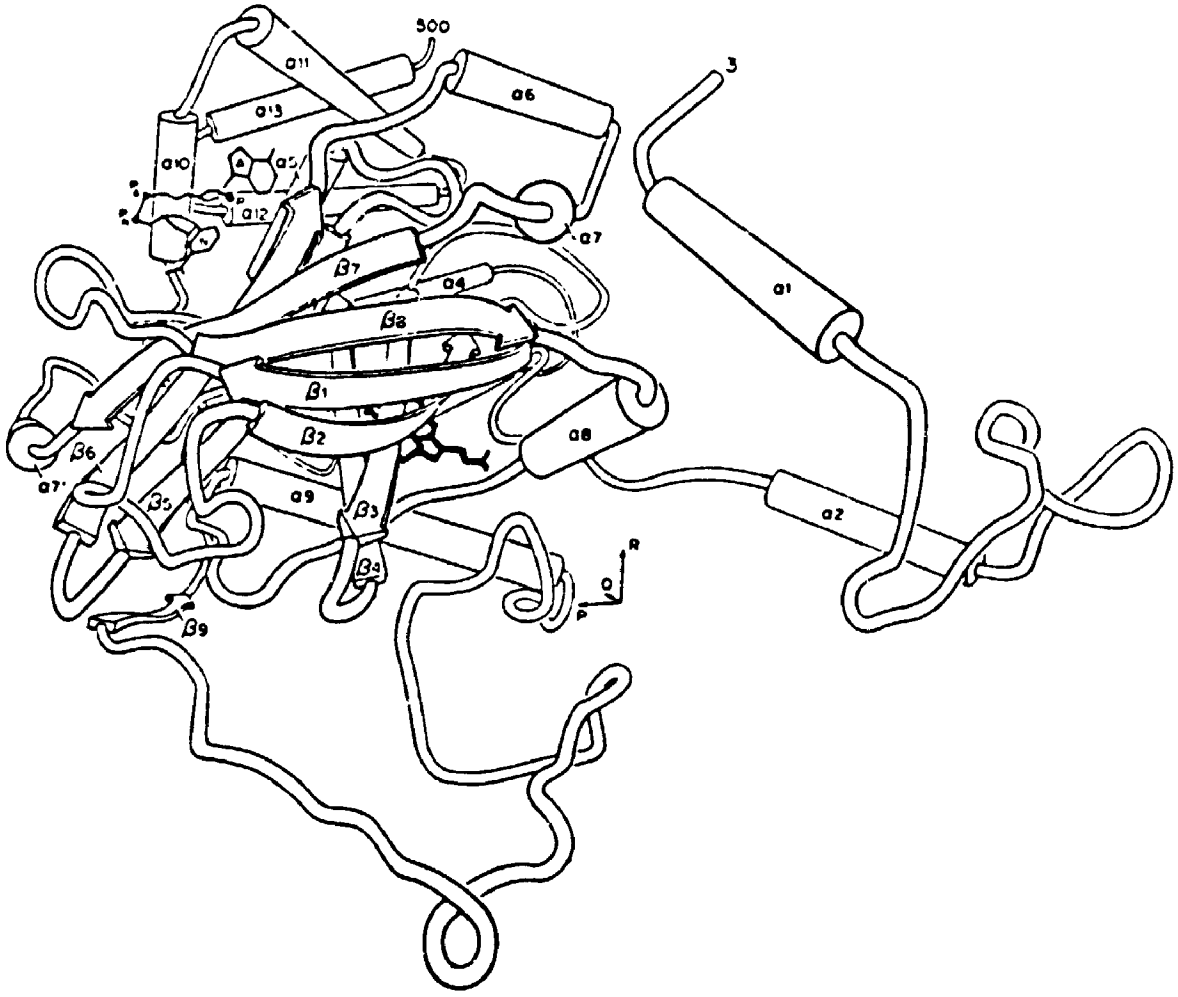
500
3
α11
α13
α6
α10
α5
α12
α7
β7
α4
β8
α1
β1
β2
α8
β6
α7'
β5
α9
β3
α2
β4
β9
R
Q
P

In acatalasemia, the erythrocyte is most severely affected, often having less than 1% of normal activity; other tissues also display variable levels of catalase deficiency. The observation that catalase activity is reduced but not absent, suggests that the term acatalasemia in the literature is a misnomer. In fact, a deletion of the catalase gene may be lethal and has never been described in mammals. In the Japanese population, acatalasemia is attributed to the absence of catalase mRNA (Wen *et al.*, 1988). Molecular analysis of fibroblasts from these affected individuals has revealed a single base substitution in the genomic DNA, resulting in a splicing mutation and the lack of mRNA production (Wen *et al.*, 1990). Clinical manifestations include ulcerating, often gangrenous, oral lesions. In contrast, the fibroblasts of the Swiss-type acatalasemia contain normal levels of mRNA, but have significantly reduced levels of catalase polypeptide. An amino acid replacement in the coding region is suggested to be responsible for a structural mutation (Crawford *et al.*, 1988). This is thought to lead to an unstable protein which phenotypically results in only mild clinical symptoms.

1.3. Mouse Catalase:

In mice, catalase is coded by a single structural gene (*Cas-1*) (Holmes and Duley, 1975; Bailley, unpublished) that has been mapped to chromosome 2, approximately 26 cM from the *agouti* locus and located in linkage group V (Dickerman *et al.*, 1968). *Cas-1* produces a single 2.4 kb message (Shaffer *et al.*, 1987; El-Hage and Singh, 1989), which is consistent in size with the catalase mRNA produced in tissues of human (Quan *et al.*, 1986) and rat (Furuta *et al.*, 1986). Once the polypeptide is synthesized, it undergoes posttranslational modifications (Masters *et al.*, 1986) which produce two distinct polypeptides that combine to yield five tetrameric isozymes (Holmes and Masters, 1970). The production of these multiple isozymes in mouse kidney has been suggested to involve an additional regulatory gene, *Ce-2* (Hoffman and Grieshaber, 1976).

Variations in the level of catalase activity have been demonstrated among tissues in the mouse (Novak *et al.*, 1978; Schisler and Singh, 1987). The highest levels of catalase activity are found in the liver, kidney and erythrocytes, while the lowest levels are detected in connective tissue. Ganschow and Schimke (1969, 1970) have suggested that liver catalase is under the control of a regulatory gene, *Ce-1*, which affects the enzyme activity

by altering the rate of degradation. In addition to tissue-specificity, variations in the level of erythrocyte and liver catalase activity have been reported in different inbred strains of mice (Heston *et al.*, 1965; Hoffman and Rechcigl, 1971; Novak *et al.*, 1978; Schisler and Singh, 1987, 1991). Based on the enzyme activity in the blood, Schisler and Singh (1991) categorized mouse strains as "normal" (BALB/c, C3H/HeAnl/*Cas-1*^{a}), "hypocatalasemic" (C57BL/6J, 129/ReJ) and "acatalasemic" (C3H/HeAnl/*Cas-1*^{b}). They also evaluated the genetic basis for the enzyme activity variations among strains and suggested the involvement of additional transacting regulatory factor(s). These strains offer the best known genetic system for studying the regulation and physiological significance of this housekeeping enzyme and its associated defects and disorders.

The development of the acatalasemic genotype, C3H/HeAnl/*Cas-1*^{b}, by mutation and breeding (Feinstein *et al.*, 1966; Feinstein, 1973) has provided additional valuable material toward understanding the expression and regulation of catalase. Because of the near absence of catalase activity in the blood and kidney of this strain of mice, they are sensitive to H_2O_2 (Feinstein, 1973). Although biochemical and physical studies of the mutant catalase have provided valuable insights into the nature of this genetic defect, the molecular basis of this tissue-specific mutation has not been established.

In 1987, Shaffer *et al.* suggested that the genetic defect that produces the tissue-specific reduction of catalase expression in the acatalasemic strain C3H/HeAnl/*Cas-1*^{b} is not due to rearrangements of DNA within the catalase structural gene. Furthermore, this mutation does not act at the level of gene transcription, but rather at the level of translation and/or catalase protein turnover. Recently, Shaffer and Preston (1990) identified a glutamine^{11} to histidine substitution in the first major α-helix of the catalase subunit in C3H/HeAnl/*Cas-1*^{b} which they suggested destabilizes the polypeptide. In addition, Shaffer *et al.* (1990) have shown a single amino acid replacement (alanine^{117} to threonine) located within the heme binding site of catalase in the hypocatalasemic strain C57BL/6J. These mice have approximately 60% of the liver catalase activity found in normal strains. A change in this region is postulated to disrupt the hydrophobic channel and diminish the catalytic efficiency of this enzyme in C57BL/6J. These replacements in the *Cas-1* coding region however, cannot alone account for the tissue-specific reduction in enzyme levels, specifically in kidney and blood of C3H/HeAnl/*Cas-1*^{b}. This suggests a role for additional genetic determinants as hypothesized by Schisler

and Singh (1991). Moreover, the well characterized tissue-specific expression profile of the mouse catalase gene in a number of established genetic strains and mutations provides valuable material for studies on the regulation of expression of this important housekeeping gene.

It was the aim of this study to determine the molecular mechanisms involved in *Cas-1* expression and explain the variation in activity among tissues and strains of mice. *Cas-1* expression was investigated in multiple tissues at the levels of mRNA (northern and dot blots), polypeptide (western blots), and enzyme activity in normal, hypocatalasemic and acatalasemic strains. A more specific objective of this project was to further characterize the molecular defect leading to acatalasemia and understand the role this defect may play in the tissue-specific expression of catalase in mice.

It may be pointed out that at birth the fetus leaves a hypoxic uterine environment and enters an environment rich in oxygen. This transition poses a significant oxidative stress on the newborn, and can result in the generation of toxic reactive oxygen species (Rickett and Kelly, 1990). Numerous studies have demonstrated an accumulation of SOD, GSH-Px and catalase in the lung during the final period of gestation (Yam *et al.*, 1978; Tanswell and Freeman, 1984; Gerdin *et al.*, 1985; Kelly and Rickett, 1987; Sosenko and Frank, 1987). These increases have been hypothesized to prepare the pulmonary system for the acute change in oxygen concentration that occurs at birth. This late gestational increase in antioxidant enzymes in this tissue is thought to be mediated by increased levels of mRNA (Hass *et al.*, 1989; Clerch *et al.*, 1991). The temporal expression of these enzymes in other tissues, however, has not been studied, particularly at late gestational age.

Preliminary studies by Holmes (1971) on the ontogeny of catalase activity revealed that fetal mouse liver catalase had approximately one-tenth the activity of adult tissue. A complete developmental profile of catalase activity in addition to other antioxidants from guinea pig liver has shown increases at late gestation as well (Rickett and Kelly (1990). In mice, El-Hage and Singh (1989, 1990) have shown that the expression of the 2.4 kb catalase transcript is detectable as early as 8 days post mating and increases during 13-18 days after mating, particularly in the liver. They have also shown that liver catalase activity exhibits an increase with *in utero* development and growth. Interestingly, the relative mRNA levels at these stages are higher than the relative enzyme activity values as compared to adults (El-Hage and Singh,

1989). These results suggest that the catalase mRNA may accumulate *in utero* and the primary transcript may undergo efficient processing and translation only after birth with the onset of independent respiration. The fact that the liver, unlike lung, is not directly exposed to higher oxygen concentrations at birth suggests that expression of antioxidant enzymes in the liver may be related to the rate of metabolism of the organ, rather than the partial pressure of oxygen (de Haan *et al.*, 1994).

The spatial and temporal pattern of catalase gene expression during mouse embryonic development has not been studied and becomes the focus of this study. The sensitive technique of *in situ* hybridization was used to detect *Cas-1* mRNA in differentiating tissues on serial sections of paraffin-embedded embryos. These experiments will aid in understanding the possible regulatory mechanisms involved in the expression of *Cas-1* in different tissues during embryonic development.

1.4. Gene Regulation:

a: Transcription

Protein synthesis in eukaryotic cells is a complex event and involves the molecular interaction of many components (Pain, 1986; Sonenberg, 1988). Many regulatory mechanisms for gene expression involve DNA sequences located in the flanking regions of a structural gene. The most extensively studied aspect of gene regulation is the control of transcription. Transcriptional regulation is a complicated, multilevel process involving the interactions of many transacting factors with specific *cis* acting DNA sequences located in the 5' upstream region of a gene. DNA methylation, primarily in the 5' flanking region, has been suggested as a mechanism for the regulation of gene expression in animal cells (Cedar, 1988) and is thought to inhibit gene expression by disrupting the protein-DNA interactions required for transcription (Eden and Cedar, 1994). Addition of a methyl group to the fifth carbon residue of cytosine is the most common DNA modification and in eukaryotes predominantly involves CpG dinucleotides (Cooper, 1983). The promoter region of many vertebrate genes, including some tissue-specific genes and most known housekeeping genes which lack a TATA box, are known to contain "CpG islands" (Bird, 1986). Such islands (>200 bases) have a GC content above 50% and a high frequency of CpG dinucleotides relative to the bulk of the genome (Bird, 1987). Razin and Cedar (1991) have demonstrated that there is

a correlation between gene expression and undermethylation of DNA. The presence of methylation may therefore act to repress transcription.

Most housekeeping genes, which are constitutively expressed, are typically unmethylated (Bird, 1986). These genes may not be affected by this inhibitory mechanism and are therefore available for constitutive expression in all cell types. In contrast, most tissue-specific genes are methylated at CpG residues and rendered transcriptionally inactive (Cedar, 1988) in early stages of embryogenesis. At later stages, the methylation profile may be altered by demethylation of tissue-specific genes in the cell types in which they are expressed. Moreover, tissue-specific gene expression during gametogenesis has also been demonstrated to involve changes in DNA methylation patterns (Kafri *et al.*, 1992). CpG sites were found to be methylated in sperm DNA but not methylated in mature oocytes, indicating that the paternal and maternal genomes have different profiles of methylation. These sites however, are demethylated in both parental genomes during early embryogenesis, providing a mechanism for removing differences in specific gene methylation patterns and allowing for the normal program of development. Prior to organogenesis, *de novo* methylation occurs which serves to re-establish the adult methylation pattern. The mechanisms involved in demethylation and remethylation are not yet known, however they appear to be important to the processes of tissue-specific gene expression, particularly during embryogenesis.

Mouse catalase is a known housekeeping enzyme with differential tissue-specific expression. The transcriptional regulation of the catalase gene *Cas-1* has not been experimentally demonstrated and the correlation between gene expression and DNA methylation, if any, has not been attempted. One of the objectives of this study therefore, was to experimentally evaluate the 5' regulatory region of the *Cas-1* gene in a number of different tissues for potential differences in DNA methylation. Results from these experiments could provide a model for understanding the transcriptional regulation of catalase and housekeeping genes in general.

b: Posttranscription

Posttranscriptional regulation of genes is now considered to be important in the expression of many eukaryotic genes. It may involve mRNA stability (Peltz *et al.*, 1991), regulation of translation (Kozak, 1992), and post-translational modifications (Darnell *et al.*, 1986). Synthesized proteins may

undergo posttranslational modifications, including the addition of signal sequences and glycosylation which are necessary for their function.

The poly (A) tail has in principle been shown to be important in mRNA stability (Hentze, 1991). In general, polyadenylated substrates are degraded more slowly than their deadenylated counterparts, suggesting that deadenylated messages are more susceptible to nucleolytic attack. Furthermore, removal of the poly (A) tail usually precedes the degradation of many mRNAs. Recent evidence now argues that additional sequences in the 3' untranslated region (3' UTR) may also confer mRNA instability. For example, unique sequences in the 3' UTRs of many cytokine and lymphokine mRNAs have been shown to be responsible for their rate of degradation in the cytoplasm (Bickel *et al.*, 1992). The cytosolic protein, adenosine-uridine binding factor (AUBF) is shown to complex with four tandem repeats (AUUUA) of an RNA transcript and is dependent on both the nucleotide sequence and secondary structure (Gillis and Malter, 1991). More recently, Alberta *et al.* (1994), have shown that the recognition site for this protein in regulating *c-myc* mRNA stability is not the AUUUA motif itself but a 39 base uridine-rich domain adjacent to this element. How these AU-rich regions induce instability is not fully understood, however the AUBF-RNA complex is thought to generate a destabilizing signal which may increase the susceptibility to exonuclease digestion. Deletion of the AU-rich region from the normal *c-fos* gene increases the steady state level of its mRNA and converts it to an oncogene (Gillis and Malter, 1991) with the ability to transform cells (Meijlink *et al.*, 1985). Similarly, the tumourigenicity of mast cells is enhanced when IL-3 is overexpressed, a result of an AU-rich 3' UTR deletion (Wodnar-Filipowicz and Moroni, 1990).

The synthesis of human transferrin receptor (TfR), which is responsible for cellular iron uptake, is also shown to be regulated posttranscriptionally by altering mRNA stability (Mullner *et al.*, 1989). A cytosolic protein, the iron-responsive element binding protein (IRE-BP), regulates TfR by binding to a conserved RNA motif, the iron-responsive element (IRE) in the 3' UTR of the mRNA. The sequence of the IRE has the potential to form five similar stem loop structures that are important for binding the IRE-BP. The regulation of TfR is dependent on intracellular iron levels and it is thought that when iron is in low abundance, TfR synthesis is enhanced by increasing the stability of the mRNA through the interaction between IRE-BP and the IRE (Hentze *et al.*, 1989). Interestingly, the same protein that binds to the 3' UTR of TfR also binds to a

single stem loop structure located in the 5' UTR of ferritin mRNA where it regulates translation of ferritin by iron (Theil, 1990). Although these two mRNAs act in different ways, this type of concerted regulation is not well documented. This may define a general strategy for using similar mRNA sequences to coordinate the synthesis of two metabolically related proteins.

An increase in catalase activity in neonatal rat lung was shown to be associated with a rise in the concentration of catalase mRNA in response to hyperoxia encountered at birth (Clerch *et al.*, 1991). Unlike late gestational changes, this elevation is associated with a doubling of the half-life of catalase mRNA and not a change in the rate of transcription. These authors suggested that this increase in catalase activity is mediated posttranscriptionally, in part by increased mRNA stability. More recently, Clerch and Massaro (1992) have demonstrated the presence of a protein(s) from neonatal rat lung that interacts specifically with catalase mRNA, perhaps the 3' UTR, to form mRNA-protein complexes. These interactions are subject to a reversible sulfhydryl switch mechanism, since in the reduced state, the strength of mRNA-protein binding complexes is increased. Clerch and Massaro have also suggested that during hyperoxia, the mRNA-binding protein complex formation may be affected by the presence of iron, thereby oxidizing the RNA-binding protein and diminishing the binding to catalase mRNA. The hydroxyl radical can be formed by the reaction of iron with elevated levels of H_2O_2. This increase in mRNA stability (as a result of decreased protein binding) could therefore provide the cell with a unique mechanism against hydroxyl radical induced damage. In general, although a possible role for the mRNA-binding proteins in the regulation of rat catalase gene expression is recognized, the molecular nature and the dynamics of this interaction are still not known.

c: Translation

Translation of mRNA is another important mechanism which cells can utilize to regulate the expression of their genes. Although the complexity of this mechanism is relatively well recognized, the processes by which mRNA translation is regulated remains to be elucidated. It may be pointed out that translational regulation is known to play a crucial role in programming early embryonic development (Richter, 1991). In many organisms early development relies on pre-existing maternally synthesized mRNAs for protein synthesis. Many of these mRNAs are stored in a translationally inactive state (masked) until a particular stage of development (Sommerville, 1992). This translational

repression is thought to be brought about by the interaction of specific RNA sequences with masking (repressor) proteins. Standart *et al.*, (1990) have shown that in clam oocytes, sequences 120-140 nucleotides long and located in the 3' UTR of ribonucleotide reductase and cyclin A mRNAs, can mediate translational inhibition *in vitro*. Removal of the 3' UTR or treatment of the oocytes with injected antisense oligonucleotides reverses the inhibitory effect and permits the translation of these mRNAs. Extensive experimentation has demonstrated that specific sequences in the 3' UTRs are required for the binding of masking proteins which act to repress translation.

The translation of eukaryotic protamine 2 mRNA (a nuclear protein predominantly expressed during spermatogenesis) has also been suggested to be translationally repressed *in vitro* (Kwon and Hecht, 1993). The 3' UTR of this gene contains a putative stem loop structure which is capable of binding to an 18 kDa protein derived from testicular cytoplasmic extracts. This complex is thought to stabilize a specific RNA conformation, thereby sterically interfering with the process of translation. At later stages of male differentiation, this protein no longer binds the mRNA, enabling the protamine mRNA to be translated. This protein, therefore, plays a primary role in translational repression during male germ cell differentiation. Although this regulation involves an mRNA-binding protein complex, the influence of other proteins cannot be ruled out.

Translational regulation of stored maternal messages can also occur by the removal or addition of the poly (A) tail. Wickens (1990) has demonstrated that critical signals lie in the 3' UTR and mRNAs containing the consensus sequence UUUUUUAU receive a poly (A) tail and are translationally active while those that lack this sequence rapidly lose their tails and are translationally inert. Although the mechanisms involved are not fully understood, this process is temporally regulated and is dependent on poly (A) tail length. Furthermore, it has been suggested that RNA-protein interactions with this consensus sequence or other 3' UTR motifs may regulate changes in the state of polyadenylation (Jackson and Standart, 1990). These changes may arise from interactions involving sequences from the coding region, the 5' and/or the 3' UTR. This "cross talk" supported by RNA-protein interactions, could influence upstream events such as translation initiation or reinitiation. This could result from a rearrangement of secondary structures throughout the whole mRNA

dependent on changes at one end of the molecule. Alternatively, it may involve some direct interaction between 5' and 3' elements.

The efficiency of translational regulation is known to be influenced by 5' UTR mRNA structure including the m7G cap, the primary sequence surrounding the AUG start codon, the position of the start codon, and the secondary structure upstream and downstream from the AUG start codon (Kozak, 1991a, b). An experimentally established consensus sequence [GCC(A/G)CCAUGG] is present in the 5' UTR and is required for efficient translation in many vertebrate mRNAs (Kozak, 1989a). In addition to local secondary structures, long range interactions have been shown to affect translation *in vitro* (Kozak, 1989b). Spena *et al.* (1985) have demonstrated that translation from zein mRNA, which synthesizes a major storage protein of *Zea mays*, is blocked by a hybrid formation involving inverted repeats found in the 5' and 3' UTRs. Whether such interactions have regulatory significance *in vivo* remains to be determined. However, the results reported do suggest the potential importance of the 3' UTR in the regulation of translation.

d: RNA Interaction

The interaction of RNA and protein is critical to many biological systems. The control of gene expression can be mediated by RNA-protein interactions in a variety of cellular processes, including mRNA splicing and translation (Keene and Query, 1991). Proteins are bound to RNA due to recognition of regions such as RNA termini, homopolymeric sequences and/or specific stem-loop secondary structures. Although the significance of a few RNA-protein interactions has been studied in recent years, most of such interactions remain to be evaluated.

More recent studies have offered an increasing list of genes where 3' UTRs play a significant role in their regulation. These include a deletion of the 3' UTR which has been implicated in aspartylglucosaminidase and lysosomal accumulation disease (Ikonen *et al.*, 1992) and an expansion of the triplet CTG in the 3' UTR region of the myotonin-protein kinase mRNA which is involved in the causation of myotonic dystrophy (Brook *et al.*, 1992; Fu *et al.*, 1993). Interestingly, the degree of CTG expansion correlates with familial anticipation (Aslandis *et al.*, 1992). However, the mechanism of abnormal expression of this unusual mutation is not known and remains speculative.

The 3' UTR of eukaryotic mRNA, which varies greatly in length, has been perceived as uninhabited and void of important regulatory information. It was

thought to be useful only to carry the signals necessary to form the stable end of the mRNA (Wickens, 1993). Although the functions of the 5' UTR in gene regulation (particularly in transcription) are now well established, the 3' UTR still remains virtually uninvestigated. As previously mentioned, this region of the mRNA, has been shown to contain sequences implicated in the regulation of gene expression, which now demonstrates that this so-called barren stretch of nucleotides contains information of functional significance.

In addition to the recently documented 3' UTR mRNA-protein interactions, other events at the 3' end of the mRNA can also control posttranscriptional regulation by distinct mechanisms (Jackson, 1993). Recently, small RNAs have also been shown to regulate gene expression (Lee *et al.*, 1993; Wightman *et al.*, 1993). *Lin-14* which encodes a nuclear protein, controls the timing of developmental events in *C. elegans*. Here, the presence of a repressor mRNA (*lin-4*) is shown to regulate the expression of *lin-14* mRNA by binding to complementary sequences located in the 3' UTR of the *lin-14* mRNA, thereby inhibiting translation (Wickens and Takayama, 1994). Hennessy *et al.* (1989) have suggested that poly (U) tracts identified in the 3' UTR of thrombospondin mRNA form a duplex with the poly (A) tail and play a role in mRNA stabilization. Other mRNAs with poly (U) tracts have also been identified (Ullrich *et al.*, 1985; Sandell *et al.*, 1984; Spicer *et al.*, 1987; Rychlik *et al.*, 1987) and suggest the possible significance of RNA-RNA interactions in posttranscriptional regulation. The possible presence of mRNA-binding proteins in both of these cases however, cannot be ruled out.

The recent evidence of functional synergism and protein binding experiments suggest that the m7G cap, the 5' leader and the 3' UTR of Tobacco Mosaic Virus RNA interact to establish an efficient level of translation (Leathers *et al.*, 1993). The regulation of gene expression by RNA-RNA interactions, is accompanied by an mRNA-binding protein specific to a 35 base region of the 5' UTR and a 52 base region of the 3' UTR sequence. Although these interactions are sequence-specific, the secondary structure of the 3' UTR may be important in the formation of the mRNA-protein binding complex. The elucidation of the mechanisms underlying these interactions will provide an opportunity to explore the more versatile and complex translational machinery of eukaryotes.

The significance of the 3' UTR of *Cas-1* toward understanding the posttranscriptional regulation of mouse catalase has never been investigated and becomes another focus of this research. The 3' UTR of *Cas-1* was

investigated for the potential involvement in the multi-level regulation of catalase among tissues and strains. As a starting point, regulatory sequences in the 3' UTR were experimentally evaluated for their ability to bind protein(s) which could be involved in the differential posttranscriptional regulation of mouse catalase. The results of these experiments are discussed in detail with respect to the nature of the mRNA-protein binding interactions. Specific mRNA sequences in the 3' UTR are identified which bind protein(s) and result in the formation of an mRNA-binding complex. In addition, the protein components of these complex formations are identified and characterized. Results from these experiments will aid in the understanding of the molecular genetics and the regulation of the mammalian antioxidant enzyme catalase.

1.5. Objectives:

Overall:

1. to understand the organization and regulation of expression of the catalase gene (*Cas-1*) in mice.

Specific:

1. to obtain the complete cDNA and 5' genomic sequences of catalase gene encoding *Cas-1*. This information is necessary to complete the objectives dealing with the expression of *Cas-1*.

2. to understand the regulation of the catalase gene (*Cas-1*) during fetal development in mice.

3. to experimentally evaluate the variation in *Cas-1* expression at mRNA, protein and enzyme activity levels towards the explanation of tissue specificity of catalase.

4. to understand the molecular mechanisms involved in the variable regulation of tissue-specific expression among mouse genotypes.

5. to elucidate the molecular defect responsible for the tissue-specific acatalasemic mutation.

CHAPTER 2

MATERIALS AND METHODS

MATERIALS:

2.1. Animals:

Mice, from 8 inbred strains (BALB/c, Swiss Webster, 129/ReJ, C57BL/6J, C3H/S, C3H/HeAnl/*Cas-1*^{a} and C3H/HeAnl/*Cas-1*^{b} and ABP/Le) were used in this study. BALB/c, Swiss Webster and C3H/S were originally obtained from Canadian Breeding Farms, St. Constant, Charles River, Quebec, 129/ReJ, C57BL/6J and ABP/Le from the Jackson Laboratory, Bar Harbour, Maine. These strains of mice have been inbred (brother-sister mated) for more than 15 years in the animal quarters of the Department of Zoology at the University of Western Ontario. C3H/HeAnl/*Cas-1*^{a} and C3H/HeAnl/*Cas-1*^{b} were obtained from T.W. Clarkson, University of Rochester, New York. A recombinant inbred (R.I.) strain derived from a cross involumeving an inbred female Swiss Webster and a male C3H/HeAnl/*Cas-1*^{b} (SXC/ws-1) was generated in 1983 in the breeding facilities of the Department of Zoology. The establishment and the biochemical characterization of SXC/ws-1 is presented in Appendix 3.

All animals were housed in 28.5 cm X 11.5 cm polycarbonate cages with sawdust bedding maintained on a diet of Purina mouse chow (Purina Canada Inc.), and provided with water *ad libitum*. A 14:10 hour light-dark cycle was maintained in a thermostatically controlled (23°C) environment.

2.2. cDNA and gDNA Clones:

Two plasmids, pMCT-1 and pB 4.6, were obtained from Dr. Robert Korneluk, Ottawa, Ontario. The cDNA insert for the plasmid pMCT-1 was obtained by screening a BALB/c liver cDNA library (Stratagene Inc.) with a heterologous liver catalase cDNA clone (pCAT 41). The restriction map of the pMCT-1 insert (the largest obtained) is shown in Figure 3A and encompasses approximately 1850 bp. This clone contained the 3' untranslated region (3' UTR) and a region which codes for ~350 amino acids of *Cas-1*.

Figure 3: A: The restriction map of the insert of pMCT-1, isolated from a BALB/c cDNA library representing the most 3' region of *Cas-1* including the 3' UTR. The termination site (TAA) is indicated and the region identified by stars represents the 0.5 kb *Bam* HI/*Pst* I restriction fragment which was subcloned into the pGem-2 riboprobe vector (B). The T7 and SP6 promoters were used to generate the antisense and sense riboprobes, respectively for use in the *in situ* hybridization analysis. Enzymes represented are: Ap, *Apa* I; B, *Bam* HI; Bg, *Bgl* II; N, *Nst* I; P, *Pst* I; Xh, *Xho* I; X, *Xba* I.

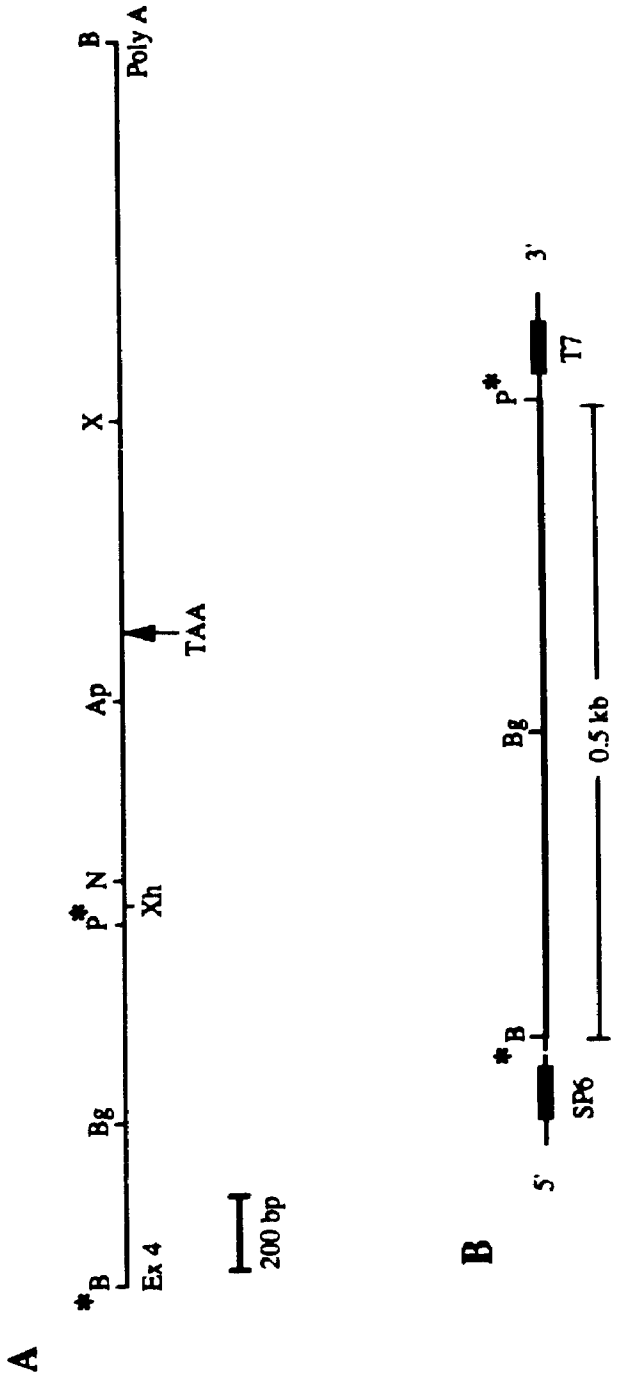
A
*B
Ex 4
Bg
P* N
Xh
Ap
TAA
X
B
Poly A
200 bp
B
*B
SP6
5'
Bg
P*
T7
3'
0.5 kb

Figure 4: A: The restriction map of the insert of pB 4.6, isolated from a BALB/c genomic library used to generate the sequence of the 5' upstream regulatory region of *Cas-1*. The translation start site (ATG) is indicated and the dotted line represents the first intron. B: The partial restriction map of pB 4.6 representing the 5' end of *Cas-1*. The identified restriction enzymes were used to subclone 4 fragments into pBluescript (SK^-) for sequence analysis. The sizes of the restriction fragments are given. The first exon/intron boundary is marked (*). Enzymes represented are: A, *Acc* I; B, *Bam* HI; P, *Pst* I; Pv, *Pvu* II; X, *Xba* I.

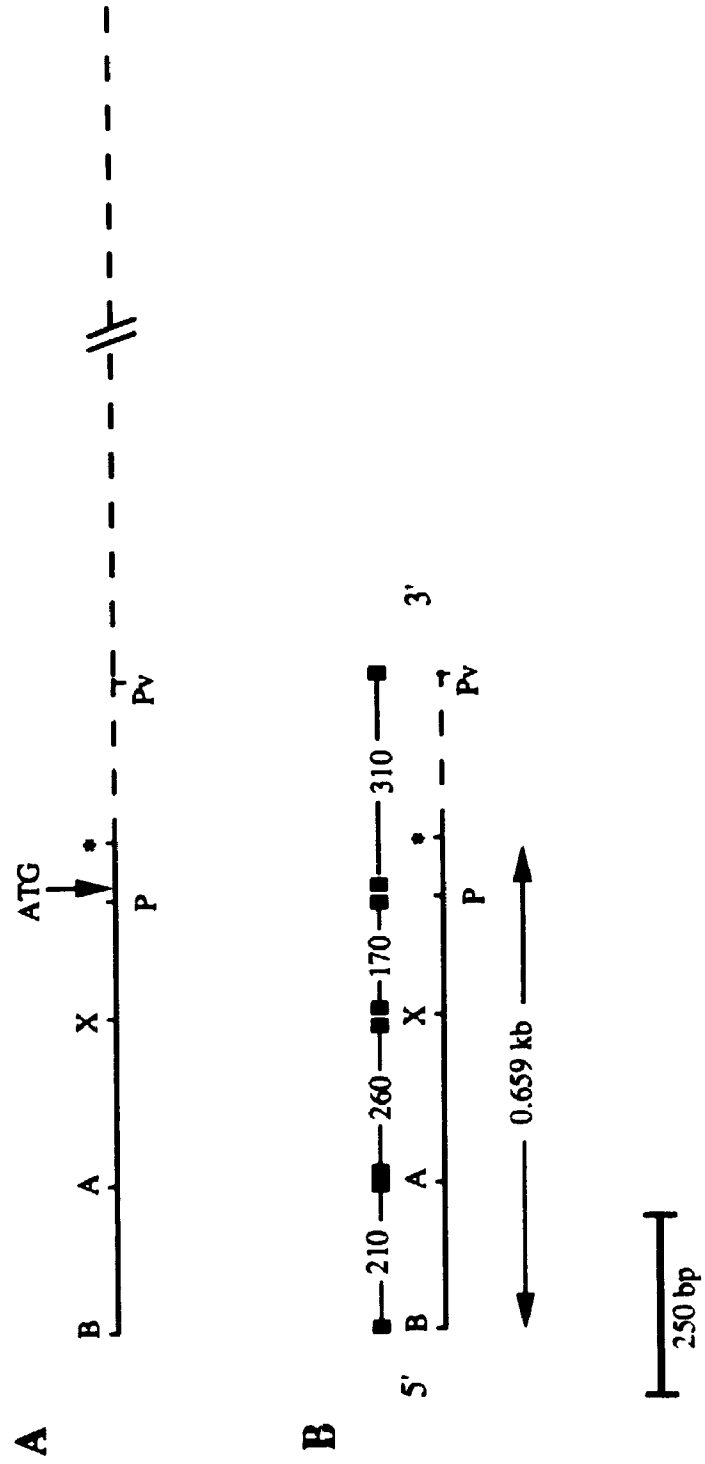
A
ATG
B
A
X
P
Pv
B
210
260
170
310
5'
3'
0.659 kb
250 bp

A BALB/c genomic liver library was screened using a human catalase promoter fragment to produce pB 4.6. This plasmid contained ~660 bp of the 5' upstream region of the *Cas-1* gene, 66 bp of exon 1, and a partial fragment from the first intron (Figure 4A).

METHODS:

A: Gene Organization

2.3. DNA Sequencing:

Cloning Strategy for Sequencing *Cas-1*:

All fragments to be sequenced were subcloned into pBluescript (SK$^-$). The fragments were separated by electrophoresis in a 0.8% low melting point agarose gel (BRL) in 1 X TAE (40mM Tris-acetate, 1.0mM EDTA), excised and purified using NACS Prepac Kit (BRL) according to the manufacturers instructions. NACS is an ion exchange resin that quantitatively binds DNA in low salt conditions (0.1M NaCl). The DNA was recovered from the column by elution with high salt (1.0M NaCl). Purified DNA fragments were ligated into compatible sites of the pBluescript (SK$^-$) plasmid (Stratagene Inc.) and transfected into XL1-Blue bacterial host cells (Stratagene Inc.). Transformed cells were grown overnight on LB agar plates (Sambrook *et al.*, 1989) with 25 µg/ml ampicillin (Sigma) which selectively allows only the growth of bacteria containing the plasmid. Random bacterial colonies were selected and grown overnight in LB supplemented with ampicillin (25 µg/ml). The presence of the appropriate insert was verified using restriction enzyme digestion of purified plasmid DNA from selected bacterial colonies. Overnight cultures of selected bacterial colonies with the desired insert yielded plasmid DNA that was used for sequencing.

DNA Sequencing Protocol:

All DNA fragments were sequenced using the dideoxynucleotide chain termination method of Sanger *et al.*, (1977). Plasmid DNA was isolated either using Magic Minipreps Columns (Promega) or using the alkaline lysis method described by Sambrook *et al.*, (1989) with modifications. Plasmid purification using Magic Miniprep columns uses the alkali lysis method of Sambrook *et al.*, (1989) followed by purification through the ion resin-based column. Alternatively, plasmid DNA was isolated from 3 ml of overnight culture using the alkali lysis method and extracted once with phenol saturated with 50mM sodium acetate pH

4.0, and once with chloroform:isoamyl alcohol (24:1) (Weickert and Chambliss, 1991). The DNA was purified by precipitation in 100% ethanol and resuspended in H_2O.

Approximately 2 µg of plasmid DNA containing the insert of interest was denatured in 0.4M NaOH for 10 min at room temperature, and an equal volume of 1.0M sodium acetate pH 5.2 was added. The DNA was precipitated at -70°C for 30 min in 3 volumes 100% ethanol and centrifuged at 12,000 x g for 10 min at 4°C. The DNA pellet was washed in 80 µl 80% ethanol, recentrifuged, air dried and resuspended in 10 µl sterile distilled H_2O. To this solution, 2 µl (0.80 µM) of the appropriate sequencing primer (M13 universal sequencing primer, or T3 pBluescript sequencing primer) and 2 µl annealing buffer (Pharmacia T7 sequencing kit, Upsala, Sweden) were added. The primer was annealed to the DNA for 20 min at 37°C, followed by 10 min at room temperature. Dideoxynucleotide sequencing of the DNA was performed using either Pharmacia's T7 Sequencing kit or USB's Sequenase kit and α ^{35}S-dATP from Dupont (Markham, Ontario).

Sequencing reactions were separated on 8% polyacrylamide 8M urea gels using either a Bio Rad Sequi-Gen Cell (0.4mm X 17cm X 50cm) and an LKB Bromma 2303 Multidrive XL 3,500 V power supply (Pharmacia) or a BRL Model S2 sequencing system (0.4mm X 31cm X 38.5cm) and a Bio Rad Model 3000xi power supply. The gels were subjected to electrophoresis at 55°C for 2, 4, 6 or 8 hr, fixed in 10% acetic acid/10% methanol for 20 min and rinsed in distilled H_2O. The gels were blotted onto Sequencing Gel filter paper (Bio Rad, Richmond, California) and dried for 1 hr in a Bio Rad Model 583 gel dryer. X-ray film (Kodak X-OMAT AR) was placed next to the gel in a film cassette and exposed 24 to 96 hr at room temperature. The film was subsequently developed according to the manufacturer's instructions using GBX developer and fixer (Kodak).

2.4. Bacteriophage Library:

cDNA Library Construction:

Messenger RNA from adult C3H/HeAnl/*Cas-1^b* kidney was isolated using PolyATract mRNA Isolation System (Promega). Kidney cells were disrupted by homogenization in extraction buffer (4M guanidine thiocyanate, 25mM sodium citrate pH 7.1) on ice. Biotinylated Oligo(dT) probe was added to the lysate and mixed well. This mixture was centrifuged at 12,000 x g for 10 min at room temperature, and the supernatant recovered. Streptavidin Magnesphere

Paramagnetic Particles (SA-PMPs) were added to the supernatant and mixed well. The SA-PMPs were captured by placing the tube in the Magnetic Stand, and the supernatant removed. Particles were washed twice in 0.5 X SSC, magnetically capturing the particles following each wash. The mRNA was eluted from the particles in RNase-free H_2O, precipitated with 1/10 volume 3M sodium acetate pH 6.0 and an equal volume isopropanol and resuspended in RNase-free H_2O (1 µg/µl). Five micrograms of poly(A)$^+$ mRNA from C3H/HeAnl/*Cas-1^b* kidney was used to construct a cDNA library using the ZAP-cDNA Synthesis Kit (Stratagene). Zap is an insertion vector equipped with multiple cloning sites within plasmid sequences that can be excised *in vivo* and converted to the plasmid vector pBluescript (SK$^-$). Synthesis of cDNA and construction of the library using the Uni-ZAP XR vector follows the supporting protocol supplied with the kit by Stratagene.

Plating and Transferring of Library:

All techniques for growing, transferring and hybridizing bacteriophage libraries are from *Current Protocols in Molecular Biology* (Ausubel *et al.*, 1987). Large (150mm) sterile polystyrene plates were used for primary library screening. Host bacteria (XL1-Blue) were grown overnight in LB (1% tryptone, 0.5% yeast extract, 1.0% NaCl pH 7.0). The next morning, 600 µl of host bacteria (OD_{600} = 0.5 in 10mM $MgSO_4$, 10% maltose) was mixed with titred phage from the cDNA library, and incubated at 37°C for 15 min. Five ml of agarose [NZY broth (0.5% NaCl, 0.2% $MgSO_4.7H_2O$, 0.5% yeast extract, 1% NZ Amine pH 7.5), 0.7% agarose (BRL)] were added and plated on 150 mm plates (NZY broth containing 1.5% agar) to give approximately 50,000 plaques/plate. The plates were incubated at 37°C for approximately 5 to 8 hr until sufficient lysis had occurred.

After lysis, the plates were refrigerated at 4°C overnight. Nitrocellulose filters (Gelman) labelled with ballpoint ink were placed on the agarose surface for 2 min to allow transfer of phage particles. Orientation of the filters on the plates was marked with a 20G needle and India ink before the filters were removed. The filters were air dried for 15 min and the phage DNA was denatured by saturating the filters (DNA side up) with 0.2M NaOH/1.5M NaCl for 1.5 min. The filters were subsequently neutralized by floating in 0.4M Tris-HCl (pH 7.6)/2 X SSC followed by 2 X SSC for 1.5 min each. The filters were air dried and then baked in a vacuum oven for 90 min at 80°C.

Hybridization:

The nitrocellulose filters were prehybridized in heat-sealed bags in 48% formamide, 4.8 X SSC, 20mM Tris-HCl pH 7.6, 1 X Denhardt's solution, 10% dextran sulphate and 0.1% SDS at 42°C for 1.5 hr. The 1.8 kb *Bam* HI/*Bam* HI fragment of the cDNA clone, pMCT-1, was random prime labelled (see Section 2.7), boiled for 10 min with 1 ml of 2 mg/ml sonicated herring sperm DNA (Sigma), and quenched on ice for 10 min. The probe was added to the prehybridized filters and hybridization was allowed to continue overnight at 42°C.

The following morning, the filters were removed from the bags, and washed three times in low stringency buffer (2 X SSC/0.1% SDS), 15 min each at room temperature. The filters were then washed in a high stringency wash buffer (0.2 X SSC/0.1% SDS) at 55°C for 20 min, wrapped in plastic wrap and exposed to X-OMAT RP film (Eastman Kodak Company, Rochester, New York) for 3 hr at -70°C with a Quanta Detail-T intensifier screen. The films were developed using Kodak's GBX developer and fixer.

Purification of Bacteriophage Clones:

Plaques which were positively hybridized on the primary plates were identified by aligning the orientation marks on the filters, film and primary plates. The plaques were isolated by inserting sterile toothpicks first into the area on the primary plate, and then onto a grid-marked secondary plate. Secondary plates were made by plating 200 µl of XL1-Blue in 0.7% agarose onto an 82mm petri dish with 20 ml of NZY agar. Approximately 30 stabs were picked for each positive primary clone. The plates were grown for approximately 6 hr at 37°C until lysis was complete. The phage were then transferred to nitrocellulose filters and hybridized as previously described. Positive plaques from the secondary screening were further purified by inserting a sterile toothpick into the positive plaque and immersing in 1 ml of SM buffer (0.58% NaCl, 0.2% $MgSO_4.7H_2O$, 50 mM Tris-HCl pH 7.5, 0.1% gelatin) for 5 min. Serial dilutions of this stock were then plated. Plates with 10 to 50 well separated plaques were used for transfer and hybridization, as above. A quaternary screening was performed in some cases to ensure complete purification. Single plaques which gave strong signals following hybridization were used to make pure phage stocks. A sterile toothpick was inserted into the plaque and placed into 500 µl SM buffer containing 20 µl chloroform, mixed thoroughly and let sit for 2 hr at room temperature and stored at 4°C. pBluescript SK$^-$ phagemids were recovered by *in vivo* excision with the use of R408 helper phage (Stratagene Inc.) according to the cDNA synthesis kit

supporting protocol. The rescued phagemids with the cloned DNA inserts (200 µl) were incubated with 200 µl XL1-Blue host bacteria (OD_{600} = 1.0) and plated at several concentrations onto 82mm LB agar plates (LB containing 15% agar) with 50 µg/ml ampicillin, and incubated at 37°C overnight.

Isolation of DNA and Characterization of Clones:

Single colonies were picked and grown overnight at 37°C in 10 ml LB with 50 µg/ml ampicillin. Plasmid DNA was isolated by alkaline lysis as described by Sambrook *et al.* (1989). A 1.5 ml microfuge tube was filled with 1.5 ml of overnight culture and the bacteria collected by centrifugation (10,000 x g, 1 min). The supernatant was removed and a further 1.5 ml of bacterial culture collected. The pellet (from three ml of culture) was resuspended in 100 µl of cold 50mM glucose, 10mM EDTA, 25mM Tris-HCl pH 8.0. After allowing this mixture to incubate at room temperature for 5 min, 200 µl of freshly prepared 0.2N NaOH, 1% SDS were added and the microfuge tube inverted to mix the contents and incubated on ice for 5 min. Potassium acetate (5M, 150 µl) was added, incubated on ice for 5 min and pelleted in a microfuge for 5 min at 4°C. The plasmid DNA was purified by phenol/chloroform extraction, precipitated with 2 volume 100% ethanol at -20°C for 5 min and recovered by centrifugation at 12,000 x g for 5 min at 4°C. The DNA was resuspended in 20 µl TE pH 8.0 with 50 µg/ml RNase A and incubated at room temperature for a further 30 min. Five µl of DNA was digested with *Eco* RI plus *Xho* I in a standard reaction for 2 hr at 37°C and run on a 0.8% agarose gel in 1 X TBE (85mM Tris-borate, 2mM EDTA) to detect the presence of cDNA inserts.

Plasmid DNAs digested to release the cDNA inserts were subjected to electrophoresis on a 0.8% agarose gel, blotted onto nylon membrane (Biotrace, R.P.) and hybridized with the pMCT-1 probe for confirmation of *Cas-1* specific sequences. Positive hybridization signals confirmed the presence of *Cas-1* specific cDNA inserts from the kidney mRNA (cDNA) of the genotype C3H/HeAnl/*Cas-1*^{b}. The plasmid DNAs containing *Cas-1* specific inserts were isolated from overnight bacterial cultures using either the acid-phenol mini-prep procedure or the Magic Miniprep columns (Promega). A fragment of approximately 400 bp containing the 3' UTR was identified and sequenced (section 2.3).

B: Gene Expression

2.5. Catalase Enzyme Activity Assays:

Tissue Collection

The method of tissue collection followed Schisler and Singh (1991). Animals were sacrificed; liver and kidney were excised, washed in distilled water and homogenized in 0.07M phosphate buffer, pH 7.2 containing 0.25M sucrose and 1% Triton X-100. Supernatants obtained after centrifugation of the homogenate at 9,000 x g for 30 min at 4°C were stored at -70°C until needed for the enzyme assays. Blood was collected by cardiac puncture or with a heparinized syringe from the thoracic cavity and centrifuged (Eppendorf microcentrifuge) for 1 min at 15,600 x g. The erythrocyte sediment was washed three times with isotonic NaCl and stored at -70°C.

Enzyme Assays:

As a preliminary indicator of enzyme activity, blood samples were obtained from mouse tails and assayed fresh or stored at -70°C. These samples were screened for relative catalase activity using the "fizz test" (Feinstein, 1973). Five µl of whole blood was added to 50 µl of 3% H_2O_2 in a glass test tube at room temperature. The presence of catalase is detected by the decomposition of H_2O_2 resulting in the vigorous production of oxygen that manifests as bubbles. Blood samples tested, were scored for the presence of catalase (fizzing) or the absence of catalase (no fizzing). This preliminary test is often used to identify strains of mice with high and low (no) catalase activities.

Evidence for the presence of catalase enzyme activity was also demonstrated by electrophoresis following Harris and Hopkinson (1976). Tissue homogenates were subjected to electrophoresis on a 5% polyacrylamide separating gel (1.5 mm, no SDS) with a 3% stacking gel under native conditions (0.25M Tris-HCl pH 6.8, 0.2M glycine) at 4°C for 20 min at 30mA followed by 45 min at 35mA. The resulting gel was immersed in 0.06% H_2O_2, incubated for 15 min at room temperature and subsequently developed with 2% potassium ferricyanide reagent, 2% ferric chloride (50:50). Catalase activity appeared as yellow zones on a blue-green background. The gel was photographed with transillumination using Kodak film (2415) and developed using HC 110 for moderate contrast.

In order to quantify the catalase enzyme activity, the UV assay of Aebi (1984) was used. In this system, the decomposition of H_2O_2 is followed by

observing the decrease in absorbance at 240 nm with time. The difference in absorbance after a defined reaction period forms the basis for the measurement of catalase activity. The specific protocol for detection of catalase enzyme activity followed Schisler and Singh (1991) which included ethanol treatment of the supernatant (0.01 ml ethanol/ml supernatant) for 30 min on ice to ensure full enzyme activation (Cohen *et al.*, 1970). Appropriate quantities of supernatant were then diluted to 2 ml with a 50mM phosphate buffer pH 7.0 prepared by dissolving each of (a) 6.81 g KH_2PO_4 and (b) 13.90 g $NaHPO_4.7H_2O$ in 1 l H_2O and mixing solutions (a) and (b) in the proportion of 1:1.55 in a quartz cuvette equilibrated at 20°C. The reaction was started by adding 1 ml of 30mM H_2O_2 substrate prepared in phosphate buffer. The absorbance at 240 nm was measured at 2 sec intervals for 18 sec in a DU 8 spectrophotometer (Beckman). One unit of catalase will decompose 1.0 µmole of H_2O_2 per min at pH 7.0 and 25°C (Aebi, 1983). Catalase activities were expressed in Bergmeyer Units/ mg protein. The method of Bradford (1976) with bovine serum albumin (BSA) as a standard was the basis for the protein determination for all samples. Measurements of enzyme activity for a given sample represent a mean of three replications from a single animal. At least three animals from each strain were tested.

2.6. Western Blotting and Analysis of Catalase Polypeptide:

Tissue Collection, Gel Electrophoresis and Blotting:

Liver, and kidneys were excised from animals and homogenized in 10 volumes phosphate buffered saline (PBS) containing 1% Triton X-100. Blood was collected and rinsed in PBS to remove serum. Supernatants were recovered following centrifugation at 3,000 rpm (IEC Clinical) at room temperature for 10 min. All homogenates were stored at -70°C until needed. Total protein was determined using the Bradford assay (Bradford, 1976).

A 10% SDS-polyacrylamide gel for a Mini-Protean II apparatus (Bio Rad) was prepared with 0.375M Tris-HCl, 0.1% SDS pH 8.8 followed by a 4% stacking gel made up with 0.125M Tris-HCl, 0.1% SDS pH 6.8. Protein from liver (3 µg), kidney (4 µg) and blood (15 µg) was dissolved in a final volume of 5 µl PBS with 1% Triton X-100. Ten microliters of 2 X sample buffer [0.125M Tris-HCl, 10% glycerol, 0.07M SDS, 2% 2-mercaptoethanol, 0.1% bromophenol blue (w/v) pH 6.8] were added and the samples denatured at 95°C for 10 min. The samples were loaded on the gel and the subunits separated electrophoretically in 0.25M

Tris-HCl, 0.2M glycine, 0.003M SDS, pH 8.3, at 30mA for 20 min followed by 35mA for 45 min. After electrophoresis, the apparatus was dismantled, and the gel equilibriated in transfer buffer [25mM Tris-HCl, 192mM glycine (BDH), 20% methanol pH 8.3] for 15 min at room temperature. The proteins were subsequently transferred to a nitrocellulose membrane (Schleicher and Schuell) using a Bio Rad Trans-Blot apparatus at 100V for 1 hr. The apparatus was disassembled, the membrane removed and used for the detection of the catalase polypeptide. To verify that equal amounts of sample were loaded, duplicate gels were included in the same experiment and the proteins stained with Coomassie blue following electrophoresis.

Detection of Catalase Polypeptide:

The catalase polypeptide was detected using the ProtoBlot western Blot AP System (Promega, Madison, WI). The membrane was blocked with 1% BSA (w/v) in TBST [(10mM Tris-HCl, pH 8.0, 150mM NaCl, 0.05% Tween 20 detergent, Sigma)] at 25°C for 30 minutes. The primary antibody used in these experiments was purchased from Biodesign Inc. It was a polyclonal anti-human erythrocyte catalase antibody raised in rabbit against the intact protein. This antibody was added to the membrane at a dilution of 1 in 400 in TBST and incubated at 25°C for 60 min, and subsequently washed three times with TBST. The membrane was incubated at 25°C for 30 min in the presence of a secondary antibody (goat anti-rabbit IgG conjugated to alkaline phosphatase in TBST). To detect the presence of the catalase polypeptide the blot was colour developed with NBT/BCIP.

Quantification of *Cas-1* polypeptide:

Quantification of the catalase specific protein band was done by scanning the blots using a Pharmacia laser densitometer (LKB UltraScan XL). The program was designed such that the densitometer scanned each band at three different positions. The values obtained are internally averaged and a mean value for each band is given. The peak heights of the signals were compared to 100 ng bovine liver catalase (Boehringer Mannheim Canada) as a control and data are presented as catalase polypeptide/mg protein.

2.7. RNA Analysis:

RNA Extraction:

Total RNA was extracted from liver, kidney and serum-free blood from different strains of mice using the guanidinium thiocyanate method of

Chomczynski and Sacchi (1987). Liver and kidney were weighed and immediately homogenized in a 1:10 (w/v) denaturing solution [4M guanidinium thiocyanate (BRL), 25mM sodium citrate pH 7.0 (BDH), 0.5% Sarkosyl (Sigma), 0.1M 2-mercaptoethanol] on ice. The volume of whole blood was measured and 1.5 volumes denaturing solution was added on ice. The RNA was extracted by adding 1/10th volume 2M sodium acetate (pH 4.0), an equal volume water-saturated phenol, 1/5 volume chloroform-isoamyl alcohol (49:1) and centrifuging at 10,000 x g for 20 min at 4°C in an SS 34 rotor (Sorvall). The aqueous layer was transferred to another tube and the RNA was precipitated with an equal volume of isopropanol overnight at -20°C. The RNA was pelleted at 10,000 x g for 20 min at 4°C (Sorvall SS 34 rotor), and dissolved in 0.3 ml of cold denaturing solution, and precipitated with an equal volume of isopropanol at -20°C for 1 hr. The RNA was recovered by centrifugation at 10,000 x g at 4°C for 10 min, air dried, and redissolved in DEPC-treated H_2O (5C - 500 µl). RNA was heated at 65°C for 5 min and microfuged at room temperature for 5 min. The supernatant was recovered and stored at -70°C until use. The concentration of RNA was evaluated by UV spectrophotometry using a Beckman DU 8 spectrophotometer at 260 nm.

RNA associated with polysomes was isolated using the microfractionation method of De Sousa *et al.* (1993) with minor modifications. Forty milligrams of kidney tissue from adult (3 to 6 months) C3H/HeAnl/*Cas-1*^{a} and C3H/HeAnl/*Cas-1*^{b}, were homogenized on ice in 1.25 ml of lysis buffer containing 1% NP-40, 0.4% sodium deoxycholate, 112 U/ml RNAsin (Promega, Madison, WI), 10 µg/ml cycloheximide in TSM/EGTA buffer [40mM Tris-HCl, 150mM NaCl, 20mM magnesium acetate, 10mM Ethylene glycol-bis [β-aminoethylether]-N,N,N'N'-tetraacetic acid (EGTA), 10mM dithiothreitol (DTT)]. The homogenate was centrifuged for 3 minutes at 24,000 rpm at 4°C, in a TLA-100 rotor of a Beckman tabletop ultracentrifuge, to pellet nuciei and mitochondria. The postmitochondrial supernatant was layered over 40% sucrose in TSM/EGTA and centrifuged in the same rotor for 40 min at 50,000 rpm at 4°C forming a polyribosomal pellet and a subribosomal supernatant.

The subribosomal supernatant was withdrawn and transferred to a microfuge tube. One tenth volume of sodium acetate (20 µl of 3M, pH 6.0) and 2.5 volumes of ethanol were added for precipitation overnight at -20°C. The subribosomal precipitate was recovered following microcentrifugation and dissolved in 40 µl solubilization buffer then 220 µl extraction buffer [4M

guanidinium thiocyanate (Gibco/ BRL), 25mM sodium citrate pH 7.0, containing 0.5% Sarkosyl and 100mM 2-mercaptoethanol; Chomczynski and Sacchi, 1987] were added. The polyribosomal pellet was dissolved in 40 µl solubilization buffer (10mM Tris-HCl, 1mM EDTA pH 8.0, 100 U/ml RNAsin, 10mM DTT), and 220 µl of extraction buffer were added and the sample stored overnight at -20°C. The RNA from the ribosomal and subribosomal fractions was purified by standard phenol/chloroform extraction followed by ethanol precipitation. The concentration of RNA was obtained using a DU 640 Spectrophotometer (Beckman). Purified RNA was stored at -70°C until use in the dot blot assay.

Gel Electrophoresis:

A 1.5% agarose gel was made up with 20mM MOPS (Sigma), 5mM sodium acetate, 1mM EDTA, pH 7.0 and 5% formaldehyde (v/v). Twenty-five micrograms of total cellular RNA was lyophilized and resuspended in 25 µl sample buffer (52.8% deionized formamide [BDH], 20.0mM MOPS [3-(N-morpholino) propanesulfonic acid], 5mM sodium acetate, 1mM EDTA pH 7.0, 16.9% formaldehyde, 7% deionized RNase-free H_2O, 7% glycerol [BRL], 0.56 (w/v) bromophenol blue [Sigma]). The samples were denatured at 65°C for 15 min and 1 µg of ethidium bromide (Sigma) was added, and the samples loaded on the gel (15 X 20 cm). RNA was separated electrophoretically in 20mM MOPS, 5mM sodium acetate, 1mM EDTA pH 7.0 at 30V for 12 to 18 hr. After electrophoresis, the gel was photographed using a 302 nm Spectroline transilluminator (model TR-302) with a Kodak Wratten #9 filter and Polaroid type 665 PN film.

Northern Transfer:

The gels were prepared for transfer by soaking in 0.05M NaOH, 1 X SSC (0.15M NaCl, 0.015M sodium citrate pH 7.2) for 15 min followed by two 10 min soaks in 10 X SSC at room temperature. The gels were placed upside-down on a sheet of Whatman 3MM paper covering a polyurethane sponge. Biotrace RP nylon membrane (Gelman Sciences, Ann Arbor, Michigan) cut the same size as the gel, wetted with distilled H_2O and soaked in 10 X SSC for 5 min, was placed on top of the gel. Plastic wrap was placed around the edges of the membrane to ensure an even transfer. Three pieces of 3MM Whatman paper and 10 cm of paper towels cut to size were weighted on top. RNA was transferred using 10 X SSC buffer for ~ 6 hr with frequent changes of paper towels. The apparatus was disassembled, then the membrane was removed and baked at 80°C for 2 hr in a vacuum oven.

RNA Dot Blotting:

Total RNA (17 µg) and polysomal RNA (9 µg) was lyophilized and resuspended in 85 µl of 0.25mM EDTA/0.1% SDS. An equivalent volume of non-polysomal RNA to that of 9 µg of polysomal RNA was also lyophilized and resuspended in 85 µl 0.25mM EDTA/0.1% SDS. An equal volume of 3:2 of 20 X SSC (3M NaCl, 0.4M sodium citrate pH 7.2): 37% formaldehyde was added to the samples for denaturation and incubated 15 min at 65°C, followed by quenching on ice. The samples for total RNA were diluted in 10 X SSC to 20 µg/ml, 10 µg/ml, and 2 µg/ml. The samples for polysomal RNA were diluted in 10 X SSC to 10 µg/ml, 4 µg/ml, 2 µg/ml or 0.2 µg/ml. Five hundred microliters of each sample dilution (10, 5, 1, or 0.1 µg total RNA; 5, 2 and 1 µg polysomal RNA) was applied to Biotrace RP membrane (Gelman Sciences, Ann Arbor, Michigan) prewetted with 10 X SSC in a dot blot apparatus (Bio Rad). The samples were vacuumed through the wells and rinsed with 200 µl 10 X SSC. The apparatus was disassembled and the membrane air dried and baked at 80°C for 2 hr.

Probe Labelling and Hybridization:

The cDNA probe for the mouse catalase gene pMCT-1 (Figure 3A) was digested with *Bam* HI, run on a 0.8% low melting point agarose gel in 1 X TAE (40mM Tris-acetate, 1mM EDTA, pH 7.2) and the 1.8 kb band excised. The agarose containing the gel fragment was melted at 70°C for 20 min and diluted with three volumes sterile H_2O. DNA from this solution (1.0 µg) was labelled with α-^{32}P dCTP (3000 Ci/mmol; ICN Biochemicals) using BRL random prime labelling kit to a specific activity of 1.0 x 10^8 cpm/µg to 1.0 x 10^9 cpm/µg. A cDNA probe for 18S rRNA was obtained from Dr. C. Naus, University of Western Ontario, and served as a control. This cDNA (50 ng) was nick translated according to the manufacturer's directions (BRL) using α-^{32}P dCTP (3000 Ci/mmol; ICN Biochemicals) to a specific activity of 2.0 x 10^7 cpm/µg to 7 x 10^7 cpm/µg.

Membranes from both Northern blots and RNA dot blots were prehybridized in 14 ml of 4.7 X SSPE (0.7M NaCl, 50mM $NaH_2PO_4.H_2O$, 5mM EDTA), 4.7 X Denhardt's (0.5% polyvinylpyrrolidone, 0.5% bovine serum albumin, 0.5% Ficoll; Denhardt, 1966), 0.1% SDS, 2.8 mg denatured herring sperm DNA, 10% dextran sulphate, 0.35% Blotto (skim milk powder) and 50% formamide) for 1 to 1.5 hr at 42°C. The radiolabelled cDNA probe, pMCT-1, was denatured by boiling for 10 min, quenched on ice 5 min, added to the prehybridized blots and incubated at 42°C for 24 hr. The hybridization solution

was removed and the blots were subsequently washed twice with 2 X SSC/0.5% SDS for 15 min each at 37°C with constant agitation followed by a final wash at 37°C in 0.2 X SSC/0.5% SDS for 15 min. Membranes were covered in plastic wrap, exposed to Kodak X-Omat RP film with intensifying screens at -70°C for 1 to 4 days. The membranes were subsequently stripped by immersing in boiling 0.1 X SSC/0.5% SDS for 10 min with constant agitation, and rehybridized with the radiolabelled probe for 18S rRNA.

Quantification of *Cas-1* mRNA:

Cas-1-specific mRNAs were quantified from autoradiograms of total RNA dot blots hybridized with the 1.8 kb cDNA catalase probe (pMCT-1) by laser densitometry (LKB UltraScan XL). Catalase-specific mRNA values obtained from densitometer readings per autoradiogram were standardized using its corresponding 18S rRNA values from the same blot. Three animals per strain were evaluated for each tissue (liver, kidney and blood) with three replications. This experimental design generated comparable estimates for catalase mRNA relative to 18S rRNA in different tissues of mice.

2.8. *In situ* Hybridization:

Tissue Collection, Fixation and Sectioning:

Female Swiss Webster (SW) mice, 11 weeks of age were superovulated by intraperitoneal (i.p.) injection of 5 units of pregnant mare's serum gonadotropin (PMSG; Sigma), followed by 5 U human chorionic gonadotropin (HCG; Sigma) 48 hr later. Each female was placed with a mature SW male overnight. The presence of a copulatory plug the following morning indicated successful mating (day 1 gestation). Pregnant females were sacrificed to collect fetuses representing days 13 and 18 *post conceptus*. Fetuses were dissected out in Sorenson's buffer pH 7.0 and immersion-fixed in buffered 4% paraformaldehyde overnight at 4°C. Adult liver was removed and cut into 2 cm cubes and immersion-fixed as well. The tissues were subsequently processed the following day on a 16 hour cycle on a Histomatic Tissue Processor (Fisher, Model 166), and embedded in paraffin. Adult liver and sagittal sections of fetuses were cut at 6 μm on a microtome and collected on gelatinized and poly-L lysine (Sigma) coated microscope slides.

Hybridization Procedure:

In situ hybridization was performed using modifications from Simmons *et al.*, (1989). Deparaffinized slides were pretreated by sequential immersion in

0.2N HCl for 20 min, 2 X SSC (1 X SSC = 0.15M NaCl, 0.015M sodium citrate, pH 7.4) for 30 min, proteinase K (BMC), 25 µg/ml for 15 min at 37°C, acetic anhydride in 0.1M triethanolamine HCl buffer pH 8.0 for 10 min, rehydrated in graded alcohols and air dried.

The cDNA insert from pMCT-1 was excised with *Bam* HI and *Pst* I to remove the poly (A) tail and the resulting 550 bp insert was subcloned into the pGem-2 vector (Promega). The restriction map of the clone and the cloning strategy used in this study is shown in Figure 2B. Radiolabelled RNA probes were synthesized in the presence of ^{35}S-UTP (Amersham) using an RNA transcription kit (Promega). In this construct, T7 promoter-driven transcription yields antisense RNA which is complementary to catalase mRNA. On the other hand, the SP6 promoter-driven transcription yields sense mRNA to be used as a negative control. The labelled probes were size-reduced by limited alkaline hydrolysis (Cox *et al.*, 1984) and had specific activities of 1.9 to 2.9 x 10^9 cpm/µg.

The hybridization mixture contained 0.2 µg/ml ^{35}S-labelled RNA transcripts, 50mM dithiothreitol (DTT), 0.3M NaCl, 50% (v/v) deionized formamide, 10% (w/v) dextran sulphate, 0.2 mg/ml sheared herring sperm DNA, 0.125 mg/ml yeast tRNA, 0.02% (w/v) Ficoll, 0.02% (w/v) polyvinylpyrrolidone, 10mM Tris-HCl pH 7.4, 1mM EDTA, and 0.1% Triton X-100. The mixture was applied to pretreated slides, coverslipped, and incubated at 45°C for 4 hr. Following hybridization, the slides were washed twice in 4 X SSC with 5mM DTT for 10 min, once in 50 µg/ml RNase A (BMC) in 0.5M NaCl and 10mM Tris-HCl pH 8.0 for 30 min at 37°C, twice in 0.5M NaCl and 10mM Tris-HCl pH 8.0 for 15 min at 37°C, twice in 0.1 X SSC with 5mM DTT and 0.1% SDS for 10 min at 50°C, 2 X SSC for 10 min, dehydrated in graded alcohols each containing 0.3M ammonium acetate, and air dried. Slides were dipped in NTB-2 nuclear track emulsion (Eastman Kodak Company, Rochester, New York) diluted (1:1) with 0.6M ammonium acetate and exposed for 2 days at 4°C. The slides were subsequently developed in D19 (Eastman Kodak Company) for 5 min at 15°C, fixed with 30% sodium thiosulfate for 5 min and counterstained with Ehrlich's hematoxylin.

All microscopy for *in situ* hybridization analyses was performed using a Photomicroscope III (Zeiss, Inc). Photography with brightfield and darkfield microscopy was performed using Kodak 2415 film developed with HC 110 under high contrast conditions.

Slides were prepared from three fetuses at each of two developmental stages. They were evaluated for the general pattern of tissue morphology and silver grains on different cells and tissue types. Although there was a tissue-specific distribution for silver grains at both development stages, conclusions about the expression of the catalase gene could only be made following quantitative evaluation of such observations. Data were therefore collected on a representative slide for the adult liver, day 13 and day 18 fetuses by quantitating the cell density and number of silver grains.

Quantification of *Cas-1* mRNA:

Each slide was evaluated using brightfield microscopy for characterization of cell types, cellular structures and the number of cells in a defined area. Darkfield microscopy was used to count silver grains per defined area on the same slides. Different numbers of silver grains were observed on different areas of each slide following hybridization with the labelled sense and the antisense riboprobes. Grains were counted in defined areas with and without (blank) tissue on the same slide. It was apparent that the number of silver grains was significantly higher on the tissue-containing areas particularly with hybridization using the antisense probe. Silver grain counts on tissues were corrected for grains on a representative area of the same slide without tissue (blank). Five random areas were counted for the number of silver grains on day 13 and day 18 fetal tissues, while ten such numbers were generated for the adult liver. For each count of silver grains for an area, the number of cells in the same area was recorded using brightfield microscopy. It is therefore possible to express these observations as grains per cell for all experiments. The difference between grain counts generated by antisense and sense ^{35}S-labelled riboprobes was used to assess the expression of the catalase message in a tissue at a given stage of development.

2.9. *Hpa* II-PCR Analysis of 5' UTR:

Isolation of Genomic DNA:

Genomic DNA was isolated from liver, brain, kidney and blood from male Swiss Webster mice. Liver, kidney, and brain previously frozen at -70°C was ground to fine powder in liquid nitrogen and 5 volumes of extraction buffer (10mM Tris-HCl, 0.1M EDTA, 20 µg/ml RNase A, 0.5% SDS, pH 8.0) was added and inverted repeatedly until mixed. Pronase E (BMC) was added to a final concentration of 1 mg/ml and incubated on a rocker at 37°C overnight. Blood

samples previously frozen at -70°C were thawed on ice, and 2 volumes of Hanks Balanced Salt Solution (HBSS pH 7.5, Gibco/BRL) was added. This mixture was centrifuged at 3,000 rpm for 10 min at 15°C, and the wash procedure repeated twice more. The cell pellet was resuspended in 3 ml TNE_2 (10mM Tris-HCl pH 8.0, 10mM NaCl, 2mM EDTA), and 0.3% SDS was added to the cell mixture and incubated at 56°C for approximately 1 hr until all lumps disappeared. Proteinase K was added to a final concentration of 1 µg/ml and the sample incubated at 56°C overnight. Following overnight incubation to digest proteins, all DNA samples were extracted with an equal volume Tris-HCl saturated phenol pH 8.0, followed by extractions with an equal volume of phenol/chloroform/isoamyl alcohol (25:24:1), and chloroform/isoamyl alcohol (24:1). The DNA was precipitated with 1/10 volume 3M sodium acetate, pH 6.0, and 2.5 volumes 100% ethanol at -20°C for 30 min and recovered by centrifugation at 10,000 rpm in a Sorvall SS 34 rotor for 20 min at 4°C. The pellet was washed with 70% ethanol and resuspended in TE (10mM Tris-HCl, 1mM EDTA pH 8.0). DNA was assessed using a Beckman DU 8 spectrophotometer.

Amplification of *Cas-1* Promoter Region:

A region of *Cas-1* 5' upstream regulatory element was amplified from the genomic DNA of four tissues using the polymerase chain reaction (PCR). The primers used were developed based on sequences obtained in this study. Figure 21 shows the position and orientation of the primers (P1 and P2) in the genomic sequence which amplifies a fragment of 278 bp. They were synthesized using an Oligo 1000 DNA Synthesis System (Beckman). The synthesized primer DNA was cleaved with ammonium hydroxide, eluted from the column and deprotected according to the manufacturer's directions. DNA was precipitated by the addition of an equal volume of glacial acetic acid and 3 volumes 100% ethanol at -20°C for 1 hr. DNA was recovered by centrifugation at 12,000 x g at 4°C and the pellet washed with 100% ethanol, air dried and resuspended in sterile distilled H_2O. Primer concentration was determined using a DU 640 Spectrophotometer (Beckman).

Approximately 25 ng high molecular weight genomic DNA, either uncut, *Msp* I digested or *Hpa* II digested was used as a template in this reaction. Twenty picomoles of each primer (P1 (For): GTCCCAGCACCACCTTTCGCTC, P2 (Rev) CTGCGGAACGTGAGACAGCAGG) and 0.25mM dATP, 0.25mM dCTP, 0.25mM dGTP, 0.25mM dTTP, 1X reaction buffer (500mM KCl, 100mM Tris-HCl pH 8.8, 1% Triton X-100), 3mM $MgCl_2$, 20 pmol of each primer P3, P4

(control; Figure 8), and 2.5 units of Taq polymerase (Promega, Fisher Scientific) was added to the template. Samples were overlaid with 50 µl mineral oil prior to amplification. All reactions were denatured for 5 min at 95°C and then subjected to 30 cycles of PCR in a Perkin Elmer Cetus Thermal Cycler. Amplification conditions consisted of primer annealing at 65°C for 1 min, elongation at 72°C for 1 min and denaturation at 95°C for 1 min. The final amplification cycle was followed by a 30 min extension at 72°C and the samples stored at 4°C. Ten microliters of each reaction mixture was subjected to electrophoresis in an 8% polyacrylamide gel at 150V for 45 min, stained in ethidium bromide for 20 min and photographed as described in Section 2.7.

2.10. Sequence Comparison of 3' UTRs Among Strains:

Amplification of 3' UTR:

Genomic DNA from brain tissue of seven strains of mice (BALB/c, C3H/HeAnl/*Cas-1*^{a}, C3H/HeAnl/*Cas-1*^{b}, C57BL/6J, 129/ReJ, C3H/S, and Swiss Webster) and the acatalasemic recombinant inbred line SXC/sw-1 with well characterized catalase expression was isolated as described in section 2.9 and used as a template in the PCR amplification. The primers (P3 and P4) used in these experiments were based on the sequences obtained from this study (Figure 8). P3 and P4 were obtained from Vetrogen Corp., London and amplify a fragment of 328 bp from the 3' UTR of *Cas-1*. Approximately 1 µg of high molecular weight genomic DNA was used in the reaction as a template. Twenty pmol of each primer (P3: CTCCTATTACCTCATGGTCTGG, P4: GCATCAACATAATCCAAGTGGG) and 0.25mM dATP, 0.25mM dCTP, 0.25mM dGTP, 0.25mM dTTP, 1 X reaction buffer (500mM KCl, 100mM Tris-HCl, pH 8.8, 1% Triton X-100), 3mM $MgCl_2$ and 2.5 units of Taq DNA polymerase (Promega, Fisher Scientific) were added to the template DNA. The final reaction volume was made up to 50 µl with sterile distilled H_2O and sealed with 50 µl of mineral oil (Sigma, St. Louis, Missouri). Thermocycling was performed in a Perkin-Elmer Cetus Thermal Cycler under the following conditions. After an initial melt at 94°C for 7 min, 30 cycles of 94°C for 1 min, 60°C for 1 min, and 72°C for 1 min were performed. A 30 min extension period (72°C) followed the 30 cycles. The samples were stored at 4°C until further analysis.

SSCP Analysis:

To determine potential DNA sequence differences among the 3' UTR of *Cas-1* from the seven strains of mice, single strand conformation polymorphism

analysis (SSCP) were performed. Ten microliters of PCR amplified DNA fragment (described above) was added to 10 µl of loading dye (95% formamide, 20mM EDTA, 1% xylene cyanol, 1% bromophenol blue), and heated at 100°C for 10 min and quenched on ice 5 min. Samples were subjected to electrophoresis on an 8% non-denaturing mini polyacrylamide gel in 1 X TBE at 150V for approximately 1 hr at 4°C.

Subcloning of PCR Fragments:

PCR products generated from the eight mouse genotypes were subcloned into pBluescript vector DNA (Stratagene Inc.) for sequencing. The amplification products were purified by Tris-HCl-saturated phenol extraction followed by phenol/chloroform/isoamyl alcohol (25:24:1) and chloroform/isoamyl (24:1) extractions. The amplified DNA was precipitated by the addition of 1/10 volume 3M sodium acetate pH 6.0 and 2.5 volumes 100% ethanol and incubated at -20°C for 30 min. DNA was recovered by centrifugation at 12,000 x g for 25 min at 4°C, and resuspended in 43 µl sterile distilled H_2O. Amplification products were blunt ended using 10U T4 DNA polymerase (Promega) in 5.0 µl T4 DNA polymerase buffer (33mM Tris-acetate pH 7.9, 66mM potassium acetate, 10mM magnesium acetate, 0.5mM DTT, 0.1mg/ml bovine serum albumin) and 0.5mM dATP, 0.5mM dCTP, 0.5mM dGTP, 0.5mM dTTP. After incubating at 37°C for 30 min, the solution was brought up to 100 µl with sterile distilled H_2O and extracted once with an equal volume of Tris-HCl saturated phenol/chloroform/isoamyl alcohol and then once with chloroform/isoamyl alcohol. The DNA was precipitated at -20°C for 30 min in the presence of 1/10 volume of 3M sodium acetate pH 6.0 and 3 volumes 100% ethanol. The DNA was recovered by centrifugation in a Sorvall RC5C high speed centrifuge (DuPont) for 60 min, 12,000 x g at 4°C. The DNA pellet was washed with 80% ethanol, air dried, and dissolved in 10 µl of H_2O by incubating for 10 min at 37°C.

The DNA was phosphorylated by incubating with 10U of T4 polynucleotide kinase in a 20 µl reaction volume containing 1 X ligation buffer (50mM Tris-HCl pH 7.5, 7mM $MgCl_2$, 1mM DTT) and 1mM ATP at 37°C for 30 min. The enzyme was inactivated by incubating the mixture at 70°C for 30 min and the DNA purified by phenol, phenol/chloroform/isoamyl alcohol and chloroform/isoamyl alcohol extractions. The DNA was ethanol precipitated at -20°C for 30 min and the pellet was resuspended in 8 µl sterile distilled H_2O and stored at 4°C until used in cloning reaction.

DNA from the vector pBluescript was linearized with *Eco* RV to generate identical cohesive ends, which were dephosphorylated prior to ligation with 50U calf intestinal alkaline phosphatase (Pharmacia) in One-Phor-All Buffer Plus (10mM Tris-acetate pH 7.5, 10mM magnesium acetate, 50mM potassium acetate) at 37°C for 15 min followed by 55°C for 45 min. The enzyme was inactivated by the addition of 0.5% SDS, 5mM EDTA, 0.1 mg/ml proteinase K, and incubated at 56°C for 30 min. The vector DNA was purified by phenol/chloroform extractions and ethanol precipitated at -20°C for 30 min. The pellet was recovered by centrifugation at 12,000 x g at 4°C for 15 min and dissolved in 50 µl H_2O.

Ligations were performed according to Sambrook *et al.* (1989). The DNA was combined in a 1:1 (insert:vector) mass ratio with 6 Weiss U of bacteriophage T4 DNA ligase in 100mM Tris-HCl pH 7.6, 10mM $MgCl_2$, 20mM DTT, 1mM ATP and the ligation allowed to proceed overnight at 16°C. Following enzyme inactivation at 65°C for 30 min, the ligated DNA was used in the transformation procedure described by Davis *et al.* (1986).

Competent XL1-Blue cells were transformed by inoculating 200 µl of cells with 10 µl of ligation reaction. This mixture was placed on ice for 30 min, heat shocked at 42°C for 2 min, 1 ml of LB broth was added and the cells equilibrated at 37°C for 1 hr before plating. Transformed bacteria were plated on 50 µg/ml ampicillin LB agar plates (1% NaCl, 1% Bacto-Tryptone, 0.5% yeast extract) with Xgal (5-bromo-4-chloro-3-indoyl-β-D-galactoside, 20 µg/ml) and IPTG (Isopropylthio-β-D-galactoside, 0.1mM). After incubation for 18 to 24 hr, white colonies were picked and grown in 10 ml LB broth with 50 µg/ml ampicillin overnight at 37°C. DNA was isolated by the 'mini-prep' method described previously (section 2.3) and digested with the appropriate restriction enzymes. Electrophoresis on an agarose mini-gel was used to verify the presence of the desired insert in the plasmid. DNA from recombinant plasmids with an insert of the appropriate size was sequenced as described in section 2.3.

2.11. Gel Shift Assay for the Detection of mRNA-protein Complexes:

All reagents, solutions and buffers used for this assay were made up with DEPC-treated H_2O. Double distilled H_2O was rendered RNase free by treatment with 1% (w/v) diethylpyrocarbonate (DEPC; ICN) overnight at 22°C and subsequently autoclaved to eliminate all traces of DEPC. All glassware, including

the gel box, glass plates, beakers, flasks etc., were treated with DEPC-water, rinsed and/or autoclaved before use.

Development of mRNA Probes:

Seven cDNA fragments from *Cas-1* representing different regions of the 3' UTR were used in this study (see Figure 35). Unless specified, they were cloned in the pBluescript vector to generate ^{32}P-labelled mRNA in a transcription reaction. The fragments include the following: (1) a 1300 bp fragment consisting of approximately 180 carboxy terminal amino acids and the entire 3' UTR, including the poly (A) tail; (2) a 470 bp fragment consisting of the most 3' terminal sequences of the 3' UTR, including the poly (A) tail; (3) a 420 bp fragment containing the most 3' terminal region of the 3' UTR excluding the poly (A) tail; (4) a 190 bp fragment consisting mainly of the $(CA)_{31}$ near repeat; (5) a 134 bp fragment containing the $(CA)_{31}$ near repeat, cloned into the *Eco* RI site of pGem 3Z (Promega Corp.) to reduce vector sequences in the resulting transcripts; (6) a 43 bp fragment in pGem 3Z containing $(T)_{15}$; and (7) a 142 bp fragment in pGem 3Z containing $(TGTGC)_7$. All fragments were sequenced (Sequenase, USB) to confirm their orientation and assure identity. The rat liver catalase cDNA (Furuta *et al.*, 1986) was cloned into pGem 4Z (1130 bp fragment coding for 100 carboxy terminal amino acids and 830 bp of 3' non-coding region), kindly provided by Dr. Linda Clerch (Georgetown University, Washington, U.S.A.) and was used as a positive control in mRNA binding assays.

Template DNA was linearized with the appropriate enzyme, purified by ethanol precipitation and ^{32}P-labelled cRNA sense strands were synthesized with specific activity > 10^8 cpm/ µg using Promega's transcription protocol with T7 RNA polymerase and ^{32}P-CTP, 800 Ci/mmol (Amersham). The RNA was extracted with equal volumes of phenol/chloroform and chloroform, and precipitated overnight at -20°C with 1/10 volume sodium acetate, pH 5.5, and 2 volumes 100% ethanol. The labelled probe was pelleted by centrifugation at 12,000 x g for 30 min at 4°C, air dried, and dissolved in formamide loading buffer (80% formamide, 1mM EDTA, 0.1% bromophenol blue, 0.1% xylene cyanol). The sample was heated at 85°C for 2 min and loaded onto an 8% non-denaturing polyacrylamide gel. After electrophoresis in 1 X TBE (89mM Tris-borate, pH 8.0, 2mM EDTA), the gel was exposed to X-ray film (XRP-1) for 45 sec, and the film developed. The film with the detected band was realigned with the gel, the band excised, crushed with a spatula and the radiolabelled cRNA eluted at 37°C for 3 hr in 0.5M ammonium acetate, 1mM EDTA. The eluate was placed in a new

microfuge tube and precipitated overnight in 100% ethanol at -20°C followed by centrifugation at 12,000 x g for 30 min at 4°C, and air dried. The pellet was subsequently resuspended in water to ~1 x 10^4 cpm/ µl and stored at -20°C until used in the binding assay.

Unlabelled cRNA transcripts were also prepared using Promega's protocol for the synthesis of large amounts of RNA (Promega, 1991). Following the transcription reaction, 50U RNase free DNase I (Pharmacia) was added and incubated at 37°C for 30 min. The unlabelled cRNA transcripts were purified by phenol/chloroform, chloroform extracted, precipitated with ethanol at -20°C and dissolved in RNase-free water. The concentration of the unlabelled probe was estimated based on spectrophotometric absorbance at 260 nm using a Beckman DU 640 spectrophotometer.

Collection of Tissue Homogenates:

Mice from the Swiss Webster, 129/ReJ, C57BL/6J, C3H/HeAnl/*Cas-1^a* and C3H/HeAnl/*Cas-1^b* strains were sacrificed and immediately perfused with phosphate buffered saline (PBS) pH 7.4. Cellular extracts were obtained from excised liver, kidney and lung by homogenizing the organ (0.5ml homogenization buffer / 0.1 g organ) on ice in buffer containing 25mM Tris-HCl pH 7.0, 0.1mM EDTA, 1% Triton X-100, 40mM KCl, 0.1mM Phenylmethylsulfonylfluoride (PMSF; BMC), 10 µg/ml leupeptin (BMC). The homogenate was centrifuged at 12,000 x g for 10 min at 4°C. The supernatant was recovered, the protein concentration determined (Bradford, 1976), and aliquots stored at -70°C until use in the mRNA binding assay. Whole blood was extracted by cardiac puncture with a 21G needle and 1 ml syringe pretreated with EDTA to prevent clotting. Red blood cells were pelleted in a microfuge for 5 min at 12,000 x g and the plasma removed. The resulting RBC pellets were immediately frozen at -70°C until needed. Prior to use in the mRNA-binding assay, the protein concentration was determined using the Bradford assay (1976).

Polysomes were isolated following the procedure of Clemens (1983) using RNase-free glassware and solutions. Liver (1 g) was excised and homogenized on ice in 3 volumes cold polysome buffer (0.25M sucrose, 0.1M KCl, 5mM magnesium acetate, 6mM 2-mercaptoethanol, 20mM Tris-HCl, pH 7.4). Cellular debris, plasma membranes and mitochondria were removed by centrifugation at 10,000 x g for 10 min at 4°C. The supernatant was retained, and Triton X-100 was added to final concentration of 1% (v/v). This mixture was layered over an equal volume of polysome buffer containing 1.0M sucrose in 13.2 ml polyallomer

centrifuge tubes (Beckman) and centrifuged in an SW 41 rotor for 2.5 hr at 222,000 x g (36,000 rpm) at 4°C in an L8-70M Beckman Ultracentrifuge. The supernatant was removed and the polysome pellet was resuspended in polysome buffer lacking sucrose and stored at -70°C. The protein concentration was determined using the method of Bradford (1976) prior to use.

mRNA-binding, Electrophoresis, and Fluorography:

Tissue extracts (50 µg protein) were incubated with 10^4 cpm of ^{32}P-labelled cRNA in 15 µl of buffer containing 5% glycerol, 40mM KCl, 3mM $MgCl_2$, and 10mM HEPES (Sigma), pH 7.6 for 30 min at 22°C. The incubation reaction was subsequently treated with 2U RNase T1 (BRL) for 15 min at 22°C followed by 6 µg/ml heparin (Sigma) for 15 min at 22°C. One unit of RNase T1 hydrolyzes 1 A_{260} unit of yeast RNA to acid-soluble material in 15 min at 37°C (BRL specification). RNase T1 hydrolyzes the region of the RNA probe not protected by bound protein while heparin destabilizes any non-specific interactions involving the RNA and protein. The negative control contained no tissue homogenate and was otherwise subjected to the same treatment. Competition experiments were used to demonstrate the sequence specificity of an observed mRNA-protein complex, when present. This involves competition with unlabelled cRNA specific to the sequence under study (same fragment) or non-specific competition involving unlabelled yeast tRNA (BMC). To determine if the complexes that bound to the target RNA were protein(s), extracts in the buffer were preincubated with an excess (50 µg/ml) of proteinase K (BMC) for 10 min at 22°C, followed by the incubation with cRNA.

Incubation mixtures representing the appropriate combination of experimental conditions were subjected to electrophoresis on a low cross-linking, 4% polyacrylamide gel (acrylamide:bis-acrylamide 60:1) containing 89mM Tris-borate (pH 8.0) and 2mM EDTA. Electrophoresis was carried out using a Vertical 15.17 Gel Electrophoresis System (BRL) with 1.5 mm spacers at 100 V for 3 hr (~10 cm) at room temperature (22°C). The gel was transferred onto filter paper, dried and exposed to X-ray film (Kodak XRP-1) at -70°C for 1 or 2 days with an intensifying screen.

Characterization of Proteins:

Radiolabelled RNA was incubated with protein extracts (liver, kidney, lung and blood) as previously described. Immediately following this incubation, the microcentrifuge tubes were uncapped and placed on ice 5 cm below the light source in a UV Stratalinker 1800 (Stratagene) and exposed to UV light at 254 nm

delivering 780 mJ/cm^2. RNase A was added to a final concentration of 1 µg/µl and incubated at 37°C for 20 min. Heparin (6 µg/ml) and 10 µl sample buffer (0.125M Tris-HCl, 20% glycerol, 2% SDS, 2% 2-mercaptoethanol, 1% bromophenol blue) was added, then the reaction mixtures were boiled 5 min and quenched on ice. The samples were separated by electrophoresis in a 10% SDS polyacrylamide gel at 150V for approximately 45 min. The apparatus was dismantled, the gel transferred to filter paper, dried on a Bio Rad Model 443 dryer and exposed to X-ray film (Kodak XRP-1) at -70°C for 3 to 8 days with an intensifying screen. The sizes of the UV cross-linked proteins were determined using low range and broad range SDS-PAGE protein markers (Bio Rad), which were included as standards for each electrophoretic run.

2.12. Statistical Analyses:

Quantitative data generated for grain counts from *in situ* hybridization, catalase enzyme activity, mRNA using dot blots and polypeptide using western blots from different tissues and genotypes were statistically evaluated. The statistical assessment included the use of means, variances, standard error of the means and analysis of variance. The Student's t-test was used to evaluate significant differences between all pairwise comparisons. Regression and correlation analyses were executed using the computer program Cricket Graph (Cricket Software, Malvern PA). Sliding base composition and homology matrix analyses were done using the DNA Inspector program (Textco Inc.)

CHAPTER 3

RESULTS

A: ORGANIZATION OF THE CATALASE GENE IN MICE:

3.1. Complete cDNA Sequence of *Cas-1*:

Catalase is encoded by a single gene in the mouse called *Cas-1* (Holmes and Duley, 1975; Bailley, unpublished) and is localized to chromosome 2 approximately 48 cM from the centromere (Maltais *et al.*, 1994). To generate the complete sequence of the cDNA of *Cas-1*, several clones were used. The cDNA insert from pMCT-1 was sequenced in both directions which generated the partial sequence (1050 bp) of the coding region and the 3' UTR. Additional sequence analysis of 534 bp was provided by Dr. Korneluk and completed the sequence of the coding region of *Cas-1* . The genomic clone pB 4.6 was used to sequence the first exon and the 5' upstream genomic region of *Cas-1*. Figure 4B shows the partial restriction map of the most 5' region of pB 4.6 and includes the sites used to subclone 4 non-overlapping fragments. A *Pst* I/ *Pvu* II fragment of ~310 bp was used to sequence exon 1 and establish the position of the first intron. An *Xba* I/*Pst* I fragment (~170 bp) was sequenced to reveal the 5' UTR upstream of the translation start site. An *Acc* I/*Xba*I fragment (~260 bp) and a *Bam* HI/ *Acc* I fragment (~210 bp) completed the sequence of 659 bp of the 5' upstream region.

The first complete cDNA sequence of *Cas-1* from the BALB/c mouse strain encompassing the coding region plus the 5' and 3' untranslated regions (UTR) is shown in Figure 5. It has been submitted to Genbank with the accession number L 25069. The 5' untranslated region of the gene is 87 nucleotides in length and has a G + C content of 62%. The coding sequence is 1,584 bp encoding 528 amino acids. The positions of the introns which divide the gene into 11 exons are indicated based on the organization of the human gene (Quan *et al.*, 1986). The position of the first intron was confirmed by sequencing the mouse genomic clone pB 4.6 and is also indicated in Figure 5. The 3' noncoding region of this mouse cDNA contains 752 bp and has an G + C content of 39.9% (18.3% - guanine, 21.6% - cytosine). A consensus polyadenylation signal AATAAA is located 14 residues upstream of the poly (A) tract. The length of the complete cDNA is 2423 bp and the sliding base composition analysis for the entire gene is shown in

Figure 5. The complete nucleotide cDNA sequence for BALB/c *Cas-1* with predicted amino acids. The 5' and 3' untranslated regions and the positions of the putative introns (*) based on the human sequence (Quan *et al.*, 1986) are included. The position of the first intron is confirmed from the sequence analysis of pB 4.6 (✠). The consensus polyadenylation signal is underlined. Genbank Accession Number: L 25069.

```
ATTGCCTTCTCCGGGTGGAGACCAGACCGCTGCGTCCGTCCCTGCTGTCTCACGTTCCGCAGCTCTGCAGCTCCGCAATCCTACACCATGTCGGAC
                                                                                                M  S  D

AGTCGC GACCCAGCCAGCGACCAGATGAAGCAGTGGAAGGAGCAGCGGGGCCTCGCAGAGACCTGATGTCCTGACCACCGGAGGCGGGAACCCAATA
 4   R  D  P  A  S  D  Q  M  K  Q  W  K  E  Q  R  A  S  Q  R  P  D  V  L  T  T  G  G  G  N  P  I

GGAGATAAACTTAATATCATGACCGCGGGGTCCCGAGGGCCCCTCCTCGTTCAGGATGTGGTTTTCACTGACGAGATGGCACACTTTGACAGAGAG
36  G  D  K  L  N  I  M  T  A  G  S  R  G  P  L  L  V  Q  D  V  V  F  T  D  E  M  A  H  F  D  R  E

CGGATTCCTGAGAGAGTGGTACACGCAAAAGGAGCAGGTGCTTTTGGATACTTTGAGGTCACCCACGATATCACCAGATACTCCAAGGGAAAGGTG
68  R  I  P  E  R  V  V  H  A  K  G  A  G  A  F  G  Y  F  E  V  T  H  D  I  T  R  Y  S  K  G  K  V

TTTGAGCATATTGGAAAGAGGACCCCTATTGCCGTTCGGTTCTCCACAGTCGCTGGAGAGTCAGGCTCAGCTGACACAGTTCGTGACCCTCGGGGG
100  F  E  H  I  G  K  R  T  P  I  A  V  R  F  S  T  V  A  G  E  S  G  S  A  D  T  V  R  D  P  R  G

TTTGCAGTGAAATTTTACACTGAAGATGGTAACTGGGATCTTGTGGGAAACAACACCCCTATTTTCTTCATCAGGGATGCCATATTGTTTCCATCC
132  F  A  V  K  F  Y  T  E  D  G  N  W  D  L  V  G  N  N  T  P  I  F  F  I  R  D  A  I  L  F  P  S

TTTATCCATAGCCAGAAGAGAAACCCACAGACTCACCTGAAGGATCCTGACATGGTCTGGGACTTCTGGAGTCTTCGTCCCGAGTCTCTCCATCAG
164  F  I  H  S  Q  K  R  N  P  Q  T  H  L  K  D  P  D  M  V  W  D  F  W  S  L  R  P  E  S  L  H  Q

GTTTCTTTCTTGTTCAGTGACCGAGGGATTCCCGATGGTCACCGGCACATGAATGGCTATGGATCACACACCTTCAAGTTGGTTAATGCAGATGGA
196  V  S  F  L  F  S  D  R  G  I  P  D  G  H  R  H  M  N  G  Y  G  S  H  T  F  K  L  V  N  A  D  G

GAGGCAGTCTATTGCAAGTTCCATTACAAGACCGACCAGGGCATCAAAAACTTGCCTGTTGGAGAGGCAGGAAGGCTTGCTCAGGAAGATCCGGAT
228  E  A  V  Y  C  K  F  H  Y  K  T  D  Q  G  I  K  N  L  P  V  G  E  A  G  R  L  A  Q  E  D  P  D

TATGGCCTCCGAGATCTTTTCAATGCCATCGCCAATGGCAATTACCCGTCCTGGACGTTTTACATCCAGGTCATGACTTTTAAGGAGGCAGAAACT
260  Y  G  L  R  D  L  F  N  A  I  A  N  G  N  Y  P  S  W  T  F  Y  I  Q  V  M  T  F  K  E  A  E  T

TTCCCATTTAATCCATTTGATCTGACCAAGGTTTGGCCTCACAAGGACTACCCTCTTATACCAGTTGGCAAAGTGGTTTTAAACAAAAATCCAGTT
292  F  P  F  N  P  F  D  L  T  K  V  W  P  H  K  D  Y  P  L  I  P  V  G  K  V  V  L  N  K  N  P  V

AATTACTTTGCTGAAGTTGAACAGATGGCTTTTGACCCAAGCAATATGCCCCCTGGCATCGAGCCCAGCCCTGACAAAAAGCTTCAGGGCCGCCTT
324  N  Y  F  A  E  V  F  Q  M  A  F  D  P  S  N  M  P  P  G  I  E  P  S  P  D  K  K  L  Q  G  R  L

TTTGCCTACCCGGACACTCACCGCCACCGCCTGGGACCCAACTATCTGCAGATACCTGTGAACTTTCCCTACCGCGCTCGAGTGGCCAACTACCAG
356  F  A  Y  P  D  T  H  R  H  R  L  G  P  N  Y  L  Q  I  P  V  N  C  P  Y  R  A  R  V  A  N  Y  Q

CGTGATGGCCCCATGTGCATGCATGACAACCAGGGTGGTGCCCCCAACTATTACCCCAACAGCTTCAGCGCACCAGAGCAGCAGCGCTCAGCCCTG
388  R  D  G  P  M  C  M  H  D  N  Q  G  G  A  P  N  Y  Y  P  N  S  F  S  A  P  E  Q  Q  R  S  A  L

GAGCACAGCGTCCAGTGCGCTGTAGATGTGAAACGCTTCAACAGTGCTAATGAAGACAATGTCACTCAGGTGCGGACATTCTACACAAAGGTGTTG
420  E  H  S  V  Q  C  A  V  D  V  K  R  F  N  S  A  N  E  D  N  V  T  Q  V  R  T  F  Y  T  K  V  L

AATGAGGAGGAGAGGAAACGCCTGTGTGAGAACATTGCCGGCCACCTGAAGGACGCTCAGCTTTTCATTCAGAAGAAAGCGGTCAAGAATTTCACT
452  N  E  E  E  R  K  R  L  C  E  N  I  A  G  H  L  K  D  A  Q  L  F  I  Q  K  K  A  V  K  N  F  T

GACGTCCACCCTGACTATGGGGCCCGCATCCAGGCTCTTCTGGACAAGTACAACGCTGAGAAGCCTAAGAACGCAATTCACACCTACACGCAGGCC
484  D  V  H  P  D  Y  G  A  R  I  Q  A  L  L  D  K  Y  N  A  E  K  P  K  N  A  I  H  T  Y  T  Q  A

GGCTCTCACATGGCTGCGAAGGGAAAAGCTAACCTGTAACTCCGGTGCTCAGCCTCCGCTGAGGAGACCTCTCGTGAAGCCGAGCCTGAGGATCAC
516  G  S  H  M  A  A  K  G  K  A  N  L  End
CTGTAATCAACGCTCGATGGATTCTCCCCCGCCGGAGCGCAGACTCACGCTGATGACTTTAAAACGATAATCCGGGCTTCTAGAGTGAATGATAAC
CATGCTTTTGATGCCGTTTCCTGAAGGGAAATGAAAGGTTAGGGCTTAGCAATCATTTAACAGAAACATGGATCTAATAGGACTTCTGTTTGGATT
ATTCATTTAAATGACTACATTTAAAATGATTACAAGAAAGGTGTTCTAGCCAGAAACATGACTTGATTAGACAAGATAAAAATCTTGGCGAGAATA
GTGTATTCTCCTATTACCTCATGGTCTGGTATATATACAATACAACACACATACCACACACACACACACATGCAATACACACACTACACACACATA
CACACACTCACACACACTCATACACACACATGAAGAGATGATAAAGATGGCCCACTCAGAATTTTTTTTTTATTTTTCTAAGGTCCTTATAAGCAA
AACCATACTTGCATCATGTCTTCCAAAAGTAACTTTAGCACTGTTGAAACTTAATGTTTATTCCTGTGCTGTGCGGTGCTGTGCTGTGCTGTGCTG
TGCAGCTAATCAGATTCTTGTTTTTTCCCACTTGGATTATGTTGATGCTAATACGCAGTGATTTCACATAGGATGATTTGTACTTGCTTACATTTT
TACAATAAAATGATCTACATGG
```

Figure 6. In general, this cDNA has 49% G + C, with A, T, G and C represented in approximately equal proportions. There are apparent high and low G + C regions along the length of the coding sequence. Further, the high G + C content in the 5' UTR and the high A + T content of the 3' UTR is also evident from this figure.

To identify putative regulatory elements associated with *Cas-1*, approximately 660 bp of the 5' upstream genomic region of BALB/c were evaluated (Figure 7). The sequence features of this region include the following: 47% G + C, at least one GC box and two potential CCAAT boxes. No TATA box is evident in this sequence. Although there is very little sequence similarity between the 5' upstream region of the human and mouse catalase genes, this region of the human gene (CAT) also lacks a TATA box. The human sequence also contains a third CCAAT box (Quan *et al.*, 1986) not found in *Cas-1*. Further analysis of the *Cas-1* sequence shows that the region containing approximately 300 bp upstream of the translation initiation site is 65% G+C, representative of a CpG island.

The 3' UTR of BALB/c *Cas-1* is 752 bp, and sequence analysis of this region reveals three unusual near repeats: $(CA)_{31}$, $(T)_{15}$ and $(TGTGC)_7$. Figure 8 shows the sequence of the 3' UTR from BALB/c and the three regions of interest are indicated. This sequence has been submitted to Genbank with the accession number L 25070.

Figure 9 shows the complete cDNA and amino acid sequence of *Cas-1* compared to and aligned with other mammalian catalases reported to date (rat, human and bovine). No gaps or rearrangements were needed to align the sequences, except for bovine catalase which is 20 amino acids shorter at the carboxy terminus compared to other mammalian catalases. All other differences are accounted for by substitutions. There is an amino acid identity of 94.5%, 91.2% and 89.0% between mouse and rat, bovine, and human catalase respectively. A homology matrix analysis was used to evaluate identities among the mammalian catalases at the level of DNA sequence. Figure 10 shows dot matrix analyses of the coding region (1584 nt), the 3' (752 nt) and 5' (87 nt) UTRs involving pairwise comparisons of the mouse (BALB/c) sequence with rat and human. A relatively high degree of sequence identity in the coding region is observed between mouse and rat (93.8%; Figure 10A), mouse and human (85.8%; Figure 10B) and rat and human (85.2%; Figure 10C).

Pairwise comparison of the catalase 3' UTR from the three species also

Figure 6. Sliding G + C composition of the complete mouse *Cas-1* cDNA. (Analysis length = 30, offset = 5). Translation start and stop sites are indicated by arrows.

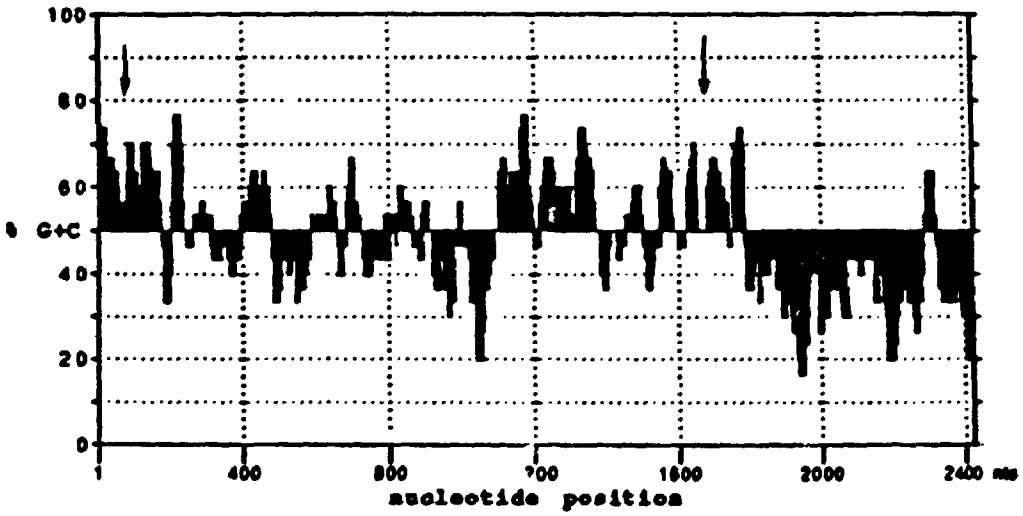
100
80
60
% G+C
40
20
0
1
400
800
700
1600
2000
2400 nts
nucleotide position

Figure 7. Genomic sequence of the 5' upstream region of *Cas-1* (659 nt). The transcribed segment is consistent with the rat (Furuta *et al.*, 1986), and human (Quan *et al.*, 1986) and is identified by capital letters, along with the first codon. The putative CCAAT and GC boxes are underlined. Genbank Accession Number: L 25070.

```
       gatccccct ctccccacaa acaaagagct tttcagtatt
      cttccgggga gaaaatggag gagcctgtca ctgcagtcaa
      tccaggccac tttggcacag tggaccaagt cacaagtcgg
      atttctacag atttcacaga ggaggagatc cgcaccgatc
-500  tgaagtaaga ttaaacactt tctgagtgtt tttacagtaa
      attattggta tacagcttgg taaatgataa tgagtgagaa
      aggaagaaaa aaaccaccca caaattagta gcaaacaaag
      taagcaaagt gagaaacttt gcacagagga attggaccct
      gagctgtgac tctcagaggt cagagaacac cagcagggtc
-300  ccagcaccac ctttcgctcc ccacccgtct ccccagtctc
      ttcctatccg gggggtccac ctccgggagc ccccacttct
      cgccccaccc tccttccaat cccgtccttt ctagagttcc
      agtggccaat caggaggcgg ccgtcccaag ggtggggggc
      ggtgctgatt ggtggagcct gaagtcacca ctccagcggg
-100  cctggccaac aagATTGCCT TCTCCGGGTG GAGACCAGAC

      CGCTGCGTCC GTCCCTGCTG TCTCACGTTC CGCAGCTCTG

      CAGCTCCGCA ATCCTACACC.ATG
```

Figure 8. DNA sequence of the 3' UTR of the BALB/c *Cas-1*. Three unusual near repeats of this region are marked [$(CA)_{31}$ - dotted underline, $(T)_{15}$ - boxed and $(TGTGC)_7$ - solid underline]. Oligonucleotide primers (P3 and P4) used to PCR amplify the 3' UTR from other strains and genotypes are indicated by arrows .

follows a similar pattern. Interestingly, there are repeated sequences midway through the 3' UTR of mouse, which show striking identity to such sequences in a similar region of rat (Figure 10D). These repeats include a number of CAs present in both rat and mouse 3' UTRs. On the other hand, such comparisons of the 3' UTRs between mouse and human (Figure 10E) or rat and human (Figure 10F), show very little identity and are localized to a few dispersed small fragments only. It should be pointed out that the sequence of the 3' UTR of human catalase has no CA repeats. To date this repeat is specific only to the rodent catalase sequence.

The length of 5' UTR sequence among the three mammalian species is variable; the human has 68 nucleotides, rat 83 nucleotides and mouse 87 nucleotides. A dot matrix homology plot between mouse and rat for this region shows a relatively high degree of identity (87.3%; Figure 10G), while such plots between mouse and human (60.9%; Figure 10H) or rat and human (51.7%; Figure 10I) show less sequence identity under identical conditions. This observation may suggest a species-specific 5' regulatory sequence divergence for this housekeeping gene.

A detailed DNA sequence comparison of the 5' UTRs from the three mammalian species is shown in the multiple sequence alignment in Figure 11. It allows the identification of conserved regulatory features. Three short regions which are identical among the three species are indicated (some not picked up in homology matrix under the conditions used). Two (TGCCT and GGGTGGAGACC) are located at the 5' end and one (GTTCCGCA) is more 3'. These sequences were searched through Keybank of Consensus Sequences (Genbank) in order to assess their possible regulatory significance. Several consensus sequences were identified and may be important. It has been shown that TGCCT is a site for topoisomerase I which is known to play a role in strand exchange in the recombinational process (Been *et al.*, 1984). The sequence GGGTGG could function to regulate expression of this gene since it has been described as a viral enhancer (Martin *et al.*, 1985; Jalinot and Kedinger, 1986) and functions as an enhancer in the histocompatibility gene of mouse (Kimura *et al.*, 1986). Conservation of these sequences with known regulatory functions among the three mammalian species may suggest the regulatory role of the 5' UTR sequence in the expression of *Cas-1*. No consensus sequences were identified from Genbank which were similar to GTTCCGCA. However, a single nucleotide difference in this sequence observed in the 5' UTR of rat and human

Figure 9. A comparison involving the BALB/c *Cas-1* coding region sequence and its deduced amino acid sequence (Mus) with the nucleotide (bottom) and amino acid sequence (top) of rat (Rat; Furuta *et al.*, 1986) and human (Hum; Quan *et al.*, 1986). The nucleotide sequence of bovine catalase is not available; however the amino acid sequence (Bov; Schroeder *et al.*, 1982) is included for comparison. Dashes represent identical nucleotides or amino acids relative to the 'ATG' translation start site.

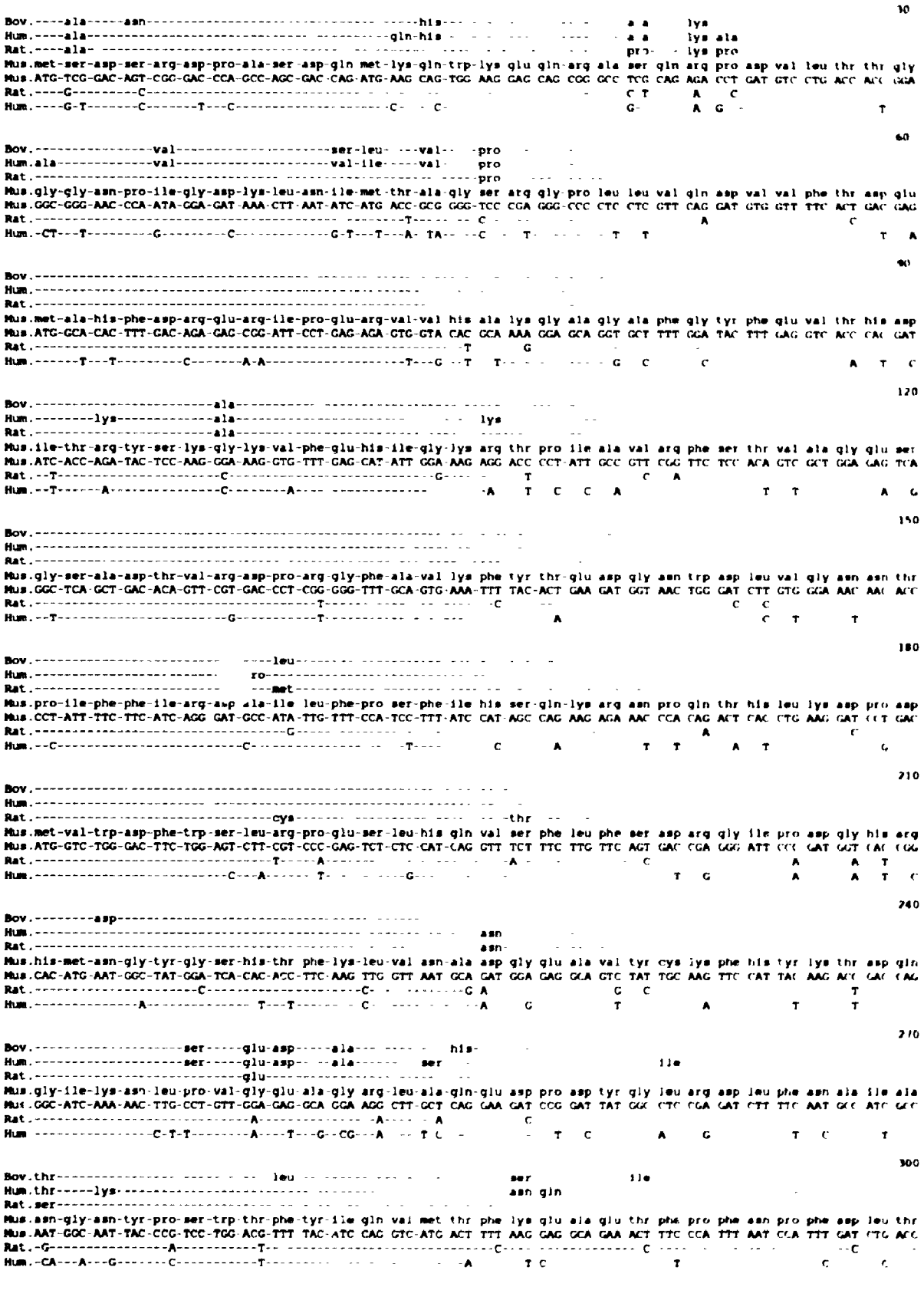

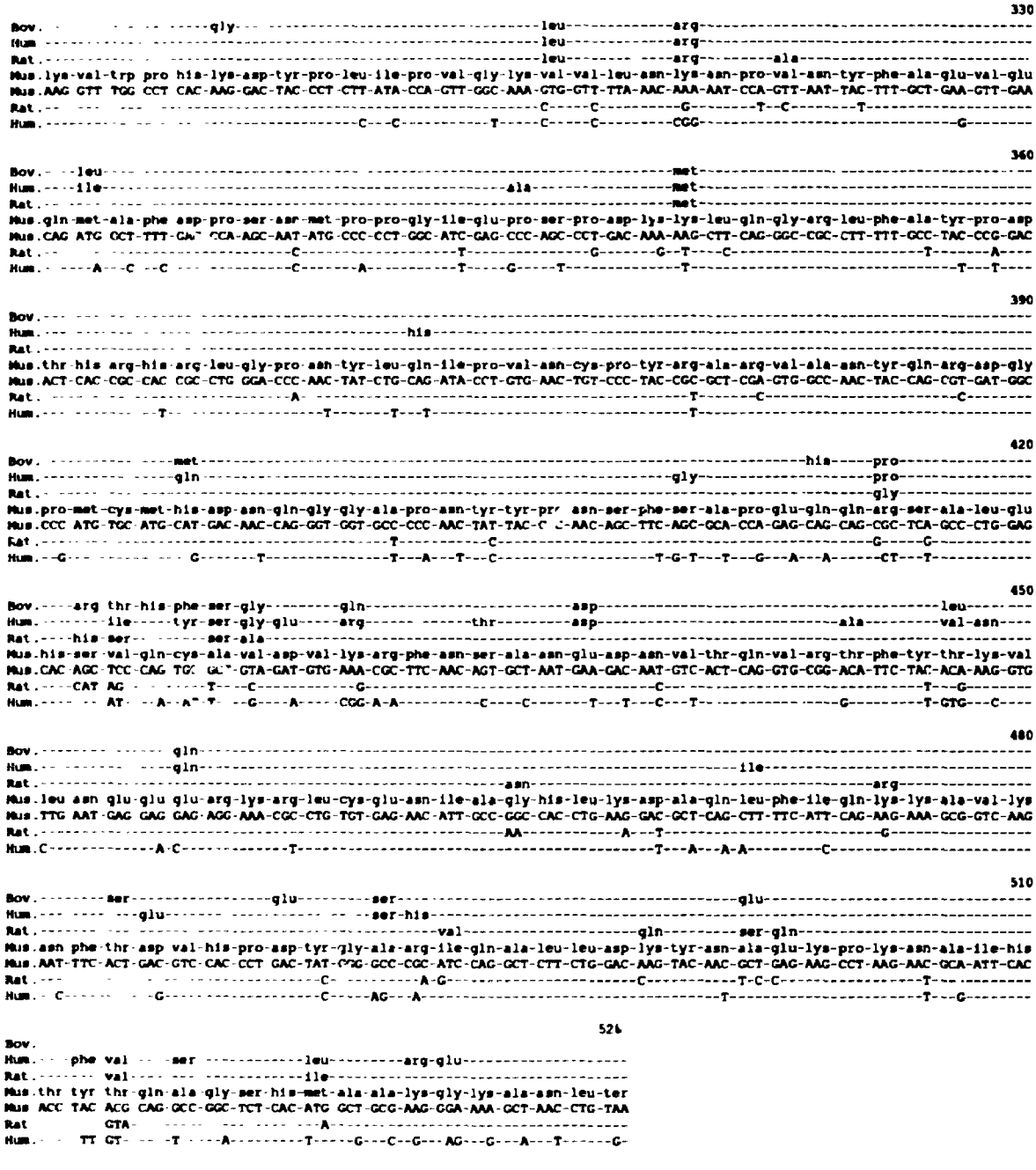

Figure 10. Dot matrix homology analyses involving catalase sequences of the mouse and rat (A, D and G), mouse and human (B, E, and H) and rat and human (C, F, I). A, B and C - coding regions (1584 nt); D, E and F - 3' UTR (mouse - 752 nt; rat - 828 nt; human - 627 nt); G, H and I - 5' UTR (mouse - 87 nt; rat - 83 nt; human - 68 nt).

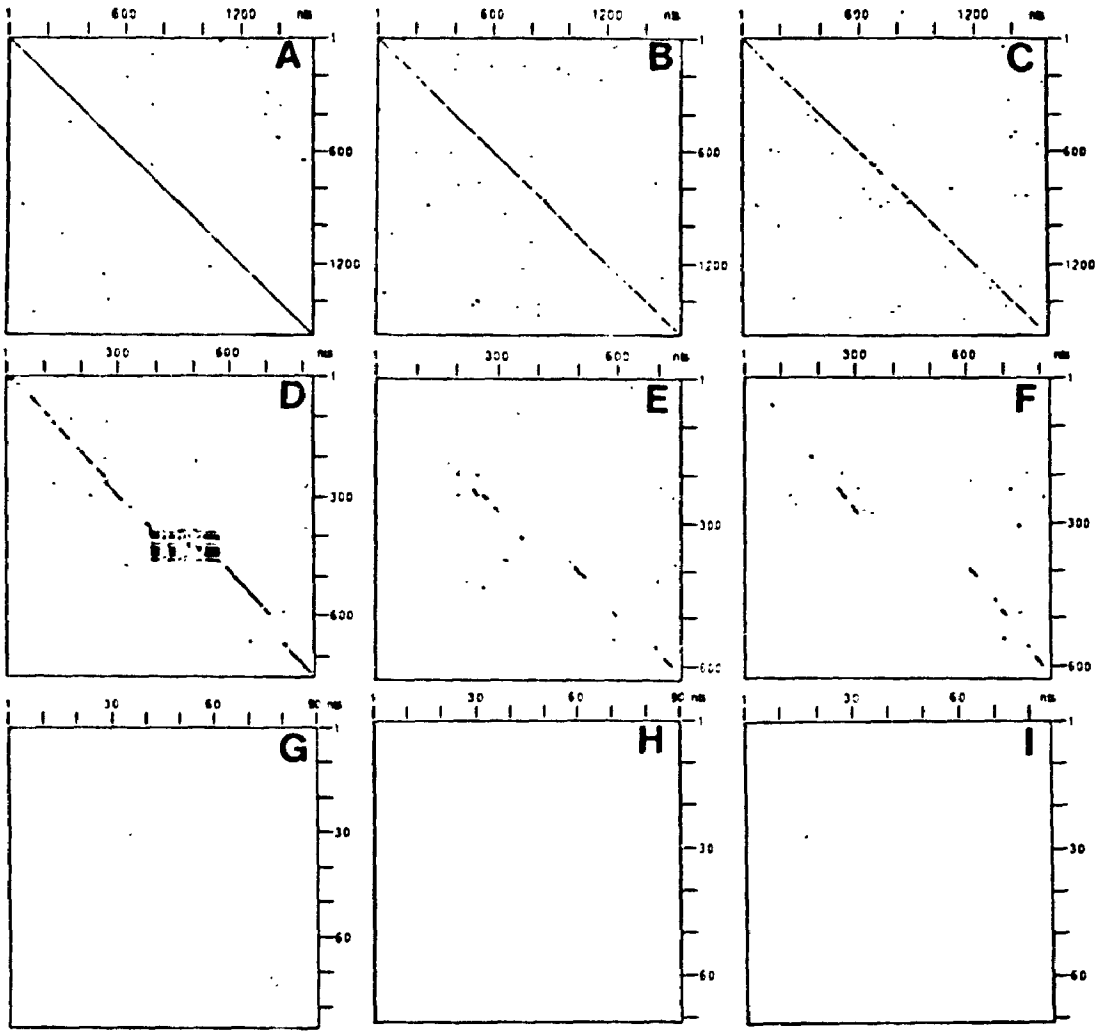
A
B
C
D
E
F
G
H
I
600
1200
300
30
60

follows a similar pattern. Interestingly, there are repeated sequences midway through the 3' UTR of mouse, which show striking identity to such sequences in a similar region of rat (Figure 10D). These repeats include a number of CAs present in both rat and mouse 3' UTRs. On the other hand, such comparisons of the 3' UTRs between mouse and human (Figure 10E) or rat and human (Figure 10F), show very little identity and are localized to a few dispersed small fragments only. It should be pointed out that the sequence of the 3' UTR of human catalase has no CA repeats. To date this repeat is specific only to the rodent catalase sequence.

The length of 5' UTR sequence among the three mammalian species is variable; the human has 68 nucleotides, rat 83 nucleotides and mouse 87 nucleotides. A dot matrix homology plot between mouse and rat for this region shows a relatively high degree of identity (87.3%; Figure 10G), while such plots between mouse and human (60.9%; Figure 10H) or rat and human (51.7%; Figure 10I) show less sequence identity under identical conditions. This observation may suggest a species-specific 5' regulatory sequence divergence for this housekeeping gene.

A detailed DNA sequence comparison of the 5' UTRs from the three mammalian species is shown in the multiple sequence alignment in Figure 11. It allows the identification of conserved regulatory features. Three short regions which are identical among the three species are indicated (some not picked up in homology matrix under the conditions used). Two (TGCCT and GGGTGGAGACC) are located at the 5' end and one (GTTCCGCA) is more 3'. These sequences were searched through Keybank of Consensus Sequences (Genbank) in order to assess their possible regulatory significance. Several consensus sequences were identified and may be important. It has been shown that TGCCT is a site for topoisomerase I which is known to play a role in strand exchange in the recombinational process (Been *et al.*, 1984). The sequence GGGTGG could function to regulate expression of this gene since it has been described as a viral enhancer (Martin *et al.*, 1985; Jalinot and Kedinger, 1986) and functions as an enhancer in the histocompatibility gene of mouse (Kimura *et al.*, 1986). Conservation of these sequences with known regulatory functions among the three mammalian species may suggest the regulatory role of the 5' UTR sequence in the expression of *Cas-1*. No consensus sequences were identified from Genbank which were similar to GTTCCGCA. However, a single nucleotide difference in this sequence observed in the 5' UTR of rat and human

Figure 11. 5' UTR sequence alignment involving mouse (M), rat (R) and human (H) indicating at least 3 conserved regions (Bold).

M ATTGCCTTCTCCGGGTGGAGACCAGACCGCTGCGTCCGTCCCTGCTGTCTCACGTTCCGCAGCTCTGCAGCTCCGCAATCCTACACCATG

R ATTGCCTACCCCGGGTGGAGACC GT GCT CGTCCGGCCCTCTTGCCTCACGTTCTGCAGCTCTGCAGCTCCGCAATCCTACACCATG

H TGCCTGCTGAGGGTGGAGACCCACGAGCCGAGGCC TCC TGCAGT GTTCTGCA C AGCAA ACCGC A C G CTATG

catalase genes may shed doubt with respect to this region and its possible regulatory significance.

3.2. The *Cas-1* Encoded Polypeptide:

The derived amino acid sequence of the mouse catalase cDNA was used in a multiple sequence alignment involving all available catalase sequences in GenBank. At the time of this analysis, the database included sequences from 22 divergent species ranging from prokaryotes to higher eukaryotes. Catalases appear to represent a well conserved group of proteins and have been phylogenetically constructed (von Ossowski *et al.*, 1993). The mouse polypeptide region of amino acids 26 to 370 shows extensive conservation of the sequences in all higher eukaryotes, plants and animals. Approximately 40% of the amino acids of this region are identical in all eukaryotic sequences available for analysis. Most of the divergence among eukaryotic sequences appears associated with the last 157 amino acids of this mouse polypeptide. The evolutionary pattern in this region reflects a number of regionalized deletions specific to different groups of eukaryotes (e.g. yeast, plants, *Drosophila* and mammals). Among the mammals, the bovine sequence is shorter by 20 terminal amino acids, and may represent such an evolutionary phenomenon. In prokaryotes, the general divergence of this polypeptide, which is greater than 700 amino acids, also appears to be confined to the carboxy terminus of this polypeptide.

The highest region of amino acid identity involves the core sequences which contain the structural domains defined in the bovine catalase structure (Murthy *et al.*, 1981). Figure 12 shows the amino acid alignment of the catalase polypeptide among four mammalian species - mouse, rat, human and bovine. This figure also identifies the four structural domains and the α and β pleats based on the crystallographic structure of bovine catalase by Fita and Rossmann (1985). Amino acids involved in heme or substrate interactions are also indicated. Comparison among these four species reveals amino acid variability in the first structural domain. This region consists of approximately 70 amino terminal amino acids and is thought to interact with neighbouring subunits (Murthy *et al.*, 1981). It is interesting that this region exhibits similarities unique to mammals, and may represent an evolutionary divergence for species specific tetramer formation. A high degree of conservation is observed among the four species in the second functional domain which contains amino acids involved in heme and subunit interactions as well as an 8-stranded antiparallel β-barrel and

Figure 12. Alignment of amino acid sequences of catalase from four mammalian species - mouse (M), rat (R), human (H) and bovine (B). The four functional domains are identified by arrowheads and the alpha (α) and beta (β) pleats are identified by boxes and are based on the crystallographic structure of bovine catalase of Fita and Rossmann (1985). Amino acids with direct interaction with the heme molecule (open diamonds) and the substrate channel (closed diamonds) are marked. Note the high degree of conservation of this polypeptide across species with the exception of the region represented by β9 (Bold).

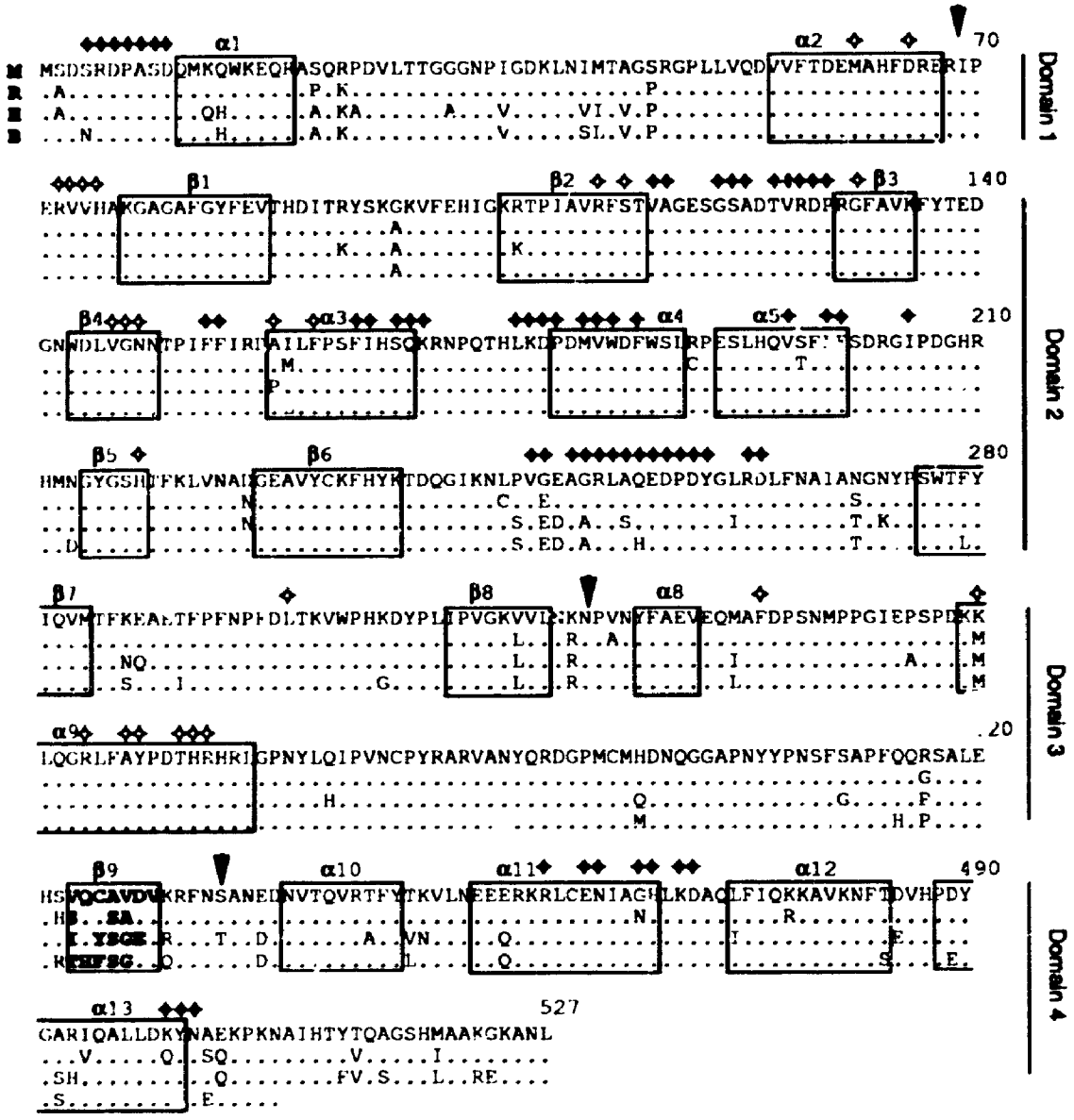
Domain 1
Domain 2
Domain 3
Domain 4

five α-helices. This region represents the active center of the molecule and amino acid conservation in this region reflects its functional importance as a hemoprotein. Comparative analysis in the third structural domain reveals extensive amino acid variability specific to the β9 pleat region (423-429) of this polypeptide (Figure 12). This region, although not involved in direct interaction with the heme molecule or the substrate channel, may be involved in intersubunit contacts to form the quaternary structure. Amino acid variability in this region may reflect species-specificity for the catalase protein. A high degree of amino acid conservation is observed among catalase polypeptides of mammals in the fourth structural domain, which contains 4 α-helices and makes up the external part of the molecule.

B: EXPRESSION OF THE *Cas-1* GENE IN MICE:

3.3. Developmental Pattern and Profile:

Figure 13 shows a representative northern blot hybridized with ^{32}P-labelled pMCT-1 on total RNA from embryonic (15 days and 18 days *post conceptus*) and adult liver. The catalase cDNA probe detects the single 2.4 kb transcript which increases in intensity during development. This observation follows El-Hage and Singh (1989, 1990) who observed the presence of this transcript as early as day 8 of gestation (onset of organogenesis). During the course of this investigation, the spatial and temporal pattern of catalase gene expression in mouse embryos was evaluated using *in situ* hybridization, a technique sensitive to the detection of low abundant mRNAs (Davis *et al.*, 1986; Simmons *et al.*, 1989).

In order to address the technical success of this protocol, paraffin sections of adult mouse liver, which is known to express catalase, were hybridized with ^{35}S-labelled sense (negative control) and antisense mouse catalase riboprobes. A hematoxylin and eosin stained section of the adult mouse liver (Figure 14A) was used to evaluate the morphology and quantify cell numbers per area. It shows epithelial cells, numerous sinusoids, and fully differentiated, relatively large hepatocytes. Molecular hybridization of this tissue section with the sense probe revealed few silver grains under darkfield (Figure 14B). Here, the grain counts on the tissue differ minimally from the number of silver grains not on the tissue. When a serial section of this tissue was hybridized with the antisense riboprobe (Figure 14C), an abundance of silver grains was observed. Further, a brightfield evaluation of this section following counterstaining with hematoxylin to

Figure 13. A: Ethidium bromide stained formamide gel of total RNA (25 µg) from liver of embryonic (18 and 15 days *post conceptus*) and adult Swiss Webster (Adult). Note the prominent 18S and 28S rRNA bands. RNA from this gel was transferred to nylon membrane and hybridized with the random prime labelled *Cas-1* cDNA. B: Representative northern blot of samples from the gel shown in A. Note the presence of a single 2.4 kb band at all stages of development.

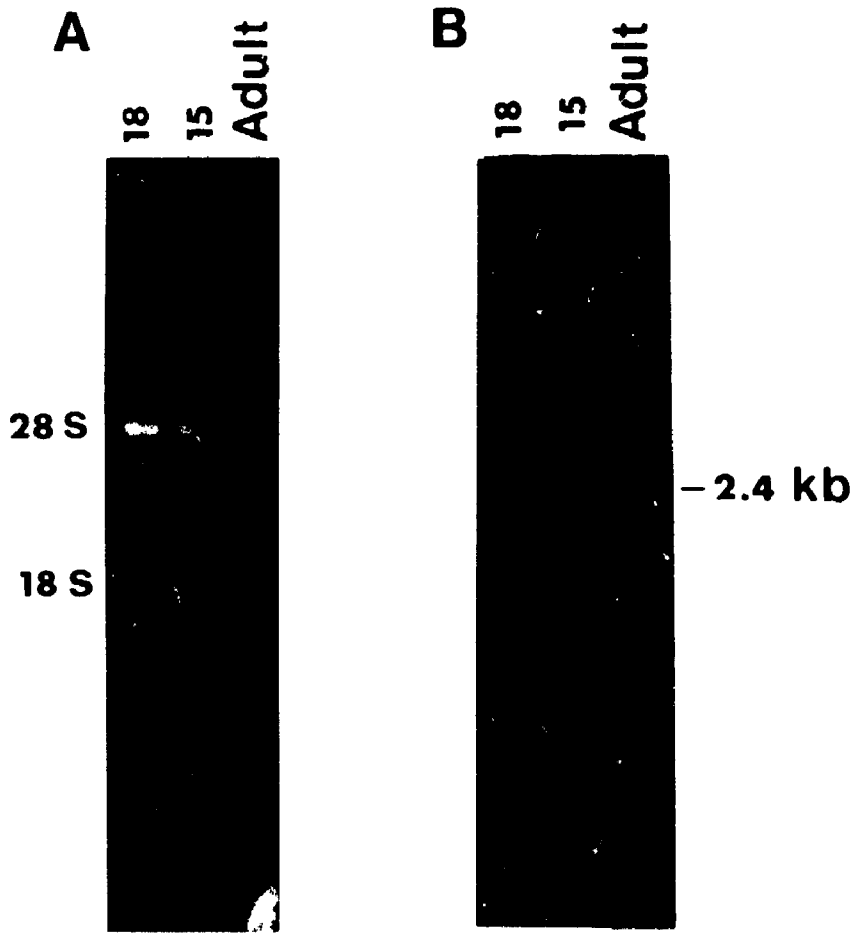
A
18
15
Adult
28 S
18 S
B
18
15
Adult
2.4 kb

Figure 14. *In situ* hybridization analysis of *Cas-1* expression in adult mouse liver. A: Brightfield, stained with hematoxylin and eosin shows numerous sinusoids (thick arrows) and large hepatocytes (thin arrow). Serial sections (darkfield) hybridized with the sense probe (B) and the antisense probe (C). D: Brightfield of C to show the distribution of the silver grains on the cells. Bar = 100 μm.

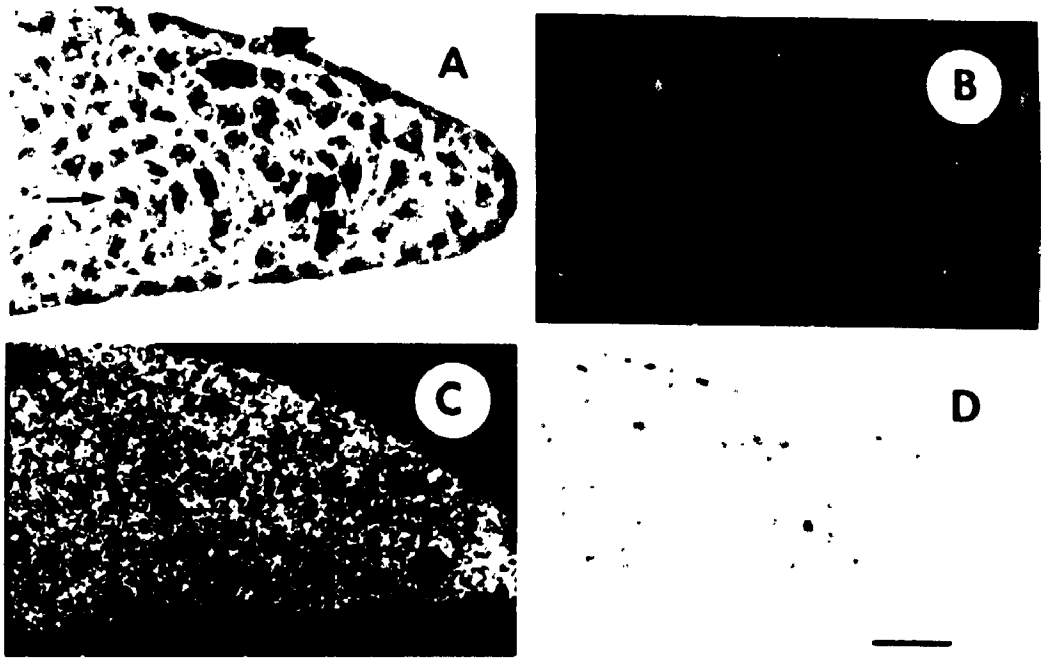
A
B
C
D

enable identification of the nuclei of individual cells, shows cell density and an apparent distribution of silver grains on the nucleus as well as on the cytoplasm (Figure 14D). These results suggest that hybridizable catalase mRNA was present in the adult liver and the transcript for this housekeeping gene in this tissue was detectable throughout the cell.

The same experimental conditions were applied to study the spatial and temporal expression of the catalase gene during development in mice. Paraffin sections from 18 day and 13 day fetuses were subjected to this *in situ* hybridization and evaluation protocol. In day 13 and day 18 fetuses, the silver grains were primarily localized to the liver followed by brain cells or their progenitors. The grain counts on these two tissues were quantified and evaluated at these developmental stages. Figure 15 shows representative tissue differences seen with the application of antisense riboprobe in 18 day fetuses. At this developmental stage, the number of silver grains is elevated in liver as compared to the surrounding tissue types, including gut [Figures 15A and C (brightfield) and 15B and D (darkfield)], skeletal tissue [Figures 15E (brightfield) and 15F (darkfield)], developing vertebrae [Figure 15G (darkfield)] and mesenchyme [Figure 15H (darkfield)]. A similar tissue distribution of grains on day 13 fetuses is seen in Figure 16. For example, higher silver grain counts were observed in liver and heart [Figures 16A (brightfield) and 16B (darkfield)] as compared to the surrounding mesenchyme cells [Figures 16E (brightfield) and 16F (darkfield)]. Figures 16C (brightfield) and 16D (darkfield) show high silver grain counts localized to a region of nucleated red blood cells in the tail bud. One may therefore conclude that the undifferentiated tissue (e.g. mesenchyme) has lower catalase mRNA levels than nucleated red blood cells at this stage of development. These data suggest that the tissue-specificity of the *Cas-1* expression is established early in development.

To accurately evaluate the developmental expression of the catalase gene in mice, a comparison of the same tissue at different developmental stages was made. Molecular hybridizations of sense and antisense riboprobes to day 13 and day 18 fetal sections were analyzed in detail for developmental expression of catalase in the liver, brain and mesenchyme. The liver and brain are easily identified and reasonably differentiated at the two developmental stages studied and show relatively high silver grain counts using the antisense probe as compared to the sense control.

In day 13 fetal liver (Fig 17A, brightfield), there are numerous sinusoids,

Figure 15. *In situ* hybridization analysis of catalase expression in 18 day mouse fetuses showing representative tissue differences with the antisense ribroprobe. Brightfield (A, C) and darkfield (B, D) photographs showing elevated numbers of silver grains on liver (L) compared to gut (G). E: brightfield and F: darkfield representation of fetal skeletal muscle. Darkfield views of developing vertebrae (DV) and mesenchyme (M) are shown in G and H respectively. Bar = 100 μm.

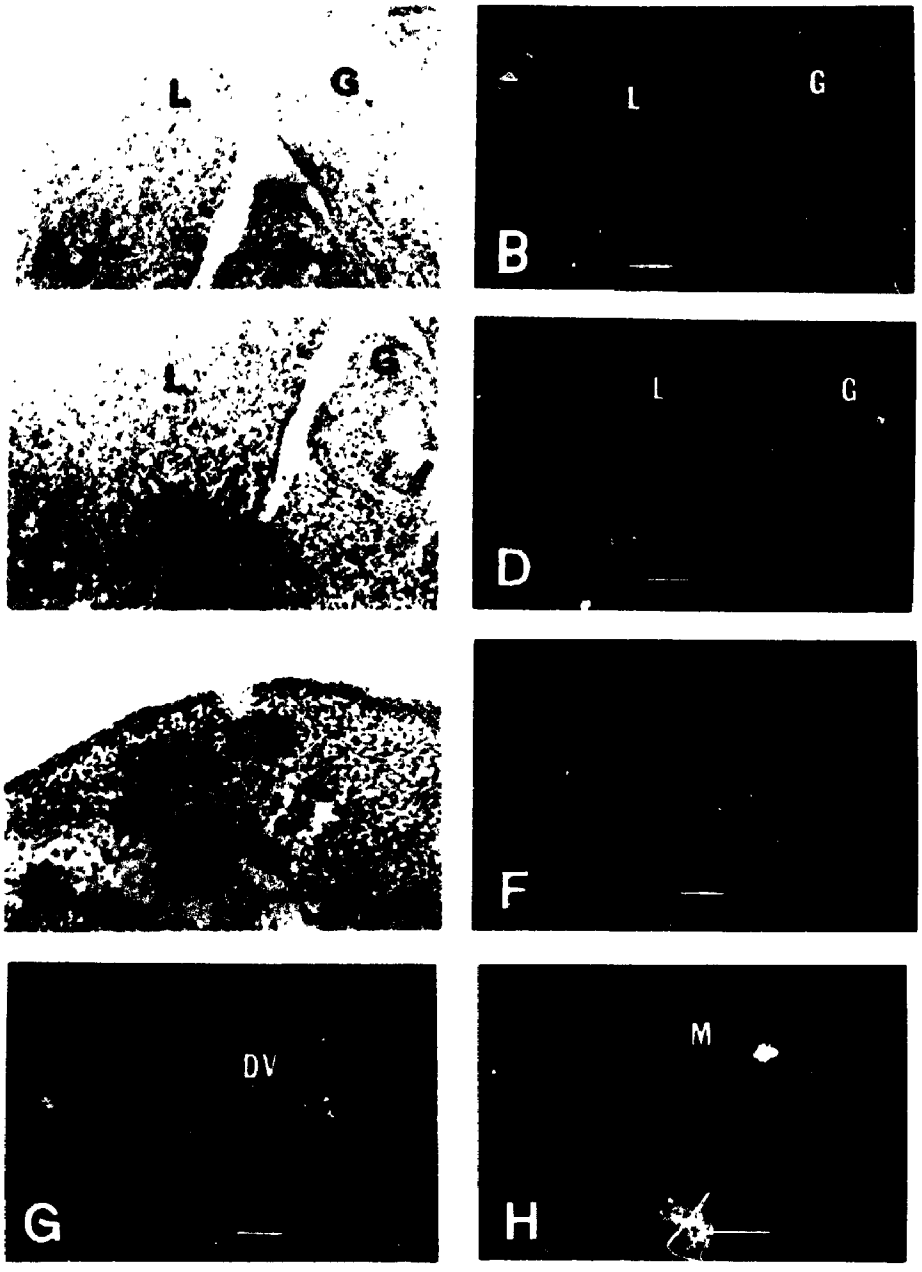
L
G
B
L
G
D
L
G
F
DV
G
M
H

Figure 16. Representative tissue differences seen with antisense riboprobe on 13 day mouse fetuses. Brightfield (A) and darkfield (B) photographs of the liver (L) and heart (H) showing tissue-specific hybridization. Brightfield (C) and darkfield (D) of the tail region showing specific hybridization to nucleated red blood cells (arrow). Brightfield (E) and darkfield (F) representation of mesenchyme (a negatively expressing tissue) showing background hybridization. Bar = 100 μm.

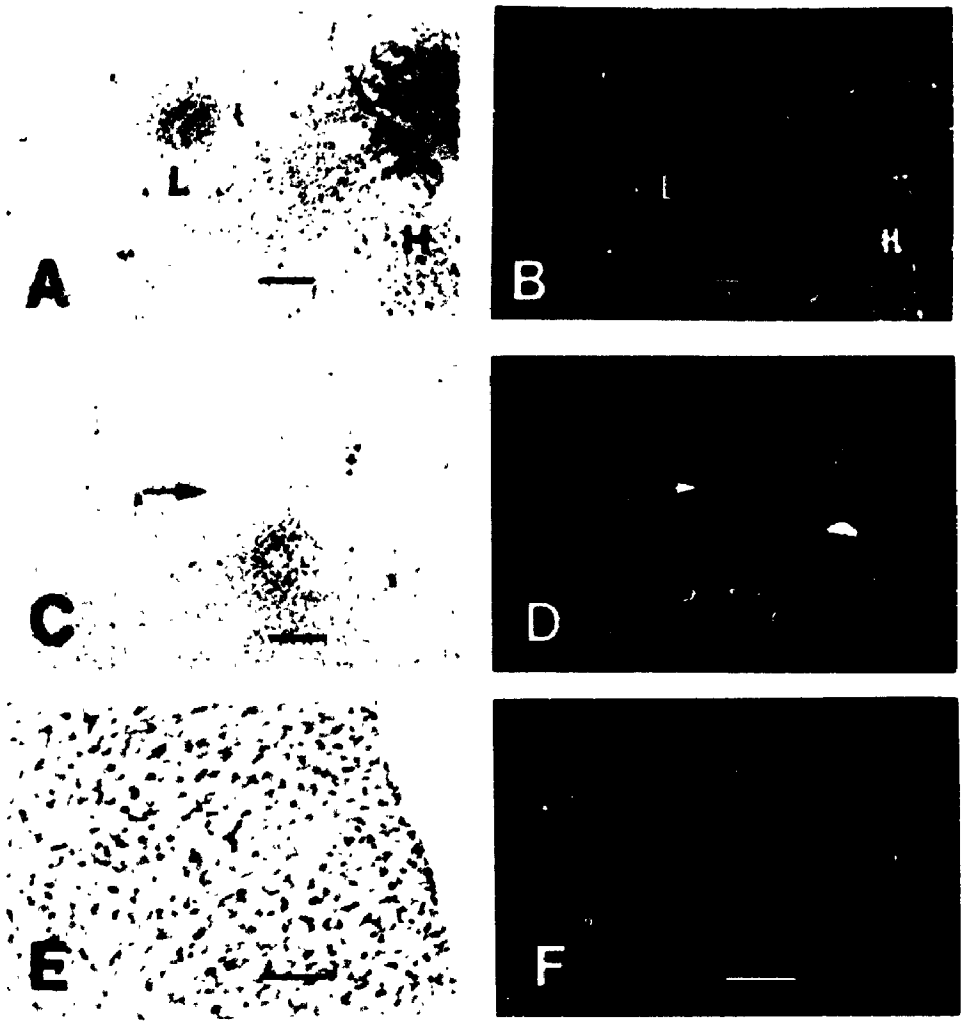
A
L
H
B
C
D
E
F

and the tissue is hemopoetic, highly dividing and rapidly differentiating. The serial section hybridization of this tissue by the sense and antisense riboprobe showed that relative grain counts were significantly higher with the antisense probe (Figure 17B) as compared to the sense probe (not shown). In comparison, the 18 day fetal liver is more differentiated, with higher number of cells in a given area but still hemopoetic (Figure 17C, brightfield). A number of sinusoids are also visible at this stage in this tissue. The *in situ* hybridization analysis shows that, as in day 13 fetuses, the grain density is higher with the antisense probe (Figure 17D) than with the sense probe. The grain count on the adult liver cells (Figure 17C) is remarkably elevated as compared to the fetal stages. Further, the density of silver grains on the 18 day fetal liver (Figure 17D) is higher than the day 13 fetuses (Figure 17B).

The brain of the 13 day fetuses possesses actively dividing progenitors in their initial stages of differentiation with clear gaps and migrating cells (Figure 17E, brightfield). Subsequent observations of *in situ* hybridizations on such fetuses shows that the gene-specific riboprobe is able to detect expression of catalase. Here, the number of silver grains generated by the antisense probe (Figure 17F) is lower than that of the liver. The brain of the day 18 fetuses is highly differentiated [Figure 17G, (brightfield) as an example] and individual cell types can be recognized. Here, the cells are densely packed, having reached their level of differentiation and organization with neural development nearing completion. The *in situ* hybridization on serial sections yielded a higher number of cell-specific silver grains on the brain cells at this stage of development, with the antisense probe (Figure 17H). A comparison of the *in situ* results shows that the density of silver grains on the brain cells is noticeably elevated in the section of the 18 day fetus (Figure 17H) as compared to the 13 day fetus (Figure 17F).

The observed differences in silver grain density may not be due to differences in gene expression alone and could be due to a combination of factors. For example, given a comparable level of gene activity, two tissues with different cell densities will yield different silver grain counts per area. Further characterization of the data is necessary, therefore, in order to offer a realistic view of the tissue- and cell-specific catalase gene expression in developing fetuses. It would require a quantitative approach which must include evaluation of cell number. I collected data on the number of silver grains, and the number of cells in a defined area on recognizable tissues at two stages (day 13 and 18) of fetal development. A summary of the results on three tissues at day 13, 18 and

Figure 17. Developmental expression of *Cas-1* in liver and brain of mouse fetuses. Brightfield analysis of day 13 liver (A) shows sinusoids (arrow) and differentiating cells; silver grains following hybridization with the antisense riboprobe (B, darkfield); day 18 liver (C, brightfield), relatively differentiated tissue with sinusoids (arrow); D: Darkfield-hybridization with the antisense riboprobe. Brain tissue of day 13 fetuses (E, brightfield) and with silver grains following antisense riboprobe hybridization (F, darkfield); day 18 brain brightfield (G) and darkfield (H). Bar = 100 μm.

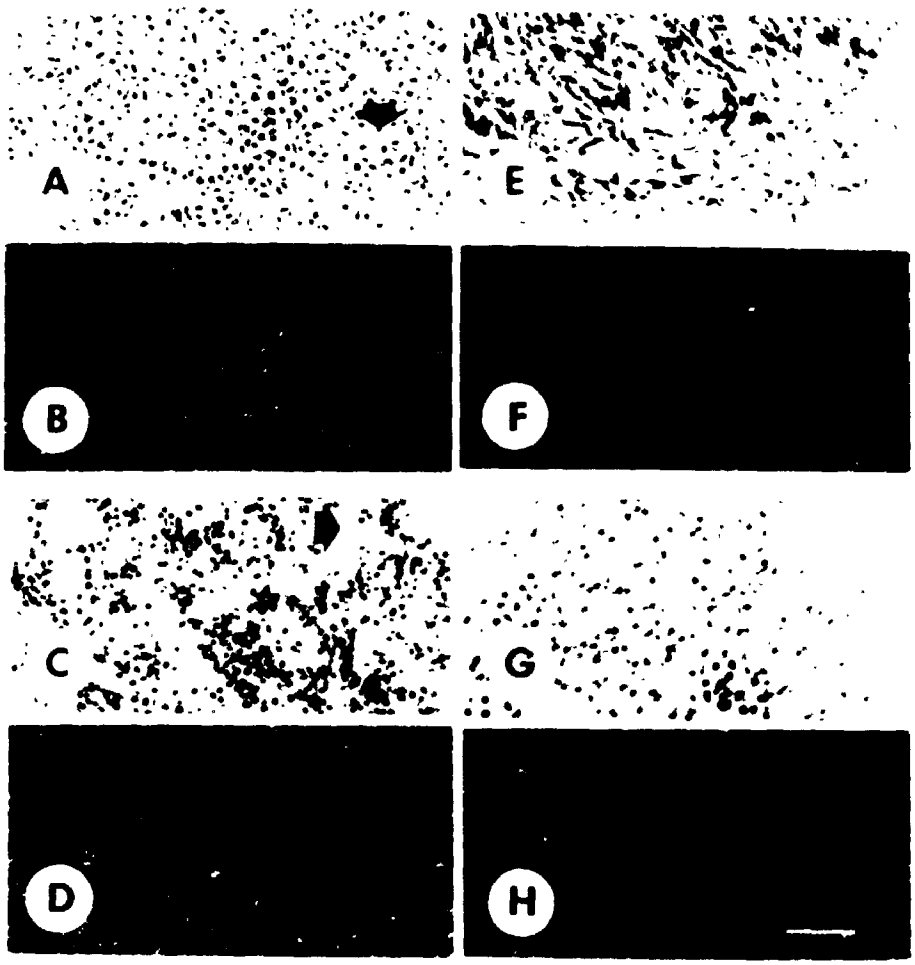
A
E
B
F
C
G
D
H
LIVER
BRAIN

adult liver is given in Table 1 It is apparent that the cell density changes during the differentiation of the liver; 65 cells per 3600 μm^2 at day 13, 99 at day 18 and 13 in the adult. The number of silver grains is significantly higher following hybridization with the antisense probe than the sense probe particularly in the liver and the brain at all stages studied. These data suggest that the cells of these tissues express the catalase gene to different degrees. Expression increases with development and differentiation. On the other hand, the mesenchyme cells of the 13 day fetuses were non-expressing and expression of this gene in these cells takes place after day 13.

The relative expression of catalase on a per cell basis (including a correction for the silver grains observed with sense (negative control) riboprobe, is given in Figure 18. It is clear that the expression of the catalase gene follows a tissue-specific temporal pattern. It is highly expressed in the liver cells and to a lesser extent in brain cells, starting early in embryogenesis. There appears to be little or no catalase message in undifferentiated mesenchyme cells at day 13, while expression of this mRNA is evident at later stages (day 18) of fetal development. The increases observed in *Cas-1* mRNA expression, particularly in brain and liver are expected for a gene under tissue- and development-dependent regulatory elements.

A substantial increase in the catalase polypeptide in adult liver as compared to 14 day fetal liver could also be demonstrated by western blotting (Figure 19). Here, the polypeptide was not apparent in day 14 liver while a single polypeptide band was observed in the liver of the adult. These results more accurately reflect the enzyme levels observed during development. This is consistent with the hypothesis that *Cas-1* mRNA transcripts may accumulate *in utero*, and are translated efficiently only after birth with the onset of independent aerobic respiration when this enzyme is needed (El-Hage and Singh, 1990).

3.4. Tissue-Specificity of *Cas-1* Expression:

Catalase enzyme activity from different tissues of adult BALB/c mice was quantified using spectrophotometric analysis. Figure 20A shows that the catalase activity is highest in the liver followed by kidney and blood. To determine whether *Cas-1* expression is regulated transcriptionally or posttranscriptionally, the three representative tissues of the BALB/c mice were quantitatively evaluated for polypeptide abundance by western blot (Figure 20B) and mRNA abundance by dot blot (Figure 20C). Correlations between the levels of enzyme mRNA, activity or polypeptide across the three tissues are shown in

Table 1. Silver grain counts on different tissues following *in situ* hybridization with antisense and sense ^{35}S-labelled riboprobes. The riboprobe represents the 550 bp fragment of the mouse catalase cDNA clone pMCT-1.

		GRAINS PER 3600 μm^2			GRAINS PER CELL		
Dev. Stage	Tissue	Sense	Antisense	#Cells/3600 μm^2	Sense	Antisense	p
13 day	Liver	50.40 ± 3.97	96.60 ± 4.53	65.2 ± 1.62	0.78 ± 0.08	1.49 ± 0.09	<0.001
	Brain	22.80 ± 0.86	35.60 ± 2.71	72.0 ± 1.00	0.32 ± 0.01	0.49 ± 0.04	<0.002
	Mesenchyme	30.20 ± 1.20	29.80 ± 2.74	64.0 ± 2.68	0.47 ± 0.03	0.47 ± 0.04	0.865
18 day	Liver	93.60 ± 4.07	203.80 ± 5.50	99.0 ± 2.47	0.94 ± 0.06	2.06 ± 0.07	<0.001
	Brain	26.60 ± 1.25	84.80 ± 4.21	45.8 ± 1.20	0.58 ± 0.02	1.86 ± 0.14	<0.001
	Mesenchyme	35.80 ± 2.65	65.20 ± 3.34	64.6 ± 1.03	0.56 ± 0.05	1.01 ± 0.04	<0.001
Adult	Liver	77.80 ± 1.76	166.00 ± 4.39	13.4 ±0.45	5.88 ± 0.28	12.52 ± 0.53	<0.001

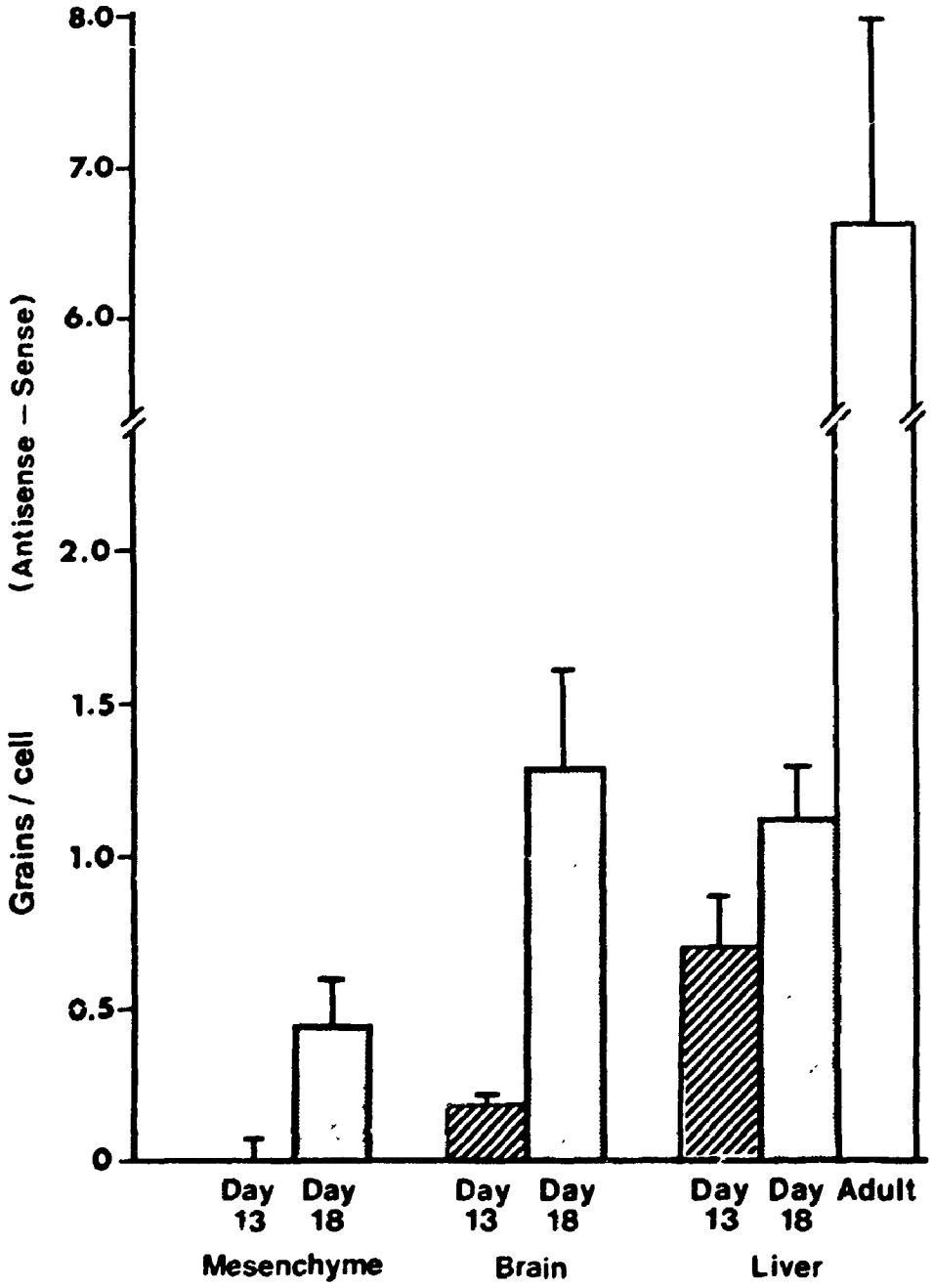
8.0
7.0
6.0
2.0
1.5
1.0
0.5
0
Grains / cell (Antisense – Sense)
Day 13
Day 18
Mesenchyme
Day 13
Day 18
Brain
Day 13
Day 18
Adult
Liver

Figure 18. Expression of *Cas-1* mRNA in mesenchyme, brain and liver of day 13 and day 18 fetuses. Values are expressed as grains per cell ± S.E.M., corrected for the silver grains observed with sense riboprobe. Values for the adult liver are included for comparison.

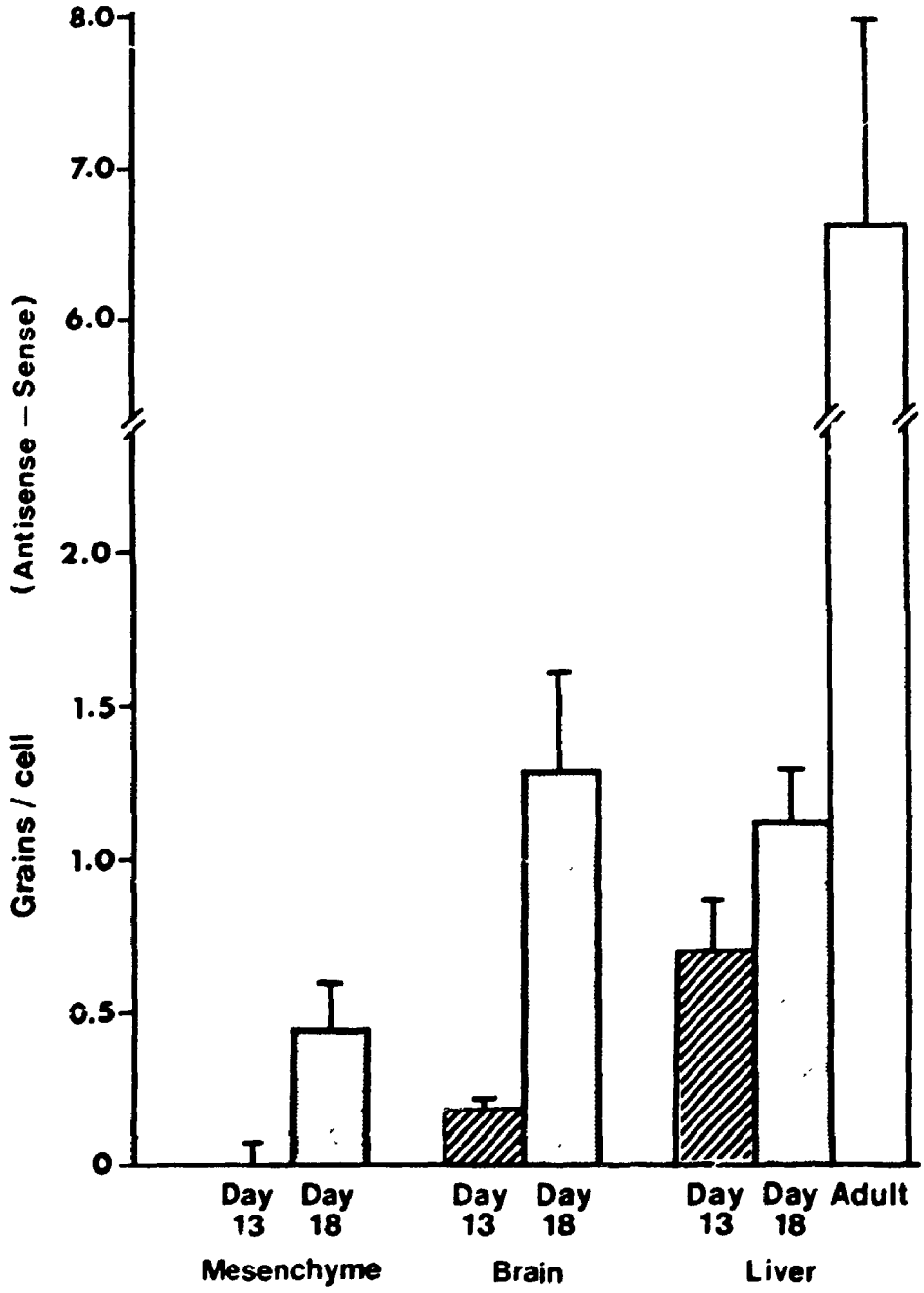
8.0
7.0
6.0
2.0
1.5
1.0
0.5
0
Grains / cell (Antisense – Sense)
Day 13
Day 18
Mesenchyme
Day 13
Day 18
Brain
Day 13
Day 18
Adult
Liver

Figure 19. Catalase polypeptide analysis of liver from a 14 day fetus and adult C3H/HeAnl/*Cas-1*^{a}. Total protein from embryonic (E - 10 μg) and adult (A - 5 μg) liver were subjected to electrophoresis in 10% SDS polyacrylamide gel with a 4% stacking gel and stained with Coomassie blue (A). The separated polypeptides from a duplicate gel were transferred to a nitrocellulose membrane and reacted with polyclonal antihuman catalase antibody to generate the western blot (B). Lane C contains purified bovine catalase polypeptide, a positive control. Arrows show the catalase polypeptide.

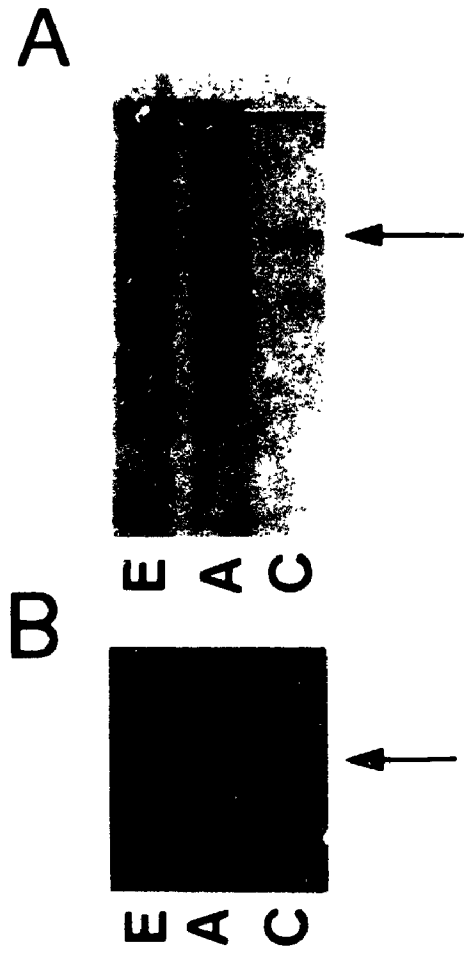
A
E
A
C
B
E
A
C

Figure 20. Expression pattern of *Cas-1* in liver, kidney and blood of BALB/c at the level of enzyme activity (A), polypeptide by western blot analysis (B) and mRNA level by dot blot analysis (C). A correlation between mRNA and polypeptide in addition to mRNA and enzyme activity is shown in D. S.E.M = standard error of the mean.

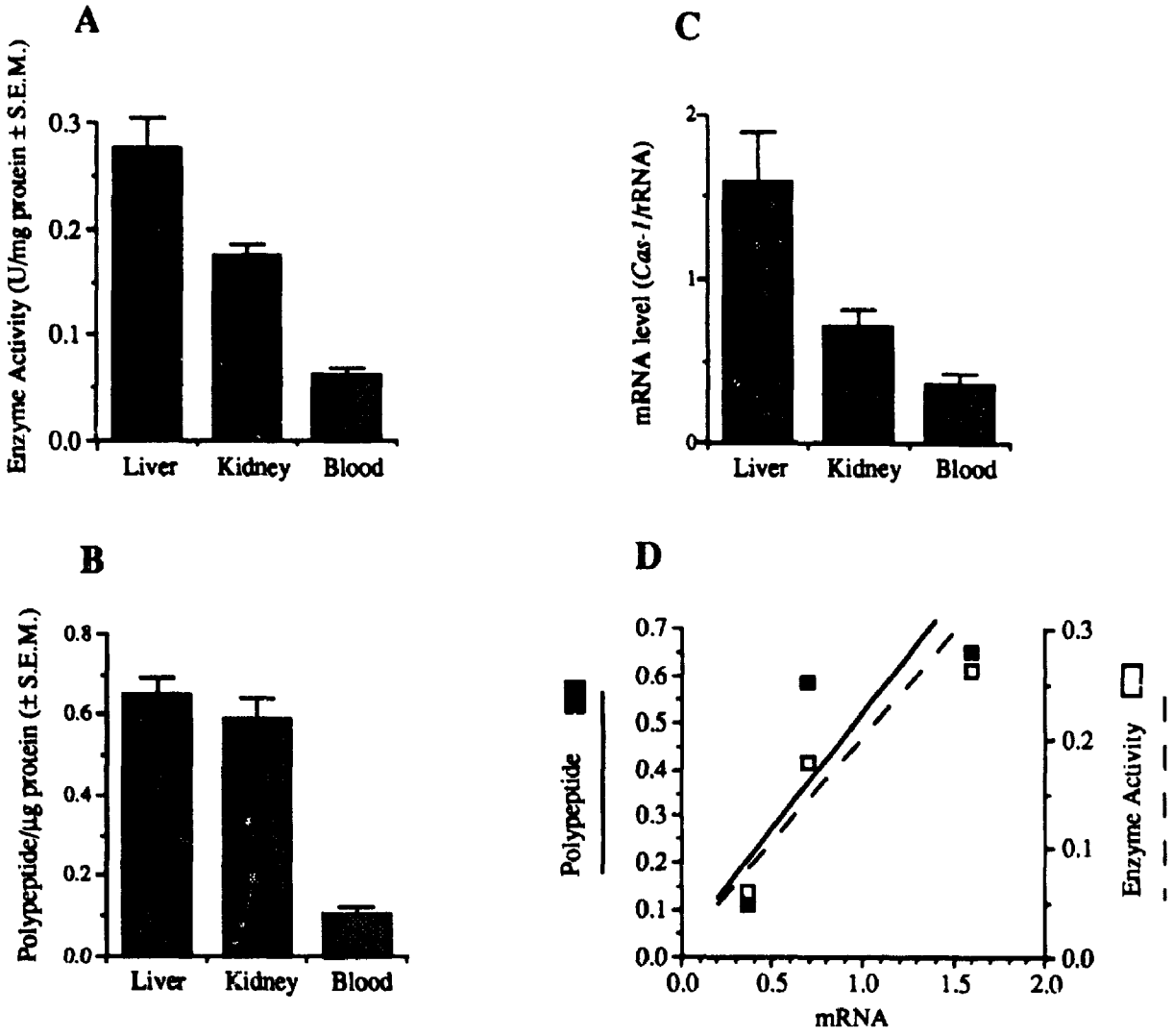
A
Enzyme Activity (U/mg protein ± S.E.M.)
0.3
0.2
0.1
0.0
Liver
Kidney
Blood
C
mRNA level (Cas-1/rRNA)
2
1
0
Liver
Kidney
Blood
B
Polypeptide/µg protein (± S.E.M.)
0.8
0.6
0.4
0.2
0.0
Liver
Kidney
Blood
D
Polypeptide
Enzyme Activity
0.7
0.6
0.5
0.4
0.3
0.2
0.1
0.0
0.3
0.2
0.1
0.0
0.0
0.5
1.0
1.5
2.0
mRNA

Figure 20D. It suggests that the tissue-specific enzyme activity follows closely the level of the polypeptide as seen on the western blots as well as the level of mRNA detected by the *Cas-1* cDNA quantified using dot blots in replicated experiments. The relative mRNA level therefore could be viewed as the determining factor for the tissue-specific expression of this housekeeping gene. The most logical explanation for the results presented in Figure 20 involves tissue-specific regulation of *Cas-1* by the rate of transcription or mRNA stability.

In general, transcriptional regulation is determined by the 5' upstream regulatory region of most housekeeping genes which is often associated with CpG methylation. As shown in Figure 21, sequence analysis of the 5' upstream regulatory region of the *Cas-1* gene reveals 21 potential methylation sensitive CpG dinucleotides. The distribution of these sites in the upstream 659 bp appears uneven (Figure 21). Figure 22 shows that the region representing 0 to -300 bp contains most of the CpG dinucleotides (17 out of 21). This region also exhibits a high G + C content (65%) as compared to the G + C content of the larger 659 bp region (47%). The 300 bp of this 5' upstream region also includes three sites (CCGG) specific to the isoschizomers *Msp* I and *Hpa* II (Figure 21). The two enzymes recognize the same sequence, however *Hpa* II lacks the ability to cleave DNA when the cytosine residue of a CpG dinucleotide is methylated. Thus the presence of a product when PCR is performed following *Hpa* II digestion would suggest methylation of the CCGG sites (Rodenhiser *et al.*, 1993). Two primers, P1 and P2 (Figure 21) were constructed to evaluate the methylation specificity of this region by *Hpa* II PCR methodology. To confirm that P1 and P2 are specific primers and the expected fragment of 278 bp is amplified from uncut genomic DNA from the 5' upstream region of *Cas-1*, PCR products were digested with *Msp* I and *Hpa* II. Figure 23A shows the expected 278 bp amplification product using P1 and P2 (left) and 4 predicted DNA fragments (161, 52, 50, and 15 bp) following enzyme digestion (right). PCR reactions also included an internal control. P3 and P4 primers (Figure 8) yield a 328 bp product of the *Cas-1* gene which contains no CCGG sites. Figure 23B shows the result of the *Hpa* II PCR amplification using genomic DNA from four tissues and appropriate controls. DNA from each tissue was amplified under three conditions: uncut, *Hpa* II and *Msp* I digested. The uncut DNA from each tissue yielded the expected 278 bp fragment using primers P1 and P2 and a 328 bp product by P3 and P4. However, only the 328 bp band was observed following the *Msp* I or *Hpa* II digestions. To date, no tissues have been identified for which this region can be

Figure 21. Genomic sequence of the 659 nt of the 5' *Cas-1* region identifying 21 CpG dinucleotides (dots). Three *Msp* I/*Hpa* II restriction enzyme sites (CCGG) are boxed, and the oligonucleotide primers (P1 and P2) used to PCR amplify this region are shown by arrows.

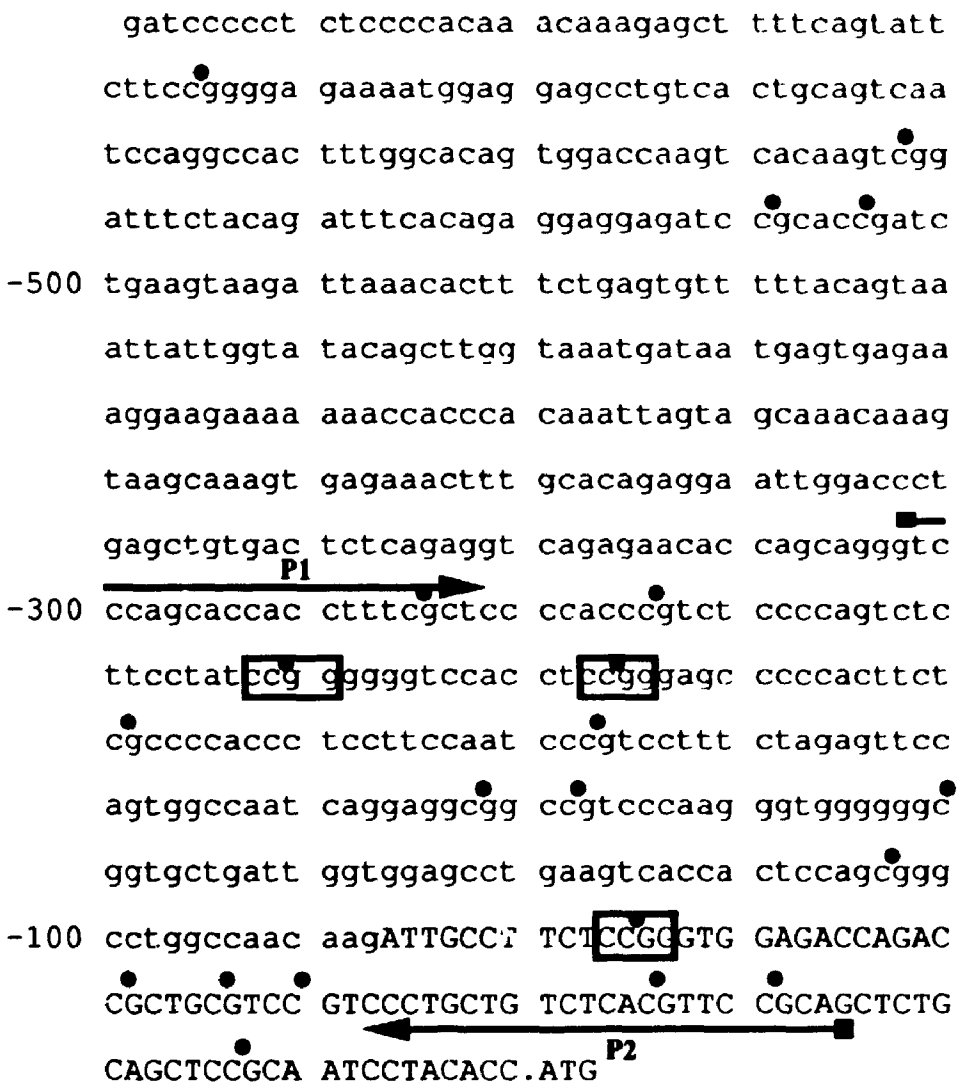
gatccccct ctccccacaa acaaagagct tttcagtatt
cttccgggga gaaaatggag gagcctgtca ctgcagtcaa
tccaggccac tttggcacag tggaccaagt cacaagtcgg
atttctacag atttcacaga ggaggagatc cgcaccgatc
-500 tgaagtaaga ttaaacactt tctgagtgtt tttacagtaa
attattggta tacagcttgg taaatgataa tgagtgagaa
aggaagaaaa aaaccaccca caaattagta gcaaacaaag
taagcaaagt gagaaacttt gcacagagga attggaccct
gagctgtgac tctcagaggt cagagaacac cagcagggtc
P1
-300 ccagcaccac ctttcgctcc ccacccgtct ccccagtctc
ttcctatccg gggggtccac ctccgggagc ccccacttct
cgccccaccc tccttccaat cccgtccttt ctagagttcc
agtggccaat caggaggcgg ccgtcccaag ggtggggggc
ggtgctgatt ggtggagcct gaagtcacca ctccagcggg
-100 cctggccaac aagATTGCCT TCTCCGGGTG GAGACCAGAC
CGCTGCGTCC GTCCCTGCTG TCTCACGTTC CGCAGCTCTG
P2
CAGCTCCGCA ATCCTACACC.ATG

Figure 22. The CpG content of the *Cas-1* 5' UTR. Data are expressed as: O (observed number of CpGs per 100 bp)/E (expected number of CpGs per 100 bp). E = number of C residues x number of G residues / 100. Numbers in brackets represent actual CpG dinucleotides.

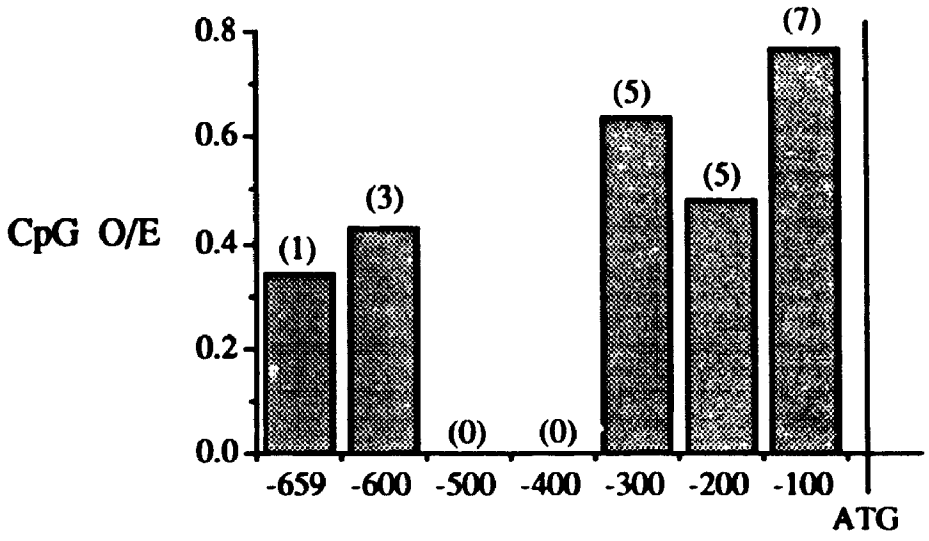
CpG O/E
0.8
0.6
0.4
0.2
0.0
(1)
(3)
(0)
(0)
(5)
(5)
(7)
-659
-600
-500
-400
-300
-200
-100
ATG

Figure 23. PCR amplification of genomic DNA from mouse. Two sets of primers were used in each reaction: P1 and P2 amplify a 278 bp fragment from the 5' upstream region (5) which contains three *Msp* I/*Hpa* II (CCGG) sites; P3 and P4 amplify a 328 bp fragment (Figure 8) from the 3' UTR with no CCGG sequences and is used as an internal control for each PCR reaction (c). A: Left - PCR amplification of genomic DNA from mouse brain (U). Right - The PCR products were digested with either *Msp* I (M) or *Hpa* II (H) and 4 expected digestion products are identified from the three known CCGG sites in the 5' upstream region only while the control 3' UTR is unaffected. B: PCR amplification (using the two sets of primers) of genomic DNA from mouse brain (Br), liver (L), kidney (K), and blood (Bl). The DNA was digested with *Hpa* II (H) or *Msp* I (M) or uncut (U) prior to amplification. S = standard 1 kb ladder of molecular weight markers (bp) (BRL).

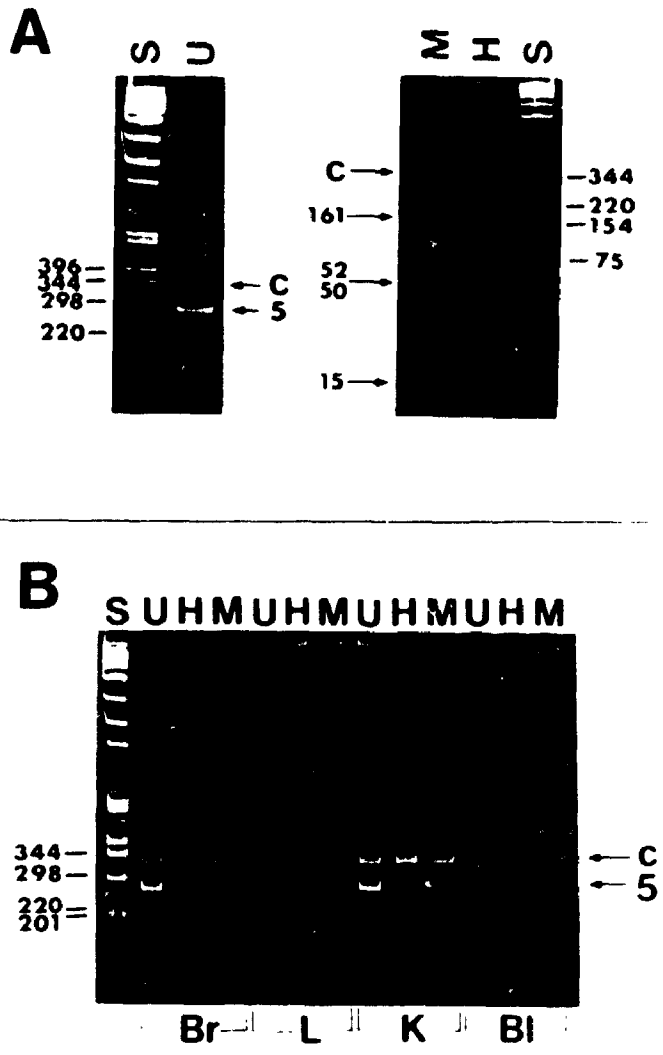
A
S U
M H S
C
161
52
50
15
344
220
154
75
396
344
298
220
C
5
B
S U H M U H M U H M U H M
344
298
220
201
C
5
Br
L
K
Bl

amplified following *Hpa* II digestions. All DNA samples used here represent tissues where catalase is expressed, although to varying degrees. The results obtained in this experiment argue that at least one of the three CCGG sites contained in the 5' region encompassed by P1 and P2 is not methylated and thereby cut by *Hpa* II in all DNA samples. The role for CpG methylation in transcriptional regulation of this housekeeping gene however, cannot be ruled out.

3.5. Expression of *Cas-1* in Genetic Strains of Mice:

Table 2 shows enzyme activities in the liver (A), kidney (B), and blood (C) for seven genotypes of mice that include six established strains (BALB/c, Swiss Webster (S.W.), C3H/HeAnl/*Cas-1*^{a}, 129/ReJ, C57BL/6J, C3H/HeAnl/*Cas-1*^{b}) and a recombinant inbred (R.I.) line generated in our laboratory from an original cross involving S.W. and C3H/HeAnl/*Cas-1*^{b} (SXC/ws-1). This R.I. line was studied at 20 generations of brother-sister matings and considered homozygous for almost all genetic loci.

It is apparent from this table that the catalase enzyme activity follows a tissue-specific pattern in all genotypes studied. Analysis of variance on each tissue indicated that among-strain differences in catalase activity were highly significant ($p < 0.01$). Catalase activity is relatively high in the liver, low in the kidney and even lower in the blood. It ranges from 0.118 and 0.389 U/mg protein in the liver, 0.018 to 0.183 U/mg protein in the kidney and 0.005 to 0.084 U/mg protein in the blood. More importantly, within a given tissue type, all mouse genotypes do not have the same level of enzyme activity. S.W. for example has a relatively higher level of enzyme activity in all tissues and C57BL/6J has relatively lower level of catalase activity in all tissues. These strains are referred to as "normal" and "hypocatalasemic" respectively. This study also includes results on an acatalasemic mutation which is represented by C3H/HeAnl/*Cas-1*^{b} and the R.I. line SXC/ws-1. The effect of this mutation is apparent on the expression of catalase in kidney and blood only. Unlike liver, where the catalase activity in the acatalasemic genotype is normal, the kidney catalase activity is reduced by a factor of ten and the blood catalase activity is barely detectable. The molecular determinants of the genotype-dependent tissue-specific expression of the catalase activity remain poorly understood, and elucidating these determinants forms one of the objectives of this study. The pattern of catalase expression was evaluated at the level of mRNA and protein (western blot) in the three tissues of the representative genotypes (normal,

Table 2: Catalase activity of liver (A), kidney (B) and red blood cell lysate (C) (Bergmeyer Units/mg protein ± S.E.M. around the number of animals) from six mouse strains and an R.I. line derived from Swiss Webster X C3H/HeAnl/*Cas-1*^{b} (SXC/ws-1).

A

Strain	Enzyme Activity	No. Animals	No. Replications
BALB/c	0.279 ± 0.017	4	3
Swiss Webster	0.389 ± 0.013	3	3
C3H/HeAnl/*Cas-1*^{a}	0.273 ± 0.047	3	3
129/ReJ	0.254 ± 0.033	3	3
C57BL/6J	0.118 ± 0.009	3	3
C3H/HeAnl/*Cas-1*^{b}	0.347 ± 0.049	4	3
SXC/ws-1	0.290 ± 0.084	3	3

B

Strain	Enzyme Activity	No. Animals	No. Replications
BALB/c	0.175 ± 0.009	3	3
Swiss Webster	0.183 ± 0.018	3	3
C3H/HeAnl/*Cas-1*^{a}	0.117 ± 0.016	3	3
129/ReJ	0.115 ± 0.016	3	3
C57BL/6J	0.111 ± 0.010	3	3
C3H/HeAnl/*Cas-1*^{b}	0.018 ± 0.004	3	3
SXC/ws-1	0.020 ± 0.001	3	3

C

Strain	Enzyme Activity	No. Animals	No. Replications
BALB/c	0.058 ± 0.006	4	3
Swiss Webster	0.076 ± 0.004	3	3
C3H/HeAnl/*Cas-1*^{a}	0.039 ± 0.010	3	3
129/ReJ	0.084 ± 0.017	3	3
C57BL/6J	0.065 ± 0.011	3	3
C3H/HeAnl/*Cas-1*^{b}	0.005 ± 0.001	4	3
SXC/ws-1	0.006 ± 0.001	4	3

hypocatalasemic and acatalasemic). Posttranscriptional regulation of catalase was evaluated by the possible involvement of mRNA-binding proteins.

Representative northern blots for liver, kidney and blood of the three representative strains of mice is shown in Figure 24. Before the RNA was transferred to nylon membranes, the ethidium bromide stained agarose gels were photographed with UV transillumination (EB) to demonstrate the presence of comparable amounts of undegraded total RNA. Northern blots hybridized with the mouse catalase cDNA probe, pMCT-1, yielded a single 2.4 kb message specific to the *Cas-1* gene present in all tissues and strains examined. The same blots were also hybridized with an 18S rRNA probe used as a control. Representative dot blots which were used to quantify the *Cas-1*-specific mRNA in the three tissues are shown in Figure 25. For each tissue, three replications on three individuals for three different amounts of RNA (1, 5 and 10 µg) were quantified for *Cas-1* mRNA in relation to 18S rRNA. Statistical analyses for the quantification of *Cas-1* mRNA from these experiments is given in Appendix 1. Analysis of variance on each tissue indicated that in general among-individual differences were not significant. This allowed a quantitative dot blot comparison among the tissues of the three strains. Table 3 shows the mean catalase mRNA levels using 1 and 10 µg total RNA (within the linear range of quantification) from liver, kidney and blood from 3 individuals of the three representative strains. In general, liver has a higher level of mRNA followed by kidney and blood. Within each tissue, the mRNA levels do not differ significantly among strains when comparing 1 µg ($p > 0.60$) or 10 µg total RNA ($p > 0.95$). Such results suggest that strain differences in enzyme activity for a given tissue are not accomplished at the level of mRNA. This also suggests that the tissue-specific decrease in enzyme activity of the acatalasemic strain is not a result of decreased transcription or the instability of its mRNA.

To determine whether the acatalasemic mutation results from the differential ability of the *Cas-1* mRNA in kidney and blood to be translated, polysomal and non-polysomal RNA was isolated from kidney of C3H/HeAnl/*Cas-1*^{b} and C3H/HeAnl/*Cas-1*^{a} and was compared to total kidney RNA by dot blot analysis. Figure 26 shows the results of this study and demonstrates that the amount of mRNA associated with the polysomes and the RNA from the non-polysomal fraction do not appear to differ between the normal and acatalasemic mouse strains. These data demonstrate that *Cas-1* mRNA is present in comparable amounts on the translational machinery in the kidney of both the

Figure 24. Representative northern blot results for catalase mRNA from liver, kidney and blood of BALB/c (Balb), C3H/HeAnl/*Cas-1*^{b} (Cs^{b}), and 129/ReJ (ReJ). RNA (25 mg) from the ethidium bromide stained gel (EB) was blotted onto nylon and hybridized with the pMCT-1 cDNA probe which yeilds a single 2.4 kb message (*Cas-1*) in all tissues and genotypes. The blots were rehybridized with 18S rRNA used as a control (18S).

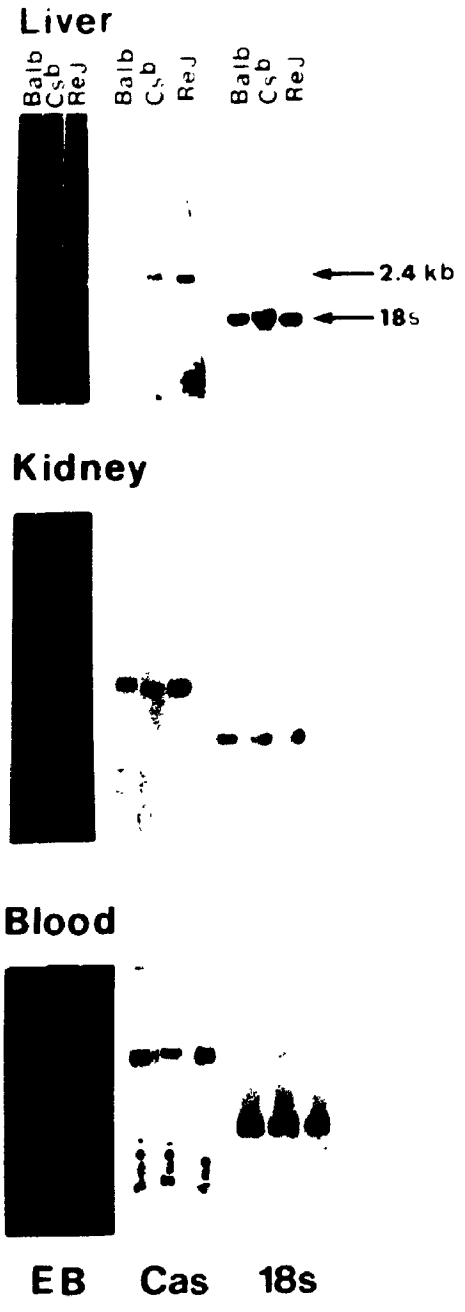
Liver
Balb
CsB
ReJ
Balb
CsB
ReJ
Balb
CsB
ReJ
2.4 kb
18s
Kidney
Blood
EB
Cas
18s

Figure 25. Dot blot results for catalase mRNA from liver, kidney and blood of BALB/c (Balb), C3H/HeAnl/*Cas-1*^{b} (Cs^{b}), and 129/ReJ (ReJ). Total cellular RNA from 3 individuals at three different quantities (10, 5 and 1 μg) from the three strains were denatured and blotted onto nylon membrane. Samples were hybridized with the *Cas-1* probe (Cat), followed by rehybridization with 18S rRNA probe (rRNA) as a control.

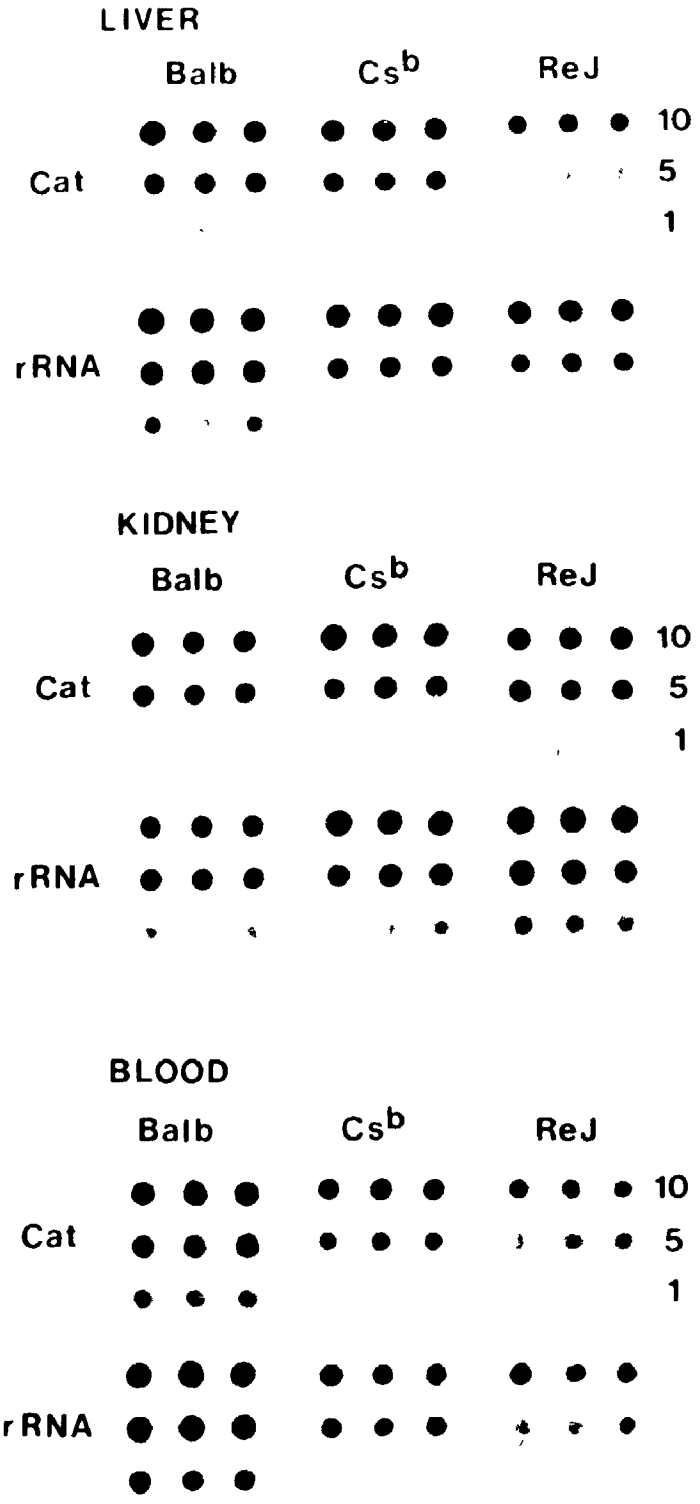
LIVER
Balb
Cs^b
ReJ
10
Cat
5
1
rRNA
KIDNEY
Balb
Cs^b
ReJ
10
Cat
5
1
rRNA
BLOOD
Balb
Cs^b
ReJ
10
Cat
5
1
rRNA

Table 3: Mean *Cas-1* mRNA levels ± S.E.M. (3 scans from each of 3 individuals) of liver, kidney and blood representative of normal (BALB/c), hypocatalasemic (129/ReJ) and acatalasemic (C3H/HeAnl/*Cas-1*^{b}) strains. Here, 1 µg and 10 µg of dot blotted total RNA was scanned three times for each individual using an LKB Densitometer and expressed as a ratio of *Cas-1* mRNA/18S rRNA present (control). A complete statistical analysis of mRNA levels is given in Appendix 1.

Strain	Tissue		
1 µg total RNA	Liver	Kidney	Blood
BALB/c	1.593 ± 0.172	0.720 ± 0.102	0.360 ± 0.073
129/ReJ	1.383 ± 0.072	0.534 ± 0.162	0.401 ± 0.032
C3H/HeAnl/*Cas-1*^{b}	1.487 ± 0.226	0.833 ± 0.190	0.436 ± 0.033
10 µg total RNA	Liver	Kidney	Blood
BALB/c	1.357 ± 0.125	0.827 ± 0.055	0.639 ± 0.188
129/ReJ	1.360 ± 0.01[illegible]	0.702 ± 0.195	0.712 ± 0.038
C3H/HeAnl/*Cas-1*^{b}	1.327 ± 0.041	0.902 ± 0.177	0.505 ± 0.096

Figure 26. Representative dot blot results for *Cas-1*-specific mRNA from total RNA (Total), mRNA associated with polysomes (P) and mRNA in the non-polysomal fraction (NP) from kidney of C3H/HeAnl/*Cas-1*^{a} (Cs^{a}), and C3H/HeAnl/*Cas-1*^{b} (Cs^{b}). Total cellular RNA (three replications), polysomal mRNA (two replications) at three different quantities (5, 2 and 1 μg) and non polysomal mRNA (two replications, the same volume as that of polysomal RNA) from the two strains were denatured and blotted onto nylon membrane. The blot was hybridized with the pMCT-1 probe and exposed to X-ray film overnight.

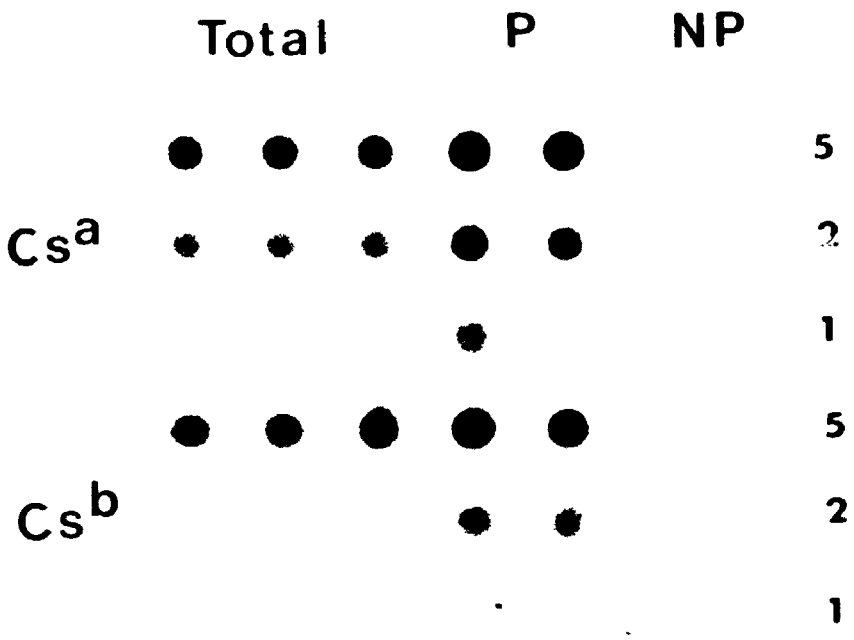
Total
P
NP
Cs^a
Cs^b
5
2
1
5
2
1

normal and acatalasemic strains. The effect of the tissue-specific mutation in C3H/HeAnl/*Cas-1^b* therefore must occur at a stage following the recruitment of the mRNA to the polysomes.

As the next logical step, catalase polypeptides from three tissues of representative strains of mice [BALB/c (normal), C3H/HeAnl/*Cas-1^b* (acatalasemic) and 129/ReJ (hypocatalasemic)] were evaluated by protein gel electrophoresis and western blot analysis. Figure 27A shows a Coomassie blue stained gel of protein from liver, kidney and blood of the three representative strains demonstrating comparable amounts of undegraded samples. A duplicate gel was transferred to a nitrocellulose membrane and reacted with an antihuman catalase antibody. The resulting western blot is shown in Figure 27B. It shows that the antibody used recognized mouse catalase as a single polypeptide comparable to the bovine catalase used as a control. This single polypeptide band was present in the liver of all genotypes. The presence of this polypeptide in the kidney and blood, however, is limited to the strains characterized as normal and hypocatalasemic only. Therefore, the absence of the catalase polypeptide in the kidney and blood of the acatalasemic mutants, must represent the basic feature of these genotypes. Densitometric scanning of western blots was performed to quantify the catalase-specific polypeptide levels in three tissues of normal (BALB/c), hypocatalasemic (129/ReJ and C57BL/6J) and acatalasemic (C3H/HeAnl/*Cas-1^b*) strains of mice. Appendix 2 contains data analysed to demonstrate linearity between protein quantity and polypeptide staining. Table 4 summarizes the results of the catalase polypeptide as compared to 100 ng of bovine catalase control. It is apparent that although the catalase polypeptide levels in liver do not differ significantly among strains ($p > 0.99$), the polypeptide is nearly absent in kidney and blood of C3H/HeAnl/*Cas-1^b*.

It is important to note that catalase polypeptides in the blood are predominantly located in red cells which largely contribute to the catalase enzyme activity observed in this tissue. Although blood is a heterogeneous tissue with a variety of cell types that possess specialized properties and functions, red blood cells make up a large portion of the tissue. These cells are enucleate and thus do not undergo active transcription, but the protein is expressed in these cells. Figure 28 shows a representative western blot of proteins isolated from red and white blood cells, compared to whole blood of the BALB/c mouse strain. Even when very large amounts of total protein from white blood cells are used few, if any, catalase polypeptide subunits are detected

Figure 27. Catalase polypeptide analysis of three tissues of BALB/c (B), 129/ReJ (R) and C3H/HeAnl/*Cas-1*^{b} (C). A: Total protein from liver (3 µg), kidney (4 µg) and blood (15 µg) was subjected to electrophoresis in a 10% SDS polyacrylamide gel with a 4% stacking gel and stained with Coomassie blue. B: The separated polypeptides from a duplicate gel were transferred to nitrocellulose membrane and reacted with a polyclonal anti-human catalase antibody to generate the western blot. Co = purified bovine catalase polypeptide, a positive control. Arrow shows catalase polypeptide.

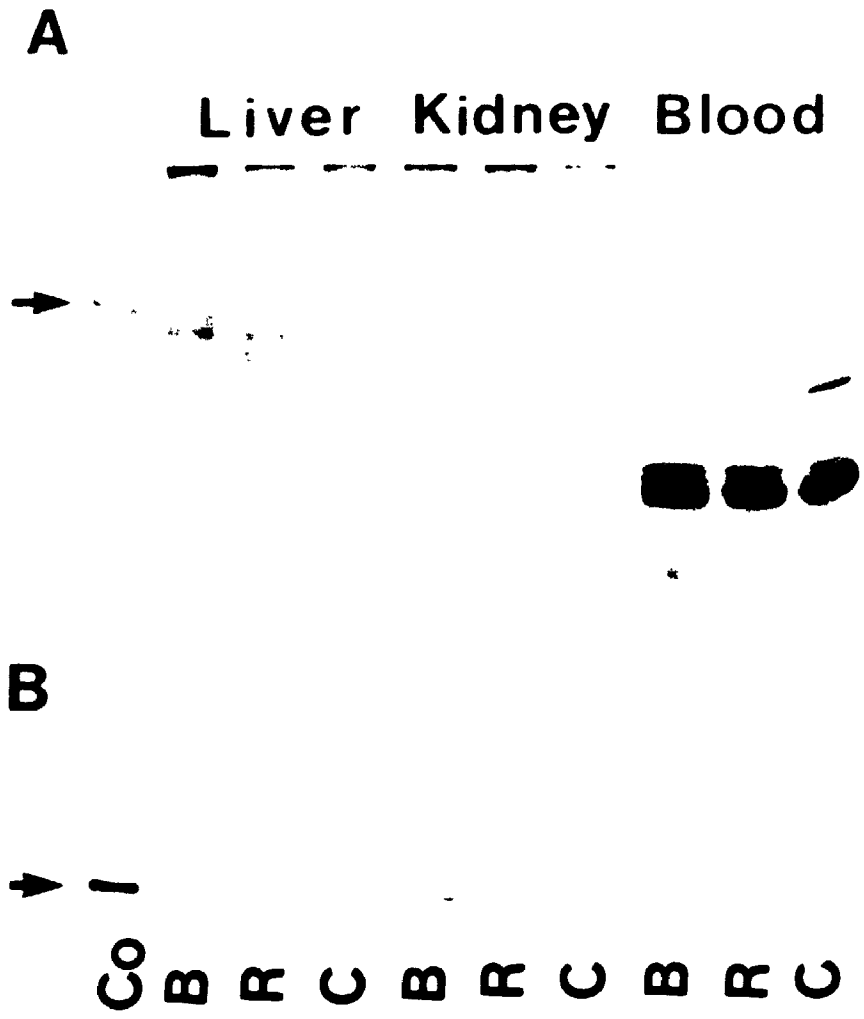
A
Liver Kidney Blood
B
Co B R C B R C B R C

Table 4: Mean *Cas-1* polypeptide levels ± S.E.M. (3 scans per band from 3 individuals) of liver, kidney and blood of normal (BALB/c), hypocatalasemic (C57BL/6J, 129/ReJ) and acatalasemic (C3H/HeAnl/*Cas-1^b*) strains of mice. Data are corrected for 100 ng bovine catalase control polypeptide and expressed per mg protein. ND = not detected.

	Polypeptide	No. Animals
LIVER		
BALB/c	0.652 ± 0.039	3
C57BL/6J	0.414 ± 0.033	3
129/ReJ	0.5[illegible] ± 0.046	3
C3H/HeAnl/*Cas-1^b*	0.660 ± 0.030	3
KIDNEY		
BALB/c	0.592 ± 0.046	3
C57BL/6J	0.352 ± 0.024	3
129/ReJ	0.409 ± 0.017	3
C3H/HeAnl/*Cas-1^b*	N.D.	5
BLOOD		
BALB/c	0.108 ± 0.014	3
C57BL/6J	0.250 ± 0.025	3
129/ReJ	0.197 ± 0.024	3
C3H/HeAnl/*Cas-1^b*	N.D.	3

Figure 28. Catalase polypeptide analysis of purified red blood cells (RBC), white blood cells (WBC) and whole blood from BALB/c (Balb). Protein samples from BALB/c blood (10 μg), RBCs (3.0 X 10^6 cells) and WBCs (3.0 X 10^4 cells) were separated on a 10% SDS polyacrylamide gel with a 4% stacking gel and stained with Coomassie blue (A). Protein samples from a duplicate gel were transferred to nitrocellulose and the western blot was generated (B). Arrow shows catalase polypeptide. C = bovine catalase control.

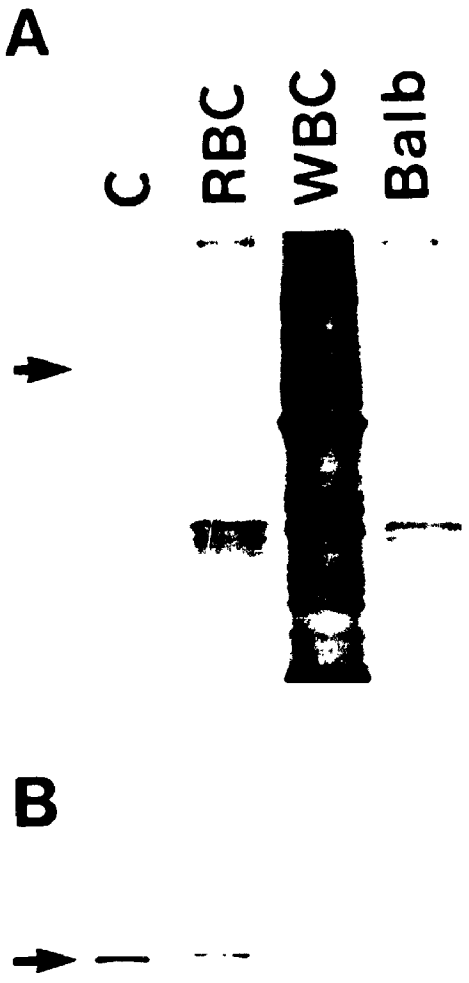
A
C
RBC
WBC
Balb
B

compared to whole blood and red blood cells. The blood-specific acatalasemic mutation therefore, could be specific to red blood cells.

Figure 29 summarizes the results on *Cas-1* expression in three tissues of three selected strains of mice [BALB/c (normal), 129/ReJ (hypocatalasemic) and C3H/HeAnl/*Cas-1*^{b} (acatalasemic)]. At the level of enzyme activity these strains are well characterized (Table 2; Schisler and Singh, 1987). The strains studied have comparable catalase activity in the liver but differ for the activity seen in the kidney and blood, the most obvious difference being the dramatic decrease in activity observed in the latter two tissues of C3H/HeAnl/*Cas-1*^{b}. Figure 29 also includes the quantitative analyses of mRNA levels from the tissues of these representative strains. It is apparent that the *Cas-1* mRNA, although tissue-specific (higher in liver than in kidney and blood), is not significantly different among genotypes for the three tissues ($p < 0.51$). On the other hand, western blot analysis shows that the three strains exhibit a unique and tissue-specific pattern of polypeptides. The results on the three tissues of the C3H/HeAnl/*Cas-1*^{b}, are of particular interest in this context. This strain has normal expression patterns (mRNA, polypeptide and enzyme activity) in the liver but an unusual pattern in kidney and blood. Although these two tissues have near normal levels of mRNA, there is no detectable polypeptide in kidney and blood. Comparisons of the catalase polypeptide levels with enzyme activity in all tissues among the three strains show a direct correlation between these two parameters, and is most evident in the kidney and blood of C3H/HeAnl/*Cas-1*^{b}. Moreover, the mRNA levels within each tissue do not correspond to the amount of polypeptide or enzyme activity levels.

Catalase activity determined by the method of Harris and Hopkinson (1976) yielded similar results. Figure 30A shows protein homogenates from liver, kidney and blood of the three representative strains separated in a polyacrylamide gel under non-denaturing conditions and stained for enzyme activity. The wide vertical bands observed for each tissue represent specific epigenetic modifications resulting in the production of variable isoforms as expected (Masters *et al.*, 1986). Comparison among the strains shows that catalase activity in C3H/HeAnl/*Cas-1*^{b} is low or absent in kidney and blood, which is consistent with the spectrophotometric assays. Under the electrophoretic conditions used here however, the catalase activity also appears to be low in the liver. Western blot analysis of the same proteins in their native conformation is presented in Figure 30B. In the livers of the three representative strains, the

Figure 29. A summary of results on tissue-specific *Cas-1* expression from three strains of mice representing normal (BALB/c), hypocatalasemic (129/ReJ) and acatalasemic (C3H/HeAnl/*Cas-1*^{b}) in liver (A), kidney (B), and blood (C).□ = mRNA (*Cas-1* /rRNA ± S.E.M.), ▨= enzyme activity (U/mg protein ± S.E.M.), ■ = polypeptide (catalase protein /mg protein ± S.E.M.). Note a drastic reduction/ absence of polypeptide and enzyme activity values in the kidney and blood for C3H/HeAnl/*Cas-1*^{b} only.

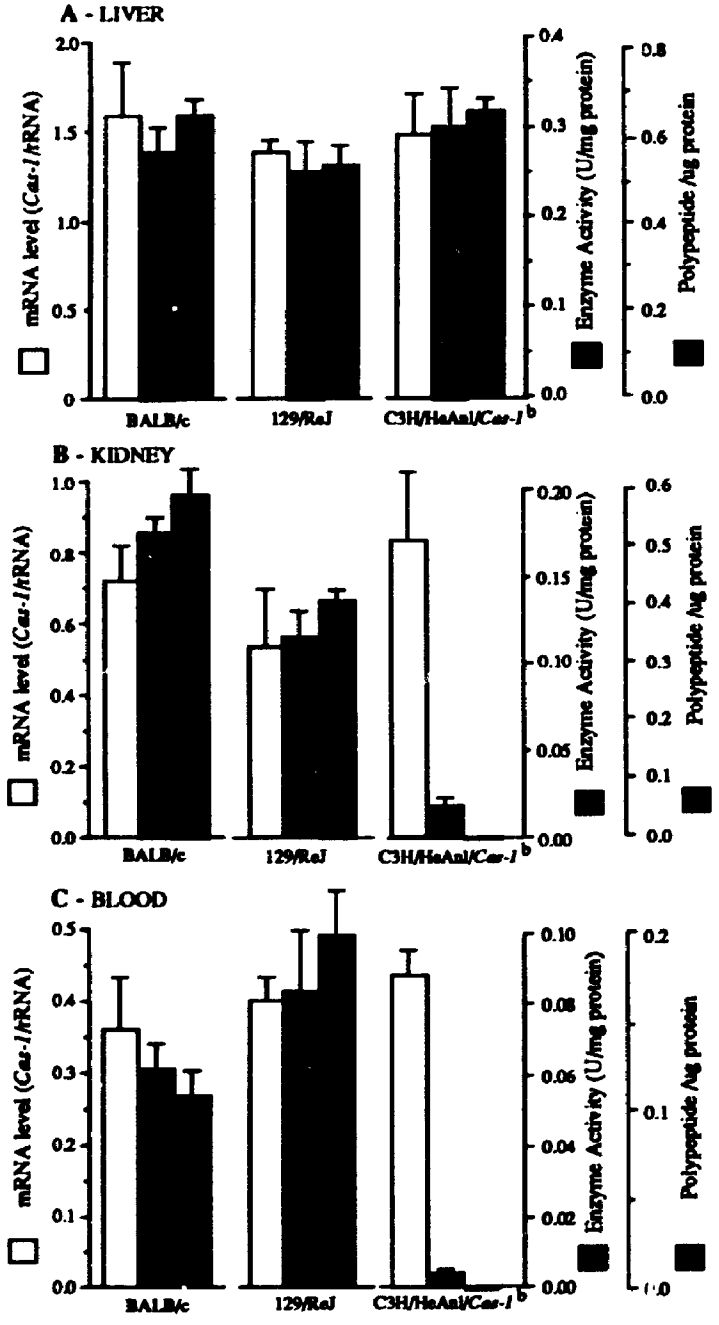
A - LIVER
mRNA level (Cas-1/hRNA)
Enzyme Activity (U/mg protein)
Polypeptide /ug protein
BALB/c
129/ReJ
C3H/HeAnl/Cas-1 b
B - KIDNEY
mRNA level (Cas-1/hRNA)
Enzyme Activity (U/mg protein)
Polypeptide /ug protein
BALB/c
129/ReJ
C3H/HeAnl/Cas-1 b
C - BLOOD
mRNA level (Cas-1/hRNA)
Enzyme Activity (U/mg protein)
Polypeptide /ug protein
BALB/c
129/ReJ
C3H/HeAnl/Cas-1 b

Figure 30. A: Catalase activity in liver, kidney and blood from representative individuals of BALB/c (Balb), C3H/HeAnl/*Cas-1*^{b} (Cs^{b}) and C57BL/6J (C57) visualized by staining the native protein in the polyacrylamide gel. B: Western blot analysis of native catalase protein from the same homogenates used in A. Co = bovine catalase control.

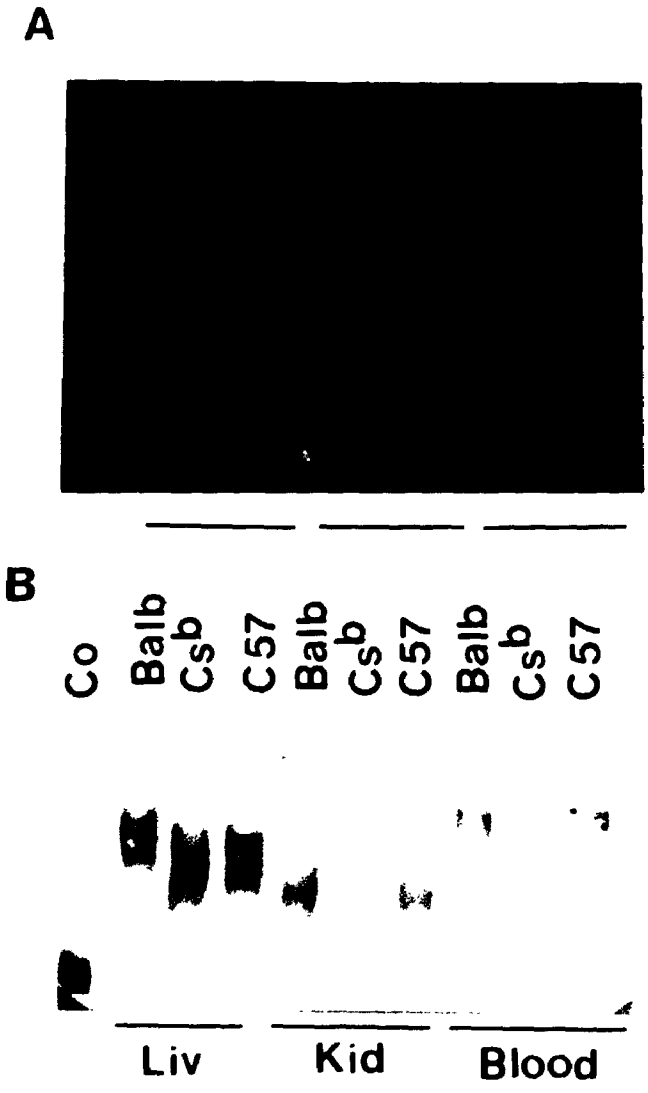
A
B
Co
Balb
Csb
C57
Balb
Csb
C57
Balb
Csb
C57
Liv
Kid
Blood

functional catalase protein appears to be intact, suggesting that the electrophoretic conditions used here may disrupt enzyme activity in the liver of C3H/HeAnl/*Cas-1^b* that is detectable in the spectrophotometric assay. In the kidney and blood of this acatalasemic strain, however, there is little or no evidence of catalase protein (Figure 30B). These data suggest that the catalase activity variation seen among the three strains is reflected in the differences seen at the level of the protein. This difference may result from variation at the level of posttranslational regulation and/or differential stability of the protein under certain physiological conditions.

The interest in the genetics of mouse catalase was initiated by reports on the drastic reduction of enzyme activity in the acatalasemic strain C3H/HeAnl/*Cas-1^b* generated following mutation and breeding (Feinstein *et al.*, 1966). Furthermore, this acatalasemic phenotype was established in a new genetic background and may provide additional biological material for the evaluation of the expression of the acatalasemic mutation. This recombinant inbred (R.I.) has been breeding true for more than 30 generations. It resulted from a mating between a female Swiss Webster and a male C3H/HeAnl/*Cas-1^b* and was used to study the genetic segregation of enzyme activity of catalase (Schisler and Singh, 1991). The resulting line SXC/ws-1 also possesses a newly arisen "belted" phenotype which was determined to be allelic to ABP/Le (*bt/bt*) by crossing and complementation experiments. Extensive biochemical and genetic characterization of SXC/ws-1 is described in Appendix 3. Figure 31 shows a representative animal from this line which is characterized by an irregular belt of albino hair located transversely across the back posterior to the midline on a black (dorsal)/ dark grey (ventral) background. A complete belt around the body is infrequent and most animals appear as shown. These animals breed true for the belted phenotype which behaves as an autosomal recessive trait. Preliminary screening of 13 mice from this R.I. line (10 males, 3 females) with the "fizz" test suggested that all animals were apparently negative for blood catalase activity. Three tissues (liver, kidney and blood) from three males each of the two parental strains [S.W. (normal) and C3H/HeAnl/*Cas-1^b* (acatalasemic)] and SXC/ws-1 were analyzed for catalase properties using a number of criteria. Figure 32 shows the level of catalase activity determined by spectrophotometry (A) and native polyacrylamide gel assay (B) accompanied by its Coomassie blue stained counterpart. As compared to S.W., catalase activities in C3H/HeAnl/*Cas-1^b* and SXC/ws-1 ranged from ~ 80% in liver, 10% in kidney and 6% in whole

Figure 31. Dorsal (A) and ventral (B) view of a typical 6-month old SXC/ws-1 (R.I.) mouse illustrating the white "belt" across the back posterior to the midline.

A

B

Figure 32. Catalase activity in liver, kidney and blood from Swiss Webster (S)., C3H/HeAnl/*Cas-1*^{b} (C) and SXC/ws-1 (CS). A: Mean catalase activity in the three tissues using the spectrophotometric assay (U/mg protein ± S.E.). B: Proteins from liver (30 µg), kidney (30 µg), and blood (50 µg) of representative individuals from the three genotypes were separated by electrophoresis under native conditions. Catalase activity was visualized using a colourimetric assay to detect native proteins within the polyacrylamide gel. A duplicate gel with homogenates from individuals in B was stained with Coomassie blue and is included. Bovine catalase control = 20 ng (Co).

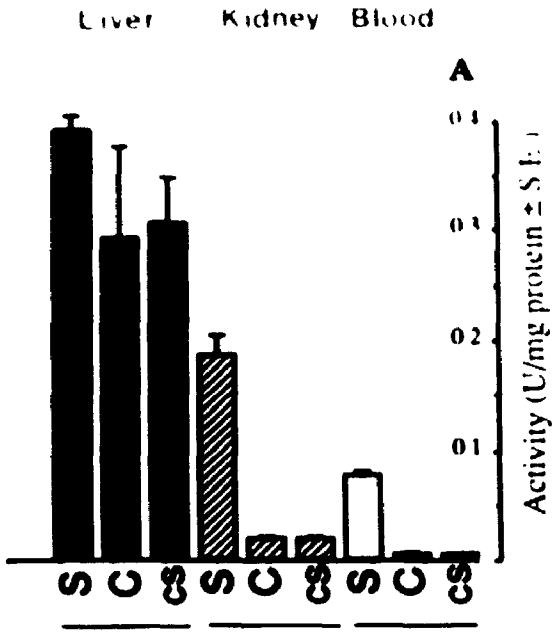
Liver
Kidney
Blood
A
0.4
0.3
0.2
0.1
Activity (U/mg protein ± S.E.)
S C CS S C CS S C CS

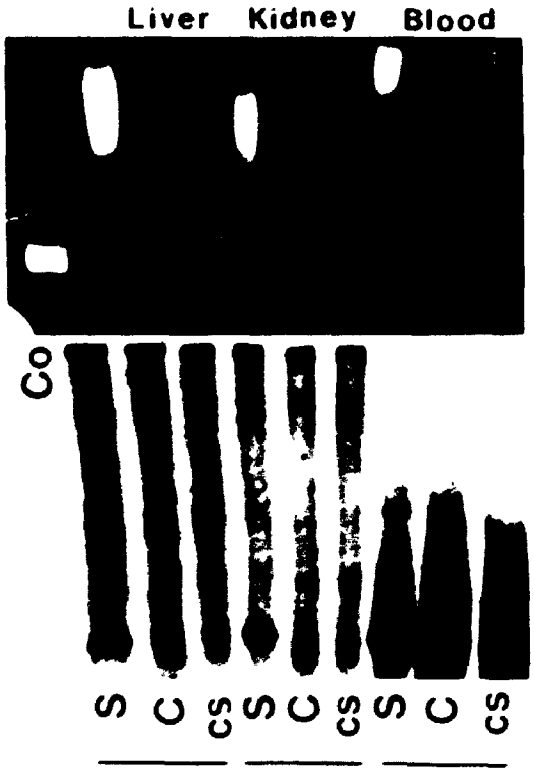
Liver
Kidney
Blood
Co
S C CS S C CS S C CS

blood lysate. The results on the native polyacrylamide gel show that the enzyme activities of the three tissues in C3H/HeAnl/*Cas-1*^{b} are similar to SXC/ws-1 and are dramatically reduced as compared to S.W.. Furthermore, western blot analysis of immunologically reactive catalase protein subunits in the three tissues showed a reduction in the polypeptide in C3H/HeAnl/*Cas-1*^{b} and SXC/ws-1 kidney as well as whole blood lysate (Figure 33B). Figure 33A is the coomassie blue stained polyacrylamide gel presented to demonstrate that the observed decrease in the catalase polypeptide is not a result of degraded protein or unequal sample loading. The quantitative results on different tissues of the known acatalasemic strain (C3H/HeAnl/*Cas-1*^{b}) are identical/ similar to the new line, SXC/ws-1 which suggest that the acatalasemic mutation has been successfully established in a novel genetic background. These homozygous genotypes may provide additional material for the evaluation of the tissue-specific expression of the acatalasemic mutation.

The results presented thus far suggest that the tissue-specific expression of this gene is explained by mRNA levels and is probably regulated transcriptionally. However, the strain differences must involve posttranscriptional regulation which may or may not be associated with the coding region of this polypeptide. A comprehensive experimental evaluation therefore must include the coding and non-coding UTR sequences.

a. Comparison of the *Cas-1* coding sequences among strains of mice:

Comparison of the coding sequence of BALB/c *Cas-1* to the coding region of three other mouse strains reveals a number of changes at the level of DNA and amino acids (Table 5). The coding region of the BALB/c *Cas-1* gene has greater than 99% sequence identity and the *Cas-1* protein has greater than 99% amino acid similarity to C3H/HeAnl/*Cas-1*^{a}, C3H/HeAnl/*Cas-1*^{b} and C57BL/6J. A total of nine nucleotide substitutions were identified among the four mouse strains which have well characterized catalase enzyme activity, four (44%) of which represent a C → G or C → T change. These nucleotide substitutions lead to five amino acid changes among the four strains, at positions 11, 97, 117, 316 and 350. The BALB/c sequence shows three amino acid differences when compared to the other three strains; glycine^{97} rather than alanine, valine^{316} rather than leucine and lysine^{350} rather than methionine. The potential impact of these amino acid differences on enzyme activity in this or any other strain is hypothetical and remains to be experimentally established. The remaining four

Figure 33. Catalase polypeptide analysis of three tissues of Swiss Webster (S), C3H/HeAnl/*Cas-1*^{b} (C) and SXC/ws-1 (CS). Total protein from liver (3 μg), kidney (4 μg) and blood (15 μg) was subjected to electrophoresis in a 10% SDS polyacrylamide gel with a 4% stacking gel and stained with Coomassie blue (A). The separated polypeptides from a duplicate gel were transferred to nitrocellulose membrane and reacted with a polyclonal antihuman catalase antibody to generate the western blot (B). Co = purified bovine catalase polypeptide, a positive control. Arrow shows catalase polypeptide.

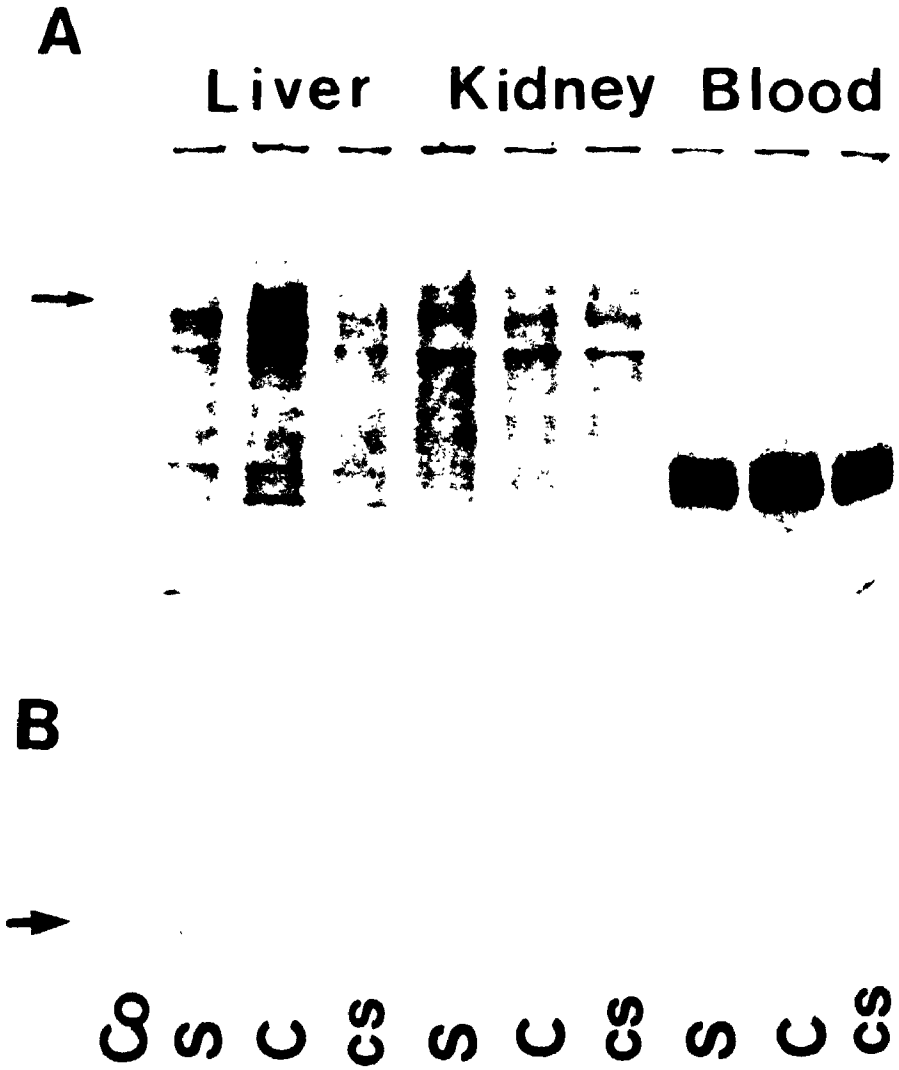
A
Liver
Kidney
Blood
B
S
C
CS
S
C
CS
S
C
CS

Table 5: Nucleotide and amino acid differences observed in catalase among strains of mice.

Strain	Amino Acid Position 11	24	97	112	117	316	350	452	464	Source
BALB/c	CAG Gln	CCT Pro	GGA Gly	CGG Arg	GCT Ala	GTG Val	AAG Lys	AAT Asn	GCC Ala	see Figure 5
Cas-1^{a}	CAG Gln	CCA Pro	GCA Ala	CGA Arg	GCT Ala	CTG Leu	ATG Met	AAT Asn	GCT Ala	Shaffer and Preston 1990
Cas-1^{b}	CAT His	CCA Pro	GCA Ala	CGA Arg	GCT Ala	CTG Leu	ATG Met	AAT Asn	GCT Ala	Shaffer and Preston 1990
C57BL/6J	CAG Gln	CCT Pro	GCA Ala	CGA Arg	ACT Thr	CTG Leu	ATG Met	AAC Asn	GCC Ala	Shaffer *et al.*, 1990

nucleotide substitutions at amino acid positions 24, 112, 452 and 464 result from a change in the wobble position and probably represent DNA polymorphisms that do not affect the polypeptide.

The coding region only of *Cas-1* from C3H/HeAnl/*Cas-1*^{b} has recently been reported, and compared to that of its congenic strain C3H/HeAnl/*Cas-1*^{a} (Table 5, Shaffer and Preston, 1990). It shows a single amino acid substitution (glutamine^{11} to histidine). If the observed amino acid change at position 11 is responsible for the acatalasemic phenotype, then it is possible that transient transfection of mutant cultured fibroblasts with the normal *Cas-1* gene could correct the defect. Preliminary experiments were performed to establish *in vitro* cultures of primary embryonic fibroblasts from the normal (C3H/HeAnl/*Cas-1*^{a}) and mutant (C3H/HeAnl/*Cas-1*^{b}) mouse strains. Western blot analysis of catalase polypeptide subunits from cultured primary embryonic fibroblasts from C3H/HeAnl/*Cas-1*^{a} demonstrated that even with increasing amounts of total protein (up to 30 μg), the production of the catalase protein appears to be substantially reduced or absent (data not shown). This suggests that the culture conditions used were not conducive for catalase production. As a result, this experimental approach was terminated. The contribution of the single amino acid substitution in C3H/HeAnl/*Cas-1*^{b} to the tissue-specific phenotype therefore remains to be experimentally demonstrated.

b. Comparison of *Cas-1* 3' UTR sequences among different strains of mice:

The 3' UTR of the mouse catalase gene (Figure 8) although not unusual with respect to size, has sequence features that are not commonly found in this region of genes and could be biologically significant. These features include near repeats of $(CA)_{31}$, $(T)_{15}$ and $(TGTGC)_{7}$. To determine the potential regulatory role of the 3' UTR in the expression of Cas-*1*, sequence comparisons were made from the region of the 3' UTR which contains these unusual repeats from eight mouse genotypes. Polymerase Chain Reaction (PCR) analysis using oligonucleotide primers 3 and 4 (Figure 8) was used to amplify a 328 bp fragment from BALB/c, 129/ReJ, C57BL/6J, C3H/S, C3H/HeAnl/*Cas-1*^{a}, C3H/HeAnl/*Cas-1*^{b}, Swiss Webster and the acatalasemic R.I. line SXC/ws-1. Figure 34A shows the presence of a single 328 bp band in seven inbred strains. To determine if there are base composition differences observed among those strains indicating sequence variation, single strand conformation polymorphism (SSCP) analysis was performed. Figure 34B shows two high molecular weight bands representing

Figure 34. A: PCR amplification of the 3' UTR from 7 strains of mice demonstrating the presence of a 328 bp fragment (arrow). B: Single strand conformation polymorphism (SSCP) analysis on PCR products from the 7 strains of mice. The 328 bp fragment of double stranded DNA is indicated by an arrowhead and the resulting single strands of DNA are shown by arrows. S = standard molecular weight (bp)

A

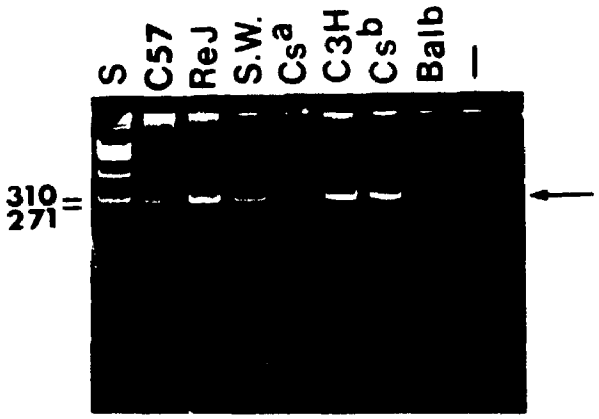
S
C57
ReJ
S.W.
Cs^a
C3H
Cs^b
Balb
—
310
271

B

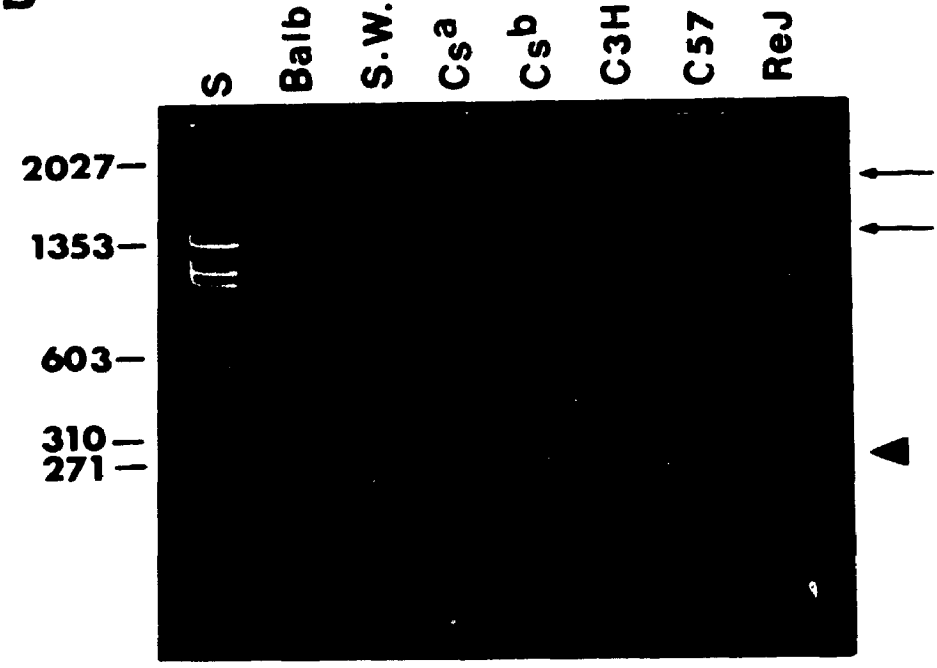
S
Balb
S.W.
Cs^a
Cs^b
C3H
C57
ReJ
2027
1353
603
310
271

the two single DNA strands in a unique conformation in each strain. These preliminary results show that no variation in base composition of the 3' UTRs exists among the strains tested. To confirm these results the PCR products from the seven strains and the R.I. line were subsequently cloned and sequenced in both directions. The three unusual repeats $(CA)_{31}$, $(TGTGC)_7$, and $(T)_{15}$ from all genotypes had identical sequences (data not shown). This suggests that some factor other than the primary sequence may be responsible for variation in gene expression of *Cas*-1. In addition, sequencing of 400 bp of the 3' terminus from a kidney cDNA library of C3H/HeAnl/*Cas-1*^{b} showed that this region is identical to that found in BALB/c. The conservation of sequences in this region of *Cas-1* suggests the potential functional importance in this species.

c. Evaluation of 3' UTR sequences in protein interactions: Possible role in posttranscriptional regulation:

The catalase-specific mRNA levels of kidney, liver and blood of the three mouse strains studied here are not significantly different, yet there is a significant difference in their enzyme activity and the level of polypeptide. This difference therefore could not be attributed to differential transcription or stability of the mRNA. Also, it is logical to argue that the tissue-specific differences in catalase activity observed among the genotypes studied could involve posttranscriptional regulation and may involve mRNA binding protein(s). Since the complete cDNA sequence of this mouse gene, including the 3' UTR is now known, gel mobility shift assays were performed involving labelled mRNA and strain-specific homogenates from different tissues. Such an experimental approach for the explanation of the posttranscriptional regulation of the mouse catalase is also supported by recent results on the rat catalase by Clerch and Massaro (1992). They have shown that the 3' UTR of rat catalase binds to specific protein(s) in *in vitro* experiments. Although the significance of this observation including the specificity of this binding remains to be established, they concluded that these proteins are involved in posttranscriptional regulation of the rat catalase.

The rat catalase 3' UTR is the only other mammalian catalase studied to date which is known to contain the three unusual repeats, namely $(CA)_{31}$, $(T)_{15}$ and $(TGTGC)_7$. Here, the T repeats are comparable in number while the CA repeat is much larger in the rat sequence (Furuta *et al.*, 1986). Interestingly, the pentamer TGTGC is not present in the 3' UTR of rat catalase and is unique to *Cas-1*.

Figure 35. Restriction maps of 7 cDNA fragments of *Cas-1* (solid line) which are transcribed (wavy line) and used in gel mobility shift assays. RNA 1 is ~1300 nt long and includes the entire 3' UTR plus ~435 nt encoding the last 145 amino acids. RNA 2 contains ~470 nt of the 3' UTR. RNA 3 consists of ~420 nt of the 3' UTR; the poly (A) tail has been removed. RNA 4 is 190 nt long and consists primarily of $(CA)_{31}$ from the 3' UTR of *Cas-1*. RNAs 5 (134 nt), 6 (34 nt) and 7 (140 nt) contain three unusual near repeats $(CA)_{31}$, $(U)_{15}$, and $(UGUGC)_7$ respectively. Partial cDNAs which produce RNA transcripts 5, 6 and 7 were subcloned into the *Eco* RI site of pGEM 3Z to minimize vector sequences in the transcripts. Others were subcloned into pBluescript (SK^-). T7 and T3 represent promoter sites for RNA polymerase. Restriction enzymes: A, *Ava* II; Ap, *Apa* I; B, *Bam* HI; D, *Dra* II; E, *Eco* RI; EV, *Eco* RV; H, *Hind* III; K, *Kpn* I; M, *Mbo* II; Mn, *Mnl* I; N, *Nsi* I; P, *Pst* I; S, *Sma* I; X, *Xba* I; Xh, *Xho* I.

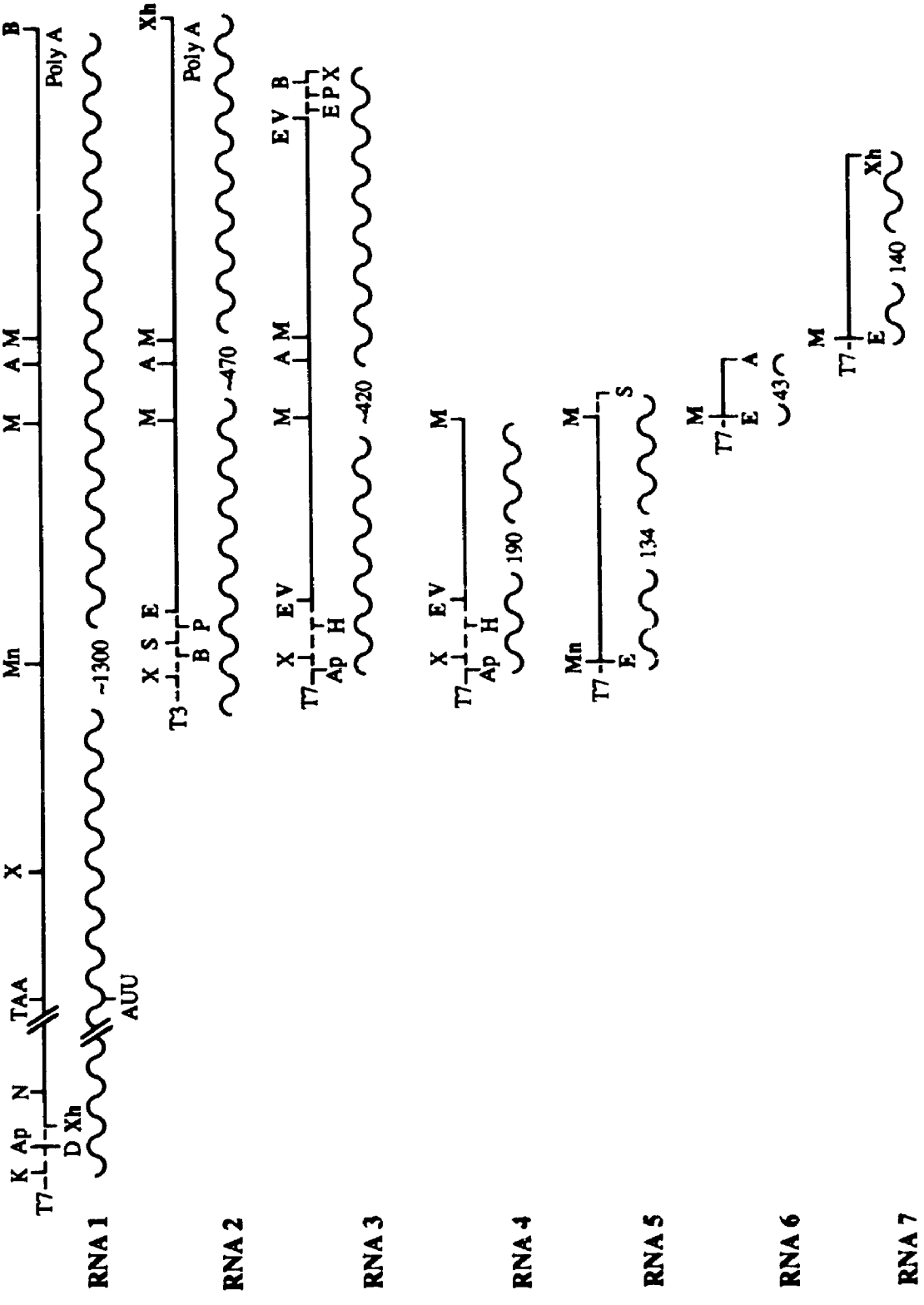
RNA 1
K Ap N
T7
D Xh
TAA
AUU
X
Mn
M A M
B
Poly A
~1300
RNA 2
X S E
T3
B P
M A M
Xh
Poly A
~470
RNA 3
X E V
T7
Ap H
M A M
E V B
T T
E P X
~420
RNA 4
X E V
T7
Ap H
M
190
RNA 5
Mn
T7
E
M
S
134
RNA 6
M
T7
E A
~43
RNA 7
M
T7
E
Xh
140

Demonstration of mouse catalase mRNA-protein complexes:

In this study, different regions of the mouse catalase 3' UTR were evaluated for their ability to recognize and bind to proteins in different tissue homogenates. Figure 35 shows 7 fragments cloned into pBluescript or pGEM 3Z representing regions of the mouse catalase cDNA clone pMCT-1. They were used to generate specific cRNAs by transcription reactions. RNA 1, the longest transcript (~1300 nt) contains the entire 3' UTR (752 nt) including the poly (A) tail plus the last 435 bases of the encoding mRNA. This transcript was used in preliminary experiments to demonstrate the presence of mRNA-protein complexes. RNA 2 contains only the 3' UTR including the poly (A) tail (~470 nt). The poly (A) tail was subsequently removed and the resulting transcript (RNA 3) contains only ~420 nt of the 3' UTR. RNA transcripts 1, 2 and 3 contain the three unusual features of this region of *Cas-1* [$(CA)_{31}$, $(U)_{15}$, and $(UGUGC)_7$] identified and discussed earlier. RNA 4 (190 nt) is a transcript which resulted from the removal of $(U)_{15}$ and $(UGUGC)_7$ from the 3' UTR and contains only the near repeat $(CA)_{31}$. All strain and tissue comparisons were made using small RNA transcripts specific to each of the three unusual regions (RNAs 5, 6 and 7). RNA 5 consists only of the mouse catalase $(CA)_{31}$ sequence (134 nt) while RNA 6 contains 43 nt of $(U)_{15}$ and RNA 7 the $(UGUGC)_7$ repeat (140 nt). In addition, a 1500 nt transcript from the rat catalase gene containing the 3' UTR (Clerch and Massaro, 1992) was used to establish and refine optimal conditions for the formation of mRNA-protein complexes.

The gel mobility shift results from preliminary experiments with ^{32}P-labelled RNA 1 and neonatal mouse lung homogenate (S.W.) are shown in Figure 36. A single band is observed. A similar band shift is also observed with the rat neonatal lung homogenate. The formation of this complex decreases upon competition with increasing amounts of unlabelled RNA 1 transcript (Figure 36A) while addition of a non-specific competitor RNA (tRNA) does not affect the formation of the complex (Figure 36B). Figure 36B also demonstrates that the factor which binds to RNA 1 is protein in nature since pre-incubation of the tissue homogenate with proteinase K eliminates all evidence of the complex. Such results argue that the homogenate factor involved in the slow migrating mRNA complex is(are) protein(s) which recognize and bind to mRNA in a sequence-specific manner. Interestingly, when rat neonatal lung homogenate or S.W. neonatal lung homogenate were incubated with the ^{32}P-labelled rat RNA

Figure 36. Gel mobility shift assay involving ^{32}P-labelled RNA 1 and lung homogenates from neonatal mouse (S.W.) and neonatal rat (Rat). A: Competition assay with increasing amounts of unlabelled RNA 1 (100, 200 and 600 ng). B: Incubation of the mouse homogenate with non-specific competitor (tRNA) and pre-incubation of the homogenate with proteinase K (PK). Arrows show mouse catalase mRNA-protein complex. RNA 1 = transcript with no homogenate added (control). C: Gel shift assay involving protein homogenates and the rat catalase probe (control) showing three complexes (arrowheads). Brackets indicate free RNA probe.

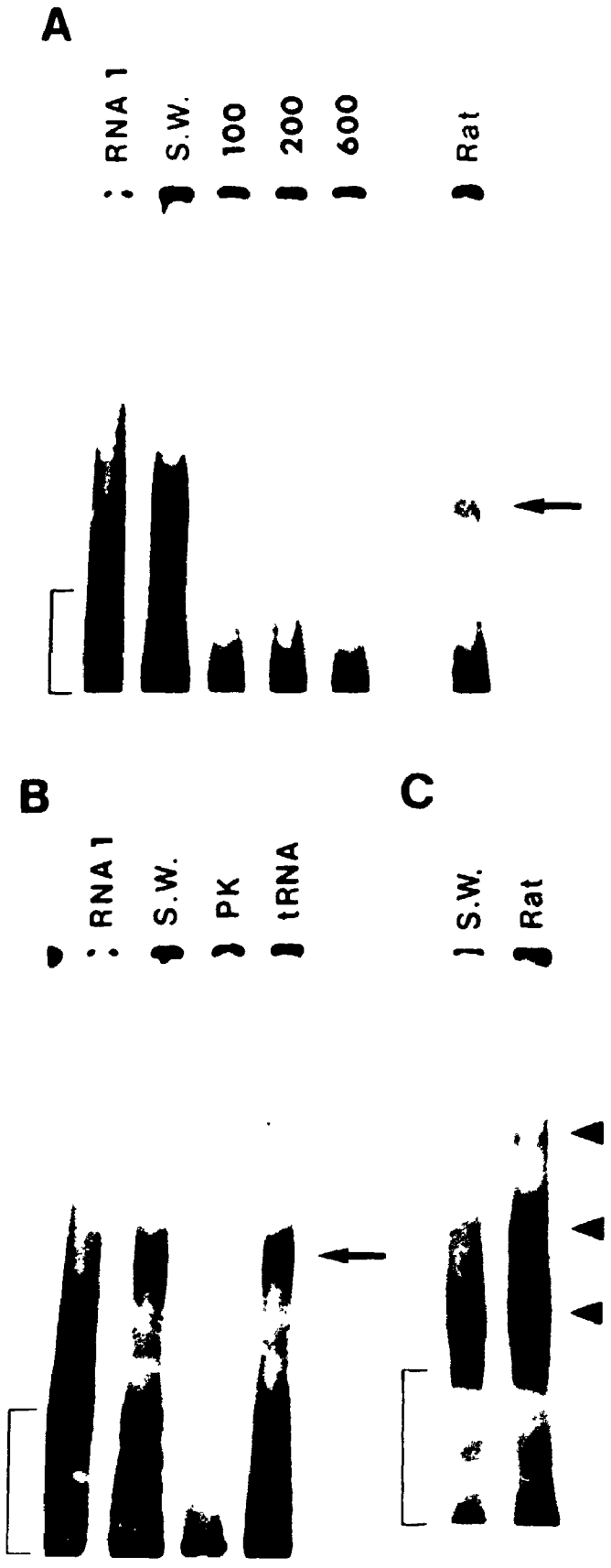
A
RNA 1
S.W.
100
200
600
Rat
B
RNA 1
S.W.
PK
tRNA
C
S.W.
Rat

(control), 3 complexes were observed (Figure 36C). It may be pointed out that the sequence of the rat catalase 3' UTR is not identical to the mouse 3' UTR. The formation of mRNA-protein complexes therefore must be specific to the sequence of the RNA transcript used.

Sequence-specificity of mRNA-protein complexes:

To determine what specific sequence of the mouse catalase mRNA is specific to protein bindings, ^{32}P-labelled mRNAs with specific regions of the 3' UTR (Figure 35) were used in gel mobility shift assays. RNAs 2, 3 and 4 were used in such assays under the same experimental conditions as used for RNA 1. Figure 37 shows the experimental results on RNA 2 [~470 nt of 3' UTR + poly (A) tail], RNA 3 [~420 nt of 3' UTR lacking poly (A) tail], and RNA 4 [190 nt of 3' UTR containing only $(CA)_{31}$]. This figure also includes uncut RNA transcripts (U) and incubations of the transcripts with RNase T1 in the absence of the homogenate (control - T1). RNase T1 specifically attacks the 3' phosphate groups of G residues and cleaves the 5' phosphate linkage of the adjacent nucleotide. Numerous pieces of different sized RNAs can result and appear as partial digestion products not seen in the presence of the homogenate. Comparable patterns are observed in the T1 control lanes of RNAs 2 and 3 since the nucleotide composition and length of the intact RNAs are similar and differ only with respect to the poly (A) tail. In mRNA-protein binding experiments, however, RNase T1 will cleave all RNA probe not protected by bound protein. When incubated with S.W. neonatal lung homogenate, each labelled RNA transcript yields a single complex migrating to a similar position in the gel. This complex appears similar to the complex observed for RNA 1. It is interesting to note that three complexes were observed when the labelled rat RNA was incubated with rat neonatal lung homogenate (positive control). Although the significance of the results are unknown, these experiments establish the presence of protein(s) which bind to the 3' UTR of *Cas-1*.

To further evaluate the 3' UTR sequence-specificity in protein recognition and binding, three specific sequences from the *Cas-1* 3' UTR [$(CA)_{31}$, $(U)_{15}$ and $(UGUGC)_7$] were evaluated. cDNAs consisting of each of the sequences $(CA)_{31}$, $(T)_{15}$ and $(TGTGC)_7$ were subcloned into pGEM 3Z. The ^{32}P-labelled mRNA transcripts 5, 6 and 7 were subjected to electrophoresis on a 4% polyacrylamide gel, eluted and further purified from this matrix and used in the mRNA-protein gel shift assay. Figure 38A shows the relative size and demonstrates the production of complete and undegraded transcripts used in all subsequent experiments.

Figure 37. Gel mobility shift assay involving incubation of RNAs 2, 3 and 4 with mouse neonatal lung homogenate (S.W.) Open arrows (left) represent uncut transcript (U) and dotted line indicates partial digestion of the transcript with RNase T1 in the absence of protein homogenate (T1). Arrows (right) indicate a single mRNA-protein complex. Rat catalase transcript incubated with rat neonatal lung homogenate was used as a control (Rat) and yields three complexes (arrowheads). Free RNA is shown in brackets.

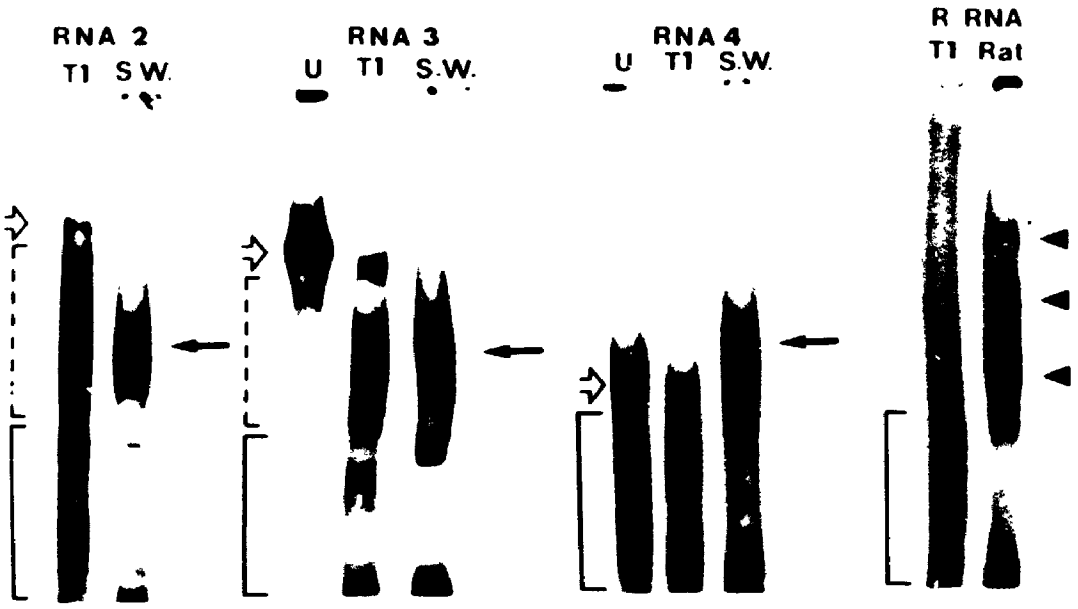
RNA 2
T1 S.W.
RNA 3
U T1 S.W.
RNA 4
U T1 S.W.
R RNA
T1 Rat

Figure 38. A: ^{32}P-labelled RNA 5 [containing $(CA)_{31}$ - 134 nt], RNA 6 [containing $(U)_{15}$ - 43 nt] and RNA 7 [containing $(UGUGC)_7$ - 140 nt] separated on an 8% polyacrylamide gel prior to purification. B: Gel mobility shift assay involving RNAs 5, 6 and 7 incubated with mouse (S.W.) neonatal lung homogenate. At least two complexes (a, b) and (x, y) are identified which involve protein homogenates with RNA 5 and RNA 6 respectively. Free RNA is indicated by brackets.

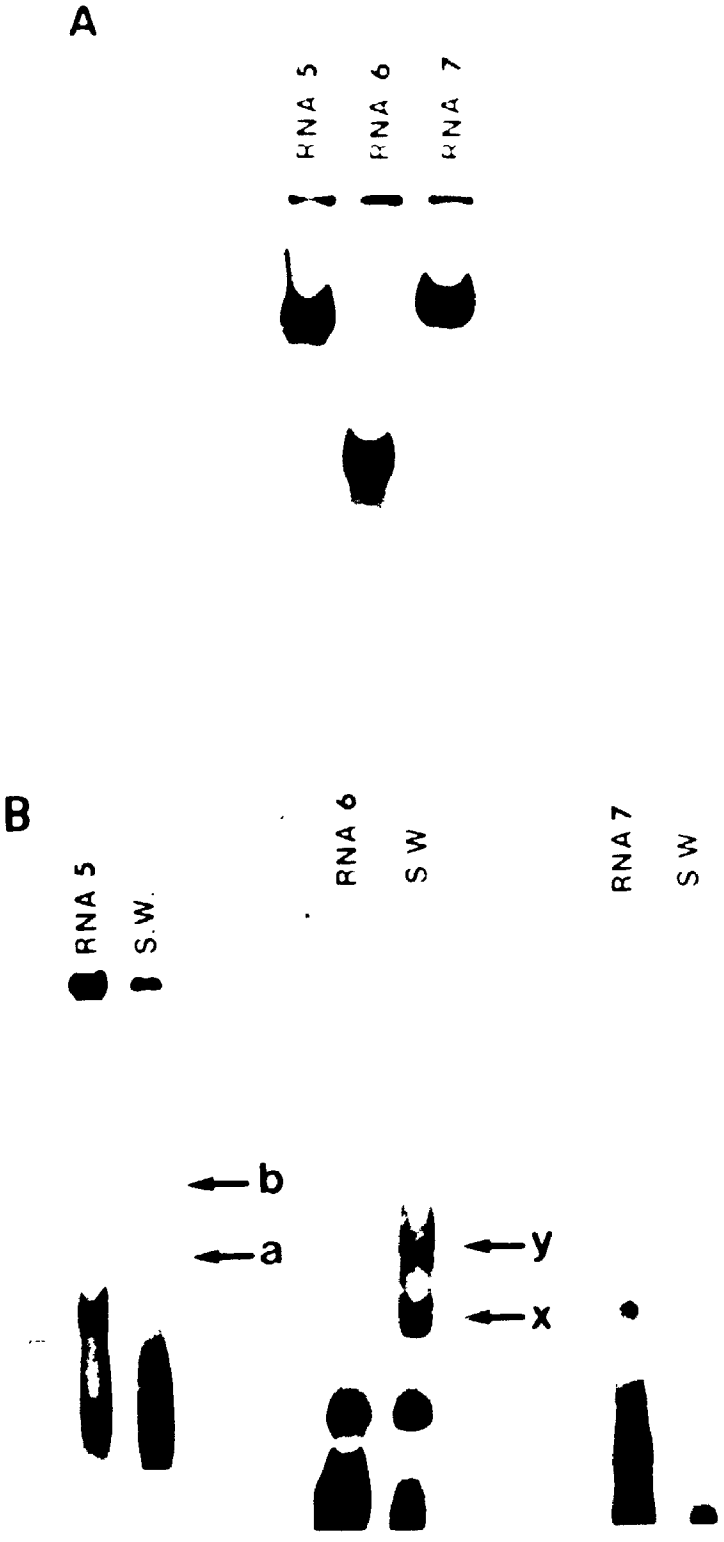
A
RNA 5
RNA 6
RNA 7
B
RNA 5
S.W.
RNA 6
S W
RNA 7
S W
b
a
y
x

Figure 38B shows that at least two complexes (a, b) are resolvable when S.W. neonatal lung homogenate was incubated with RNA 5, which is small (134 nt) and consists mainly of $(CA)_{31}$. Similarly, when RNA 6 (43 nt fragment which contains $(U)_{15}$) was used in the gel shift assay with the same lung homogenate, two different complexes are seen (x, y - Figure 38B). Under the conditions used in these assays, no mRNA-protein complexes were observed with the use of RNA 7 [140 nt of $(UGUGC)_7$] in repeated experiments.

Additional refinements and specific competition assays were performed to establish the sequence-specificity of the observed mRNA-binding proteins. Competition experiments involved incubating ^{32}P-labelled RNA transcripts with the protein homogenate in the presence of increasing amounts of the same unlabelled transcripts. The protein homogenate used in these experiments was from adult S.W. liver, since the complexes formed were better resolved than those from the neonatal lung. Figure 39A shows the presence of 3 mRNA-protein complexes when RNA 5 is incubated with the liver homogenate (Figure 39A: a,b and c). Incubation of ^{32}P-labelled RNA 5 and the protein homogenate in the presence of unlabelled $(CA)_{31}$ transcript shows a consistent decrease in the intensity of the three complexes at increasing concentrations of unlabelled RNA. These data show that the formation of these complexes is sequence-specific. Addition of a non-competitor (tRNA) to the incubation mixture has no effect on these complexes. Pre-incubation of the homogenate with proteinase K (PK) eliminates all traces of complex formation, suggesting that the observed complexes have a protein(s) component. Figure 39B shows similar results with RNA 6 which contains $(U)_{15}$ and three complexes are identified (x, y and z). The sequence-specificity of binding was demonstrated by a decrease in complex formation following incubation of ^{32}P-labelled RNA 6 with homogenate and unlabelled RNA 6 transcripts. Incubation in the presence of the non-competitor tRNA does not affect the complexes and pre-incubation of the homogenate with proteinase K eliminates all mRNA-protein complexes. No complexes were formed with RNA 7 which contains $(UGUGC)_7$ under the conditions used here (Figure 39C). The nucleotide sequence of the two RNAs (5 and 6) that recognize proteins in tissue homogenates and yield complexes in gel shift assays are presented in Figure 40. Both RNA 5 and RNA 6 consist of sequences that lack the potential to form secondary structures. This may suggest that protein(s) involved recognize these regions in a sequence- rather than structure-specific manner.

Figure 39. A: Gel mobility shift assay involving labelled RNA 5 and mouse (S.W.) liver homogenate yields three complexes (a, b and c). Competition assay involving increasing amounts of unlabelled RNA 5 (36, 360 and 3600 ng), non-specific competitor yeast tRNA or pre-incubation of homogenate with proteinase K (PK). B: Gel mobility shift assay involving labelled RNA 6 and mouse (S.W.) adult liver homogenate produces three complexes (x, y and z). Competition assay using increasing amounts of unlabelled RNA 6 (40, 400 and 4000 ng), yeast tRNA or pretreatment of the homogenate with proteinase K (PK). C: Gel mobility shift assay involving labelled RNA 7 and mouse (S.W.) adult liver homogenate. Free probe is indicated by brackets.

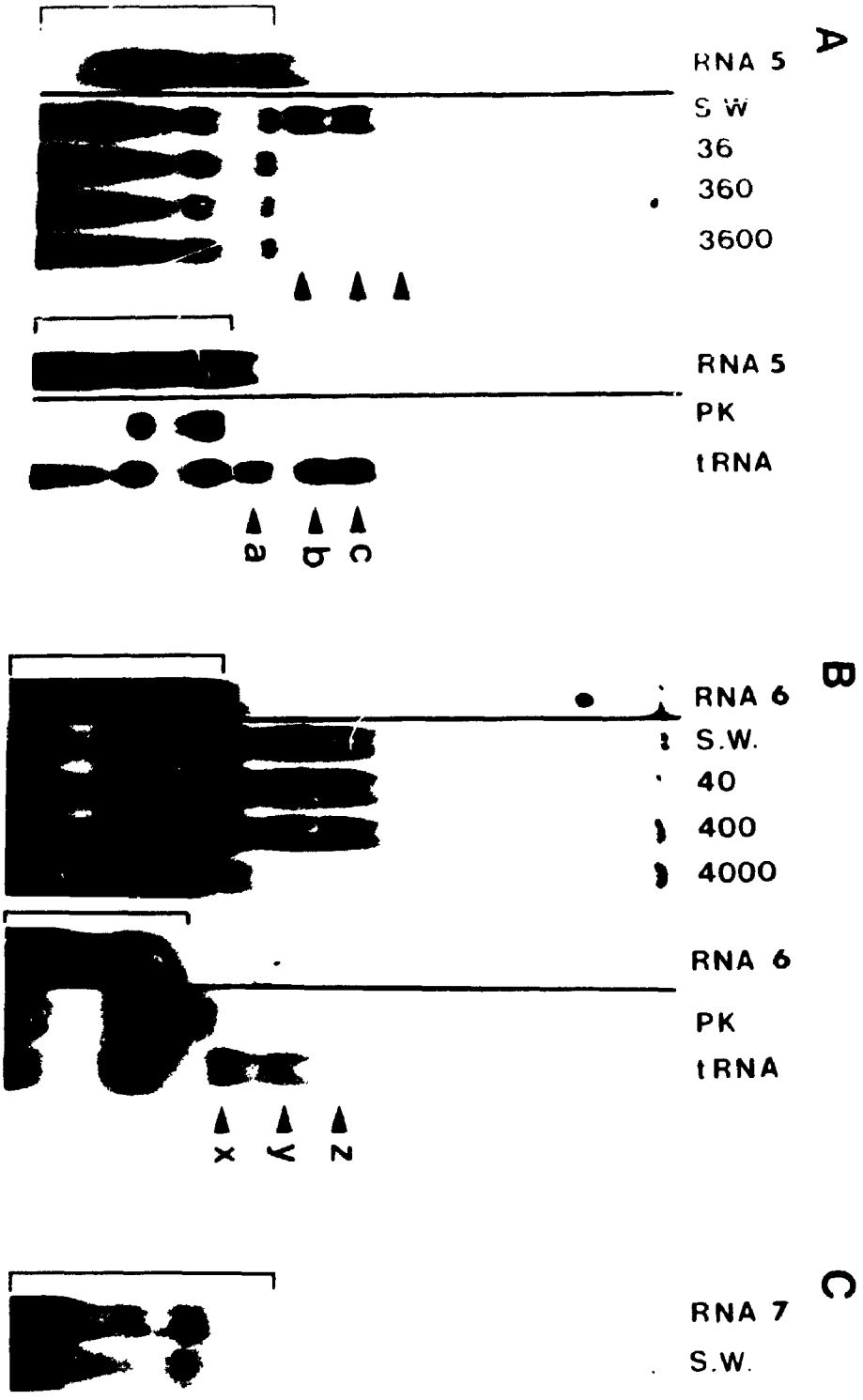
A
RNA 5
S W
36
360
3600
RNA 5
PK
tRNA
a
b
c
B
RNA 6
S.W.
40
400
4000
RNA 6
PK
tRNA
x
y
z
C
RNA 7
S.W.

Figure 40. Sequence of RNA transcripts 5 and 6 involved in the sequence-specific formation of protein(s) complexes. The cDNAs were cloned into the vector pGEM 3Z and transcripts synthesized using the T7 promoter. Vector sequences contained in the transcripts are underlined.

RNA 5

T7 GGGCG GGUAUAUAUACAAUACAACACACAUACCACACACACACACACA
UGCAAUACACACACUACACACACAUACACACACUCACACACACUCAUAC
ACACACAUGAAGAGAUGAUAA UUCGAGCUCGGUACCC

RNA 6

T7 GGGCG GCCCACUCAGAAUUUUUUUUUUAUUUUUCUAAG

To determine whether the protein(s) that are binding to the $(CA)_{31}$ containing mouse catalase mRNA (RNA 5) are different than those that are binding to the $(U)_{15}$ containing mRNA (RNA 6), cross competition experiments were performed. Figure 41A shows that when labelled RNA 5 was incubated with the mouse liver homogenate in the presence of an excess of unlabelled RNA 6, the three complexes (a, b and c) specific to RNA 5 were unaffected. Similarly when labelled RNA 6 was incubated with the same homogenate in the presence of an excess of unlabelled RNA 5, the formation of complexes x, y and z specific to RNA 6 were unaffected (Figure 41B). This suggests that the protein(s) which bind to RNA 5 are apparently different than those that recognize and bind to RNA 6-specific sequences.

Tissue-specificity of catalase mRNA-binding protein(s) in genetic strains of mice:

One of the objectives of this research, was to identify the molecular mechanisms involved in tissue-specific *Cas-1* expression among different genetic strains of mice. Having determined the sequence-specificity of RNAs 5 and 6 involved in the mRNA-protein binding complex formation, it was of interest to investigate the formation of these complexes in different tissues from mice of different genetic backgrounds. Variation in mRNA-protein binding complexes among strains could explain differences in *Cas-1* regulation at the level of translation or later.

Adult tissues (liver, kidney and lung) from five strains of mice representing normal (S.W., C3H/HeAnl/*Cas-1*^{a}), hypocatalasemic (C57BL/6J and 129/ReJ) and acatalasemic (C3H/HeAnl/*Cas-1*^{b}) were evaluated for the formation of mRNA-protein binding complexes using RNAs 5, 6 and 7 [containing the near repeats $(CA)_{31}$, $(U)_{15}$ and $(UGUGC)_7$ respectively)]. Figure 42A shows the presence of three mRNA-binding complexes (a, b and c) when labelled RNA 5 is incubated with homogenates from adult liver and kidney of all five strains. However, such complexes are absent when adult lung tissue homogenate was used from any strain in such experiments. The mRNA-protein binding complexes observed using neonatal lung homogenates were not consistently observed and were therefore not included in this experiment. The observed differences in mRNA-protein complexes among tissues is not commonly reported in the literature. Characterization of catalase mRNA-protein complexes was also evaluated on red blood cells, a tissue where the acatalasemic phenotype is manifested in mice. Figure 42B shows the presence of three complexes (arrows)

Figure 41. Gel mobility shift assay involving mouse (S.W.) liver homogenate and RNA 5 yielding complexes a, b and c and RNA 6 yielding complexes x, y and z. A: Cross competition assay involving the addition of unlabelled RNA 6 (4.0 and 8.0 μg) to the incubation mixture containing labelled RNA 5. B: Cross competition assay involving the addition of unlabelled RNA 5 (3.6 and 7.2 μg) to the incubation mixture containing labelled RNA 6. Free probe is indicated by brackets.

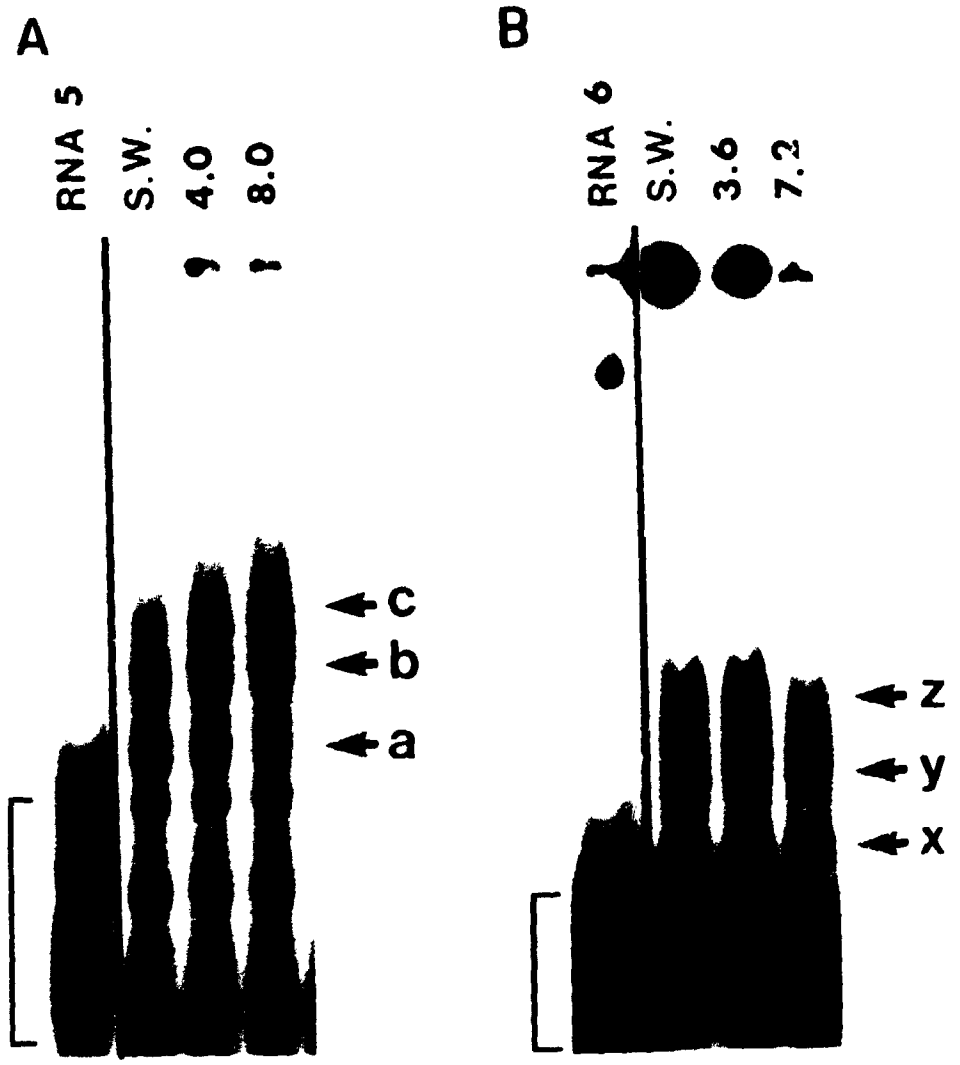
A
RNA 5
S.W.
4.0
8.0
c
b
a
B
RNA 6
S.W.
3.6
7.2
z
y
x

Figure 42. Gel mobility shift assay involving incubation of labelled RNA 5 [containing $(CA)_{31}$] with homogenates from adult liver, kidney and lung from 5 strains of mice and rat neonatal lung as a control (A). Complexes a, b and c are marked. B: Gel mobility shift assay involving RNA 5 and protein homogenate from red blood cells of acatalasemic (Cs^b) and normal (Cs^a) mouse strains. Three complexes are indicated by arrows. Free probe is bracketed.


A
RNA 5
Rat
S W
C57
Cs^a
Cs^b
ReJ
S.W.
C57
Cs^a
Cs^b
ReJ
S.W.
C57
Cs^a
Cs^b
ReJ
Liver
Kidney
Lung
a
b
c
B
RNA 5
Cs^b
Cs^a
RBC

in two strains [(C3H/HeAnl/*Cas-1*^{a}) Cs^a and (C3H/HeAnl/*Cas-1*^{b}) Cs^b] that differ in catalase enzyme and protein levels. Interestingly, the migration of the complexes differs from that of kidney and liver, and may represent the presence of different protein(s) involved in tissue-specific expression. It is clear however, that there is no difference in the migration of the complexes between the acatalasemic strain Cs^b and its normal congenic counterpart.

Figure 43 shows a similar experiment with labelled RNA 6. The formation of complexes x, y and z are consistently observed when RNA 6 is incubated with liver, kidney or lung homogenates from the five mouse strains (Figure 43A). Neonatal lung homogenate from two strains (S.W. and C57) also shows the presence of protein complexes. Catalase mRNA-protein complexes specific to RNA 6 were also evaluated in red blood cells of the acatalasemic strain [(C3H/HeAnl/*Cas-1*^{b}) Cs^b] and the normal control [(C3H/HeAnl/*Cas-1*^{a}) Cs^a]. Figure 43B shows the presence of three complexes (arrows) which may or may not be the same as those identified in liver, kidney or lung. Although there is no strain variation observed in the migration of the liver- and RBC-specific complexes, protein complexes y and z of kidney appear variable among strains. A similar strain variation in the formation of these two complexes is apparent in lung homogenates as well. The migration patterns of y and z complexes is also variable between neonatal and adult lung homogenates.

As a negative control towards the substantiation of these observations, ^{32}P-labelled RNA 7 was used in gel mobility shift assays with adult liver, kidney and lung homogenates from the five mouse strains under the same experimental conditions. The results of such an experiment are presented in Figure 44 and shows that no complexes are observed in any tissue and strain investigated. It is therefore concluded that the $(CA)_{31}$- and $(U)_{15}$- specific sequences of the mouse catalase mRNA are primary sites for recognition and binding by mRNA-binding proteins. They may be expressed in a tissue-specific manner, follow a developmental course and differ among genotypes.

Characterization of *Cas-1* 3' UTR binding proteins:

Further characterization of the proteins involved in the formation of catalase mRNA binding complexes specific to RNA 5 was evaluated in liver, kidney and red blood cells from inbred mice including the acatalasemic and normal strains (Cs^b and Cs^a respectively). The protein(s) associated with this transcript were UV cross-linked and separated on a 10% SDS polyacrylamide gel to determine the number and sizes of the protein(s) involved. Figure 45 shows

Figure 43. A: Gel mobility shift assay involving incubation of labelled RNA 6 [containing $(U)_{15}$] with homogenates from adult liver, kidney and lung from 5 strains of mice. Neonatal mouse homogenates (S.W.) and (C57) are included for comparison and rat neonatal lung homogenate as a control (Rat). Complexes x, y and z are marked. B: Gel mobility shift assay involving RNA 6 and protein homogenate from red blood cells of acatalasemic (Cs^b) and normal (Cs^a) mouse strains. Three complexes are indicated by arrows. Free probe is bracketed.

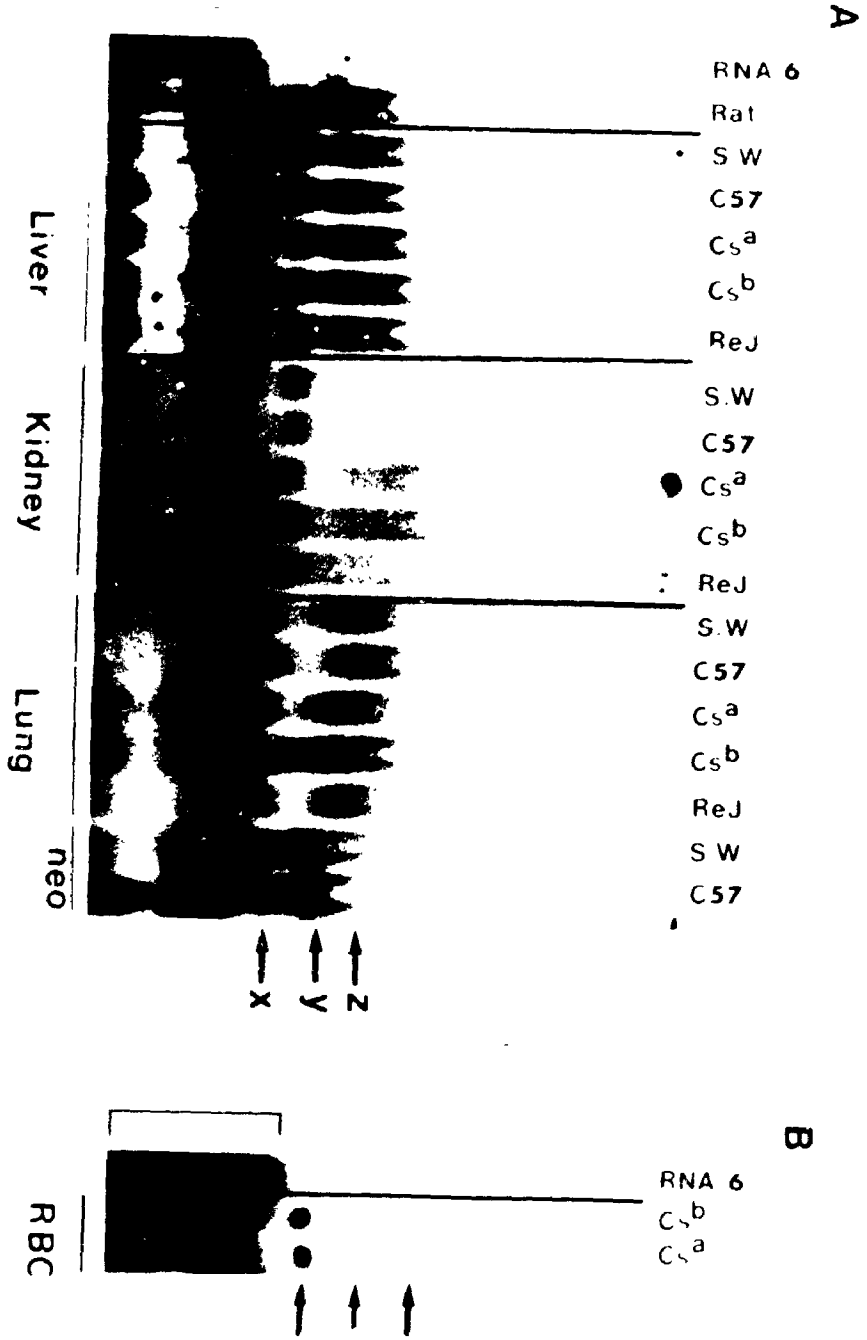
A
RNA 6
Rat
S.W
C57
Cs^a
Cs^b
ReJ
S.W
C57
Cs^a
Cs^b
ReJ
S.W
C57
Cs^a
Cs^b
ReJ
S.W
C57
Liver
Kidney
Lung
neo
x
y
z
B
RNA 6
Cs^b
Cs^a
RBC

Figure 44. Gel mobility shift assay involving the incubation of labelled RNA 7 [containing $(UGUGC)_7$] with homogenates from adult liver, kidney and lung from 5 mouse strains. Free probe is indicated by a bracket.

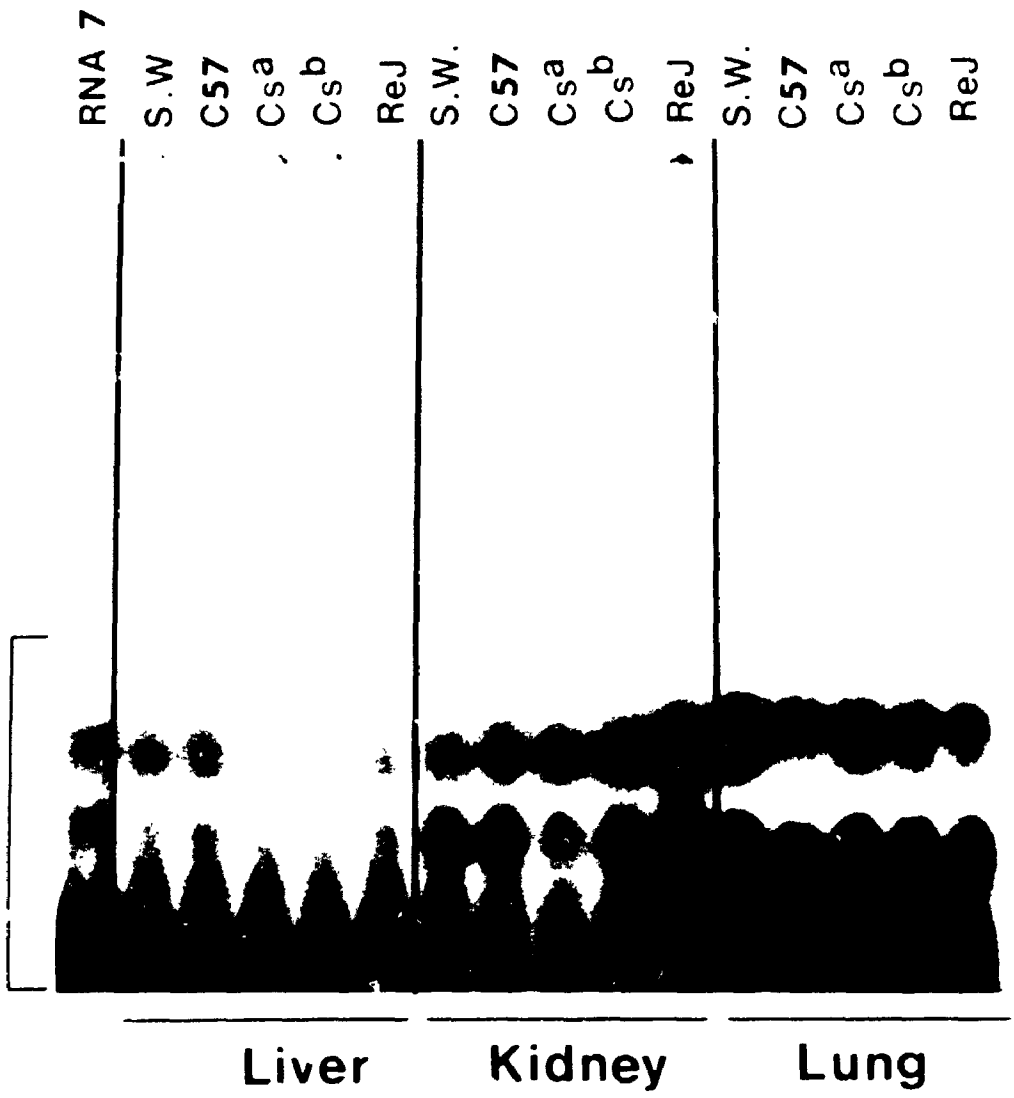
RNA 7
S.W
C57
Csa
Csb
ReJ
S.W.
C57
Csa
Csb
ReJ
S.W.
C57
Csa
Csb
ReJ
Liver
Kidney
Lung

Figure 45. Electrophoretic separation of mRNA-binding complexes following UV crosslinking of RNA 5 and associated protein(s) from liver, kidney and red blood cells of different inbred mouse strains. Homogenates were incubated with RNA 5, subjected to UV irradiation (+UV) and sequentially treated with RNase A and heparin prior to separation through a 10% SDS polyacrylamide gel. Incubation of homogenate with labelled RNA 5 in the absence of UV crosslinking is included as negative controls (-UV). A single protein band of ~69 kDa is indicated by an arrow. RNA 5 = transcript +UV, a negative control. Molecular weight protein standards (Bio Rad) were included on each gel during the electrophoretic separation and are indicated on the left in kDa.

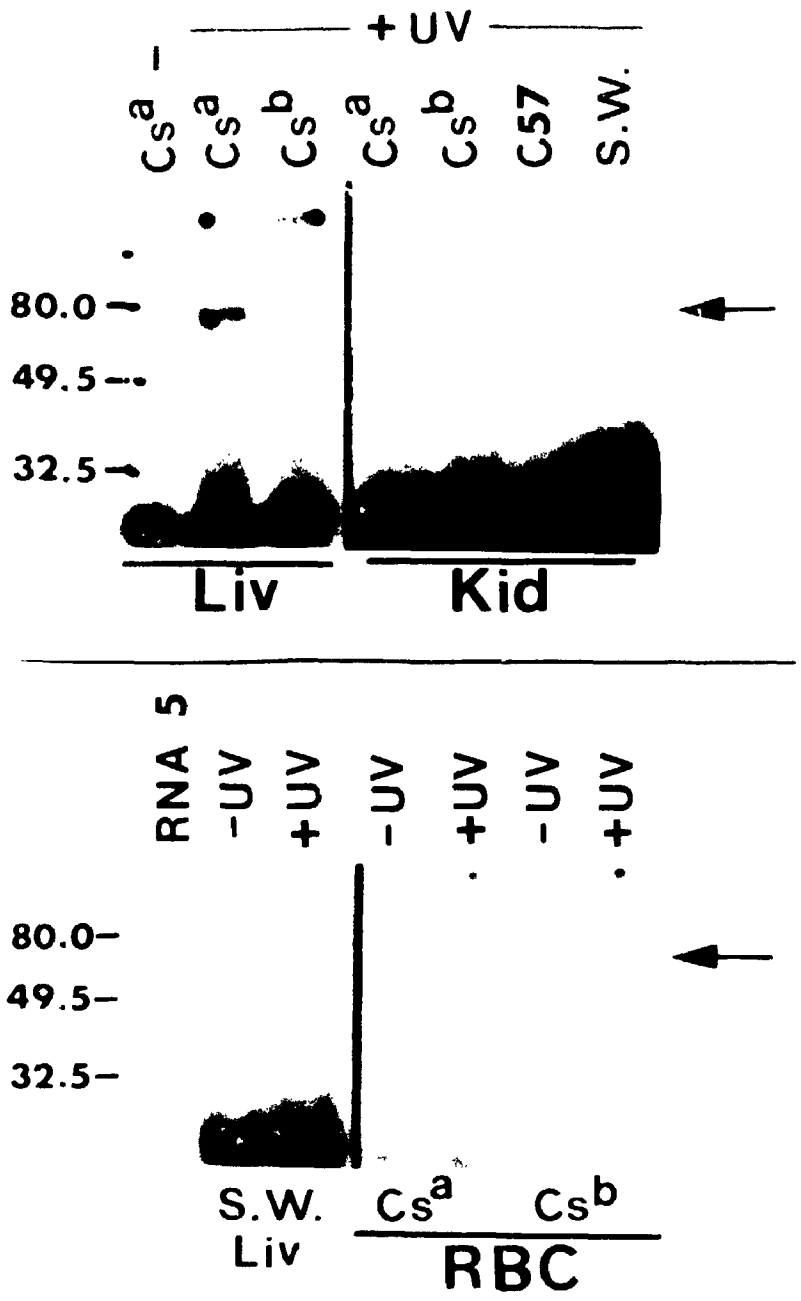
+UV
Cs^a
Cs^a
Cs^b
Cs^a
Cs^b
C57
S.W.
80.0
49.5
32.5
Liv
Kid
RNA 5
-UV
+UV
-UV
+UV
-UV
+UV
80.0
49.5
32.5
S.W. Liv
Cs^a
Cs^b
RBC

that in all tissues and strains tested, a single high molecular weight band of approximately 69 kDa is present (arrow) when the complexes were UV cross-linked compared to the control (- UV). This suggests that some similar protein(s) are involved in the formation of complexes in different tissues. It should be noted that particularly in the liver of Cs^a (C3H/HeAnl/*Cas-1*^{a}), several smaller molecular weight bands (~37.5 and ~50 kDa) were observed. The presence of these bands however was not consistent in repeated experiments and may represent individual polypeptides that became separated from a larger complex under denaturing conditions.

To determine if the mRNA-binding protein(s) specific to the $(CA)_{31}$ sequence could play a role in translation, the polysomes from liver homogenates of a number of strains were isolated and the proteins associated with this fraction were evaluated in the gel mobility shift assay. Figure 46A shows that when proteins associated with polysomes of S.W., Cs^a, and Cs^b were incubated with labelled RNA 5, at least two (perhaps three) complexes were observed. The pattern of migration does not appear to differ among strains and therefore does not reflect the decrease in catalase activity and protein polypeptide observed in C3H/HeAnl/*Cas-1*^{b}. The migration of the complexes associated with polysomes however, is different from that observed for total liver homogenate (a, b and c). This suggests that in addition to the ~69 kDa protein identified by UV cross-linking, there may be other proteins involved in the formation of these complexes. Some may specifically be associated with the polysomes, reflecting their possible interaction with the translational machinery. The contribution of other non-polysomal proteins to the formation of the complexes cannot be ruled out. To further investigate the possible involvement of proteins from cellular fractions other than polysomes, a UV cross-linking experiment was performed with homogenates from the polysome and the non-polysome fraction from kidney (a tissue where the acatalasemic phenotype is manifested in mice) of C3H/HeAnl/*Cas-1*^{a} (Cs^a) and C3H/HeAnl/*Cas-1*^{b} (Cs^b). Figure 46B shows the presence of a single high molecular weight band similar in migration to the ~69 kDa in the total liver homogenate and the polysome fraction. Results from the non-polysome fraction show that in both the acatalasemic and normal strains, there are two proteins: one similar in size to the ~69 kDa band and an additional higher molecular weight protein (> 100 kDa). Although the function of these proteins is not known, these data reflect the complex nature of the formation of the catalase mRNA-binding complexes. In addition, it suggests the possible

Figure 46. A: Gel mobility shift assay involving labelled RNA 5 and protein homogenates from polysome liver fractions of Cs^a, Cs^b and S.W. S.W. liver homogenate is included as a control. The three complexes (a, b and c) are marked. Free probe is indicated by a bracket. B: Electrophoretic separation of RNA 5 UV crosslinked to associated protein(s) from polysome (P) and non-polysome (NP) kidney fractions. Liver homogenates (Liv) were included as controls. Note the presence of two protein bands in the non-polysome fraction of Cs^a and Cs^b (arrows). The lower band is seen in all tissues and strains and represents ~69kDa by comparison to conrol (Liv).

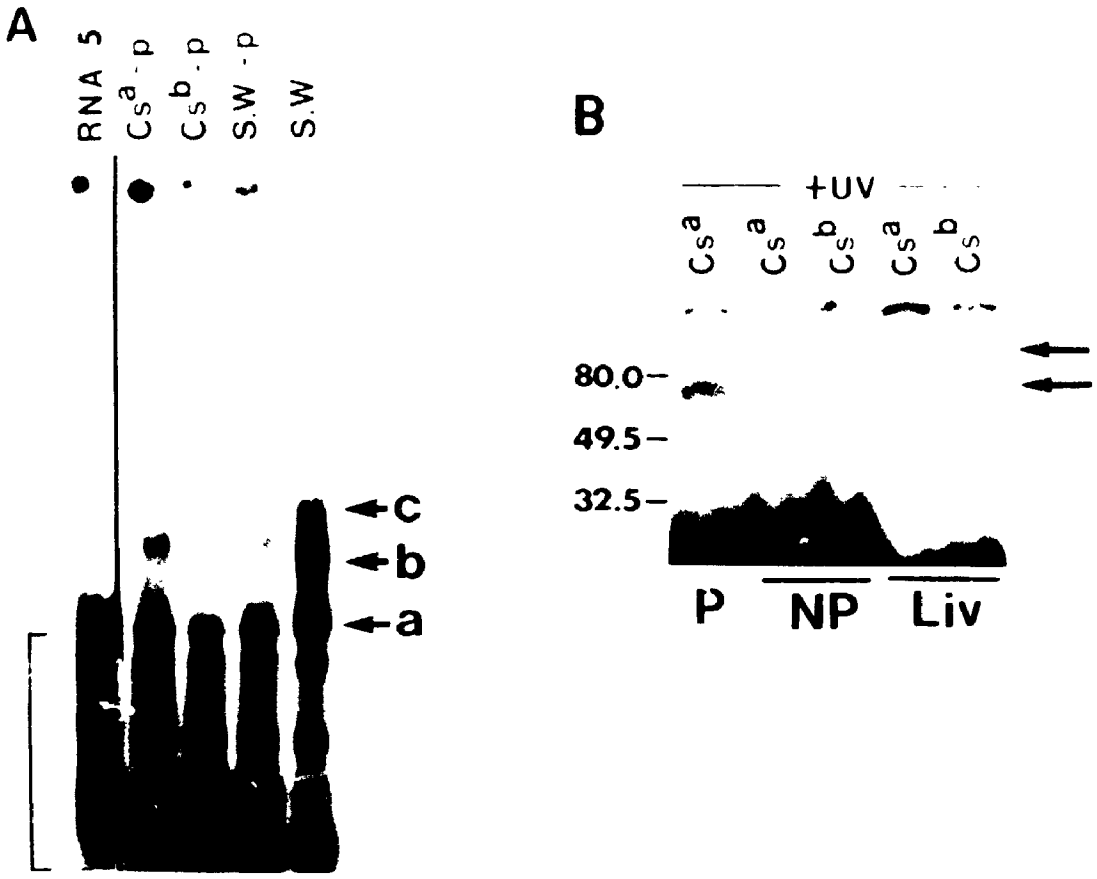
A
RNA 5
Cs^a-p
Cs^b-p
S.W-p
S.W
c
b
a
B
+UV
Cs^a
Cs^a
Cs^b
Cs^a
Cs^b
80.0
49.5
32.5
P
NP
Liv

involvement of a number of proteins from the cellular as well as polysomal components of the tissue.

Further characterization of the number and sizes of protein(s) involved in the formation of complexes x, y and z involving labelled RNA 6 (containing $(U)_{15}$) and liver, kidney and lung homogenates from adult and neonate mice is shown in Figure 47. Here, protein homogenates were incubated with labelled RNA 6, UV cross-linked, and subjected to electrophoresis in a 10% SDS polyacrylamide gel. In all tissues examined, two protein bands were identified (~38 and ~47 kDa), suggesting that similar protein(s) are involved in the formation of mRNA-binding complexes in different tissues. It is interesting to note that unlike kidney, the ~38 kDa protein from liver and lung appears to be more prominent than the ~47 kDa protein from the same tissue. The significance of this observation remains to be elucidated. The presence of the same or similar identified proteins was also observed when comparing the results using homogenates from adult and neonatal lung from four mouse strains. However, the migration of the complexes under non-denaturing conditions appears as if they are different (Figure 43). Here, the contribution of additional factor(s) in the adult or neonatal lung tissue cannot be ruled out.

To determine the involvement of mRNA-binding protein(s) specific to the $(U)_{15}$ sequence in translation, polysomes from liver homogenates of number of strains were isolated. The proteins associated with this fraction were evaluated in the gel mobility shift assay using labelled RNA 6 and the result in presented in Figure 48. Although the presence of three complexes (x, y and z) was observed in S.W. liver homogenate (control), only two of the complexes (x and y) were seen in the liver polysomes of (C3H/HeAnl/*Cas-1*^{a}) Cs^a, (C3H/HeAnl/*Cas-1*^{b}) Cs^b and Swiss Webster (S.W.). There is no difference in the liver polysomal proteins associated from RNA 6 from different strains including Cs^b that represents the acatalasemic mutation. Furthermore, UV crosslinking of protein(s) from the liver polysomes of (C3H/HeAnl/*Cas-1*^{a}) Cs^a and (C3H/HeAnl/*Cas-1*^{b}) Cs^b revealed a single protein band of approximately 38 kDa in both strains (Figure 48B). This protein is present in all tissues and strains evaluated to date (Figure 47) and reflects on its possible interaction with the translational machinery. The absence of the ~47 kDa protein suggests that it is not associated with the polysome, however the functional significance of this protein remains to be determined.

The experiments described above suggest that two specific sequences of the mouse catalase mRNA [$(CA)_{31}$ and $(U)_{15}$ located in the 3' UTR] bind to

Figure 47. Electrophoretic separation of RNA 6 UV crosslinked to associated protein(s) from liver, kidney and lung (A-adult, N-neonate) from different mouse strains. Homogenates were incubated with labelled RNA 6, subjected to UV crosslinking (+UV) and treated with RNase A and heparin, prior to 10% SDS-PAGE. Incubation with homogenate in the absence of UV crossliniking was included as negative controls (-UV). Two protein bands (~38 and ~47 kDa) are identified with arrows. Molecular weight protein standards (Bio Rad) are included on each gel and are indicated on the left in kDa. RNA 6 = transcript +UV, a negative control.

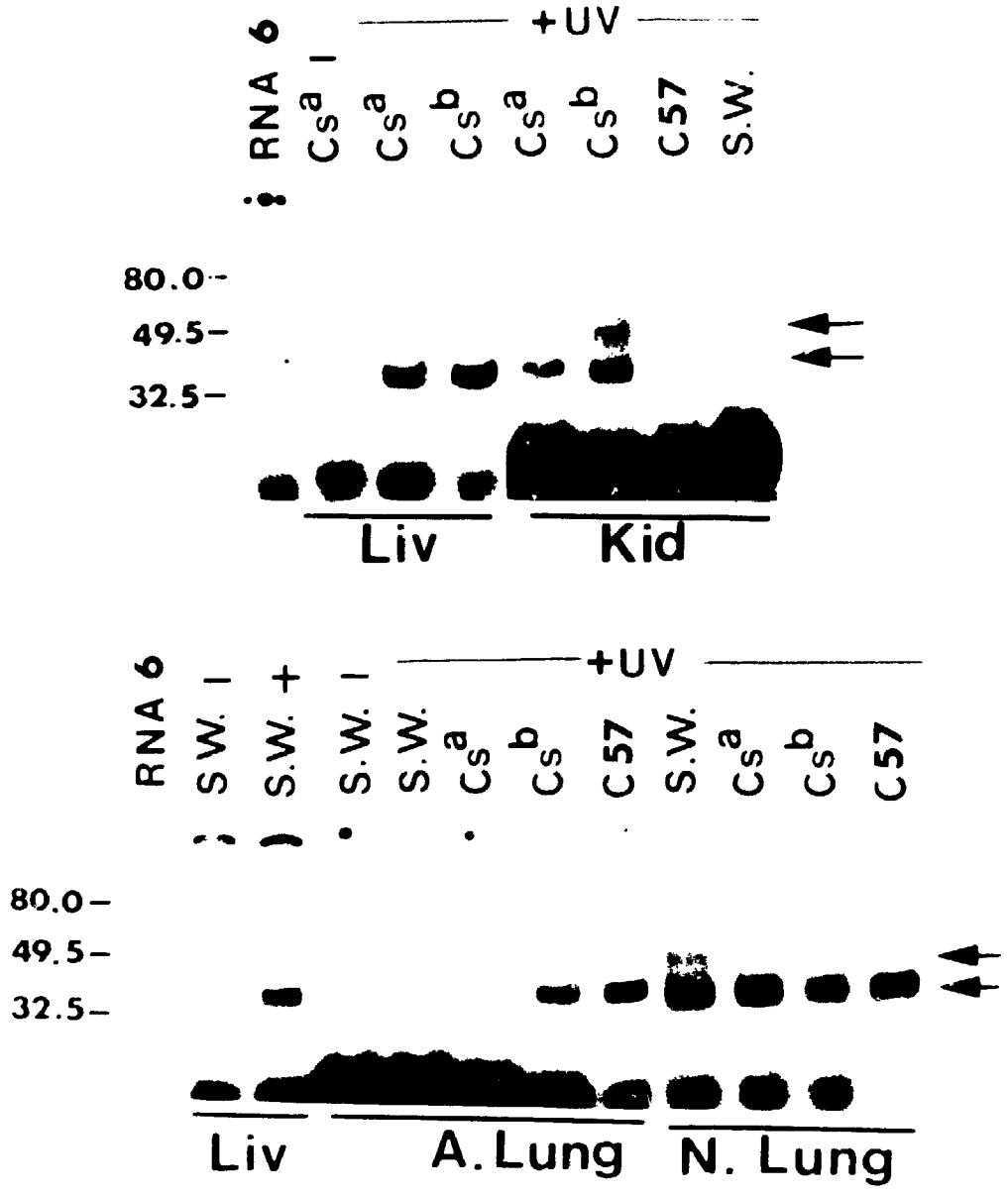
RNA 6
+UV
Cs^a
Cs^a
Cs^b
Cs^a
Cs^b
C57
S.W.
80.0
49.5
32.5
Liv
Kid
RNA 6
S.W. −
S.W. +
S.W. −
+UV
S.W.
Cs^a
Cs^b
C57
S.W.
Cs^a
Cs^b
C57
80.0
49.5
32.5
Liv
A.Lung
N. Lung

Figure 48. A: Gel mobility shift assay involving labelled RNA 6 and protein homogenates from polysome liver fractions of Cs^a, Cs^b and S.W. S.W. liver homogenate was included as a control. The three complexes (x, y and z) are marked. Free probe is indicated by a bracket. B: Electrophoretic separation of mRNA-binding complexes involving UV crosslinked RNA 6 to associated protein(s) from liver homogenates of Cs^a and Cs^b isolated polysomes (+UV). Cs^b Liver (+UV) was included as a positive control. The presence of a single band of ~38 kDa (compared to control) in the polysome fraction of both strains is indicated by an arrow.

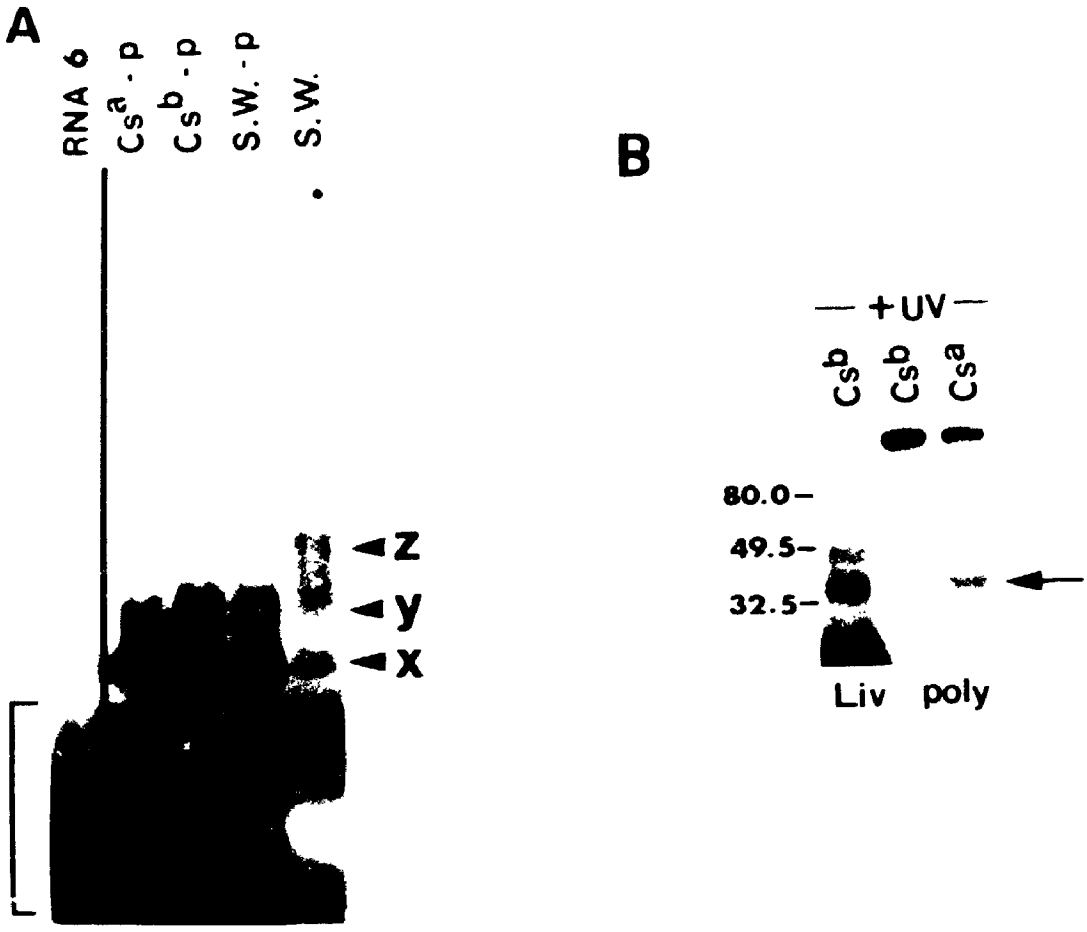
A
RNA 6
Cs^a - p
Cs^b - p
S.W. - p
S.W.
z
y
x
B
— + UV —
Cs^b
Cs^b
Cs^a
80.0 –
49.5 –
32.5 –
Liv
poly

cytosolic proteins present in most polysomal fractions evaluated. The two sequences are specific for different proteins that are found in most tissues in adults and neonates. It is tempting to suggest that such interactions may be involved in posttranscriptional regulation of mouse catalase. However, such a suggestion must remain hypothetical until characterization of the proteins involved, including the experimental evidence for the functional significance of the mRNA-protein complexes observed during the course of this study, is completed.

CHAPTER 4

DISCUSSION

Molecular mechanisms associated with the regulation of eukaryotic housekeeping genes in general remain poorly understood. Such an understanding is critical to interpreting the harmonious tasks which most cells efficiently execute. Regulatory studies on most of these genes have lagged behind the genes involved in development and differentiation. One of the reasons is the lack of well characterized mutations in any model organism. It is important to note that regulatory elements associated with some of these genes including mouse catalase have been hypothesized based on linkage studies (Hoffman and Grieshaber, 1974; 1976) and studies involving genetic complementation and segregation (Schisler and Singh, 1991 among others). Over the years, studies on the mouse catalase benefited from an extensive investigation of biochemical properties and characterization of genetic strains of mice which show variability in the tissue-specific catalase activity (Rechcigl and Heston, 1963; Heston *et al.*, 1965; Rechcigl and Heston, 1967; Ganschow and Schimke, 1969; Hoffman and Rechcigl, 1971; Holmes and Masters, 1972; Hoffman and Grieshaber, 1974; 1976; Schisler and Singh, 1987; 1991).

The mouse catalase provides a suitable model system for the evaluation and understanding of the regulation of housekeeping genes. A number of important features in this context include the following. Catalase is encoded by a single gene (*Cas-1*) (Bailley, unpublished) and localized to chromosome 2 (Maltais *et al.*, 1994). The sequence of the partial cDNA has recently been published (Shaffer and Preston, 1990). There is a well characterized tissue-specific expression of this enzyme during development and aging (Schisler and Singh, 1987; El-Hage and Singh, 1990, Reimer and Singh, 1990). Extensive segregation studies on genetic crosses have hypothesized possible molecular determinants that regulate the tissue-specific expression in this model system (Schisler and Singh, 1991). The nature of such determinants remains a challenge for the future and represents an ultimate goal of this research.

As a first step towards the molecular evaluation of the regulation of mouse catalase expression, it was necessary to obtain the complete cDNA

sequence and to clone and characterize the 5' genomic sequence associated with *Cas-1*. The sequence data were then complemented by quantitative studies on the expression of the catalase gene in a number of tissues in different genetic strains of mice at the level of mRNA, polypeptide and enzyme activity. In addition, the spatial and temporal pattern of *Cas-1* mRNA expression was evaluated during fetal development and differentiation by *in situ* hybridization. The involvement of the 5' upstream regulatory region was evaluated for the pattern of CpG methylation towards an explanation of the observed tissue specificity. Upon evaluation of the complete cDNA sequence obtained, it was recognized that the molecular mechanisms involved in the regulation of *Cas-1* among strains and genotypes may involve unusual features identified in the 3' UTR of this gene. The possible involvement of this region in posttranscriptional regulation was experimentally investigated by sequence comparisons among mouse strains in addition to gel mobility shift assays for the identification of specific mRNA-binding complexes and proteins.

A: SEQUENCE ORGANIZATION OF THE MOUSE CATALASE GENE (*Cas-1*):

4.1. Complete cDNA:

The complete cDNA of the mouse catalase which has been generated for the first time in this investigation is 2423 nt and corresponds to the results obtained using northern blot analysis (Shaffer *et al.*, 1987; El-Hage and Singh, 1989; 1990). It contains 87 nt of 5' and 752 nt of 3' untranslated regions plus 1584 nt of coding sequences (Figure 5). The BALB/c *Cas-1* coding region corresponds to the published results on mouse (Shaffer and Preston, 1990; Shaffer *et al.*, 1990), rat (Furuta *et al.*, 1986) and human (Quan *et al.*, 1986). Features such as signals for translation and gene organization appear conserved among mammalian catalase gene including the position of the first intron established for mouse *Cas-1* during the course of this study (Figure 5). It corresponds to the human CAT gene (Quan *et al.*, 1986). Other exon/intron boundaries for *Cas-1* although not experimentally established are compatible to the reported human gene (Quan *et al.*, 1986). The proposed ATG translation initiation site (Figure 5) follows Shaffer and Preston (1990). The flanking sequence ACACCATGT is a close match to the consensus (Kozak, 1991a; 1991b) for the translation initiation codon and another ATG does not exist for up to 571 bp upstream.

There is a high (> 89.0%) amino acid identity among the known sequences from mammalian species (mouse, rat, human and bovine). A recent report by von Ossowski *et al.*, (1993) have shown that within each of the groupings of animal, plant and fungal catalases, a high degree of identity (> 95% confidence using neighbour-joining and parsimony analyses) has been maintained throughout the length of the primary sequence. Comparisons of the amino acid sequence among the divergent species, including prokaryotes, show a striking similarity in the middle of the polypeptide from prokaryotes to eukaryotes. These two groups usually differ at the amino and carboxy ends of this protein. Most of the divergence among the eukaryotic sequences also appears to result from blocks of deletions and additions, and are specific to particular groups (yeast versus plant etc.). These variations are compatible with rearrangements (e.g. exon shuffling) as major evolutionary mechanisms for this polypeptide. They may also explain the functional differences among different eukaryotes.

Comparisons among mammalian species have revealed that in addition to rearrangements, amino acid replacements specific to certain regions may also play a significant role in the divergence of this polypeptide. In particular, the first 35 amino acids of the first structural domain of this polypeptide possess a relatively high level of amino acid replacements when compared to other functional domains of mammalian catalases (Figure 12). This region is thought to be involved in subunit interaction and may therefore represent an evolutionary divergence for species-specific tetramerization by this polypeptide. Another area of interest is the β9 region, located between amino acids 423-429 (Figure 12). As supported by the crystallographic structure of the bovine catalase by Fita and Rossmann (1985), β9 is not involved in direct interaction with the heme molecule or the substrate channel and may be able to accommodate neutral substitutions. This region of the polypeptide, however, has been suggested to be involved in intersubunit contacts in the formation of the quaternary structure and may be hypothesized to be responsible for mammalian species specificity of the catalase protein. The remainder of the polypeptide, which includes domain two (involved in heme and substrate channel formation) and domain four (the hydrophobic channel) appears to be highly conserved among mammalian species and may reflect the common functional element of the enzyme.

Catalase is known to be localized to the peroxisomes, particularly in liver, and is directed by the use of a topogenic signals located in the fourth domain near the carboxy terminus (van den Bosch *et al.*, 1992). The tripeptide signal (serine-histidine-leucine) was shown to contain the peroxisome-targeting information of human catalase (Gould *et al.*, 1988). When this region is compared to other mammalian species, the tripeptide is represented by serine-histidine-isoleucine in rat and serine-histidine-methionine in mouse. These latter two tripeptides are less likely to act as topogenic signals, since results of mutagenesis suggest that leucine cannot be replaced by other amino acids in this triplet signal (Osumi and Fujiki, 1990). However, if this tripeptide is important in catalase trafficking into peroxisomes perhaps this can explain the differences in catalase expression among species. Interestingly, bovine catalase is 20 amino acids shorter than other mammalian sequences at the carboxy terminus and does not contain any potential topogenic signals.

To date, no sequence comparisons have been made involving the 5' and 3' UTRs of the catalase gene. Sequences for the untranslated regions of the cDNA of catalase in three mammalian species are now known and include mouse (this study), human (Quan *et al.*, 1986) and rat (Furuta *et al.*, 1986). Dot matrix homology analyses comparing 3' UTRs demonstrate a unique sequence homology among rodents. The sequences which show high identity are specific and unusual and include near repeats containing $(CA)_{31}$ and $(T)_{15}$ as defined in Figure 8. An additional unusual near repeat unique to mouse catalase is also identified [$(TGTGC)_7$]. Observations on the 3' UTR sequence of human catalase reveal that only the poly (T) is present however is much smaller [$(T)_{10}$]. This may represent an evolutionary divergence specific for rodent catalases. The potential significance of these unusual near repeat sequences will be eluded to and discussed later.

The length of the 5' UTR is variable among mammalian species (68 - human, 83 - rat and 87 - mouse). Two regions of sequence similarity among these species include TGCCT and GGGTGG which have known regulatory functions. TGCCT has been suggested to play a role in strand exchange in the recombinational process (Been *et al.*, 1984), while GGGTGG is thought to act as an enhancer in viruses (Martin *et al.*, 1985; Jalinot and Kedinger, 1986) and in the histocompatability gene of mouse (Kimura *et al.*, 1986). The conservation of these sequences among mammalian catalase cDNA may suggest a regulatory

role of the 5' UTR in the expression of *Cas-1*. The molecular mechanisms for this regulation however remain to be experimentally established for *Cas-1*.

4.2. 5' Genomic Sequences:

The first report consisting of mouse 5' genomic sequence analysis of *Cas-1* is presented in this thesis (Figure 7). Sequencing of this region is based on non-overlapping DNA fragments. The only other sequence from this region is reported for the human catalase gene, *CAT* (Quan *et al.*, 1986). Comparison of the sequences between these two species reveals that there is a high degree of sequence variability in this region. Differences in this region may also explain species-specific regulation of catalase expression. Although the regulation involving this region of human *CAT* has not been investigated, there are a number of sequence features that are common between the human and mouse catalase 5' genomic region. For example, the human and mouse catalase genes contain CCAAT boxes and a GC box. Interestingly, neither of them contain a TATA box which has been observed in this region of other housekeeping genes. This suggests that the catalase gene likely developed an "unconventional" method of accomplishing mRNA transcription specific to the requirements of the cell.

This 5' genomic region of mouse and human also contains a "CG island". This property is characteristic of most housekeeping genes, and is now known to be involved in the repression of transcriptional regulation through methylation of CpG dinucleotides in this region (Boyes and Bird, 1991). The presence of this feature in the human and mouse catalase genes suggests the potential for a common mechanism of transcriptional regulation. A more extensive investigation of the pattern of methylation at the 5' end of *Cas-1* and its involvement in tissue-specificity is discussed later.

B: EXPRESSION OF *Cas-1* GENE IN MICE

4.3. Developmental Pattern and Profile:

At birth, a fetus is subjected to a significant increase in the levels of oxygen compared to the *in utero* environment. This transition results in a significant oxidant stress (Rickett and Kelly, 1990). It has been suggested that these oxidants are neutralized by a substantial increase in the antioxidant enzymes superoxide dismutase (SOD), glutathione peroxidase (Gpx) and catalase in the lungs of fetuses from different species (Frank and Groscclose,

1984; Tanswell and Freeman, 1984; Gerdin *et al.*, 1985; Frank and Sosenko, 1987). These increases are apparent in late gestation which may prepare the pulmonary system for the acute change in oxygen concentration encountered during birth with the onset of independent respiration. Recently de Haan *et al.* (1994) have shown that the increase in enzyme activity of SOD and Gpx during late gestation is not limited to the lungs alone. The increase in these enzymes and their associated mRNAs is also apparent in tissues including liver and stomach. The molecular mechanisms for this up-regulation during late gestation remain to be explained, however, the data in this study suggest it is not correlated with oxygen exposure in these organs. The reasons for these increases are more complex and may perhaps involve other factors.

Studies on mouse liver catalase have shown that the enzyme activity increases during embryonic development and exhibits a sharp elevation at birth that remains relatively high into adult life (Holmes, 1971; El-Hage and Singh, 1990). El-Hage and Singh (1989) further observed that the catalase mRNA level increase during late gestation is more dramatic than the level of enzyme activity. Such results are interpreted to mean that the catalase mRNA may accumulate *in utero* and is efficiently translated only after birth when the enzyme is needed during independent aerobic respiration. Although these studies demonstrate that the expression is higher in developing liver, they do not identify specific cell types that synthesize the catalase message during development and differentiation. The sensitive technique of *in situ* hybridization was therefore applied to paraffin-embedded whole mouse fetuses to determine spatial and temporal expression of the catalase gene.

The results included in this thesis show that the mouse catalase gene begins active transcription in a tissue-specific manner prior to day 13 of fetal development. The resulting mRNA is particularly detectable in differentiating hepatocytes at day 13, which increases with development and growth (Reimer and Singh, 1990). This expression is not limited to the hepatocytes at this stage of development, since the *Cas-1* mRNA is also shown to be expressed in brain but very low levels in mesenchyme. *Cas-1* mRNA, when present, appears evenly distributed throughout the cells. Unlike liver, the level of expression in the brain is relatively low, which could argue for the significance of liver in the metabolism of toxic oxygen radicals. These data are consistent with El-Hage and Singh (1989) who showed that the catalase gene in mice is transcribed at the onset of organogenesis and is expressed in a tissue-specific manner. The

molecular regulation of the tissue-specific expression of mouse catalase remains to be determined.

4.4. Tissue-Specificity of *Cas-1* Expression:

Cas-1 expression was evaluated by catalase enzyme activity, polypeptide (western blot analysis) and mRNA (northern and dot blot analyses) and was quantified from different tissues of BALB/c mice. As expected, the enzyme activity is highest in the liver, intermediate in the kidney and lowest in the blood among the tissues evaluated. It should be noted that blood is a heterogeneous tissue consisting of various cell types with specific properties and features. The catalase activity is predominantly expressed in red blood cells, however mRNA is found only in nucleated white blood cells. Caution should therefore be used when analysing catalase expression in this tissue. Quantification of the catalase polypeptide and *Cas-1*-specific mRNA show a similar trend across the tissues. Correlations among the results for three levels of *Cas-1* expression suggest that the tissue-specific enzyme activity follows the level of polypeptide and the mRNA levels (Figure 20). It is therefore concluded that the tissue-specific expression of this housekeeping gene is accomplished at the level of mRNA by the rate of transcription or mRNA stability.

Transcriptional regulation is the most common explanation for the tissue-specific expression of genes in eukaryotes. This mechanism of regulation has been extensively studied. In general, it represents a complex but highly specific interaction of specialized protein(s) with DNA sequences in the 5' upstream region of the gene (e.g. promoter). This regulation in part accounts for the orchestration of genetic programs for cell growth and differentiation including the establishment and maintenance of the differentiated state. Sequencing of the *Cas-1* upstream region from BALB/c mouse (~ 660 bp) reveals the presence of two canonical CCAAT sequences and a GC box (Figure 7). This region is GC rich as expected for most eukaryotic promoters but lacks a TATA box. Lack of a TATA box in the promoter region of a number of housekeeping genes expressed in most cells has been reported (Dynan, 1986). The mechanism by which specific transcription is accomplished by TATAless promoters has been reviewed by Weis and Reinberg (1992). Although not conserved, most TATAless promoters contain a 17 bp element, the initiator element (Inr), which encompasses the transcription start site and contains all the information necessary for determining specific initiation of transcription. This element is

critical in positioning RNA Polymerase II and is recognized by DNA-binding proteins specific to this region. It is the interaction between these Inr-binding proteins and the components of the transcriptional machinery which provides a basis for the formation of a transcription competent complex. Although specific transcriptional proteins of the catalase TATAless promoter have not yet been characterized, it is logical to suggest that the mechanism of transcription for this TATAless gene may not differ significantly from other TATAless housekeeping genes.

The tissue-specificity at the level of transcription can potentially be attained by differential epigenetic modification in the GC rich catalase promoter. One of the most common forms of epigenetic modifications involves the methylation of eukaryotic DNA which appears to be related to differential patterns of gene activity (Bird, 1986; Holliday, 1987; Kafri *et al.*, 1992). The specific functions of DNA methylation and the consequences of modulating transcription however, remain poorly understood. In mammals, most DNA methylation is confined to the cytosine residue of CpG dinucleotides (Cooper, 1983). Methylation of the cytosine residue in this dinucleotide may suppress transcription (Razin and Cedar, 1991). Evaluation of the genomic DNA sequence of the *Cas-1* promoter reveals a number of potential methylation sensitive CpG sites (Figures 21, 22) and if involved in transcriptional regulation, may be expected to be differentially methylated. The results on the evaluation of methylation of the *Cas-1* promoter region included in this report show that in four tissues which express catalase, at least one of the three CpG dinucleotide sites tested is not methylated (Figure 23B). The *Hpa* II-PCR method used to evaluate CpG methylation does not permit the assessment of the specificity of methylation of every CpG dinucleotide in this sequence. However, the absence of methylation in at least one of the three CCGG sites would explain the observed results on *Hpa* II-PCR and indirectly suggest that the lack of 5' CpG methylation may play a role in the expression of the mouse catalase. Recently, preliminary experiments show that the catalase gene in mouse sperm is methylated at these three sites. It is hypothesized therefore, that the degree of methylation in this region may account for different levels of expression of *Cas-1* in different tissues, which remains to be experimentally established.

The regulation of mammalian catalase appears to involve different strategies in different situations, including increased transcription, mRNA stability and DNA amplification. The rate of transcription as a mechanism of

catalase regulation has been suggested by Clerch *et al.* (1991) in developing rat lung during late gestation. Furthermore, they suggested that an increase in catalase activity in response to early postnatal hyperoxia may be mediated by mRNA stability. Additionally, Yamada *et al* (1991) observed that the H_2O_2 stress in an *in vitro* system was accommodated by an increase in catalase activity by increased mRNA following DNA amplification. Such multilevel regulation of the mRNA of a housekeeping gene is not commonly reported in the literature. In fact, mammalian catalase may represent an exceptional biological system in this context.

The product of the single structural gene, *Cas-1* has been thought to be regulated tissue-specifically by a number of segregating loci in studies on genetic crosses. Ganschow and Schimke (1970) have identified a gene, *Ce-1*, which appears to affect the degradation of the enzyme in liver. Moreover, Hoffman and Grieshaber (1976) have suggested the involvement of an additional regulatory gene, *Ce-2*, which acts posttranslationally to alter the electrophoretic mobility of kidney catalase by binding directly to the molecule or by altering its charge distribution. More recently, extensive analyses by Schisler and Singh (1991) showed that the tissue-specific expression of catalase is genotype- or strain- specific. This permitted the evaluation of involved genetic determinants. They have shown that the expression of murine catalase involves a complex system of spatial and temporal genetic regulators, which may interact with *Cas-1* mRNA or its product to produce the observed catalase phenotype. This regulation may involve as yet uncharacterized transacting regulatory factors which may act at multiple levels including transcription, posttranscription and translation.

4.5. *Cas-1* Expression Pattern in Strains and Genotypes of Mice:

Catalase enzyme activity, polypeptide (western blot analysis) and mRNA (northern and dot blot analyses) were quantified from liver, kidney and blood of mouse strains representing normal, hypocatalasemia and acatalasemia (Figure 29). In general, the data show that although there is a comparable level of enzyme activity in the liver of these strains, there is a substantial reduction in catalase activity in kidney and blood, particularly in the acatalasemic strain. Analysis of the level of catalase polypeptide in these tissues and strains demonstrates that the decrease in enzyme activity is associated with a

decrease in the polypeptide. It is interesting to note that the mRNA levels in these tissues are comparable among all genotypes.

Characterization of the acatalasemic R.I. line (SXC/ws-1) generated in our breeding colony also suggests that unlike the tissue-specific expression, the regulation of catalase among mouse genotypes is not related to transcription or stability of the mRNA. The difference among genotypes must result from posttranscriptional regulation and/or differential stability of the protein under certain physiological conditions. An incorrectly spliced mRNA leading to a 2.4 kb message not detectable under the conditions used however, cannot be ruled out. These studies complement the segregation studies of Schisler and Singh (1991) and suggest that the enzyme activity variation among strains is regulated by additional transacting genetic determinants. The molecular nature, the mechanism(s) associated with such genetic elements, and their possible role in posttranscriptional regulation however remain hypothetical.

Posttranscriptional regulation may involve sequences in the coding or non-coding region of *Cas-1*. The coding region may ultimately determine the property of the polypeptide (stability, interactions, etc.) by altering the amino acid sequence while the non-coding region may play a role in translational regulation of the *Cas-1* mRNA (Sonenberg, 1994). The non-coding region may require additional transacting factors (e.g. mRNA-binding proteins) to be operational in the translational regulation of the *Cas-1* mRNA (Clerch and Massaro, 1992). The observations and results on the coding region and non-coding regions of the *Cas-1* mRNA will be discussed separately.

a. Comparison of the *Cas-1* DNA sequences among genetic strains of mice

It is now possible to compare the coding sequence for at least four genetic strains of mice (Table 5) representing normal, hypocatalasemia and acatalasemia (this study; Shaffer *et al.*, 1990, Shaffer and Preston, 1990 respectively). The coding region sequence among the strains is similar but not identical. There are nine nucleotide substitutions which lead to five amino acid changes in the catalase polypeptide. Recently, Shaffer and Preston, 1990 have reported a single amino acid change, glutamine^{11} to histidine in the acatalasemic strain C3H/HeAnl/*Cas-1*^{b}. They suggested that since this amino acid is positioned within the first major α-helix of the catalase polypeptide subunit, any substitution in this region could dissociate the tertiary structure and

alter the stability of the molecule under certain physiological conditions. This hypothesis is compatible with results on the expression of *Cas-1* in this strain presented in Figure 29 (enzyme activity, protein and mRNA). It suggests that the effect of the glutamine^{11} to histidine mutation does not affect the *Cas-1* mRNA level (i.e. transcription or mRNA stability) but is apparent at the level of the polypeptide in a tissue-specific manner (unaffected in the liver and almost absent in the kidney and blood). The glutamine^{11} to histidine mutation could alter catalase protein turnover rates in kidney and blood and/or the specific environment of the liver could permit near normal polypeptide and enzyme activity. It may be pointed out that the complementation and segregation results involving C3H/HeAnl/*Cas-1^b* as one of the parents (Schisler and Singh, 1991) are best explained by additional transacting factors in the tissue-specific regulation of this housekeeping enzyme. The additional transacting factors apparent in genetic crosses could be hypothesized to be involved in determining the tissue-specific property of the glutamine^{11} to histidine mutation in C3H/HeAnl/*Cas-1^b*. As an alternative, the glutamine^{11} to histidine substitution could represent a polymorphism and the expression pattern in this genotype is determined by still uncharacterized transacting factor(s) involved in posttranscriptional regulation.

Towards explaining the hypocatalasemic phenotype, Shaffer *et al.* (1990) reported a threonine^{117} to alanine substitution in the strain C57BL/6J. This substitution is located in the heme binding region of the molecule (Murthy *et al.*, 1981; Fita and Rossmann, 1985). An amino acid change in this region may in theory disrupt the hydrophobic channel, leading to diminished catalytic efficiency of this enzyme. This alteration alone however could not account for the tissue-specific nature of expression of this gene in C57BL/6J and suggests a role for additional tissue-specific posttranscriptional regulators.

Other than the two amino acid replacements discussed above, Table 5 includes three additional alterations in the BALB/c sequence. One substitution, glycine^{97} to alanine is situated in the second domain where the contribution of amino acids is not thought to be critical (Figure 12). A change in this region is therefore unlikely to affect the secondary structure of the protein. Another change observed specifically in the BALB/c coding sequence is valine^{316} to leucine. Although this amino acid is located in the β8 chain, which is situated in the second functional domain, this change results in a neutral change which does not alter the polarity or the charge of the amino acid involved. The third

amino acid replacement observed in this strain is lysine^{350} to methionine which is located at the beginning of the α9 helix and located in the "wrapping domain". This amino acid does not interact directly with the substrate or the heme channel. In addition, its presence on the outer layer of the polypeptide subunit suggests that a change in this region may not disrupt catalase function. It is interesting that these three amino acid substitutions are unique to the BALB/c mouse strain and are not observed in other known mammalian species. The significance of these changes is not apparent in this study and remains to be established.

It is interesting to note that among the number of amino acid substitutions seen involving the four strains of mice, none involve the β9 region of the catalase polypeptide. The lack of substitutions in this region among mouse strains (if true for other strains not examined to date) may suggest that β9 mutations represent species-specific substitutions and may account for differences in biochemical properties of this enzyme from different species. Data included in Table 5 also could be used to comment on the nature of mutational events associated with the *Cas-1* gene. In particular, approximately 50% of the base substitutions involve a C → T transition or a C → G transversion. High mutability of the cytosine residue is well recognized in mammalian sequences (Cooper and Youssoufian, 1988) and may involve methylation of cytosine. It may be pointed out that the *Cas-1* region of the mouse genome is subject to methylation (unpublished results, this lab) which may account at least in part for the observed mutational events.

DNA sequences from the non-coding regions of the catalase gene available from Genbank for a number of species including eukaryotes and prokaryotes were compared to the BALB/c mouse sequence (data not presented). Although the 3' UTR sequence varies considerably in size, it was observed that this region of the mouse catalase gene has sequence features that are not commonly found in a similar region of other catalases. Comparison of the catalase 3' UTR sequences from mammals (Figure 10) however, show that this region of rodent (rat and mouse) is an exception and contains unusual repeat sequences (Figure 8) not identified in the same region of the human catalase. Of the three sets of near repeats present in mice [$(CA)_{31}$, $(T)_{15}$ and $(TGTGC)_7$], CA and T repeats are also found in the rat. The near T repeats in the two species are comparable in size while the CA repeat is much larger in the rat sequence (Furuta *et al*, 1986). The near pentamer repeat $(TGTGC)_7$ is

unique to mouse. The functional significance of such sequences is not known and becomes the focus of the remainder of this study.

b. Comparison of the *Cas-1* 3' UTR sequences among strains of mice

The 328 bp region of the 3' UTR of *Cas-1* (containing the unusual repeats mentioned above) was PCR amplified, cloned and sequenced bidirectionally from seven strains and the acatalasemic R.I. line of mice. The results showed no variation in SSCP analysis (Figure 34B) or in sequence comparisons (data not shown). It is interesting however, that in the coding region of this gene, a number of nucleotide substitutions are observed among the same strains. Recently, Duret *et al.* (1993) have shown that during vertebrate evolution, regions of the 3' UTR have been highly conserved from a number of genes including Na+/K+ ATPase β subunit, transferrin receptor and *c-fos*. Although these regions of high conservation do not permit conclusions about their function, there is a suggestion that these sequences are involved in posttranscriptional processes. The strong sequence conservation observed in the 3' UTR of *Cas-1* among strains and genotypes studied here may reflect the importance of this region in establishing a mechanism of posttranscriptional regulation of the catalase gene in mice. Unlike other genes reported in the literature, the conservation of the unusual near repeat sequences [$(CA)_{31}$, $(T)_{15}$ and $(TGTGC)_7$] is unique to *Cas-1* and may represent an evolutionary divergence in the regulation of mouse catalase gene expression.

The 3' UTR of an mRNA has in the past been viewed as a desert, lacking sequences with important regulatory information (Wickens, 1993). It was thought to carry only the signals necessary to form the end of the mRNA which are important in controlling mRNA stability (Jackson and Standart, 1990). It is now recognized that the often large 3' UTR can contain signals which may regulate translation and subcellular localization of an mRNA or polypeptide in addition to mRNA stability (Wickens, 1992). The mechanism by which a 3' UTR could play a regulatory role in gene expression is not well understood (Jackson, 1993). It is however, logical to argue that it may involve specific interactions with protein(s) or RNA (Wickens, 1993). The demonstration of such an interaction will further substantiate the importance of this region and its possible role in posttranscriptional regulation.

c. Evaluation of 3' UTR sequences in protein interactions: Possible role in posttranscriptional regulation

An extensive investigation on the 3' UTR of mouse *Cas-1* in this study has revealed the presence of mRNA-binding protein complexes. The three unusual repeat regions of *Cas-1* 3' UTR have been cloned and the corresponding mRNAs were subsequently generated. These transcripts were individually tested using gel mobility shift assays for their ability to bind proteins. I have shown that two regions of the 3' UTR of *Cas-1* mRNA, one of which contains $(CA)_{31}$ and the other which contains $(U)_{15}$, have the capacity to bind protein(s) *in vitro*, with sequence specificity. Moreover, these sequences bind different proteins as shown in cross competition assays (Figure 41). Clerch and Massaro (1992) have shown that the rat catalase 3' UTR, which is similar to mouse but not identical, binds to specific proteins(s) from neonatal rat lung in *in vitro* experiments. They have suggested that the formation of these mRNA-protein complexes are involved in regulating mRNA stability. The elucidation of mRNA-binding proteins to the specific regions of mouse *Cas-1* 3' UTR now provides a model to study the molecular mechanisms involved in the tissue-specific expression of catalase. These proteins may serve as transacting factors and differentially regulate catalase expression among strains and genotypes. This represents a major step in understanding the posttranscriptional regulation of mouse catalase in particular and housekeeping genes in general.

In this study, the 3' UTR region of *Cas-1* mRNA containing the near repeat $(U)_{15}$ yields at least three mRNA-binding complexes (x, y and z) which are observed in gel mobility shift assays (Figure 39). Extensive experimentation has shown that these complexes bind with sequence specificity and the protein(s) involved are unique to this region of the transcript. Comparisons involving a number of mouse strains showed that the mobility of the three protein-$(U)_{15}$ mRNA complexes do not differ in liver (Figure 43). The mobility of two of these complexes (y and z' in kidney and lung, however, appears to be variable among strains. In addition, there appears to be variability in the gel shift mobility complexes y and z in adult lung as compared to the neonatal lung homogenate. Similar complexes were also observed in blood cell lysates.

UV cross-linking studies with the near repeat $(U)_{15}$-specific mRNA-protein binding reveals the presence of two proteins (~38 and 47 kDa) in all tissues and genotypes tested in repeated experiments (Figure 47). To

the posttranscriptional regulation of mRNAs once they are localized to the cytoplasm.

Most 3' UTR mRNA-binding proteins identified to date are located primarily in the cytoplasm of mammalian cells and vary in molecular weight from 18 to 98 kDa. Although only a few proteins have been identified, one of the known regulatory proteins, the AU-rich binding factor (AUBF) has been well studied and reported to range in size from 32 to 36 kDa (Malter, 1989; Vakalopoulou *et al.*, 1991; Bickel *et al.*, 1992; Bohjanen *et al.*, 1992). Moreover, it has been shown to interact in a sequence-specific manner to multiple units of AUUUA. This protein functions mainly to stabilize a number of mRNAs including *c-myc* and *c-fos* in addition to lymphokine/cytokine mRNAs such as GM-CSF and IL-3. Due to the high U content of the mRNA sequence to which AUBF binds, it is possible that the near repeat $(U)_{15}$ containing transcript used in the studies reported in this thesis may in fact be related to these AU rich mRNAs. Furthermore, since the size of one of the proteins which binds the near repeat $(U)_{15}$ is ~38 kDa and the size range of AUBF is 32 to 36 kDa, it is possible that these two mRNA-binding proteins belong to a similar or related family of regulatory proteins. To date, no other known 3' UTR mRNA-binding proteins fall within the size range of the AUBF nor do they exhibit similar binding specificities.

It is logical to suggest that the posttranscriptional regulation of *Cas-1* may therefore involve the two proteins (~38 and 47 kDa) which bind specifically to $(U)_{15}$. Although the functions of these proteins have yet to be determined, it is possible that in part they interact with the catalase message to promote mRNA stability. This is supported by the experiments of Clerch and Massaro (1992) which also demonstrate the presence of mRNA-binding protein complexes that regulate catalase mRNA stability in rat neonatal lung homogenate. Although the ~38 kDa protein may function to regulate mRNA stability, its association with polysomes suggests that it may also function in translation. The presence of other proteins involved in the formation of the observed complexes and their contribution to the mechanisms of regulation cannot be ruled out.

The other 3' UTR of *Cas-1* mRNA which yield specific mRNA-binding complexes contains a near repeat of $(CA)_{31}$ (Figure 39). Comparisons involving a number of mouse strains showed that the mobility of the three protein-$(CA)_{31}$ mRNA complexes (a, b and c) do not differ between liver and kidney (Figure 42). In addition, it may be pointed out that these complexes do

determine whether these protein complexes may be important in the context of translation, polysomes were isolated from the livers of different mouse strains. The presence of two (x and y) mRNA-binding complexes were observed (Figure 48). Further analysis by UV cross-linking studies showed that only the smaller ~38 kDa band is associated with the polysome fraction of the tissue homogenates. This may argue for the importance of the ~38 kDa protein in the interaction with the translational machinery. The absence of the ~47 kDa protein from this fraction suggests that it is not directly involved with the translational machinery and may reflect the complexity of these mRNA-protein interactions.

The $(U)_{15}$ near repeat present in the 3' UTR of *Cas-1* mRNA is also found in rat (Furuta *et al.*, 1986) and may be important in the context of posttranscriptional regulation. Interestingly, the 3' UTR of human catalase mRNA also contains this near repeat although it is considerably smaller [$(U)_{10}$] and may or may not be significant in this context. The importance of this type of repeat is supported by other findings in the literature and may suggest its importance in the posttranscriptional regulation of catalase. Other mRNAs with poly (U) tracts in their 3' UTRs include those for the human thrombospondin (Hennessy *et al.*, 1989), human insulin receptor (Ullrich *et al.*, 1985), chick procollagen II (Shaw and Kamen, 1986), bovine acetylcholine receptor β-chain (Tanabe *et al.*, 1984), mouse urokinase plasminogen activator (Belin *et al.*, 1985), human β-actin (Tokunaga *et al.*, 1986), chick ovalbumin Y gene (Heilig *et al.*, 1982), human tissue factor (Spicer *et al.*, 1987), and human cap binding protein (Rychlik *et al.*, 1987). Although there is no known function for the poly (U) tract, it is clear that it has the potential to hybridize with the poly (A) tail forming a loop. Perhaps this duplex region plays a role in stabilization of mRNA against exonucleolytic attack as has been proposed for thrombospondin bacterial (Bilofsky *et al.*, 1986) and histone mRNAs (Raghow, 1987).

It is likely that the posttranscriptional mechanism involved in the regulation of *Cas-1* by mRNA-binding proteins is a complex one and may require the interactions of multiple elements, including multiple proteins. It is now known that the processes of nuclear cleavage and polyadenlyation of mRNAs involves a number of mRNA-binding proteins which are thought to interact and bind to form a much larger ternary complex (Sachs and Wahle, 1993). It is possible therefore, that such complex mechanisms may also exist in

the posttranscriptional regulation of mRNAs once they are localized to the cytoplasm.

Most 3' UTR mRNA-binding proteins identified to date are located primarily in the cytoplasm of mammalian cells and vary in molecular weight from 18 to 98 kDa. Although only a few proteins have been identified, one of the known regulatory proteins, the AU-rich binding factor (AUBF) has been well studied and reported to range in size from 32 to 36 kDa (Malter, 1989; Vakalopoulou *et al.*, 1991; Bickel *et al.*, 1992; Bohjanen *et al.*, 1992). Moreover, it has been shown to interact in a sequence-specific manner to multiple units of AUUUA. This protein functions mainly to stabilize a number of mRNAs including *c-myc* and *c-fos* in addition to lymphokine/cytokine mRNAs such as GM-CSF and IL-3. Due to the high U content of the mRNA sequence to which AUBF binds, it is possible that the near repeat $(U)_{15}$ containing transcript used in the studies reported in this thesis may in fact be related to these AU rich mRNAs. Furthermore, since the size of one of the proteins which binds the near repeat $(U)_{15}$ is ~38 kDa and the size range of AUBF is 32 to 36 kDa, it is possible that these two mRNA-binding proteins belong to a similar or related family of regulatory proteins. To date, no other known 3' UTR mRNA-binding proteins fall within the size range of the AUBF nor do they exhibit similar binding specificities.

It is logical to suggest that the posttranscriptional regulation of *Cas-1* may therefore involve the two proteins (~38 and 47 kDa) which bind specifically to $(U)_{15}$. Although the functions of these proteins have yet to be determined, it is possible that in part they interact with the catalase message to promote mRNA stability. This is supported by the experiments of Clerch and Massaro (1992) which also demonstrate the presence of mRNA-binding protein complexes that regulate catalase mRNA stability in rat neonatal lung homogenate. Although the ~38 kDa protein may function to regulate mRNA stability, its association with polysomes suggests that it may also function in translation. The presence of other proteins involved in the formation of the observed complexes and their contribution to the mechanisms of regulation cannot be ruled out.

The other 3' UTR of *Cas-1* mRNA which yield specific mRNA-binding complexes contains a near repeat of $(CA)_{31}$ (Figure 39). Comparisons involving a number of mouse strains showed that the mobility of the three protein-$(CA)_{31}$ mRNA complexes (a, b and c) do not differ between liver and kidney (Figure 42). In addition, it may be pointed out that these complexes do

not appear to differ among the strains tested. Interestingly, no complexes were observed which bind to $(CA)_{31}$ in lung tissue homogenate of any strain examined. The migration of the protein complexes from red blood cell lysates however, are different from those of liver and kidney suggesting the involvement of different protein(s) in the formation of mRNA-binding complexes in this tissue.

Further characterization of the $(CA)_{31}$-protein complexes by UV cross-linking studies showed that in every tissue examined, including the red blood cell lysate that exhibits the formation of complexes, a common band of ~69 kDa is present (Figure 45). This protein may represent a component of a much larger complex and the contribution of additional proteins to the formation of the tissue-specific complexes cannot be ruled out. Furthermore, this single ~69 kDa protein is found to be associated with the polysomal fraction of the tissue homogenates (Figure 48) suggesting that it may be important in the context of translation.

To the best of my knowledge there have been no reports in the literature to date which have identified mRNA-binding proteins specific to CA repeats. The involvement of proteins which bind to the 3' UTR of *Cas-1* mRNA containing $(CA)_{31}$ repeats is therefore speculative. It is tempting to offer a hypothetical model that may suggest a role for the 3' UTR of *Cas-1* in posttranscriptional gene regulation. Since the proteins which bind to the near repeat $(CA)_{31}$ are apparently different than those which bind the near repeat $(U)_{15}$, it is logical to suggest that perhaps there is a complex interaction involving both the mRNA sequences and their associated proteins which may or may not have similar functions.

Recent evidence using protein binding experiments and functional synergism suggests that the cap, the 5' leader and 3' UTR sequences of Tobacco Mosaic Virus interact with the same proteins which in turn establishes an efficient level of translation (Leathers *et al.*, 1993). This is the first report which exemplifies the complexity of posttranscriptional regulation of eukaryotic genes. In the study of mouse catalase, it is possible that this "scorpion" model can be used to explain the posttranscriptional regulation of *Cas-1*. The protein(s) which bind specifically to the near repeat $(U)_{15}$ containing region of *Cas-1* 3' UTR may act in part to regulate mRNA stability. The presence of the smaller protein (~38 kDa) associated with the polysome, however, may suggest an additional function, perhaps a translational one. In addition, the presence of the ~69 kDa protein associated with the upstream element $(CA)_{31}$ near repeat

is also associated with polysomes and may add to the bulk of the complex formation. If this putative highly complicated network is involved in translational efficiency, then it is possible that there exists a communication with the 5' upstream region of *Cas-1* gene, although this has not been demonstrated.

This "cross-talk" between sequences involving the 3' UTR and the extreme end of the poly (A) tail has been demonstrated to affect the rates of poly (A) shortening and subsequent mRNA degradation (Jackson and Standardt, 1990). The effect of coding sequences, 5' UTR sequences, and the translating ribosome on mRNA degradation rates further suggests that cross-talk exists between the 3' UTR or the poly (A) tail and far upstream sequences or events. The corollary is that events at the 3' end of the mRNA, such as changes in polyadenylation state or the interaction of specific proteins with the 3' UTR, could influence upstream events such as translation initiation or reinitiation. This cross-talk could result in a rearrangement of alternative secondary structures throughout the whole mRNA dependent on changes at one end of the molecule which may affect the regulation of gene expression. Alternatively, it may involve some direct interaction between 5' proximal and 3' proximal elements. Although this mechanism of gene regulation exists, it remains speculative and the involvement of this type of posttranscriptional regulation in the expression of *Cas-1* remains to be tested. Moreover, regulation at the level of translation cannot be ruled out in explaining the tissue-specificity of the formation of mRNA-protein complexes among the strains tested.

Recently, experiments on the regulation of *lin*-14 of *C. elegans*, a gene which controls the timing of developmental events, have shown that not only do regulatory proteins bind to specific sequences in the mRNAs which they control (Wickens and Takayama, 1994), but RNAs themselves can also act to regulate the expression of genes (Lee *et al.*, 1993; Wightman *et al.*, 1993). Here *lin*-4 RNA acts as a repressor which binds to specific sequences in the 3' UTR on *lin*-14. The formation of RNA duplexes down regulates the *lin*-14 translation. Since the TGTGC repeat in the 3' UTR of the *Cas-1* gene is not apparently involved in the binding of mRNA proteins under these conditions, it may still be important in regulation via other small RNA interactions. In the context of the scorpion model presented here, it is possible that RNA-RNA interactions may affect the cross-talk involved between the 3' UTR and the 5' regulatory regions necessary for the regulation of catalase translation. It should be pointed out that

such repeat sequences are not observed in rat or human catalase and may represent a posttranscriptional regulatory mechanism unique to mouse.

Although the research included in this thesis has identified two specific near repeat sequences $(CA)_{31}$ and $(U)_{15}$ in the 3' UTR of the *Cas-1* mRNA that form complexes with proteins present in the polyribosomal fraction of a number of tissue homogenates, the actual role of these sequences and their associated proteins remains to be experimentally established. It suggests however, that the 3' UTR of the *Cas-1* mRNA may not be barren and devoid of function. Rather, it may be important in the posttranscriptional regulation of this important antioxidant enzyme, a critical aspect of the regulation of this gene, at least in mice. The significance and role of the 3' UTR associated proteins observed during the course of this investigation must await the characterization of these proteins at the molecular level. Further experimentation in this area of research can only enhance our understanding of the contribution of the 3' UTR toward posttranscriptional gene regulation.

4.6. Summary:

Catalase is an antioxidant housekeeping enzyme which protects cells from the toxic effects of oxygen free radical metabolites by catalyzing the breakdown of H_2O_2 to H_2O and O_2. A defect in this enzyme results in elevated intracellular levels of oxidants which if not cleared effectively can result in a number of diseases including cancer. It was the aim of this project, therefore, to understand the organization and regulation of the expression of the catalase gene (*Cas-1*) in mouse. Mice from a number of different genotypes exhibit variability in tissue-specific expression and provide valuable biological material to evaluate the molecular mechanisms for the regulation of this housekeeping gene.

Catalase gene regulation was investigated at the level of transcription and posttranscription. In order to accomplish this, the complete cDNA sequence for *Cas-1*, including ~660 bp of 5' upstream regulatory elements was determined. The cDNA has 1584 nucleotides coding for a 528 amino acid polypeptide. Analysis of the 5' upstream regulatory region revealed a "CG island", two putative CCAAT boxes and a GC box, however it lacks a TATA box, typical of other housekeeping genes. This promoter was experimentally evaluated for patterns of methylation. In brain, liver, kidney and blood (all tissues which are known to express catalase), at least one of three CCGG sensitive sites tested lacked methylation. This suggests that the observed tissue-specific expression may be transcriptionally regulated.

The expression of *Cas-1* was evaluated in multiple tissues from a number of mouse genotypes using enzyme activity assays, polypeptide (western blot) and mRNA (northern and dot blot) analyses. The variability in enzyme activity observed in different tissues was shown to correlate with the level of mRNA. This suggests that tissue-specific expression of *Cas-1* is regulated at the level of transcription. The variability in enzyme activity which was observed among strains/genotypes is not, however, correlated with the level of mRNA. On the contrary, it was demonstrated to correlate with the levels of polypeptide using western blot analysis. These data suggest that the variability in catalase expression among genotypes is regulated posttranscriptionally.

The regulation of the mouse catalase gene (*Cas-1*) during fetal development was evaluted by *in situ* hybridization analysis. It was shown that the *Cas-1* gene is transcribed as early as 8 days *post conceptus* (with the formation of somites) and the transcription increases during development and differentiation. The tissue-specific enzyme expression appears to be regulated at the level of transcription since the relative mRNA level is correlated with relative enzyme activity. At birth however, with the onset of independent respiration, the enzyme activity levels, particulary in the liver, are dramatically increased relative to mRNA levels. This suggests posttranscriptional regulation at this stage of development.

The molecular basis of the tissue-specific acatalasemic mutation (C3H/HeAnl/*Cas-1^b*) was investigated. The observed amino acid subtitutions in the coding region of *Cas-1* in this strain cannot solely explain the tissue-specific mutation. Sequence analysis of the 3' UTR of the *Cas-1* gene revealed three unusual near repeats [$(CA)_{31}$, $(T)_{15}$ and $(TGTGC)_7$]. PCR analysis, cloning and sequencing revealed no sequence variation among the genotypes tested including C3H/HeAnl/*Cas-1^b*. The mRNA gel shift assay was used and identified proteins which specifically complexed to the near repeats $(CA)_{31}$ (~69 kDa), and $(U)_{15}$ (~38 and 47 kDa). Moreover, the ~69 and ~38 kDa proteins are found associated with the polysomes. It is hypothesized that the $(U)_{15}$-protein complex may be involved in mRNA stability and translation and the $(CA)_{31}$-protein complex may assist in regulation, possibly involving "cross-talk" between the 5' and 3' UTRs of this mRNA via their associated proteins.

The proteins identified in this study which bind specifically to sequences in the 3' UTR of *Cas-1* may represent transacting factors involved in the posttranscriptional regulation of this gene. Whether these protein factors contribute to the molecular understanding of the acatalasemic mutation remains unknown. The significance and the role of these 3' UTR mRNA-binding proteins must await their characterization at the molecular level.

APPENDIX 1:

Quantification of *Cas-1* mRNA by dot blots analysis

RNA dot blots were prepared and hybridized with *Cas-1* cDNA (pMCT-1) followed by rehybridization with 18S rRNA probes as specified in Methods (sect. 2.7). Statistical analyses of RNA dot blots is presented below.

The first set of experiments was performed to establish consistency in loading and scanning of dot blots. The laser densitometer (Pharmacia LKB Ultrascan XL) automatically scanned each dot three times, and the instrument internally averaged the values. In addition to these triplicate readings, replications included the use of three individuals and three different amounts of total RNA. Here, dot blots were prepared using total RNA (10, 5 and 1 μg) from the liver, kidney and blood of three strains: normal (BALB/c), hypocatalasemic (129/ReJ) and acatalasemic (C3H/HeAnl/*Cas-1*^{b}). One membrane consisted of total RNA from a single tissue with three replications from three individuals from each strain. The blot was hybridized with the *Cas-1* probe (pMCT-1) and subsequently exposed to X-ray film. The X-ray film was developed and densitometrically scanned for each strain, individual, and quantity of RNA used. The blot was stripped, and rehybridized with the 18S rRNA probe, which served as a control and used to account for variability in the total RNA loaded in each well. The X-ray film generated from this experiment was also scanned and the results compared to those of the *Cas-1* probe. The data are presented in Table I.

Analysis of variance was used to statistically evaluate the data. No difference in *Cas-1* mRNA/18S rRNA was detected among individuals in liver when 1 μg ($p > 0.90$) and 10 μg of total RNA was used. At 5 μg total RNA however, there was a significant difference observed among individuals. In kidney, no difference was detected in *Cas-1* mRNA/18S rRNA with 1 μg ($p > 0.50$), 5 μg ($p > 0.80$) and 10 μg ($p > 0.64$) of total RNA used. In blood, no significant difference was detected in *Cas-1* mRNA/18S rRNA among individuals using 1μg total RNA ($p > 0.93$), however individual differences were observed when 5 μg ($p < 0.023$) and 10 μg ($p < 0.004$) total RNA were used. In these experiments, comparisons in *Cas-1* mRNA/18S rRNA cannot be made among the three dot blots, since the X-rays generated vary in exposure time. These data, however, allow subsequent experiments to be performed with a single

individual without replications. In this way more than one tissue from multiple strains can evaluated under the same conditions, and comparisons among tissues and strains can be evaluated.

Table I. Mean *Cas-1* mRNA levels from three tissues (1 tissue per blot) of BALB/c, 129/ReJ, and C3H/HeAnl/*Cas-1*^{b} ± S.E.M. (calculated from 3 replications for 3 individuals of each strain) expressed as a ratio to 18S rRNA (*Cas-1*/rRNA).

	Total RNA (μg)		
Dot Blot 1: LIVER	1	5	10
BALB/c	0.272 ± 0.017	0.704 ± 0.043	0.745 ± 0.041
129/ReJ	0.273 ± 0.015	0.478 ± 0.016	0.640 ± 0.019
C3H/HeAnl/*Cas-1*^{b}	0.314 ± 0.015	0.782 ± 0.058	0.911 ± 0.038
Dot Blot 2: KIDNEY	1	5	10
BALB/c	0.539 ± 0.055	1.007 ± 0.095	1.192 ± 0.061
129/ReJ	0.407 ± 0.038	0.702 ± 0.069	1.144 ± 0.076
C3H/HeAnl/*Cas-1*^{b}	0.531 ± 0.043	0.919 ± 0.085	1.155 ± 0.095
Dot Blot 3: BLOOD	1	5	10
BALB/c	0.551 ± 0.074	0.519 ± 0.077	0.536 ± 0.068
129/ReJ	0.714 ± 0.119	0.652 ± 0.107	0.483 ± 0.083
C3H/HeAnl/*Cas-1*^{b}	0.696 ± 0.079	0.572 ± 0.079	0.744 ± 0.097

In order for these results to be accurately evaluated, the values obtained under the conditions used must fall within a linear range. Regression analysis was performed on each tissue from the *Cas-1* densitometric readings from each of the above blots. Data points from three random individuals from each blot were graphed for each amount of total RNA loaded. Linear regression values were determined and the data are presented in Figure I. In liver and kidney, most

Figure I: Representative *Cas-1* mRNA dot blot densitometric scans from random individuals at 1, 5 and 10 µg total RNA. The three tissues (liver, kidney and blood) are represented on different blots, therefore the scale of the densitometric readings are different and cannot be compared to one another. The regression values (r) are indicated for each line presented. Liver (A, B) - BALB/c , (C) - C3H/HeAnl/*Cas-1*^{b}. Kidney (A) - BALB/c, (B) - C3H/HeAnl/*Cas-1*^{b}, (C) - 129/ReJ. Blood (A,C) - BALB/c, (B) - C3H/HeAnl/*Cas-1*^{b}.

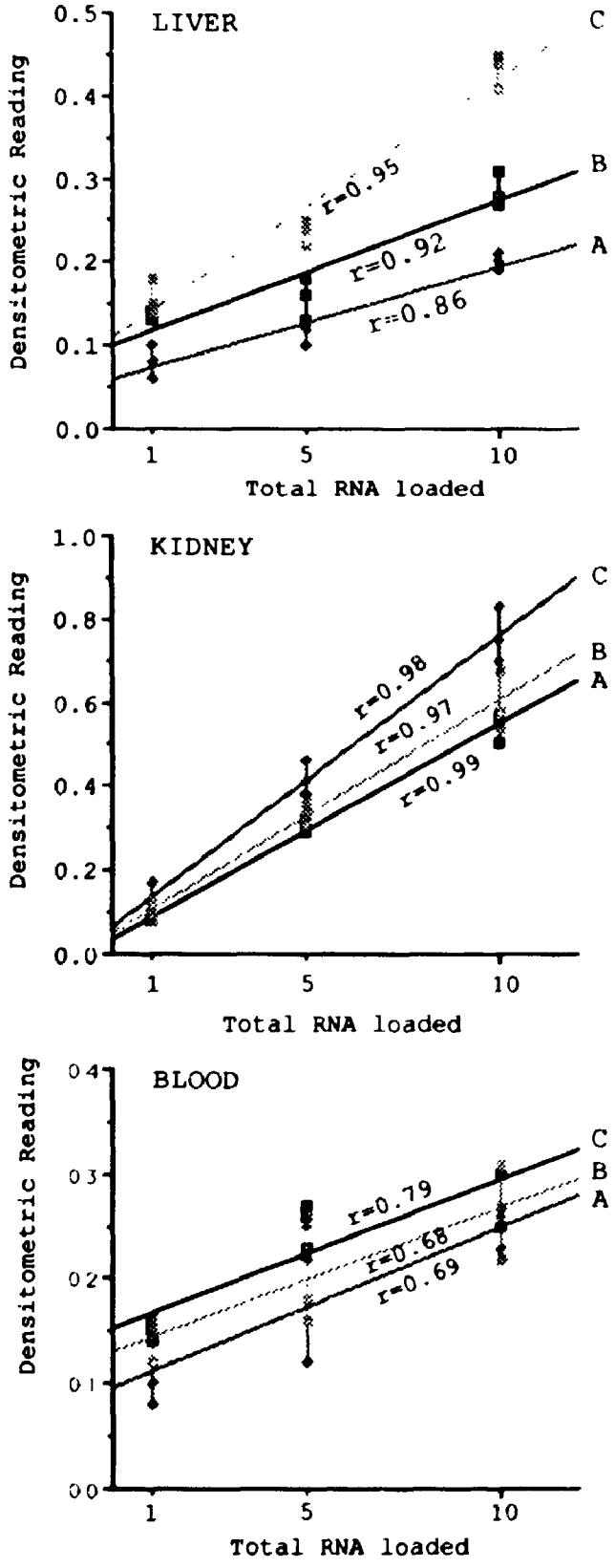
LIVER
Densitometric Reading
0.5
0.4
0.3
0.2
0.1
0.0
1
5
10
Total RNA loaded
C
B
A
r=0.95
r=0.92
r=0.86
KIDNEY
Densitometric Reading
1.0
0.8
0.6
0.4
0.2
0.0
1
5
10
Total RNA loaded
C
B
A
r=0.98
r=0.97
r=0.99
BLOOD
Densitometric Reading
0.4
0.3
0.2
0.1
0.0
1
5
10
Total RNA loaded
C
B
A
r=0.79
r=0.68
r=0.69

regression values obtained for all individuals were greater than 0.90. In blood, linear regression values ranged from 0.684 to 0.794. These results reflect the data and the values obtained using 10 µg total RNA may exceed optimum loading. In general however, these data demonstrate that the amount of RNA used in these experiments generated values that were in the linear range.

Cas-1 mRNA/18S rRNA comparisons were made among five mouse strains at 1, 5 and 10 µg of total RNA for each of liver and kidney. A single sample from each of three individuals was dot blotted from each strain for the three amounts of total RNA. The dot blots were hybridized as above, and the results are presented in Table II.

Table II. Mean *Cas-1* mRNA levels from two tissues (1 tissue per blot) of BALB/c, C3H/HeAnl/*Cas-1*^{a}, 129/ReJ, C57BL/6J and C3H/HeAnl/*Cas-1*^{b} ± S.EM.. (calculated from 1 replication from each of 3 individuals for each strain) expressed as ratio to 18S rRNA (*Cas-1*/rRNA). * represents only 1 animal from this strain which results were obtained. These data were not included in the ANOVA test.

	Total RNA (µg)		
Dot Blot 1: LIVER	1	5	10
BALB/c	1.06 ± 0.25	2.01 ± 0.16	1.88 ± 0.15
C3H/HeAnl/*Cas-1*^{a}	0.55 ± 0.11	1.04 ± 0.24	1.22 ± 0.24
129/ReJ	0.87 ± 0.07	1.54 ± 0.05	1.68 ± 0.06
C57BL/6J	0.66 ± 0.14	1.28 ± 0.23	1.63 ± 0.33
C3H/HeAnl/*Cas-1*^{b}	0.54 ± 0.15	1.26 ± 0.29	1.42 ± 0.32
Dot Blot 2: KIDNEY	1	5	10
BALB/c	0.58 ± 0.05	0.91 ± 0.18	0.70 ± 0.11
C3H/HeAnl/*Cas-1*^{a*}	0.25	0.41	0.66
129/ReJ	0.34 ± 0.04	0.54 ± 0.09	0.76 ± 0.20
C57BL/6J	0.18 ± 0.03	0.22 ± 0.08	0.31 ± 0.11
C3H/HeAnl/*Cas-1*^{b}	0.21 ± 0.01	0.17 ± 0.01	0.31 ± 0.06

Analysis of variance shows that in liver, the *Cas-1* mRNA/18S rRNA values are not significantly different among individuals ($p > 0.90$) or among strains ($p > 0.55$) when 1, 5 and 10 µg total RNA was used. In kidney, there was

also no significant difference among individuals ($p > 0.90$) with the three amounts of total RNA, however significant differences were observed among strains ($p < 0.01$) for 5 and 10 µg of total RNA. It is important to note that the *Cas-1* mRNA from the acatalasemic strain is not substantially reduced when compared to other strains, and suggests that the tissue-specific mutation is not due to transcription.

Since preliminary experiments established that there were no differences among individuals, comparisons were then made on the same dot blot among liver, kidney and blood from the three representative strains: normal (BALB/c), hypocatalasemia (129/ReJ) and acatalasemia (C3H/HeAnl/*Cas-1*^{b}). Total RNA (0.1, 1 and 10 µg) from each tissue and strain was blotted onto nitrocellulose and hybridized as above. The results of this experiment are presented inTable III.

Table III. Mean *Cas-1* mRNA levels from the liver, kidney and blood (on a single blot) of BALB/c, 129/ReJ, and C3H/HeAnl/*Cas-1*^{b} ± S.E.M. (calculated from 3 individuals for each strain) expressed as a ratio to18S rRNA (*Cas-1*/rRNA). Total RNA was used at 0.1, 1 and 10 µg. Only values obtained using 1 and 10 µg are included, since 0.1 µg of total RNA was not detectable on the dot blots.

	Total RNA (µg)	
LIVER	1.0	10.0
BALB/c	1.593 ± 0.172	1.357 ± 0.125
129/ReJ	1.383 ± 0.072	1.360 ± 0.015
C3H/HeAnl/*Cas-1*^{b}	1.487 ± 0.226	1.327 ± 0.041
KIDNEY	1.0	10.0
BALB/c	0.720 ± 0.102	0.827 ± 0.055
129/ReJ	0.534 ± 0.162	0.702 ± 0.195
C3H/HeAnl/*Cas-1*^{b}	0.833 ± 0.190	0.902 ± 0.177
BLOOD	1.0	10.0
BALB/c	0.360 ± 0.073	0.639 ± 0.188
129/ReJ	0.401 ± 0.032	0.712 ± 0.038
C3H/HeAnl/*Cas-1*^{b}	0.436 ± 0.033	0.505 ± 0.096

Analysis of variance demonstrates that when 10 µg of RNA was used, there was no significant difference observed in *Cas-1* mRNA levels among strains within the three tissues ($p > 0.95$). Moreover, the tissue specific differences in *Cas-1* mRNA levels were highly significant ($p < 0.001$). Analysis using 1 µg total RNA showed that *Cas-1* mRNA expression does not significantly differ among strains ($p > 0.60$) however tissue-specific expression of *Cas-1* mRNA does show a significant difference ($p < 0.001$). The values obtained using 1 and 10 µg RNA in this experiment are included in the results section and were used for comparative analysis and further evaluation.

APPENDIX 2: - Quantitation of polypeptide from western blots.

Western blots were prepared and reacted with polycolonal anti human catalase antibody as indicated in Methods (sect. 2.6). This experiment was performed to show that densitometric scans of bands resulting from western blots fall within the linear range and the evaluation of the relative quantitation of catalase polypeptide from tissues and genotypes is therefore satisfactory. Regression analysis was performed on a range of bovine liver catalase (BMC) from the densitometric readings from a western blot. Linear regression values were determined using 50 to 400 ng of bovine catalase and the data are presented in Figure I. This graph shows that all quantities used fall within the linear range and no quenching was observed at the highest concentration. This analysis is satisfactory to determine the relative presence or absence of the catalase polypeptide in liver, kidney and blood of the different strains of mice. On each blot, the catalase polypeptide from these tissues was evaluated using 100 ng bovine catalase polypeptide as a control to standardize the quantitative results obtained.

Figure I: Densitometric scans from 50, 100, 200 and 400 ng bovine liver catalase polypeptide. The regression value (r) is indicated and demonstrates that all protein concentrations yield values that are on a linear scale.

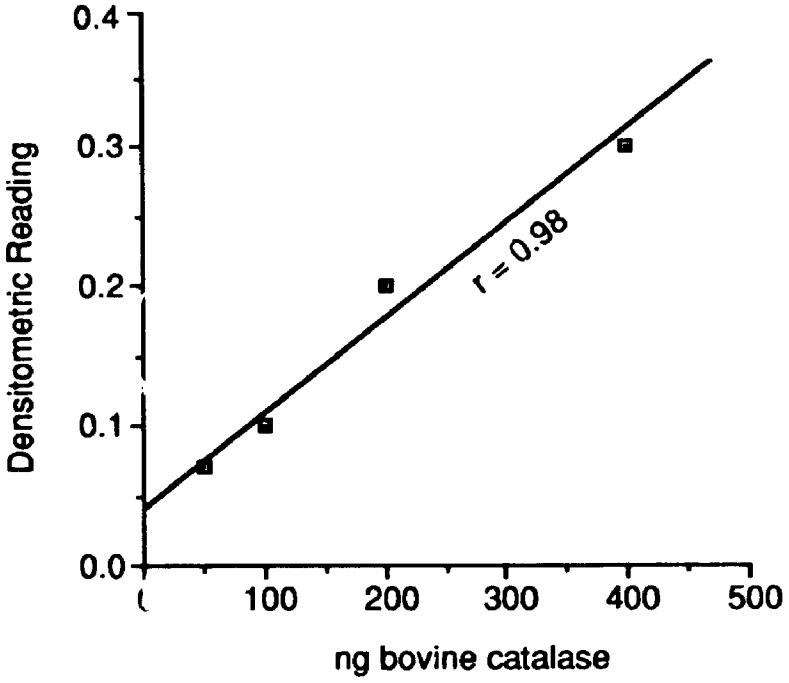
0.4
0.3
0.2
0.1
0.0
Densitometric Reading
r = 0.98
100
200
300
400
500
ng bovine catalase

APPENDIX 3

Origin and Characterization of an Acatalasemic RI Line

Numerous recombinant inbred (RI) mouse lines were established to study the genetic segregation of catalase phenotypes (Schisler and Singh, 1991). One of the RI lines developed possessed a "belted" phenotype. This RI line is registered and designated SXC/ws-1. This "belted" phenotype was first observed in 1983 in an F_2 generation of a cross involving an inbred female S.W. (white, normal catalase) and a male C3H/HeAnl/*Cas-1*^{b} (brown, acatalasemic). Four pairs of brother-sister F_1 matings produced four belted females and four belted males (out of 47 F_2 individuals) with white belts around the midsection on a brown or black background. Subsequent mating of a black "belted" female and a black "belted" male (from the F_2 generation) resulted in 50% black and 50% brown animals, all with the "belted" phenotype. Crosses involving black animals with the belt in subsequent generations resulted in 100% black "belted" animals, and have been maintained by brother-sister matings in the breeding colony for more than 20 generations since 1983.

A mouse strain with the known "belted" mutation (ABP/Le *a/a b/b bt/bt p/p se/se wa-1/wa-1* (*bt/bt*:)) has been genetically characterized and the gene for the "belted" mutation has been localized to Chromosome 15. This strain was obtained from The Jackson Laboratory and used in genetic studies involving the newly arisen RI line (SXC/ws-1). To test whether the "belted" phenotype in SXC/ws-1 is allelic to the known "belted" mutation of ABP/Le, matings were set up between SXC/ws-1 and ABP/Le. Eighteen F_1 animals were obtained from a cross involving a female SXC/ws-1 with a male ABP/Le and twenty-six F_1 animals were produced by the reciprocal cross. All animals were black and possessed the belted phenotype, however there is variability in expression of the belt. Two brother-sister matings were used to produce F_2 individuals that were scored for the presence of the belt. Forty out of 41 F_2 animals exhibited a clear visible white hair patch or belted phenotype. There is extensive variability in the amount of white hairs present, ranging from a few hairs on the dorsal or ventral surface to the presence of a complete belt around the body. The single animal with no obvious white hair patch is assumed to be due to incomplete penetrance

of the *bt* gene. These data suggest that the two mutations are indeed allelic. As expected there is also a segregation for coat colour in this generation which includes black, silver, beige and chocolate.

Mice from the SXC/ws-1 line were biochemically characterized for the catalase phenotype using four different approaches: a) the "fizz" test, b) the spectrophotometric enzyme assay, c) the PAGE / ferric chloride assay and d) SDS-PAGE western blots analysis (see Materials and Methods, section 2.5 and 2.6)

Preliminary screening of 13 mice (10 males, 3 females) with the "fizz" test suggested that all animals were apparently negative for blood catalase activity. Three tissues (liver, kidney and blood) from three males each of the two parental strains [S.W. (normal), C3H/HeAnl/*Cas-1^b* (acatalasemic)] and SXC/ws-1 were analyzed for catalase properties using a number of criteria. Results from these experiments are presented in the results section of this thesis. Using the spectrophotometric assay and the native polyacrylamide gel, catalase activities in the three tissues of C3H/HeAnl/*Cas-1^b* are similar to SXC/ws-1, and are dramatically reduced when compared to S.W. Furthermore, western blot analysis in the three tissues suggests that the reduction in catalase enzyme activity in C3H/HeAnl/*Cas-1^b* and the SXC/ws-1 kidney and whole blood lysate, could be explained by a reduction in the catalase polypeptide.

Results from the biochemical and genetic studies suggest that the acatalasemic mutation has successfully been established in a novel genetic background. Although Shaffer and Preston (1990) have identified a single nucleotide transversion in the catalase structural gene (*Cas-1*) of C3H/HeAnl/*Cas-1^b*, the tissue-specific expression of this mutation may require additional factors (Reimer *et al.*, 1994). Although the molecular basis of acatalasemia in the new RI line has not been investigated, evidence available to date implies that its genetic basis is identical to that in the C3H/HeAnl/*Cas-1^b*. This line however permits the evaluation of the expression of the acatalasemic mutation in a novel genetic background.

REFERENCES

Aebi, H. (1983). Catalase. In: *Methods of Enzymatic Analysis* H.U. Bergmeyer (Ed.), Academic Press, New York, pp. 673-684.

Aebi, H. (1984). Catalase in vitro. Methods Enzymol., 105: 121-126.

Aebi, H., and Suter, H. (1971). Acatalasemia. Adv. Hum. Genet., 2: 143-199.

Alberta, J. A., Rundell, K., and Stiles, C. D. (1994). Identification of an activity that interacts with the 3' untranslated region of c-myc mRNA and the role of its target sequence in mediating rapid mRNA degradation. J. Biol. Chem., 269(6): 4532-4538.

Ames, B. N. (1983). Dietary carcinogens and anticarcinogens: Oxygen radicals and degenerative diseases. Science, 221: 1256-1264.

Aslandis, C., Jansen, G., Amemiya, C., Shutler, G., Tsilfidis, C., Mahadevan, M., Chen, C., Alleman, J., Wormskamp, N. G. M., Vooljs, M., Buxton, J., Johnson, K., Smeets, H. J. M., Lennon, G. G., Carrano, A. V., Korneluk, R. G., Wieringa, B., and de Jong, P. J. (1992). Cloning of the essential myotonic dystrophy region: mapping of the putative defect. Nature, 355: 548-551.

Ausubel, F. M., Brent, R., Kingston, R. E., Moore, D. D., Smith, J. A., Seidman, J. G., and Struhl, K. (1987). *Current Protocols in Molecular Biology.* Green Publishing Associates, Toronto.

Aviram, I., and Shaklai, N. (1981). The association of human erythrocyte catalase with cell membrane. Arch. Biochem. Biophys., 212: 329-337.

Been, M. D., Burgess, R. R., and Champoux, J. J. (1984). Nucleotide sequence preference at rat liver and wheat germ type 1 DNA topoisomerase breakage lies in duplex SV40 DNA. Nuc. Acids Res., 12(7): 3097-3113.

Belin, D., Vassalli, J.-D., Combepine, C., Godeau, F., Nagamine, Y., Reich, E., Kocher, P., and Duvoisin, R. M. (1985). Cloning, nucleotide sequencing and expression of cDNAs encoding mouse urokinase-type plasminogen activator. Eur. J. Biochem., 148: 225-232.

Bickel, M., Iwai, Y., Pluznik, D. H., and Cohen, R. B. (1992). Binding of sequence-specific proteins to the adenosine-plus uridine rich sequences of the murine granulocyte/macrophage colony-stimulating factor mRNA. Proc. Natl. Acad. Sci., 89: 10001-10005.

Bilofsky, H. S., Burks, C., Fickett, J. W., Goad, W. B., Lewitter, F. I., Rindone, W. P., Swindell, C. D., and Tung, C.-S. (1986). The GenBank genetic sequence database. Nuc. Acids Res., 14: 1-4.

Bird, A. P. (1986). CpG-rich islands and the function of DNA methylation. Nature, 321: 209-213.

Bird, A. P. (1987). CpG islands as gene markers in the vertebrate nucleus. Trends Genet., 3: 342-347.

Bohjanen, P. R., Petryniak, B., June, C. H., Thompson, C. B., and Lindsten, T. (1992). AU RNA-binding factors differ in their binding specificities and affinities. J. Biol. Chem., 267(9): 6302-6309.

Boyes, J., and Bird, A. (1991). DNA methylation inhibits transcription indirectly via methyl-CpG binding protein. Cell, 64: 1123-1134.

Bradford, M. (1976). A rapid and sensitive method for quantitation of microgram quantities of protein utilizing the priniciple of protein-dye binding. Anal. Biochem., 72: 248-254.

Brock, J. D., McCurrach, M. E. Harley, H. G., Buckler, A. J., Church, D., Aburatani, H., Hunter. K., Stanton, V. P., Thirion, J.-P., Hudson, T., Sohn, R., Zemelman, B., Snell, R. G., Rundle, S. A., Crow, S., Davies, J., Shelbourne, P., Buxton, J., Jones, C., Juvonen, V., Johnson, K., Harper, P. S., Shaw, D. J., and Housman, D. E. (1992). Molecular basis of myotonic dystrophy: Expansion of a trinucleotide (CTG) repeat at the 3' end of a transcript encoding a protein kinase family member. Cell, 68: 799-808.

Cedar, H. (1988). DNA methylation and gene activity. Cell, 53: 3-4.

Cerutti, P. (1985). Pro oxidant states and tumor promotion. Science, 227: 375-381.

Chance, B., Sies, H., and Boveris, A. (1979). Hydroperoxide metabolism in mammalian organs. Physiol. Rev., 59: 527-605.

Chomczynski, P., and Sacchi, N. (1987). Single-step method of RNA isolation by acid guanidinium thiocyanate-phenol-chloroform extraction. Anal. Biochem., 162: 156-159.

Clemens, M. J. (1983). Purification of eukaryotic mRNA. In: *Transcription and Translation.* B. D. Hames and S. J. Higgins, (Eds.), IRL Press Ltd, Oxford, England, pp. 211-230.

Clerch, L., and Massaro, D. (1992). Oxidation-reduction-sensitive binding of lung protein to rat catalase mRNA. J. Biol. Chem., 267(5): 2853-2855.

Clerch, L. B., Iqbal, J., and Massaro, D. (1991). Perinatal rat lung catalase gene expression: Influence of corticosteroid and hyperoxia. Am. J. Physiol., 260: L428-433.

Cohen, G., Dembeic, D., and Marcus, J. (1970). Measurement of catalase activity in tissue extracts. Anal. Biochem., 34: 30-38.

Cooper, D. N. (1983). Eukaryotic DNA methylation. Hum. Genet., 64: 315-333.

Cooper, D. N., and Youssoufian, H. (1988). The CpG dinucleotide and human genetic disease. Hum. Genet., 78: 151.

Cox, K. H., Deleon, D. V., Angerer, L. M., and Angerer, R. C. (1984). Detection of mRNAs in sea urchin embryos by *in situ* hybridization using asymmetric RNA probes. Dev. Biol., 101: 485-502.

Crawford, D. R., Mirault, M.-E., Moret, R., Zbinden, I., and Cerutti, P. A. (1988). Molecular defect in human acatalasia fibroblasts. Biochem. Biophys. Res. Comm., 153(1): 59-66.

Darnell, J., Lodish, H., and Baltimore, D. (1986). *Molecular Cell Biology.* W.H. Freeman and Company, New York.

Davis, L.G., Dibner, M.D., and Battey, J.F. (1986). *Basic Methods in Molecular Biology.* Elsevier Publishing Company, New York.

de Duve. C., and Baudhuin, P. (1966). Peroxisomes, microbodies and related particles. Physiol. Rev., 46: 323.

de Haan, J. B., Martin, J. T., Francesca, C., and Ismail, K. (1994). Expression of copper/zinc superoxide dismutase and glutathione peroxidase in organs of developing mouse embryos, fetuses and neonates. Ped. Res., 35(2): 188-196.

De Sousa, P. A., Valdimarsson, G., Nicholson, B. J., and Kidder, G. M. (1993). Connexin trafficking and the control of gap junction assembly in mouse preimplantation embryos. Dev., 117: 1355-1367.

Denhardt, D. T. (1966). A membrane filter technique for the detection of complementary DNA. Biochem. Biophys. Res. Comm., 23: 641-646.

Dickerman, R. C., Feinstein, R. N., and Grahn, D. (1968). Position of acatalasemia gene in linkage group V of the mouse. J. Hered., 59: 177-178.

Duret, L., Dorkeld, F., and Gautier, C. (1993). Strong conservation of non-coding sequences during vertebrates evolution: Potential involvement in post-transcriptional regulation of gene expression. Nuc. Acids Res., 21(10): 2315-2322.

Dynan, W. S. (1986). Promoters for housekeeping genes. Trends Genet., 2: 196-197.

Eden, S., and Cedar, H. (1994). Role of DNA methylation in the regulation of transcription. Current Opin. Gen. Dev., 4: 255-259.

El-Hage, S., and Singh, S. M. (1989). Regulation of catalase-specific mRNA and its processing during development in mice. Dev. Genet., 10: 339-344.

El-Hage, S., and Singh, S. M. (1990). Temporal expression of genes encoding free radical-metabolizing enzymes is associated with higher mRNA levels during in utero development in mice. Dev. Genet., 11: 149-159.

Feinstein, R. N. (1970). Acatalasemia in the mouse and other species. Biochem. Genet., 4: 135-155.

Feinstein, R. N. (1973). Studies of acatalasemia. Birth Defects: Orig. Art. Ser., IX(2): 55-61.

Feinstein, R. N., Howard, J. B., Braun, J. T., and Seaholm, J. E. (1966). Acatalasemia and hypocatalasemia mouse mutants. Genet., 53: 923-933.

Fita, I., and Rossmann, M. G. (1985). The active center of catalase. J. Mol. Biol., 185: 21-37.

Frank, L., and Groseclose, E. E. (1984). Preparation for birth into an oxygen rich environment: the antioxidant enzymes in the developing rabbit lung. Ped. Res., 18: 240-244.

Frank, L., and Sosenko, I. R. S. (1987). Prenatal development of lung antioxidant enzymes in four species. J. Pediatr., 110: 106-110.

Fridovich, I. (1977). Oxygen is toxic. BioScience, 27(7): 462-466.

Fridovich, I. (1986). Biological effects of the superoxide radical. Arch. Biochem. Biophys., 247: 1-11.

Fu, Y.-H., Friedman, D. L., Richards, S., Pearlman, J. A., Gibbs, R. A., Pizzuti, A., Ashizawa, T., Perryman, M. B., Scarlato, G., Fenwick, R. G., and Caskey, C. T. (1993). Decreased expression of myotonin-protein kinase messenger RNA and protein in adult form of myotonic dystrophy. Science, 260: 233-238.

Furuta, S., Hayashi, H., Hijikata, M., Miyazawa, S., Osumi, T., and Hashimoto, T. (1986). Complete nucleotide sequence of cDNA and deduced amino acid sequence of rat liver catalase. Proc. Natl. Acad. Sci., 83: 313-317.

Ganschow, R. E., and Schimke, R. T. (1969). Independent genetic control of the catalytic activity and rate of degradation of catalase in mice. J. Biol. Chem., 244(17): 4649-4658.

Ganschow, R. E., and Schimke, R. T. (1970). Mutant catalase phenotypes. Biochem. Genet., 4: 157-167.

Gerdin, E., Tyden, O., and Eriksson, U. J. (1985). The development of antioxidant enzymatic defense in the perinatal rat lung. Activities of superoxide dismutase, glutathione peroxidase and catalase. Ped. Res., 19: 687-691.

Gillis, P., and Malter, J. S. (1991). The adenosine-uridine binding factor recognizes the AU-rich elements of cytokine, lymphokine and oncogene mRNAs. J. Biol. Chem., 266(5): 3172-3177.

Gould, S. J., Keller, G., and Subramani, S. (1988). Identification of peroxisomal targeting signals located at the carboxy terminus of four peroxisomal proteins. J. Cell Biol., 107: 897-905.

Halliwell, B., and Gutteridge, J. M. C. (1990). Role of free radicals and catalytic metal ions in human disease: An overview. Methods Enzymol., 186: 1-43.

Harman, D. (1982). The free-radical theory of aging. In: *Free Radicals in Biology* W. A. Pryor (Ed.), Academic Press, New York, pp. 255-275.

Harris, H., and Hopkinson, D. A. (1976). *Handbook of Enzyme Electrophoresis in Human Genetics.* American Elsevier Publishing Company, New York.

Hass, M., Iqbal, J., Clerch, L. B., Frank, L., and Massaro, D. (1989). Rat lung Cu, Zn superoxide dismutase. Isolation and sequence of a full-length cDNA and studies of enzyme induction. J. Clin. Invest., 83: 1241-1246.

Heilig, R., Muraskowsky, R., Kloepfer, C., and Mandel, J. L. (1982). The ovalbumin gene family: Complete sequence and structure of the Y gene. Nuc. Acids Res., 10: 4363-4382.

Hennessy, S. W., Frazier, B. A., Kim, D. D., Deckwerth, T. L., Baumgartel, D. M., Rotwein, P., and Frazier, W. A. (1989). Complete thrombospondin mRNA sequence includes potential regulatory sites in the 3' untranslated region. J. Cell Biol., 108: 729-736.

Hentze, M. W. (1991). Determinants and regulation of cytoplasmic mRNA stability in eukaryotic cells. Biochim. Biophys. Acta, 1090: 281-292.

Hentze, M. W., Ronault, T. A., Harford, J. B., and Klausner, R. D. (1989). Oxidation -reduction and the molecular mechanism of a regulatory RNA-protein interaction. Science, 244: 357-359.

Hessler, J. R., Morel, D. W., Lewis, L. J., and Chisolm, G. M. (1983). Lipoprotein oxidation and lipoprotein-induced cytotoxicity. Arteriosclerosis, 3: 215-222.

Heston, W. E., Hoffman, H. A., and Rechcigl, M. (1965). Genetic analysis of liver catalase activity in two substrains of C57BL mice. Genet. Res., 6: 387-397.

Hoffman, H. A., and Grieshaber, C. K. (1974). Genetic studies of murine catalase: Liver and erythrocyte catalase controlled by independent loci. J. Hered., 65: 277-279.

Hoffman, H. A., and Grieshaber, C. K. (1976). Genetic studies of murine catalase: Regulation of multiple forms of kidney catalase. Biochem. Genet., 14: 59-66.

Hoffman, H. A., and Rechcigl, M. J. (1971). Erythrocyte catalase in inbred mice. Enzyme, 12: 219-225.

Holliday, R. (1987). The inheritance of epigenetic defects. Science, 238: 163-170.

Holmes, R. S. (1971). Ontogeny of mouse liver peroxisomes and catalase isozymes. Nature New Biol., 232: 218-220.

Holmes, R. S., and Duley, J. A. (1975). Biochemical and genetic studies of peroxisomal multiple enzyme systems: a-hydroxyacid oxidase and catalase. In: *Isozymes: Molecular Structure* C. L. Markert (Ed.), Academic Press, New York, pp. 191-211.

Holmes, R. S., and Masters, C. J. (1970). Epigenetic interconversions of the multiple forms of mouse liver catalase. FEBS Lett., 11(1): 45-48.

Holmes, R. S., and Masters, C. J. (1972). Species specific features of the distribution and multiplicity of mammalian liver catalase. Arch. Biochem. Biophys., 148: 217-223.

Ikonen, E., Ulmanen, I., and Peltonen, L. (1992). Deletion of the 3' untranslated region of aspartylglucosaminidase mRNA results in a lysosomal accumulation disease. J. Biol. Chem., 267(13): 8715-8781.

Jackson, R. J. (1993). Cytoplasmic regulation of mRNA function: the importance of the 3' untranslated region. Cell, 74: 9-14.

Jackson, R. J., and Standart, N. (1990). Do the poly (A) tail and 3' untranslated region control mRNA translation? Cell, 62: 15-24.

Jalinot, P., and Kedinger, C. (1986). Negative regulatory sequences in the Ela-inducible enhancer of the adenovirus-2 early Ella promoter. Nuc. Acids Res., 14(6): 2651-2669.

Kafri, T., Ariel, M., Brandeis, M., Shemer, R., Urven, L., McCarrey, J., Cedar, H., and Razin, A. (1992). Developmental pattern of gene-specific DNA methylation in the mouse embryo and germ line. Genes Dev., 6: 705-714.

Keene, J. D., and Query, C. C. (1991). Nuclear RNA-binding proteins. Prog. Nuc. Acids Res. Mol. Biol., 41: 179-202.

Kelly, F. J., and Rickett, G. M. W. (1987). Temporal development of antioxidant in the newborn rat. Biochem. Soc. Trans., 15: 225-226.

Kensler, T. W., and Trush, M. A. (1984). Role of oxygen radicals in tumor promotion. Environ. Mutagen., 6: 593-616.

Kimura, A., Israel, A., Bail, O. L., and Kourilsky, P. (1986). Detailed analysis of mouse H-2K^b promoter: enhancer-like sequences and their role in the regulation of class I gene expression. Cell, 44: 261-272.

Kontos, H. A. (1985). Oxygen radicals in cerebral vascular injury. Circ. Res., 57: 508-516.

Kozak, M. (1989a). The scanning model for translation: an update. J. Cell Biol., 108: 229-241.

Kozak, M. (1989b). Circumstances and mechanisms of inhibition of translation by secondary structure in eucaryotic mRNAs. Mol. Cell Biol., 9(11): 5134-5142.

Kozak, M. (1991a). An analysis of vertebrate mRNA sequences: intimations of translational control. J. Cell Biol., 115(4): 887-903.

Kozak, M. (1991b). Structural features in eukaryotic mRNAs that modulate the initiation of translation. J. Biol. Chem., 266(30): 19867-19870.

Kozak, M. (1992). Regulation of translation in eukaryotic systems. Ann. Rev. Cell Biol., 8: 197-225.

Kwon, U. K., and Hecht, N. B. (1993). Binding of a phosphoprotein to the 3' untranslated region of the mouse protamine 2 mRNA temporally represses its translation. Mol. Cell. Biol., 13(10): 6547-6557.

Leathers, V., Tanguay, R., Kobayashi, M., and Gallie, D. R. (1993). A phylogenetically conserved sequence within viral 3' untranslated RNA peudoknots regulates translation. Mol. Cell Biol., 13(9): 5331-5347.

Lee, R. C., Feinbaum, R. L., and Ambros, V. (1993). The *C. elegans* heterochronic gene lin-4 encodes small RNAs with antisense complementarity to lin-14. Cell, 75: 843-854.

Maltais, L. J., Doolittle, D. P., Roderick, T. H., Hillyard, A. L., and Davisson, M. T. (1994). Locus map of mouse. Mouse Genome, 92(1): 62-85.

Malter, J. (1989). Identification of an AUUUA-specific messenger RNA binding proteins. Science, 246: 664-666.

Martin, J. D., King, D. M., Slauch, J. M., and Frisque, R. J. (1985). Differences in regulatory sequences of naturally occurring JC virus variants. J. Virol., 53: 306-311.

Masters, C., Pegg, M., and Crane, D. (1986). On the multiplicity of the enzyme catalase in mammalian liver. Mol. Cell Biochem., 70: 113-120.

Meijlink, F., Curran, T., Miller, A. D., and Verma, I. M. (1985). Removal of a 67-base pair sequence in the noncoding region of protooncogene *fos* converts it to a transforming gene. Proc. Natl. Acad. Sci., 82: 4987-4991.

Mullner, E. W., Neupert, B., and Kuhn, L. C. (1989). A specific mRNA binding factor regulates the iron-dependent stability of cytoplasmic transferrin receptor mRNA. Cell, 58: 373-382.

Murthy, M. R. N., Reid, T. J., Sicignano, A., Tanaka, N., and Rossmann, M. G. (1981). Structure of beef liver catalase. J. Mol. Biol., 152: 465-499.

Novak, R., Matkovics, B., Varga, I., and Szabo, L. (1978). Comparison of peroxide metabolism enzymes in the organs of congenic mice. Comp. Biochem. Physiol., 60B: 149-150.

Ogata, M. (1991). Acatalasemia. Hum Genet., 86: 331-340.

Osumi, T., and Fujiki, Y. (1990). Topogenesis of peroxisomal proteins. BioEssays, 12(5): 217-222.

Pain, V. M. (1986). Initiation of protein syntnesis in mammalian cells. Biochem. J., 235: 625-637.

Peltz, S. W., Brewer, G., Bernstein, P., Hart, P. A., and Ross, J. (1991). Regulation of mRNA turnover in eukaryotic cells. Critical Reviews in Eukaryotic Gene Expression, 1(2): 99-126.

Percy, M. E. (1984). Catalase: an old enzyme with a new role? Can. J. Biochem. Cell Biol., 62: 1006-1014.

Quan, F., Korneluk, R. G., Tropak, M. B., and Gravel, R. A. (1986). Isolation and characterization of the human catalase gene. Nuc. Acids Res., 14(13): 5321-5335.

Raghow, R. (1987). Regulation of messenger RNA turnover in eukaryotes. Trends Biochem. Sci., 12: 358-360.

Razin, A., and Cedar, H. (1991). DNA methylation and gene expression. Microbiol. Rev., 55(3): 451-458.

Rechcigl, M., and Heston, W. E. (1963). Tissue catalase activity in several C57BL substrains and in other strains of inbred mice. J. Natl. Cancer Inst., 30(5): 855-864.

Rechcigl, M., and Heston, W. E. (1967). Genetic regulation of enzyme activity in mammalian system by the alteration of the rates of enzyme degradation. Biochem. Biophys. Res. Comm., 27(2): 119-124.

Reimer, D. L., and Singh, S. M. (1990). In situ hybridization studies on murine catalase mRNA expression during embryonic development. Dev. Genet., 11: 318-325.

Reimer, D. L., Bailley, J., and Singh, S.M. (1994). Complete cDNA and 5' genomic sequences and multilevel regulation of the mouse catalase gene. Genomics (in press).

Richter, J. D. (1991). Translational control during early development. Bioessays, 13(4): 179-183.

Rickett, G. M. W., and Kelly, F. J. (1990). Developmental expression of antioxidant enzymes in guinea pig lung and liver. Dev., 108: 331-336.

Rodenhiser, D.I., Coulter-Mackie, M.B., and Singh, S.M. (1993). Evidence of DNA methylation in the neurofibromatosis type 1 (NF1) gene region of 17q11.2. Hum. Mol. Gen., 2(4): 439-444.

Rychlik, W., Domier, L. L., Gardner, R. R., Hellmann, G. M., and Rhoads, R. E. (1987). Amino acid sequence of the mRNA cap-binding protein from human tissues. Proc. Natl. Acad. Sci., 84: 945-949.

Sachs, A., and Wahle, E. (1993). Poly(A) tail metabolism and function in eucaryotes. J. Biol. Chem., 268(31): 22955-22958.

Sambrook, J., Fritsch, E. F., and Maniatis, T. (1989). *Molecular Cloning: A Laboratory Manual. Second Edition.* Cold Spring Harbor, New York.

Sandell, L. J., Prentice, H. J., Kravis, D., and Upholt, W. B. (1984). Structure and sequence of chicken type II procollagen gene. J. Biol. Chem., 259: 7826-7834.

Sanger, F., Nicklen, S., and Coulson, A. R. (1977). DNA sequencing with chain-terminating inhibitors. Proc. Natl. Acad. Sci., 74: 5463-5467.

Saul, R. P., Gee, P., and Ames, B. N. (1987). Free Radicals, DNA damage and aging. In: *Modern Biological Theories of Aging* H. R. Warner (Ed.), Raven Press, New York, pp. 113-129.

Schisler, N. J., and Singh, S. M. (1987). Inheritance and expression of tissue specific catalase activity during development and aging in mice. Genome, 29: 748-760.

Schisler, N. J., and Singh, S. M. (1991). A quantitative genetic analysis of tissue-specific catalase activity in *Mus musculus*. Biochem. Genet., 29(1/2), 65-89.

Schonbaum, G. R., and Chance, B. (1976). Catalase In: *The Enzymes* (3rd ed.), P.D. Boyer (Ed.), Academic Press, New York, pp. 363-408.

Schroeder, W.A., Shelton, J.R., Shelton, J.B., Robberson, B., Apell, G., Fang, R.S., and Bonaventura, J. (1982). The complete amino acid sequence of bovine liver catalase and the partial sequence of bovine erythrocyte catalase. Arch. Biochem. Biophys., 214(1): 397-421.

Shaffer, J. B., Preston, K. E., and Shepard, B. A. (1990). Nucleotide and deduced amino acid sequences of mouse catalase: molecular analysis of a low activity mutant. Nuc. Acids Res., 18: 4941.

Shaffer, J. B., and Preston, K. E. (1990). Molecular analysis of an acatalasemic mouse mutant. Biochem. Biophys. Res. Comm., 173(3): 1043-1050.

Shaffer, J. B., Sutton, R. B., and Bewley, G. C. (1987). Isolation of a cDNA clone for murine catalase and analysis of an acatalasemic mutant. J. Biol. Chem., 27: 12908-12911.

Shaw, G., and Kamen, R. (1986). A conserved AU sequence from the 3' untranslated region of GM-CSF mRNA mediates selective mRNA degradation. Cell, 46: 659-667.

Sies, H., and Cadenas, E. (1983). Biological basis of detoxification of oxygen free radicals. In *Biological Basis of Detoxification* W. Jakoby (Ed.), Academic Press, New York, pp. 181-211.

Simmons, D. M., Arriza, J. L., and Swanson, L. W. (1989). A complete protocol for in situ hybridization of messenger RNAs in brain and other tissues with radiolabeled single-stranded RNA probes. J. Histotech., 12: 169-181.

Smith, E. N., and Taylor, R. T. (1982). Acute toxicity of methanol in the folate-deficient acatalasemic mouse. Toxicol., 25: 271-287.

Sommerville, J. (1992). RNA-binding proteins: masking proteins revisited. Bioessays, 14: 337-339.

Sonenberg, N. (1988). Cap binding proteins of eucaryotic messenger RNA: Function in initiation of translation. Prog. Nuc. Acids Res. Mol. Biol., 35: 173-207.

Sonenberg, N. (1994). mRNA translation: influence of the 5' and 3' untranslated regions. Curr. Opin. Genet. Dev., 4: 310-315.

Sosenko, I. R. S., and Frank, L. (1987). Guinea pig lung development: antioxidant enzymes and premature survival in high O_2. Am. J. Physiol., 252: R693-R698.

Southorn, P. A., and Powis, G. (1988). Free radicals in medicine. II. Involvement in human disease. Mayo Clin. Proc., 63: 390-408.

Spena, A., Krause, E., and Dobberstein, B. (1985). Translation efficiency of zein mRNA is reduced by hybrid formation between 5'- and 3' -untranslated region. EMBO J., 4(9): 2153-2158.

Spicer, E. K., Horton, R., Bloem, L., Bach, R., Williams, K. R., Guha, A., Kraus, J., Lin, T.-C., Nemerson, Y., and Konigsberg, W. H. (1987). Isolation of cDNA clones coding for human tissue factor: Primary structure of the protein and cDNA. Proc. Natl. Acad. Sci., 84: 5148-5152.

Stadtman, E. R., and Oliver, C. N. (1991). Metal-catalyzed oxidation of proteins. J. Biol. Chem., 266(4): 2005-2008.

Standart, N., Dale, M., Stewart, E., and Hunt, T. (1990). Maternal mRNA from clam oocytes can be specifically unmasked in vitro by antisense RNA complementary to the 3' untranslated region. Genes Dev., 4: 2157-2168.

Tanabe, T., Noda, M., Furutani, Y., Takai, T., Takahashi, T., Tanaka, K., Hirose, T., Inayama, S., and Numa, S. (1984). Primary structure of the beta subunit precursor of calf muscle acetylcholine receptor deduced from cDNA sequence. Eur. J. Biochem., 144: 11-17.

Tanswell, J. F., and Freeman, B. A. (1984). Pulmonary antioxidant enzyme maturation in the fetal and neonatal rat. Developmental profiles. Ped. Res. 18: 584-587.

Theil, E. C. (1990). Regulation of ferritin and transferrin receptor mRNAs. J. Biol. Chem., 265(9): 4771-4774.

Titus, D. E. (1991). Synthesis of large amounts of RNA (100 µl) In: *Protocols and Applications* (2nd ed.). Promega Corporation, U.S.A. p. 59-61.

Tokunaga, K., Taniguchi, H., Yoda, K., Shimizu, M., and Sakiyama, S. (1986). Nucleotide sequence of a full-length cDNA for mouse cytoskeletal beta-actin mRNA. Nuc. Acids. Res., 14: 2829.

Ullrich, A., Bell, J. R., Chen, E. Y., Herrera, R., Petruzzelli, L. M., Dull, T. J., Gray, A., Coussens, L., Liao, Y.-C., Tsubokawa, M., Mason, A., Seeburg, P. H., Grunfeld, C., Rosen, O. M., and Ramachandran, J. (1985). Human insulin receptor and its relationship to the tyrosine kinase family of oncogenes. Nature(313): 756-761.

Vainshtein, B. K. (1974). The quaternary structure of catalase. In: *Alcohol and Aldehyde Metabolizing Systems* R. G. Thurman, J. R. Williamson, T. Yonatani, and B. Chance (Eds.), Academic Press, New York.

Vakalopoulou, E., Schaack, J., and Shenk, T. (1991). A 32-kilodalton protein binds to AU-rich domains in the 3' untranslated regions of rapidly degraded mRNAs. Mol. Cell. Biol., 11: 3355-3364.

van den Bosch, H., Schutgens, R. B. H., Wanders, R. J. A., and Tager, J. M. (1992). Biochemistry of peroxisomes. Annu. Rev. Biochem., 61: 157-197.

Varma, S. D., Chand, D., Sharma, Y. R., Kuck, J. F. J., and Richards, R. D. (1984). Oxidative stress on lens and cataract formation: Tole of light and oxygen. Curr. Eye Res., 3: 35-57.

von Ossowski, I., Hausner, G., and Loewen, P.C. (1993). Molecular evolutionary analysis based on the amino acid sequence of catalase. J. Mol. Evol., 37: 71-76.

Weickert, M. J., and Chambliss, G. H. (1991). Preparation of double stranded DNA template for sequencing using acid phenol extraction. USB Bulletin.

Weis, L., and Reinberg, D. (1992). Transcription by RNA polymerase II: Initiator-directed formation of transcription-competent complexes. FASEB, 6: 3300-3309.

Wen, J.-K., Osumi, T., and Hashimoto, T. (1990). Molecular analysis of human acatalasemia: Identification of a splicing mutation. J. Mol. Biol., 211: 383-393.

Wen, J.-K., Osumi, T., Hashimoto, T., and Ogata, M. (1988). Diminished synthesis of catalase due to the decrease in catalase mRNA in Japanese-type acatalasemia. Physiol. Chem. Phys. Med. NMR: 171-176.

Wickens, M. (1990). In the beginning is the end: regulation of poly (A) addition and removal during early development. Trends Biochem. Sci., 15: 320-324.

Wickens, M. (1992). Forward, backward, how much, when: mechanisms of poly (A) addition and removal and their role in early development. Sem. Dev. Biol., 3: 399-412.

Wickens, M. (1993). Springtime in the desert. Nature, 363: 305-306.

Wickens, M., and Takayama, K. (1994). Deviants - or emissaries. Nature, 367: 17-18.

Wightman, B., Ha, I., and Ruvkun, G. (1993). Posttranscriptional regulation of the heterochronic gene lin-14 by lin-4 mediates temporal pattern formation in *C. elegans*. Cell, 75: 855-862.

Wodnar-Filipowicz, A., and Moroni, C. (1990). Regulation of interleukin 3 mRNA expression in mast cell occurs at the posttranscriptional level and is mediated by calcium ions. Proc. Natl. Acad. Sci., 87: 777-781.

Yam, J., Frank, L., Roberts, R. J. (1978). Oxygen toxicity: comparison of lung biochemical responses in neonatal and adult rats. Ped. Res., 12: 115-119.

Yamada, M., Hashinaka, K., Inazawa, J., and Abe, T. (1991). Expression of catalase and myeloperoxidase genes in hydrogen peroxide-resistance HL-60 cells. DNA and Cell Biol., 10(10): 735-742.